UNIVERSIDADE FEDERAL DE PELOTAS
Centro de Desenvolvimento Tecnológico
Programa de Pós-Graduação em Ciência e Engenharia de Materiais

Tese

Mecanismos de absorção e adsorção de biofiltros para biorremediação de ambientes aquáticos contaminados com SARS-CoV-2 e metais pesados

Carolina Faccio Demarco

Pelotas, 2023

Carolina Faccio Demarco

Mecanismos de absorção e adsorção de biofiltros para biorremediação de ambientes aquáticos contaminados com SARS-CoV-2 e metais pesados

Tese apresentada ao Programa de Pós-Graduação em Ciência e Engenharia de Materiais da Universidade Federal de Pelotas, como requisito parcial à obtenção do título de Doutor em Ciência e Engenharia de Materiais.

Orientador: Prof. Dr. Robson Andreazza

Pelotas, 2023

Universidade Federal de Pelotas / Sistema de Bibliotecas
Catalogação na Publicação

D372m Demarco, Carolina Faccio

Mecanismos de absorção e adsorção de biofiltros para biorremediação de ambientes aquáticos contaminados com SARS-CoV-2 e metais pesados / Carolina Faccio Demarco ; Robson Andreazza, orientador. — Pelotas, 2023.

146 f. : il.

Tese (Doutorado) — Programa de Pós-Graduação em Ciência e Engenharia de Materiais, Centro de Desenvolvimento Tecnológico, Universidade Federal de Pelotas, 2023.

1. Ilhas flutuantes artificiais. 2. Fitorremediação. 3. Adsorção SARS-CoV-2. 4. Remediação cromo hexavalente. 5. Biomateriais. I. Andreazza, Robson, orient. II. Título.

CDD : 620.11063

Elaborada por Simone Godinho Maisonave CRB: 10/1733

Carolina Faccio Demarco

Mecanismos de absorção e adsorção de biofiltros para biorremediação de ambientes aquáticos contaminados com SARS-CoV-2 e metais pesados

Tese aprovada, como requisito parcial, para obtenção do grau de Doutor em Ciências e Engenharia de Materiais, Programa de Pós-Graduação em Ciência e Engenharia de Materiais, Centro de Desenvolvimento Tecnológico, Universidade Federal de Pelotas.

Data da defesa: 16/02/2023

Banca examinadora:

_____
Prof. Dr. Robson Andreazza (Orientador)
Doutor em Ciência do Solo pela Universidade Federal do Rio Grande do Sul (UFRGS).

_____
Prof. Dr. Fernando Machado Machado
Doutor em Engenharia de Minas, Metalúrgica e de Materiais pela Universidade Federal do Rio Grande do Sul (UFRGS)

_____
Prof. Dr. Flávio Manoel Rodrigues da Silva Júnior
Doutor em Ciências Fisiológicas pela Universidade Federal do Rio Grande (FURG).

_____
Prof. Dr. Filipe Selau Carlos
Doutor em Ciência do Solo pela Universidade Federal do Rio Grande do Sul (UFRGS).

_____
Prof. Dr. Simone Pieniz (Suplente)
Doutora em Microbiologia Agrícola e do Ambiente pela Universidade Federal do Rio Grande do Sul (UFRGS).

_____
Prof. Dr. Rafael Beltrame (Suplente)
Doutor em Engenharia Florestal pela Universidade Federal de Santa Maria (UFSM).

Agradecimentos

Às agências de fomento por permitir a realização desta pesquisa. O presente trabalho foi realizado com apoio da Coordenação de Aperfeiçoamento de Pessoal de Nível Superior – Brasil (CAPES) – Código de Financiamento 001, do Conselho Nacional de Desenvolvimento Científico e Tecnológico (CNPq) e Fundação de Amparo à Pesquisa do Estado do Rio Grande do Sul (FAPERGS).

Ao Professor Robson, pela orientação, amizade e incentivo ao longo desses anos.

Ao Professor Tito e doutorando Andrei pelo auxílio com as análises na Escola de Química e Alimentos da FURG.

Ao Professor Rodrigo pela pesquisa em parceria no Laboratório de Bioquímica e Biologia Molecular de Microrganismos da UFPel.

Ao Professor Anderson e doutoranda Daisa pelo auxílio e disponibilização do Laboratório de Metrologia da Química.

Ao Professor Neftali por também disponibilizar o Laboratório Novonano para realização de análises do nosso grupo de pesquisa.

Ao Centro de Desenvolvimento e Controle de Biomateriais (CDC-Bio), da faculdade de Odontologia da UFPel, pela disponibilização das análises de FT-IR.

Ao Laboratório de Ciência da Madeira da UFPel pela disponibilização das análises de TGA.

Ao Professor Marcelo do Programa de Pós-Graduação em Engenharia e Tecnologias de Processos, Universidade de Caxias do Sul, pela disponibilização do laboratório.

A todos os colegas do Laboratório de Química Ambiental, pela parceria de longa data. Agradeço também ao Professor Maurízio, pelos projetos em conjunto e pela participação em minha formação acadêmica.

Ao Filipe pelo apoio, amor e incentivo.

À minha família e todos os amigos que nos auxiliaram a enfrentar momentos pessoais tão difíceis. Agradeço aos meus pais, Claudio e Maria Inês e minha irmã Fernanda, por serem tão fortes. Agradeço especialmente à minha irmã Claudia, por ser o nosso maior exemplo de coragem e superação, e por nos fazer enxergar a vida com outro olhar.

Resumo

DEMARCO, Carolina Faccio. **Mecanismos de absorção e adsorção de biofiltros para biorremediação de ambientes aquáticos contaminados com SARS-CoV-2 e metais pesados.** Orientador: Robson Andreazza.146 f. Tese (Doutorado em Ciência e Engenharia de Materiais) – Centro de Desenvolvimento Tecnológico, Universidade Federal de Pelotas, Pelotas, 2023.

Os ambientes aquáticos são comumente afetados pelas diversas atividades antropogênicas, incluindo o lançamento de efluentes domésticos e industriais sem tratamento, atividades agrícolas e de mineração. Entre os contaminantes, os metais pesados representam grande preocupação pela toxicidade e propriedade de bioacumulação, afetando diretamente a qualidade ambiental e saúde da população. Entre as alternativas de remoção de metais pesados, a utilização de plantas como agentes de descontaminação apresenta destaque, e as macrófitas aquáticas vem sendo estudadas devido a habilidade natural de remoção de contaminantes. Primeiramente, foi realizada uma comparação entre o potencial natural de remoção de metais pesados pelas espécies de macrófitas *E. anagallis*, *H. ranunculoides*, *H. grumosa*, e *S. montevidensis* em uma área altamente antropizada no município de Pelotas/RS. Entre elas, verificou-se através dos índices de fitorremediação que *H. ranunculoides* apresentou destaque pelo fator de bioconcentração (BCF). Desse modo, a espécie *H. ranunculoides* foi selecionada para realização do estudo de avaliação dos mecanismos de resistência ao Cromo(VI), em um período de exposição de 7 dias e com avaliação de parâmetros de crescimento, pigmentos fotossintéticos, peroxidação lipídica via ensaio TBARS, compostos fenólicos totais, enzimas antioxidantes, FT-IR, teores de cromo e nutrientes, índices de fitorremediação, observações de superfície e citológicas, juntamente com análise de TGA. Verificou-se que a espécie de planta demonstrou restauração de pigmentos fotossintéticos, alteração nos grupos funcionais e nas células epidérmicas, juntamente com o aumento das concentrações de Cr(VI). Na comparação inicial entre as espécies, também verificou-se que *H. grumosa* e *S. montevidensis* destacaram-se pelo potencial de fitorremoção (g ha^{-1}). Desse modo, a espécie *H. grumosa* foi selecionada *para o* estudo de remoção de SARS-CoV-2, vírus causador da pandemia de COVID-19, a qual apresentou sérias consequências na saúde da população mundial, tendo causado mais de 6,6 milhões de mortes. O enfrentamento à pandemia demandou o desenvolvimento de diferentes pesquisas, e este trabalho encontra-se entre elas, visando desenvolver um material adsorvente para remoção de SARS-CoV-2 de águas residuárias. Para isso, a espécie *H. grumosa* foi utilizada em sua forma in natura e em forma de carvão ativado para a adsorção de SARS-CoV-2. Como resultados encontrados, destaca-se o excelente potencial de remoção encontrado: 98,44% por *H. grumosa* in natura, e 99,61% por carvão ativado produzido com *H. grumosa*. Considerando os resultados encontrados, realizou-se uma proposta inicial de dispositivos de biofiltros flutuantes a fim de aplicar as espécies *H. ranunculoides e H. grumosa* na descontaminação de cromo e SARS-CoV-2, respectivamente.

Palavras-chave: ilhas flutuantes artificiais; fitorremediação; adsorção SARS-CoV-2; remediação cromo hexavalente; biomateriais.

Abstract

DEMARCO, Carolina Faccio. **Mechanisms of absorption and adsorption of biofilters for bioremediation of aquatic environments contaminated with SARS-CoV-2 and heavy metals.** Advisor: Robson Andreazza. 146 f. Thesis (PhD in Science and Engineering of Materials) – Technological Development Center, Federal University of Pelotas, Pelotas, 2023.

Aquatic environments are commonly affected by several anthropogenic activities, including the release of untreated domestic and industrial effluents, agricultural and mining activities. Among the contaminants, heavy metals are of great concern due to its toxicity and bioaccumulation property, directly affecting the environmental quality and population health. Among the alternatives for removing heavy metals, the use of plants as decontamination agents stands out, and aquatic macrophytes have been studied due to their natural ability to remove contaminants. Firstly, a comparison was made among the natural potential for removal of heavy metals by the macrophyte species *E. anagallis*, *H. ranunculoides*, *H. grumosa*, and *S. montevidensis* in a highly anthropized area in the municipality of Pelotas/RS. Among them, it was verified through the phytoremediation indices that *H. ranunculoides* was highlighted by the bioconcentration factor (BCF). Thus, the species *H. ranunculoides* was selected to the study to evaluate the mechanisms of resistance to Chromium(VI), in an exposure period of 7 days and with the evaluation of growth parameters, photosynthetic pigments, lipid peroxidation via TBARS assay, total phenolic compounds, antioxidant enzymes, FT-IR, chromium and nutrient contents, phytoremediation indices, surface and cytological observations, along with TGA analysis. It was found that the plant species demonstrated restoration of photosynthetic pigments, alteration in functional groups and in epidermal cells, along with increased concentrations of Cr(VI). In the initial comparison between species, it was also verified that *H. grumosa* and *S. montevidensis* stood out for their phytoremoval potential (g ha^{-1}). Thus, the *H. grumosa* species was selected for the study to remove SARS-CoV-2, the virus that caused the COVID-19 pandemic, which had serious consequences for the world's population health, been responsible for more than 6.6 million of deaths. Coping with the pandemic demanded the development of different researches, and this work is among them, aiming to develop an adsorbent material to remove SARS-CoV-2 from wastewater. For this, the species *H. grumosa* was used *in natura* form and in the form of activated carbon for the adsorption of SARS-CoV-2. As results found, it is highlighted the excellent removal potential found: 98.44% by *H. grumosa* in natura, and 99.61% by activated carbon produced with *H. grumosa*. Considering the results found, an initial proposal of floating biofilter devices was made aiming to apply the species *H. ranunculoides* and *H. grumosa* in the decontamination of chromium and SARS-CoV-2, respectively.

Keywords: artificial floating islands; phytoremediation; SARS-CoV-2 adsorption; hexavalent chromium remediation; biomaterials.

Lista de Figuras

ARTIGO 1

ARTIGO 2

ARTIGO 3

ARTIGO 4

Lista de Tabelas

ARTIGO 1

ARTIGO 2

ARTIGO 3

ARTIGO 4

Lista de abreviaturas e siglas

AFI	Ilha flutuante artificial
BCF	Fator de Bioconcentração
BET	Brunauer, Emmett, Teller
BJH	Barrett- Joyner-Halenda
CAT	Catalase
C_T	Cycle Threshold
ERO	Espécie Reativa de Oxigênio
FT-IR	Fourier-transform Infrared Spectroscopy
MDA	Malondialdeído
MIP OES	Microwave-induced plasma optical emission spectrometer
PCZ	Ponto de Carga Zero
POD	Peroxidase
SEM	Scanning Electron Microscopy
SOD	Superóxido Dismutase
TBARS	Substâncias Reativas ao Ácido Tiobarbitúrico
TF	Fator de Translocação
TGA	Thermogravimetric Analysis
TPC	Compostos Fenólicos
WBE	Wastewater-Based Epidemiology
XRD	X-ray diffraction

Sumário

1 Introdução

A degradação dos recursos hídricos está intrinsecamente relacionada com a rápida urbanização, atividades industriais e formação de aglomerados urbanos em conjunto com uma gestão ineficiente de uso e ocupação do solo (LU *et al*., 2015). A liberação de poluentes através de emissões veiculares, disposição inadequada de resíduos sólidos, indústrias químicas e atividades de mineração, comumente afetam a qualidade dos solos e consequentemente a qualidade da água, devido à adição de metais pesados e outros compostos (AHMED; AHMARUZZAMAN, 2016).

A poluição da água por contaminantes orgânicos e inorgânicos representa um desafio atual, e a tentativa de remoção desses elementos é objeto de estudo de diferentes pesquisas (SAJID *et al*., 2018). Os metais pesados, em particular, apresentam propriedades de não-biodegradabilidade, toxicidade e potencial de bioacumulação, representando desse modo uma ameaça à qualidade ambiental e saúde da população (QING; YUTONG; SHENGGAO, 2015).

Outra questão de extrema relevância é presença de patógenos emergentes, que tem atraído atenção devido aos riscos que apresentam à saúde da população. Um exemplo é o SARS-CoV-2, tendo em vista a pandemia de COVID-19. A detecção de partículas virais em águas residuárias acendeu um alerta em termos de transmissão de doenças através dos sistemas de esgotamentos sanitários. No caso do SARS-CoV-2, apesar da rota significativa de transmissão ser via inalação de aerossóis, a excreção de partículas virais através das fezes, saliva e fluidos corporais fez com que cargas virais fossem detectadas em águas residuárias (LAHRICH *et al.* 2021).

Entre os processos convencionais de remoção de contaminantes de soluções aquosas, encontra-se a adsorção. Diversos estudos visam identificar novos materiais que possam ser utilizados como adsorventes, de modo a obter maior eficiência de remoção com um menor custo de produção. As biomassas vegetais, incluindo as macrófitas aquáticas, são alternativas para a produção de novos adsorventes e vem sendo estudadas devido a facilidade de obtenção dessas espécies (BIND *et al*. 2018).

Devido a sua composição e estrutura, as biomassas lignocelulósicas apresentam características que favorecem o processo adsortivo, como por exemplo, a presença dos grupamentos funcionais específicos que permitem a ligação do

material ao contaminante. Visando aumentar a eficiência do processo, os adsorventes podem ser modificados quimicamente ou fisicamente (MAIA; SOARES; GURGEL, 2021).

As macrófitas aquáticas apresentam também potencial de remoção de contaminantes no meio, servindo como filtros naturais em áreas contaminadas. Estudos demonstram que nutrientes como fósforo e nitrogênio podem ser absorvidos naturalmente (SUDIARTO; RENGGAMAN; CHOI 2019), bem como metais pesados (ALI *et al.* 2020). As macrófitas aquáticas também são responsáveis por promover um ambiente favorável ao aparecimento de microrganismos na zona de raízes, o que facilita a retenção e/ou transformação dos contaminantes. Outra característica é a redução da velocidade do fluxo da água, permitindo a redução dos sólidos dissolvidos e consequentemente reduzindo a turbidez (WANG *et al*. 2021).

Uma das formas de aplicabilidade das plantas vivas para remediação de corpos hídricos contaminados são os biofiltros do tipo ilha flutuante. O sistema consiste em um dispositivo onde as plantas permanecem flutuando na coluna de água e, as raízes realizam a filtração e permitem a formação de biofilme de microrganismos (SAMAL; KAR; TRIVEDI 2019). Para eficaz utilização desse sistema, deve-se mencionar a necessidade de retirada das plantas após a capacidade limite de remoção de contaminantes, visando evitar a reentrada dos compostos na coluna d'água devido ao processo de decomposição dos tecidos da planta (WANG *et al*. 2020). A destinação adequada dessa biomassa após a retirada é parte fundamental para garantir que não exista geração de poluição secundária e, ao mesmo tempo, permite gerar subprodutos de valor agregado. Alguns estudos já demonstraram a conversão da biomassa de macrófitas em adsorventes, produção de biogás, biochars, entre outros. Essa conversão da biomassa vai ao encontro da economia circular e produção limpa e demanda maiores estudos para efetiva aplicação (KURNIAWAN *et al*. 2021).

Desta forma, o presente trabalho propõe comparar os mecanismos naturais de fitorremediação através dos quais as macrófitas aquáticas *Enydra anagallis*, *Hydrocotyle ranunculoides*, *Hymenachne grumosa*, e *Sagittaria montevidensis* estão naturalmente removendo os metais pesados cromo, zinco, níquel, cádmio, chumbo e cobre *in situ*, em uma área altamente antropizada no município de Pelotas/RS.

Entre essas espécies, duas foram selecionadas para os experimentos posteriores. Uma delas foi utilizada como bioadsorvente – tanto in natura quanto na forma de carvão ativado e outra espécie foi utilizada em sua forma viva. Mais

especificamente, a pesquisa visa identificar os mecanismos através dos quais outra espécie de macrófita aquática - *Hymenachne grumosa,* responde ao processo adsortivo de SARS-CoV-2, tanto como bioadsorvente in natura, quando na forma de carvão ativado. Também propõe identificar os mecanismos através dos quais a macrófita aquática *Hydrocotyle ranunculoides* tolera altas concentrações de cromo (VI) em experimento de hidroponia, realizando caracterizações de parâmetros de crescimento, pigmentos fotossintéticos, peroxidação lipídica, grupamentos funcionais, observações morfológicas de superfície e citológicas. Ambas as espécies selecionadas permitiram a proposta teórica inicial de novos dispositivos de biofiltração e visam servir como base para aplicação em técnicas de biorremediação de ambientes contaminados.

2 Objetivos

2.1 Objetivos Gerais

Comparar os mecanismos naturais de fitorremediação através dos quais as macrófitas aquáticas *E. anagallis*, *H. ranunculoides*, *H. grumosa*, e *S. montevidensis* estão naturalmente removendo metais pesados. Avaliar o potencial da biomassa seca de *H. grumosa* in natura e em forma de carvão ativado para a adsorção de SARS-CoV-2, visando a obtenção de um novo adsorvente. Além disso, objetivou identificar os mecanismos de resistência ao Cromo (VI) apresentados pela espécie de macrófita aquática *H. ranunculoides* visando o entendimento dos fatores que tornam essa espécie tolerante a esse metal pesado. O estudo visou embasar a proposta de dispositivos de biofiltros para aplicação em recuperação de áreas contaminadas.

2.2 Objetivos Específicos

- Comparar o potencial natural das espécies *E. anagallis*, *H. ranunculoides*, *H. grumosa*, e *S. montevidensis* através dos índices de fitorremediação;
- Produzir os bioadsorventes *H. grumosa* in natura e *H. grumosa* carvão ativado;
- Caracterizar quimicamente, estruturalmente e morfologicamente os bioadsorventes produzidos;
- Avaliar o potencial adsortivo de SARS-CoV-2 pelos bioadsorventes *H. grumosa* in natura e *H. grumosa* carvão ativado;
- Propor a aplicação de dispositivos de biofiltração utilizando os bioadsorventes produzidos;
- Identificar os principais efeitos em *H. ranunculoides* visando entender aspectos da tolerância ao Cromo (VI);
- Caracterizar a espécie *H. ranunculoides* quanto à tolerância ao Cromo (VI) através de parâmetros de crescimento e teores de macronutrientes; pigmentos fotossintéticos; peroxidação lipídica; atividades enzimáticas; grupamentos funcionais; índices de fitorremediação; morfologia da superfície; e análise citológica.
- Propor a aplicação de dispositivos de biofiltração do tipo ilhas flutuantes utilizando a espécie *H. ranunculoides.*

3 Revisão Bibliográfica

3.1 Metais pesados

Os metais pesados são elementos presentes naturalmente no ambiente, com liberação que pode ser de origem natural, por intemperismo das rochas e pedogênese, ou por atividades antropogênicas, como por exemplo as atividades industriais e descarte inapropriado de efluentes (GARG; GAUNS, 2023). A poluição por metais pesados representa um grande risco devido ao seu potencial de permanência no ambiente e bioacumulação em plantas e animais em suas cadeias tróficas, causando danos aos organismos mesmo em baixas concentrações (INOBEME *et al*. 2023).

As consequências da presença de concentrações excessivas de metais pesados no organismo humano são, de modo geral: danos aos rins e ossos, problemas endócrinos, cardiovasculares e neurológicos, além de potencializar o desenvolvimento de câncer (RENIERI *et al*., 2019). A Tabela 1 apresenta os metais pesados mais conhecidos pelos efeitos deletérios à saúde humana, juntamente com os valores de referência estabelecidos pela World Health Organization (WHO, 2011), além de descrever os principais efeitos toxicológicos ao organismo humano.

Tabela 1 - Valores de referência em água potável e efeitos toxicológicos de alguns metais pesados à saúde humana.

Elemento	Valor de referência (mg L^{-1})	Efeitos toxicológicos
As	0,01	Alterações na pigmentação da pele; lesões nas palmas das mãos e pés; efeitos no sistema renal, gastrointestinal e cardiovascular, bem como aumento da pressão arterial; carcinogênico. Gestantes com exposição ao As apresentam aumento do risco de aborto ou nascimento prematuro.
Cd	0,003	Disfunção renal com reabsorção prejudicada de proteínas, glicose e aminoácidos; alterações pulmonares; carcinogênico.
Cr	0,05	Problemas respiratórios, renais, gastrointestinais e cardiovasculares; irritação na pele; carcinogênico.
Cu	2,0	Sangramento gastrointestinal; toxicidade hepatocelular; insuficiência renal aguda; anemia; problemas respiratórios.
Pb	0,01	Danos ao cérebro do feto; efeitos aos rins, sistema circulatório e sistema nervoso
Hg	0,006	Efeitos tóxicos nos sistemas nervoso, digestivo e imunológico e nos pulmões, rins, pele e olhos.
Ni	0,07	Efeitos de citotoxicidade, potencial mutagênico e carcinogênico, dermatite e hipersensibilidade na cavidade oral.
Zn	0,12*	Náuseas, vômito e febre.

Fonte: Adaptado de WHO (2011) e USEPA (2006)*.

3.1.1 Cromo (Cr)

O cromo apresenta número atômico 24 e massa atômica 51,996 u. O elemento tem ocorrência natural na crosta terrestre e pode existir em diferentes valências, porém, as formas mais comumente encontradas são Cr^0, Cr^{3+}e Cr^{6+}. O estado trivalente ocorre de maneira natural no ambiente, enquanto as formas Cr^{6+} e Cr^0 são normalmente geradas por processos industriais (ANASTOPOULOS *et al*., 2017).

O cromo é comumente utilizado em aplicações industriais na sua forma Cr (VI) devido à propriedade anticorrosiva, visto que a redução de Cr (VI) à Cr (III) forma camadas de precipitação que são mais estáveis em diversas condições químicas (GORNY *et al*., 2016). Desse modo, os usos mais comuns são para preservação de madeira, tratamento de couro, produção de cimento e tinta e no processo de galvanização (ANASTOPOULOS *et al*., 2017)

As principais fontes de cromo em ambientes aquáticos são a disposição inadequada de efluentes industriais, bem como lixiviação de aterros sanitários e de áreas de mineração (MISHRA; BHARAGAVA, 2016). Em meio aquoso, o elemento ocorre principalmente nos estados trivalente e hexavalente, os quais apresentam diferenças em relação a sua mobilidade, solubilidade, biodisponibilidade e toxicidade, sendo o Cr (VI) biologicamente mais tóxico do que a forma Cr (III). Enquanto o Cr (III) é caracterizado por ser um nutriente essencial ao ser humano em baixas concentrações, o Cr (VI) apresenta a característica de ser tóxico e carcinogênico (ALMEIDA *et al*., 2019).

O elemento Cr (VI) é altamente solúvel e rapidamente permeável, tendo interação com proteínas e ácidos nucléicos. Os efeitos toxicológicos do cromo em sua forma Cr (VI) advêm da possibilidade da livre difusão nas membranas celulares, bem como do forte potencial oxidativo, causando efeitos tóxicos, mutagênicos, genotóxicos e cancerígenos no organismo (MISHRA; BHARAGAVA, 2016).

A representação gráfica das possíveis fases de equilíbrio estáveis do sistema eletroquímico para o elemento Cr encontra-se na Figura 1.

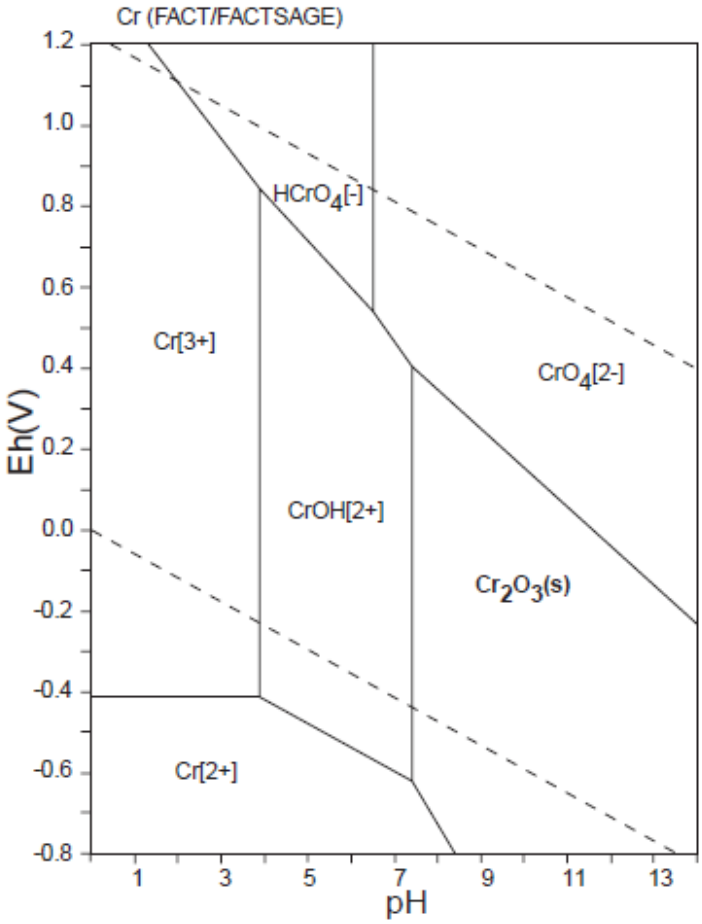

Figura 1 - Diagrama Eh-pH do sistema Cr-O-H em meio aquoso, 25°C,105 Pa.

Fonte: Takeno (2005).

3.4 Remoção de metais pesados

A remoção de metais pesados de soluções aquosos pode se dar por métodos convencionais, como por exemplo troca iônica, remoção eletroquímica, coagulação, filtração por membranas, precipitação química, entre outros (BURAKOV *et al*., 2018). Entretanto, essas técnicas apresentam algumas limitações, seja pela remoção incompleta, alto custo operacional – incrustação de membranas, necessidade de disposição de lodo, ou pela alta demanda de energia (BARAKAT, 2011). Entre os métodos convencionais utilizados para remoção de metais pesados, também encontra-se o processo de adsorção, o qual apresenta flexibilidade de design e operação, bem como um notável custo-benefício, fazendo com que essa técnica esteja entre as mais estudadas (KOBIELSKA *et al*., 2018).

3.4.1 Remoção utilizando plantas

A remoção de metais pesados do meio – tanto aquoso quanto solo, pode ser realizada também pelo metabolismo de organismos vivos. Tal técnica é denominada de biorremediação e pode utilizar fungos, leveduras, bactérias, algas, cianobactérias e plantas para a remoção do contaminante (MASSOUD *et al*., 2019).

A remoção de contaminantes utilizando plantas como agentes de descontaminação é denominada de fitorremediação. Essa técnica baseia-se no potencial das espécies de remover, estabilizar ou sequestrar compostos orgânicos ou inorgânicos – incluindo metais pesados. Desse modo, diferentes espécies vêm sendo estudadas para realizar fitorremediação, destacando as espécies hiperacumuladoras (THAKUR *et al*., 2016).

As macrófitas aquáticas apresentam propriedades que permitem a filtragem de diferentes contaminantes no meio, tornando-as favoráveis para aplicação na remoção de contaminantes. Os tecidos das partes emergentes dessas plantas são responsáveis por armazenar os nutrientes, como por exemplo o nitrogênio, que apresenta função fisiológica e de formação de biomoléculas; e o fósforo, segundo nutriente mais importante, desempenhando diversas funções metabólicas, genéticas, estruturais e regulatórias nas plantas (ALI *et al*., 2019).

O tecido das partes submersas promove área superficial para o desenvolvimento do biofilme de comunidade microbiana, promove a liberação de oxigênio, aumentando a degradação, além de absorver os nutrientes (ZHAO *et al*., 2018). Já as raízes auxiliam na redução do fluxo de escoamento, permitindo a sedimentação de partículas em suspensão maiores – reduzindo a turbidez, e promovendo também a absorção biológica de nutrientes, funcionando como filtros (LUCKE; WALKER; BEECHAM, 2019).

A remoção de metais pesados do meio requer a aplicação de plantas com tolerância à toxicidade desses elementos, visto que alguns desses atuam como micronutrientes em baixas concentrações, sendo tóxico em valores mais elevados; e outros não apresentam função biológica conhecida no metabolismo vegetal, podendo induzir efeitos tóxicos mesmo em baixas concentrações (BONANNO; VYMAZAL; CIRELLI, 2018).

3.4.1.1 Avaliação dos mecanismos de resistência

Um efeito importante causado pela presença de metais pesados nas plantas é o estresse oxidativo. Esse efeito ocasiona o aumento das espécies reativas de oxigênio (ERO), como por exemplo o radical superóxido (O_2^-), radical hidroxila, radical hidroperoxila (HO_2^-), peróxidos (O_2^{2-}), peróxido de hidrogênio (H_2O_2) e oxigênio (O_2), os quais são responsáveis por causar danos como disfunção metabólica e inclusive morte celular (ETESAMI, 2018).

Destaca-se que as ERO são parte do metabolismo natural da planta, entretanto o desequilíbrio entre a quantidade de ERO produzidas e a quantidade eliminada por processos enzimáticos e não enzimáticos é que causa o estresse oxidativo e seus respectivos efeitos deletérios (KAPOOR *et al*., 2019).

O combate ao estresse oxidativo a partir do sistema antioxidante apresenta relação direta com a espécie da planta, estágio de desenvolvimento e condições de crescimento (CLEMENTE *et al*., 2019). Para isso, as células das plantas produzem enzimas antioxidantes, como por exemplo a superóxido dismutase (SOD), as quais constituem a primeira linha de defesa contra as EROs, resultando na formação de H_2O_2 (YILMAZ; ERCAN; ERCAN, 2019). Posteriormente, há a ação coordenada de um conjunto de enzimas incluindo a catalase (CAT), peroxidase (POD), ascorbato peroxidase (APX) (YASIN *et al*., 2018).

A peroxidação lipídica refere-se à degradação oxidativa dos lipídios é causada pelo aumento excessivo de EROs, danificando a estrutura e o funcionamento das membranas devido a alteração na sua fluidez e permeabilidade (ISLAM *et al*., 2014). O malondialdeído (MDA) encontra-se entre os biomarcadores mais utilizados, devido ao fato de ser um dos produtos secundários mais conhecidos da peroxidação lipídica (RIZWAN *et al*., 2018). Desse modo, a peroxidação lipídica pode ser estimada através de medição da formação de substâncias reativas ao ácido tiobarbitúrico (TBARS) e quantificada como malondialdeído (MDA).

A quantificação dos teores de prolina também auxiliam no entendimento dos mecanismos de resistência aos metais pesados. Teores elevados são associados à resistência ao estresse, visto a comprovação do aumento de níveis desse aminoácido nos tecidos das plantas em situações de altos teores de metais pesados (BHAGYAWANT *et al*., 2019, YASIN *et al*., 2018).

Os pigmentos presentes nas plantas como, por exemplo, a clorofila a e clorofila b são responsáveis pela fotossíntese e são afetadas significativamente por estresses abióticos. Os metais pesados podem causar inibição da biossíntese de clorofila por impedimento na cadeia de transporte de elétrons fotossintéticos, e desse modo os teores desses pigmentos nas plantas são inversamente proporcionais às concentrações de metais pesados no meio (EL-KHATIB *et al*., 2020).

Os compostos fenólicos (TPC) apresentam importância morfológica e fisiológica para as plantas, além de servirem como proteção contra o estresse a partir da ação antioxidante. Esses compostos são metabólitos secundários e apresentam tendência de quelar metais pesados (KISA *et al*., 2016). Manquián-Cerda *et al*. (2016) estudando os efeitos do metal pesado Cd no crescimento de *Vaccinium corymbosum* L. verificaram o aumento dos teores de compostos fenólicos sendo mediado pelo aumento das EROs.

A atividade antioxidante pode ser avaliada pelo método DPPH (2,2-difenil-1-picril-hidrazil), visto a ampla aplicação como um radical livre empírico para esse tipo de ensaio. O aumento da atividade de eliminação de DPPH pode estar relacionada ao aumento de alguns metabólitos secundários, os quais auxiliam no aumento da defesa antioxidante (TAIE *et al*., 2019).

Os mecanismos de resistência podem ser avaliados também pela caracterização anatômica, ferramenta que permite identificar as alterações histológicas responsáveis pela tolerância aos metais pesados. As alterações mais frequentes são o acúmulo de metais em células especializadas da epiderme, tricomas e no interior do vacúolo, bem como o espessamento da parede celular (GHORI *et al*., 2019, SOUZA *et al*., 2009).

3.4.1.2 Biofiltros ilhas flutuantes artificiais

Os sistemas de biofiltros do tipo ilhas flutuantes são uma variação do sistema de wetland construído para melhoria da qualidade da água. São constituídos de vegetação sobre um suporte flutuante, permanecendo sob a superfície do corpo hídrico (CHANG *et al*., 2017). Esses sistemas apresentam a parte superior da vegetação crescendo acima do nível da água, enquanto as raízes realizam a filtração dos contaminantes em hidroponia. As raízes permitem o desenvolvimento de um

biofilme de microrganismos, os quais também apresentam mecanismos de remoção de contaminantes (BENVENUTI *et al*., 2018) (Figura 2).

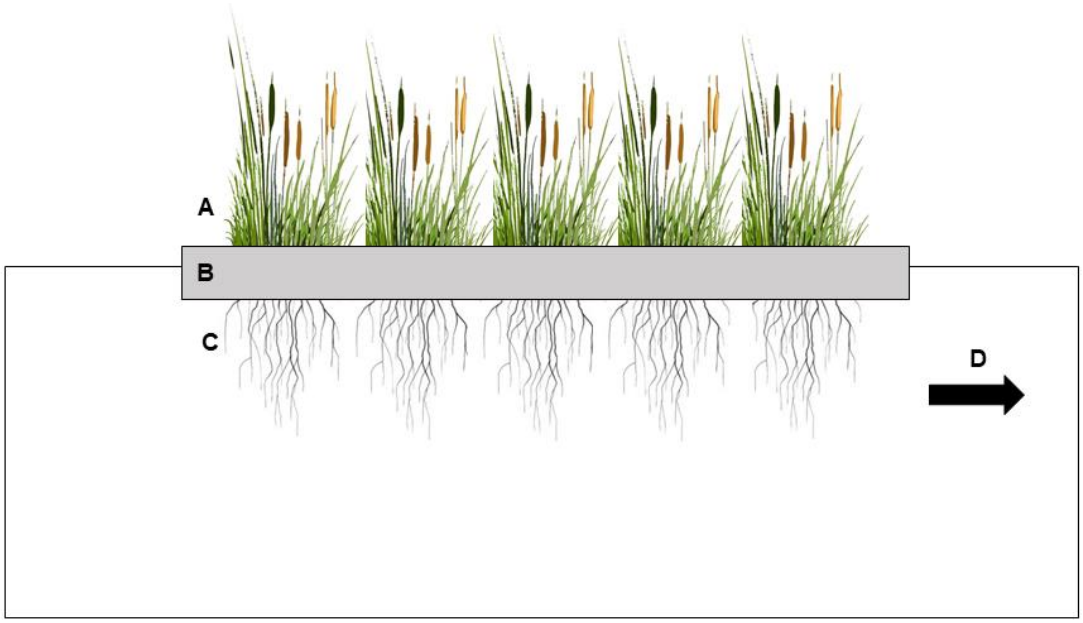

Figura 2- Representação de uma Ilha flutuante artificial (AFI), (a) parte aérea, (b) dispositivo flutuante, (c) raízes permanecendo abaixo da superfície da água, permitindo a formação de biofilme. O sistema permanece flutuando no fluxo d'água (d).

Os tipos de suporte que podem ser utilizados são usualmente constituídos de materiais como polímeros, madeira e fibra de vidro, e apresentam flutuação pela injeção de espuma ou uso de componentes ocos e vedados (LUCKE; WALKER; BEECHAM, 2019). Diferentes espécies de macrófitas aquáticas têm sido utilizadas para remediação de corpos hídricos, como a aguapé (*Eichhornia crassipes*), lentilha (*Lemna, Lemna* spp.), alface d´água (*Pistia stratiotes*), capim vetiver (*Chrysopogon zizanioides*) e caniço (*Phragmites australis*) (LU *et al*., 2018) e poderiam ser aplicadas em biofiltros do tipo ilhas artificiais.

A utilização de tecnologias combinadas, como por exemplo a adição de biofilmes ou microrganismos imobilizados podem aumentar o potencial de remoção de contaminantes a partir de ilhas flutuantes (PAVLINERI; SKOULIKIDIS; TSIHRINTZIS, 2017). Na literatura, já foi relatada a utilização de bactérias desnitrificantes imobilizadas, inclusão de sistema de aeração, adição palha de arroz e

outras fibras como substratos, visando melhorar o funcionamento desses sistemas filtrantes (SHEN *et al*., 2019).

Após o processo de remoção de contaminantes, a biomassa deve ser retirada do corpo hídrico, antes que a fase de decaimento ocorra e os nutrientes e metais pesados retirados reentrem no sistema (ZHAO *et al*., 2012). Em relação a parte da planta a ser retirada, alguns estudos já demonstraram que durante a fase inicial de crescimento da planta, as maiores concentrações de nutrientes situam-se na parte aérea, enquanto que na fase de senescência há maiores concentrações nas raízes (BI *et al*., 2019). Desse modo, destaca-se a necessidade de novos estudos visto a capacidade de retenção de contaminantes em ambas as partes do vegetal (SAMAL; KAR; TRIVEDI, 2019).

A Tabela 2 apresenta alguns estudos já realizados com ilhas flutuantes, incluindo o seu local de estudo, material de composição, espécies utilizadas e parâmetros analisados.

Tabela 2 – Estudos realizados com ilhas flutuantes artificiais.

Área de estudo	Escala	Material flutuação	Espécies de plantas	Método plantio	Parâmetros avaliados	Referência
Área rural (China)	*In situ*	Tubos PVC (40 mm) e cordas	*Oenanthe javanica; Gypsophila sp.; Rohdea Japônica; Dracaena sanderiana; Gardenia jasminoides Var. grandiflora; Gardenia jasminoides Var. prostrata* e *Salix babylonica.*	Mudas	Temperatura, pH, OD, SS, DQO, N total; P total; clorofila a.	Zhu, Li e Ketola (2011)
Canal com efluentes da aquicultura (Itália)	*In situ*	Patente Tech-IA® (EVA)	*Phragmites australis; Carex elata; Juncus effusus; Typha latifolia; Chrysopogon zizanioides; Sparganium erectumeDactylis glomerata.*	Plantas adultas	pH, temperatura, condutividade, OD, DBO, DQO, N total, NTK, N amoniacal, nitrato, P total, SS.	De Stefani *et al*. (2011)
Experimento águas pluviais sintéticas (Nova Zelândia)	Mesocosmo	[a] Patente BioHaven®	*Carex virgata; Cyperus ustulatus; Juncus edgariae; Schoenoplectus tabernaemontani.*	Mudas	Cu, Zn, turbidez, temperatura, OD, pH, macronutrientes e micronutrientes	Tanner e Headley (2011)
Experimento solução nutriente (China)	Microcosmo	PVC e espuma de polietileno	*Canna generalis; Scirpus validus;Alternanthera philoxeroides; Cyperus alternifolius; Thalia geniculata.*	Plantas adultas	DBO; DQO; N total; P total; N amoniacal e nitrato	Zhang *et al*. (2014)
Escoamento urbano de águas pluviais	Mesocosmo	Bóia circular de Poliestireno Extrudado.	*Juncus effusus*e *Carex riparia*.	Pozolana como substrato + mudas	Cd, Ni, Zn, produção biomassa.	Ladislas *et al*. (2013)
Lagoas de retenção urbana (EUA)	Mesocosmo	Cerdas de fibra de coco RoLanka™ Inc.	*Pontederia cordata* L., *Schoenoplectus tabernaemontani*	Mudas	P total, P particulado, ortofosfato, N total, N orgânico, N amoniacal, nitrato, clorofila a.	Wang e Sample (2014)

OD: oxigênio dissolvido (mg L^{-1}); DBO: demanda bioquímica de oxigênio (mg L^{-1}); DQO: demanda química de oxigênio (mg L^{-1}); SS: sólidos em suspensão; NTK: nitrogênio total Kjeldahl; [a] Fibra de poliéster entrelaçada (95% de porosidade) injetados com espuma de poliestireno para fornecer flutuabilidade;
Fonte: Adaptado de Pavlineri, Skoulikidis eTsihrintzis (2017)

3.4.1.3 Destinação da biomassa

A destinação da biomassa após a remoção de contaminantes dependerá das características e toxicidade do material, visto que há a possibilidade de contaminação secundária. As possibilidades de aplicação/destinação dessa biomassa variam desde fermentação anaeróbica, compostagem, combustão, fito-mineração, destinação em aterro sanitário e pirólise (LIU *et al*., 2019). Entre elas, a pirólise destaca-se por ser adequada para biomassas contendo metais pesados, visto a capacidade de promover a estabilização dos metais dentro da matriz de carbono, conforme estudo de Huang *et al*. (2018). A pirólise da biomassa é responsável por reduzir a massa de resíduos e degradar o material em produtos pirolíticos de valor agregado, dando origem ao denominado biocarvão, que pode ser empregado como corretivo para o solo, visto a presença de nutrientes básicos com o N, P e K, entre outros (ZHOU *et al*., 2020).

3.5 A pandemia de COVID-19

O surto de COVID-19 iniciou em Wuhan, China, em Dezembro de 2019. A nomenclatura foi dada em 7 de Janeiro de 2020, a partir da junção das iniciais de Coronavirus Disease 2019 (COVID-19). No Brasil, o primeiro caso foi confirmado em 26 de Fevereiro de 2020, e em 11 de Março de 2020, a organização mundial da saúde (OMS) declarou a pandemia do COVID-19 (WHO 2020). A partir desse momento, inúmeros foram os desafios em termos de saúde, economia, bem como aspectos políticos e sociais. Os dados apontam que, até Janeiro de 2023, o SARS-CoV-2 já infectou mais de 650 milhões de indivíduos e causou mais de 6,6 milhões de mortes no mundo (WHO 2023a).

Os principais impactos imediatos foram a superlotação dos sistemas de saúde e a busca por fabricação de Equipamentos de Proteção Individual (EPI), obras emergenciais de hospitais e criação de novos leitos de unidades de tratamento intensivo. Entre as medidas de enfrentamento da pandemia adotadas por diversos países, incluíram-se o uso de máscaras, higiene das mãos, quarentena de pessoas infectadas, bem como distanciamento social e aplicação da vacina (PAN *et al*. 2022). Com as medidas restritivas de distanciamento social e quarentena, impactos diretos foram gerados nos diversos setores – agricultura, manufatura, construção, varejo, energia, saúde e transporte (BARDHAN; BYRD; BOYD 2023).

3.5.1 SARS-CoV-2

O vírus responsável por causar a COVID-19 é o vírus SARS-CoV-2. A COVID-19 apresenta múltiplas manifestações de sintomas, incluindo não respiratórios, e essas variações ocorrem devido à idade da pessoa infectada, da variante do SARS-CoV-2 em questão e do estágio da infecção (WOJTUSIAK *et al*. 2023). Entre os principais sintomas da fase aguda incluem-se tosse seca, febre, dor de cabeça, fadiga, dor de garganta, perda de olfato e paladar, congestão nasal e náuseas (VAN KESSEL *et al*. 2022). Ainda são desconhecidos os efeitos a longo prazo da COVID-19, entretanto, as evidências apontam a presença de doenças neurológicas e de saúde mental, doenças pulmonares e cardiovasculares (SATTERFIELD *et al*. 2022).

De modo geral, os vírus apresentam a característica de serem partículas coloidais carregadas que podem ser adsorvidas por diferentes superfícies (LAHRICH *et al*., 2021). O SARS-CoV-2 apresenta a característica de ter uma fita simples de RNA com sentido positivo e pertencer à família Coronaviridae (YIN, 2020).

Diversas variantes do SARS-CoV-2 já foram relatadas, sendo divididas em Variantes de Preocupação (*Variants of Concern*, VOC) e Variantes de Interesse (*Variants of Interest*, VOI) de acordo com a Organização Mundial da Saúde. Entre as VOC, estão as variantes Alfa, Beta, Gamma, Delta e Ômicrom, sendo Ômicrom classificada em cinco linhagens principais (BA.1, BA.2, BA.3, BA.4, BA.5) e algumas sublinhagens (BA.1.1, BA.2.12.1, BA.2.11, BA.2.75, BA.4.6). Em Janeiro de 2023 não há nenhuma VOI, entretanto, algumas já relatadas foram Epsilon, Zeta, Theta, Kappa, Lambda, entre outras (WHO 2023b).

Apesar da principal rota de transmissão do SARS-CoV-2 ser através de gotículas de ar e contato, a transmissão via águas residuárias tornou-se uma preocupação crítica. Embora sem precedentes, existe o risco do SARS-CoV-2 ser transmitido via feco-oral, visto a detecção de partículas virais em urina e fezes de pacientes contaminados (ZAMHURI *et al*. 2022).

O monitoramento ambiental pode auxiliar no enfrentamento de futuras crises, visto que é um método não invasivo que pode fornecer informações importantes de indícios de infecções em níveis comunitários e servir de alerta para futuros surtos de doenças. O SARS-CoV-2, devido às suas características de transmissão, tem sido monitorado em diferentes meios, como o ar, águas residuárias e superfícies (SOLO-GABRIELE *et al*. 2023).

Uma forma de monitoramento é através da epidemiologia baseada em águas residuais (*Wastewater-Based Epidemiology – WBE*), a qual consiste em analisar marcadores visando a caracterização de poluentes emergentes e padrões de doenças em determinadas comunidades, apresentando potencial para auxiliar no entendimento dos surtos de COVID-19 (GONZALEZ *et al.* 2020). A WBE pode ser uma ferramenta essencial para rastreio de doenças e auxílio na alocação de recursos e combate a futuras pandemias (GRUBE et al. 2023).

O desenvolvimento dessa pesquisa ocorreu no momento de maior crise sanitária e hospitalar do Brasil com a pandemia de COVID-19. O país estava em um colapso no sistema de saúde conforme relatado pela Fiocruz (2021), com 25 dos 27 estados apresentando taxas de ocupação superiores a 80% dos leitos de Unidade de Terapia Intensiva (UTI) COVID-19. O epicentro do COVID-19 na América e no mundo era o Brasil, chegando a quase 4000 mortes diárias.

A crise sanitária apresenta impactos de longo prazo na saúde da população, nas esferas econômicas e sociais. Dessa forma, tornou-se urgente a necessidade de pesquisa de novas alternativas para remoção do vírus de águas e efluentes, visto a incerteza quanto ao comportamento do SARS-CoV-2 no ambiente, riscos de contaminação e demora na vacinação da população.

3.5.2 Adsorção

O processo de adsorção baseia-se na transferência do composto de interesse do meio para os sítios ativos presentes no adsorvente utilizado (OJEDOKUN; BELLO, 2016). A técnica apresenta como vantagem a fácil operação e eficiência de custo, bem como a possibilidade de regeneração do adsorvente, devido ao processo de dessorção (BURAKOV *et al*., 2018).

O fenômeno de adsorção ocorre a partir da interação do adsorvato às superfícies de um sólido – sendo nesse caso a ligação dos íons metálicos com o adsorvente. A capacidade de adsorção é dependente de fatores como as características do meio (pH, temperatura e concentração do elemento em questão), propriedades dos adsorventes (porosidade, área superficial específica, grupos funcionais presentes na superfície), bem como a dose de adsorvente utilizada e o tempo de contato (VELEMPINI; PILLAY, 2019).

Em estudos de adsorção, a ativação do adsorvente é comumente utilizada para aumentar a capacidade adsortiva, e desse modo, melhorar a eficiência do processo.

A modificação do adsorvente pode ser feita através de ativação física ou química (NAYAK *et al*., 2017).

Na ativação química podem ser utilizados agentes químicos como ácidos (H_2SO_4, H_3PO_4), bases (KOH, NaOH) e sais (Na_2CO_3, $AlCl_3$, $FeCl_3$, e $ZnCl_2$) (MAMANÍ *et al*., 2019). A utilização de ativantes alcalinos pode catalisar a desmetilação da pectina (polissacarídeos estruturais encontrados nos vegetais), fazendo com que ocorra um aumento de grupamentos funcionais COOH e desse modo facilitando a ligação dos íons metálicos na superfície do adsorvente (BIND; GOSWAMI; PRAKASH, 2018). A modificação química do adsorvente ocasiona a liberação de novos sítios ativos, melhora a estabilidade mecânica e protonação (ABDOLALI *et al*., 2015).

Por outro lado, a ativação física envolve a reação com vapores e gases contendo oxigênio, tratando-se de um processo onde o material reage com o gás oxidante – normalmente vapor de água ou CO_2, em temperaturas elevadas (de 800 a 1000 ^oC), com a energia para o processo de ativação dependendo diretamente do tipo de forno empregado. De modo geral, a ativação física permite o aumento do número de poros do material (LIEW *et al*., 2018).

Algumas modificações já relatadas previamente, como por exemplo o aumento na capacidade de adsorção de Ni (II) por *U. pinnatifida* após a modificação com $CaCl_2$ (CHEN; MA; HAN, 2008) e o aumento da remoção de Cr (VI) por várias macrófitas aquáticas após a modificação com H_2SO_4 (JOSEPH *et al*., 2019).

O fenômeno de adsorção do SARS-CoV-2 em superfícies dependem de vários fatores como a química da superfície, pH, umidade e temperatura. Esses aspectos também influenciam o processo de dessorção e a estabilidade e persistência do SARS-CoV-2, e a literatura apresenta lacunas quanto à interação entre o vírus e diferentes superfícies (JOONAKI et al., 2020).

3.5.3 Carvão ativado

O carvão ativado é um material carbonáceo composto por até 90% de carbono, e é caracterizado por apresentar uma estrutura porosa e elevada área superficial. O preparo do carvão pode se dar a partir do tratamento com gases oxidantes de precursores carbonizados e carbonização de materiais carbonosos, misturados com produtos químicos desidratantes (HEIDARINEJAD *et al*., 2020).

O carvão ativado como adsorvente apresenta grande aplicabilidade devido à área superficial, estrutura de porosa e alta capacidade de adsorção (KAUR; RANI; MAHAJAN, 2012). Entretanto, apresenta limitação de uso pelo custo, fazendo com que a busca por materiais alternativos seja estimulada, incluindo resíduos da agricultura e materiais lignocelulósicos (YAHYA; AL-QODAH; NGAH, 2015). Entre os novos materiais, a produção de carvão ativado vem sendo estudada também a partir da biomassa de macrófitas aquáticas (GONZÁLEZ-GARCÍA *et al*., 2019).

O processo de produção de carvão ativado baseia-se em duas principais etapas – a carbonização do precursor e a ativação do material carbonizado. No caso da ativação química, o processo de ativação ocorre antes da carbonização, com a impregnação utilizando $ZnCl_2$, H_3PO_4, NaOH, KOH, entre outros. Já a ativação física baseia-se na ativação em altas temperaturas (800 à 1.100 ºC), após a carbonização, sob fluxo de gases como CO_2 ou vapor de água, contribuindo para o aumento da porosidade (MAMANÍ *et al*., 2019).

Destaca-se que parâmetros como a temperatura, taxa de impregnação e o tempo são essenciais para determinar a textura e as propriedades do carvão ativado (NAYAK *et al*., 2017). Outro aspecto importante é a necessidade de realizar a lavagem do carvão após a modificação química, visando a retirada dos íons do agente ativante (YAHYA; AL-QODAH; NGAH, 2015).

4 Artigo 1

O artigo intitulado **“Bioremediation of Aquatic Environments Contaminated with Heavy Metals: A Review of Mechanisms, Solutions and Perspectives”** é apresentado conforme publicado na Revista Sustainability, ISSN: 2071-1050, fator de impacto 3.889, classificação A2 na área de Materiais, tendo sido aceito em 5 de Janeiro de 2023.

sustainability

30 MDPI

Review

Bioremediation of Aquatic Environments Contaminated with Heavy Metals: A Review of Mechanisms, Solutions and Perspectives

Carolina Faccio Demarco [1], Maurízio Silveira Quadro [2], Filipe Selau Carlos [3], Simone Pieniz [4], Luiza Beatriz Gamboa Araújo Morselli [1] and Robson Andreazza [1,*]

1 Technology Development Center, Graduate Program of Science and Materials Engineering, Pelotas 96015-560, Rio Grande do Sul, Brazil Federal University of Pelotas, Brazil; carolina.demarco@ufpel.edu.br (C.F.D.); luiza.morselli@ufpel.edu.br (L.B.G.A.M.)
2 Engineering Center, Federal University of Pelotas, Pelotas 96015-560, Rio Grande do Sul, Brazil; mausq@ufpel.edu.br
3 Faculty of Agronomy, Federal University of Pelotas, Pelotas 96015-560, Rio Grande do Sul, Brazil; filipe.selau@ufpel.edu.br
4 Faculty of Nutrition, Federal University of Pelotas, Pelotas 96015-560, Rio Grande do Sul, Brazil; simone.pieniz@ufpel.edu.br
* Correspondence: robson.andreazza@ufpel.edu.br

Abstract: The degradation of water resources is related to anthropic actions such as rapid urbanization and industrial and agricultural activities with inefficient land use and occupation management. Water pollution caused by organic and inorganic contaminants represents a current challenge for researchers and humanity. One of the techniques used to remove pollutants from aquatic environments is bioremediation, through the metabolism of living organisms, and especially phytoremediation, with plants as a decontamination agent. Aiming to demonstrate the current mechanisms, solutions, and perspectives regarding bioremediation, and especially phytoremediation in aquatic environments, a literature review was conducted, highlighting the following subjects: heavy metals as contaminants, phytoremediation, evaluation of resistance mechanisms, removal of heavy metals by microorganisms and biofilters of the artificial floating islands type. From the literature research carried out, it can be concluded that alternatives such as macrophyte plants have proved to be an effective and efficient alternative with a high potential for removal of contaminants in aquatic environments, including concomitantly with microorganisms. There was no mechanism well-defined for specific absorption of heavy metals by plants; however, some results can indicate that if there was sporadic contamination with some contaminants, the plants can be indicators with some adsorption and absorption, even with low concentration in the watercourse by the moment of the evaluation. It is necessary to study bioremediation methods, resistance mechanisms, tolerance, and removal efficiencies for each biological agent chosen. Within the bioremediation processes of aquatic environments, the use of macrophyte plants with a high capacity for phytoremediation of metals, used combined with bioremediating microorganisms, such as biofilters, is an interesting perspective to remove contaminants.

Keywords: heavy metals; macrophytes; microorganisms; biofilters; remediation

Citation: Demarco, C.F.; Quadro, M.S.; Carlos, F.S.; Pieniz, S.; Morselli, L.B.G.A.; Andreazza, R. Bioremediation of Aquatic Environments Contaminated with Heavy Metals: A Review of Mechanisms, Solutions and Perspectives. *Sustainability* **2023**, *15*, x. https://doi.org/10.3390/xxxxx

Academic Editor(s): Daizy R. Batish

Received: 22 November 2022
Revised: 30 December 2022
Accepted: 5 January 2023
Published: 11 January 2023

1. Introduction

The degradation of water resources is intrinsically related to rapid urbanization, industrial activities, agriculture, and the formation of urban agglomerates together with inefficient management of land use and occupation [1]. The release of pollutants through vehicular emissions, inadequate disposal of solid waste, chemical industries, and mining activities, commonly affect soil and, consequently, water quality due to the addition of heavy metals (HM) and other compounds [2]. Furthermore, urban land made a disproportionately large contribution to water pollution compared to other kinds of land use because intensive anthropogenic activities and urbanization can exacerbate the negative impacts on water quality [3].

Water pollution by organic and inorganic contaminants represents a current challenge, and the attempt to remove these elements is the object of study of different studies [4]. Several pollutants have recently been analyzed in the literature for their remediation by biological agents, such as pharmaceuticals and cosmetics [5]; polycyclic aromatic hydrocarbons [6]; artificial chemicals [7]; microplastics [8]; agrochemicals and pesticides [9]; primary nutrients [10]; HM [8,11–15].

Bioremediation is the most common ecologically sound biological technique to improve the natural degradation process [16]. Contamination through HM in soil and water is a major problem in developing countries, so phytoremediation is the best possible method for regions with large and moderate levels of concentration, rather than regions with high concentrations in little volume [17]. HM have properties of non-biodegradability, toxicity, and bioaccumulation potential, thus representing a threat to the environmental quality and health of the population [18]. The removal of HM from the medium—both aqueous and soil, can be performed by the metabolism of living organisms. This technique is called bioremediation and can use fungi, yeasts, bacteria, algae, cyanobacteria, and plants for the removal of the contaminant [19].

Phytoremediation is one of the bioremediation techniques and consists of the application of plants as a decontamination agent, especially aquatic macrophytes, which have the potential for removal of HM and other contaminants in the environment, serving as natural filters in contaminated areas [20]. Studies demonstrate that nutrients such as phosphorus and nitrogen can be absorbed naturally [21], as well as HM [22]. Aquatic macrophytes form a complex ecosystem based on symbiotic interaction with different microorganisms, both in natural conditions and in-built wetland systems [5].

One of the forms of applicability of living plants for remediation of contaminated water bodies is floating island biofilters. The system consists of a device where the plants remain floating in the water column and the roots perform filtration and allow the formation of biofilm of microorganisms [21]. For the effective use of this system, it is necessary to remove the plants after the limited capacity of removal of contaminants, to avoid the re-entry of the compounds into the water column due to the process of decomposition of the plant tissues [23,24]. The choice of the best method for the treatment of biomass after phytoremediation is hard to make, considering that simple combustion and gasification require a lot of care, in addition to the environmental impact caused by ash and gases [17]. The proper disposal of this biomass after removal is a key part of ensuring that there is no generation of secondary pollution and, at the same time, allows the generation of value-added by-products. For a sustainable remediation system, it is important to use plants with rapid growth and greater biomass accumulation [20].

Some studies have already demonstrated the conversion of macrophyte biomass into adsorbents, biogas production, and biochars, among others [5,21,24,25]. This conversion of biomass meets the circular economy and clean production and requires further studies for effective application [25]. Aiming to demonstrate the current mechanisms, solutions, and perspectives regarding bioremediation, and especially phytoremediation in aquatic environments, a review of the scientific literature was conducted, addressing aspects such as contaminants, phytoremediation, evaluation of resistance mechanisms, removal of HM by microorganisms and biofilters of the artificial floating islands type.

2. Heavy Metals (HMs) as Contaminants

HM is a general description for metals that are relative to high densities, atomic weights, or atomic numbers; however, for environmental studies, this term is well-used for indicating toxicity for living organisms and as a hazardous substance. Many HMs are nutrients and with high concentrations are contaminants such as Cu, Co, Zn, Cr and others [26]; however, other HMs do not have any function in living organisms and are toxic even in small concentrations such as As, Hg, Cd, Pb, and others [26]. For this reason, there are many studies and legislations for each element due to its concentration and form for toxicity and place found such as soil and water, for example.

The form of HM is also important once it can promote some key characteristic of this metal such as to improve toxicity or reduce mobility as in the case of chromium, once the oxidative phase Cr (VI), it is one of the most oxidative agents and can oxidate organic matter and tissues, and it can be more toxic in the environment, and Cr (VI) has been identified as a "Group I human carcinogen" with multisystem and multiorgan toxicity [27]. On the other hand, Cr (III) has been recommended for years as a trace element necessary for the proper functioning of organisms [28]; however, high concentrations can promote problems for living organisms and the environment.

When HMs are soluble in the watercourse, the problem of the contaminants can be exponentially increased once the solubility for microorganisms, plants, fish, and humans is increased, and all the food chain can be contaminated and biomagnification can be improved. For this reason, legislation of many governments has tables of toxicity for reference of pollution such as in Brazil [29] and in the USA [30], where limits on soil and water are proposed. These limits can be variable because of the exposure and characteristics of the watercourse, use, and limits in the country and or State.

Rivers and lakes have received high amounts of toxic metals, but more studies are necessary on the adsorption and transformation of these metals in the hyporheic zone and the exchange flux between the sediment–water interface. Fine sediments and colloidal particles can act as a carrier of HM, which may lead to higher accumulations of contaminants in the hyporheic zone and in the water itself [31]. It is important to know that the same HM that is adsorbed into a colloidal system, can be a source for delivery of this contaminant to the system and come back to the intoxication of the living microorganisms.

HMs are elements naturally appearing in the environment with a release that can be from natural origin, by weathering of rocks and pedogeneses, or by anthropogenic activities, such as industrial activities and inappropriate disposal of effluents [32]. HM pollution represents a great risk due to its potential permanence in the environment and bioaccumulation in plants and animals in their trophic chains, causing damage to organisms even at low concentrations [33].

The consequences of the presence of excessive concentrations of HM in the human body are, in general: damage to the kidneys and bones, endocrine, cardiovascular and neurological problems, in addition to potentiating the development of cancer [34]. Table 1 presents the HM best known for their deleterious effects on human health, in conjunction with the reference values established by the World Health Organization [35], in addition to describing the main toxicological effects on the human organism.

Table 1. Reference values in drinking water and toxicological effects of some HM on human health.

Element	Reference Value (mg L^{-1})	Toxicological Effects
As	0.01	Changes in skin pigmentation; lesions on the palms of the hands and feet; effects on the renal, gastrointestinal and cardiovascular system, as well as increased blood pressure; carcinogenic. Pregnant women with exposure to As have an increased risk of abortion or premature birth.
Cd	0.003	Renal dysfunction with impaired resorption of proteins, glucose, and amino acids; pulmonary alterations; carcinogenic.
Cr	0.05	Respiratory, intestinal, gastrointestinal, and cardiovascular problems; skin irritation; carcinogenic.
Cu	2.0	Gastrointestinal bleeding; hepatocellular toxicity; acute renal failure; anemia; breathing problems.
Pb	0.01	Brain damage to the fetus; affects the kidneys and circulatory and nervous systems.
Hg	0.006	Toxic effects on the nervous, digestive, and immune systems and lungs, kidneys, skin, and eyes.

Source: adapted from WHO [35].

3. Phytoremediation in Aquatic Environments

The phytoremediation technique is based on the potential of a variable of species of plants capable to remove, stabilize or kidnap organic or inorganic compounds. It is also one of the effective methods for reducing environmental contamination by HM [11]. Thus, different species have been studied to perform phytoremediation, highlighting the hyperaccumulator species [36].

Aquatic macrophytes have properties that allow the filtration of different contaminant substances in the medium, making them favorable for application in the removal of it. The tissues of the emerging parts of these plants are responsible for storing nutrients, such as nitrogen, which has physiological and biomolecule formation functions such as amino acids, proteins, and chlorophyll; and, phosphorus, which performs various metabolic, genetic, structural, and regulatory functions in plants [37].

Responsible for promoting an environment favorable to the multiplication of microorganisms in the rhizosphere, macrophytes facilitate the retention and/or transformation of contaminants. Another characteristic is the reduction of the speed of water flow, allowing the reduction of dissolved solids and consequently reducing turbidity [38].

During bioaccumulation, macrophytes store the polluting elements in their roots or transmit them to the shoots [14]. The tissue of the submerged parts allows the expansion of the surface area for the development of microbial community biofilm and promotes the release of oxygen, increasing degradation, in addition to nutrient absorption [39]. On the other hand, the roots help in reducing the flow, allowing the sedimentation of particles in larger suspension—reducing turbidity, and also promoting the biological absorption of nutrients, functioning as filters [40].

The removal of HM from the medium requires the application of plants with a tolerance to the toxicity of these elements since some of these act as micronutrients in low concentrations, being toxic at high values; and, others do not present known biological function in plant metabolism, and may induce toxic effects even at low concentrations [41]. Therefore, considering that the response of metal accumulation mechanisms differs between species [12], plant selection should mutually consider tolerance and removal capacity for phytoremediation success [7].

Phytoremediation has the advantage of being able to be applied on-site, consequently minimizing the exposure of the contaminant to other receptors and areas, as well as its benefits to efficiency and sustainability [42]. The main phytoremediation mechanisms include phytoextraction, phytostabilization, rhizofiltration, phytovolatilization, and phytodegradation. Phytoextraction can be characterized by the removal of HM through the roots and this content is translocated to the aerial part of the plant [37]. Phytostabilization, however, is based on the use of plants aiming at conversion into less bioavailable and less mobile forms [43].

Rhizofiltration consists of filtering contaminants through the root zone. In the case of HM, there may be absorption into the roots, or adsorption on the surface of the roots. Some aspects that directly influence this mechanism are the presence of root exudates, and pH, which allow the precipitation of HM [44].

Phytovolatilization is a mechanism based on the conversion of compounds to volatile forms, which are eliminated by plants through the transpiration process. Some metals that have been studied as application potential in this technique are selenium, mercury, and arsenic [45]. Phytodegradation encompasses the degradation of the contaminant through metabolic pathways. The plant then absorbs the compounds of the medium and, with the support of different enzymes, degrades them into non-toxic forms. This technique is commonly used for organic compounds [46].

4. Evaluation of Resistance Mechanisms

An important effect caused by the presence of HM in plants is oxidative stress. This effect increases the reactive oxygen species (ROS), such as superoxide radical (O2-), hydroxyl radical (OH), hydroperoxyl radical (HO2-), peroxides (O2-2), hydrogen

peroxide (H2O2), and oxygen (O2), which are responsible for causing damage such as metabolic dysfunction and even cell death [47].

It is noteworthy that ROS are part of the natural metabolism of the plant; however, the imbalance between the amount of ROS produced and the amount eliminated by enzymatic and non-enzymatic processes is the cause of oxidative stress and its respective deleterious effects [48].

The effort against oxidative stress from the antioxidant system has a direct relationship with the plant species, stage of development, and growth conditions [49]. Towards that, plant cells produce antioxidant enzymes, such as superoxide dismutase (SOD), which constitute the first line of defense against ROS, resulting in the formation of H_2O_2 [50]. Subsequently, there is a coordinated action of a set of enzymes including catalase (CAT), peroxidase (POD), and ascorbate peroxidase (APX) [51].

Lipid peroxidation refers to the oxidative degradation of lipids which is caused by the excessive ROS increase, damaging the structure and functioning of membranes due to changes in fluidity and permeability [52]. Malondialdehyde is among the most widely used biomarkers because it is one of the most well-known secondary products of lipid peroxidation [53]. Thus, lipid peroxidation can be estimated by measuring the formation of thiobarbituric acid reactive substances (TBARS) and quantified as malondialdehyde.

The quantification of proline contents also assists in understanding the mechanisms of resistance to HM. High levels are associated with stress resistance, since there is evidence of the increased quantity of this amino acid in plant tissues in situations of high levels of HM [51,54].

The pigments present in plants, such as chlorophyll a and chlorophyll b, are responsible for photosynthesis and are significantly affected by abiotic stresses. HM can cause inhibition of chlorophyll biosynthesis by hindering the transport chain of photosynthetic electrons, and thus the contents of these pigments in plants are inversely proportional to the concentrations of HM [55].

Phenolic compounds (PCT) have morphological and physiological importance for plants, besides serving as protection against stress from antioxidant action. These compounds are secondary metabolites and tend to break HM [56]. Manquián-Cerda et al. [57] studied the effects of heavy metal Cd on the growth of *Vaccinium Corymbosum* L. and verified the increase in phenolic compound contents being mediated by increased ROS.

Antioxidant activity can be evaluated by the DPPH method (2,2-diphenyl-1-picryl-hydrazyl), seen by wide application as an empirical free radical for this type of assay. The increase in DPPH elimination activity may be related to the increase in some secondary metabolites, which help in increasing antioxidant defense [58].

The resistance mechanisms can also be evaluated by anatomical characterization, a tool that allows identifying the histological changes responsible for the tolerance to HM. The most frequent changes are the accumulation of metals in specialized cells of the epidermis, trichomes, and inside the vacuole, as well as the thickening of the cell wall [59,60].

Table 2 presents several resistance mechanisms studied in aquatic macrophytes and HM.

Table 2. HM tolerance mechanisms in aquatic macrophytes.

Species	Metal	Concentration	Toxicological Effects	Reference
Macleaya cordata	Mn^{2+}	0–12 mmol L^{-1}	Cells distort and deform, black precipitates appeared in the intercellular space, mitochondria, and starch granules decrease. Chloroplasts shrink, and hungry particles increase.	[61]
Nerium indicum	Pb	3311.5–4297.08 mg kg^{-1}	Significant decrease in the acid-extractable state, a significant increase in the residue state, and a small decrease in the Fe-Mn binding state, and a small increase in the organic binding state.	[62]
	Zn	1398.33–1704.92 mg kg^{-1}		
	Cu	143.33–163.5 mg kg^{-1}		
	Cd	28.92–43.83 mg kg^{-1}		

Species	Metal	Concentration	Toxicological Effects	Reference
Pontederia cordata	Cd^{2+}	0–66 mM	Decrease in chlorophyll contents due to increased lipid peroxidation and inhibition of biosynthesis of chlorophyll precursors; inhibition of Cd translocation from roots to aerial part; SOD and POD activities without variation about control at concentrations 0.04 mM to 0.22 mM in 15 days of exposure; A concentration of 0.44 mM caused a reduction in SOD and POD.	[63]
Potamogeton pectinatus L.	Cu	0–1000 μM	Accumulation mainly in the roots; dose-dependence pattern identified; decreased levels of chlorophylls and carotenoids; Inhibition of photosynthesis; leaf damage; reduction in pigments.	[64]
Nymphaea tetragona	U	0–55 mg L^{-1}	Increased activity POD, CAT, SOD; increased MDA levels aggravate cell membrane damage; inhibition of soluble protein, chlorophyll a, chlorophyll b, and carotenoid sums.	[65]
Spirodela polyrhiza L.	Cu^{2+} Hg^{2+}	0.0–40 μM 0.0–0.4 μM	Increased SOD activity in 10 μM Cu^{+2}; 0.2 μM Hg^{+2}; CAT, at 20 μM Cu^{+2}; 0.2 μM Hg^{+2} and GPOD, at 10 μM Cu^{+2}; 0.2 μM Hg^{+2} with the fall of all activities until 40 μM Cu^{+2} and 0.4 μM Hg^{+2}.	[66]

Source: The authors.

5. Removal of HM by Microorganisms

Microorganisms have metabolic pathways that use contaminants as an energy source for their growth and development, through respiration and fermentation. However, they can also carry out degradation of the compounds through co-metabolism (without nutritional utilization of the substrate) [67].

For the efficient use of microorganisms in the removal of HM, it is necessary to make the selection of organisms resistant to the compound of interest, from the isolation technique, as well as identification of resistance mechanisms [68]. This selection can be performed in contaminated areas, which perform a natural pre-selection since they are more likely to have organisms tolerant to the stress situation.

Among the strategies for the removal of HM by microorganisms, biosorption stands out, a process where (i) dead biomass, (ii) live cultures, or (iii) extracellular polymeric substances (EPS) can be used. EPS are produced by microorganisms and present in their composition mainly polysaccharides and proteins. EPS have plenty of negative charges, allowing binding with HM; therefore, they have the potential for removal of these ions from aqueous solutions [69]. The EPS matrix confers mechanical resistance, and water and nutrient retention, and assists in the resistance of cells to various stress conditions [23].

It is noteworthy that, for biosorption to be efficient, it is necessary to analyze the physical nature of biosorbents, sorption kinetics, maximum adsorption capacity, as well as the regeneration capacity of the adsorbent and the stability of microorganisms as biosorbents [70]. Among the bacteria commonly used for metal biosorption are the genera *Bacillus*, *Pseudomonas*, and *Streptomyces* [71].

Some mechanisms of resistance of living microorganisms to heavy metal ions are illustrated in Figure 1. Active export of metal ions depends directly on special resistance genes on the chromosome or plasmid. These genes encode heavy metal transporters, performing the ion influx. For instance, one can cite enzymes called P-type ATPase, which transport specific ions through the cell membrane against a concentration gradient [72].

Extracellular sequestration of ions is responsible for reducing the toxicity of these elements to microorganisms. This mechanism allows the accumulation of HM in different biological structures and can be performed, for example, by EPS, glutathione, and biosurfactants [73]

The sequestration of metal ions can also be performed intracellularly, when the element is already inside the cell, preventing more sensitive cellular components from being affected by toxicity. In this mechanism, ions can be accumulated by cysteine-rich proteins such as metallothioneins (MTs), which have a high affinity for free metal ions [74].

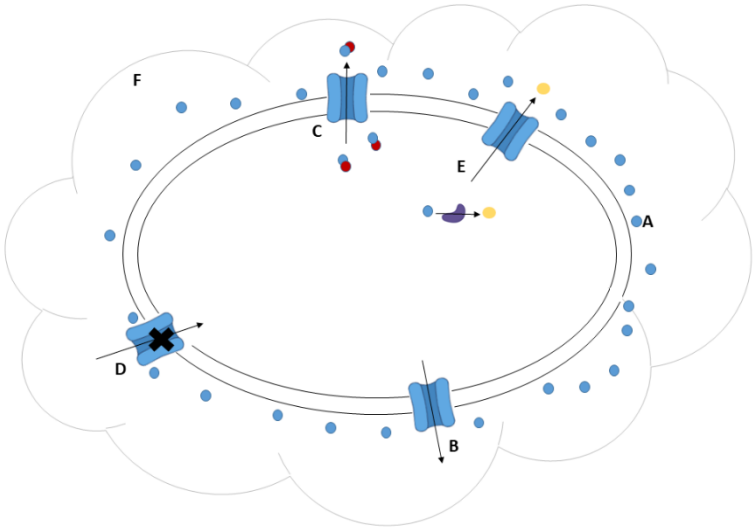

Figure 1 Mechanisms of detoxification of metal ions by microorganisms, where (a) active heavy metal ion, (b) active export, (c) heavy metal sequestration (d) control uptake (e) enzymatic detoxification, and (f) extracellular polymeric substances - EPS .

Enzymatic detoxification regulates the chemical transformation of HM into less toxic forms, conferring the ability to tolerate HM by microorganisms [75]. The mechanism is based on the redox state change, where enzymes perform oxidation and reduction reactions of metal ions. An example is the bacterium *Bacillus* sp., which is resistant to mercury by Hg reductase, responsible for reducing mercury to the metallic state, released into the medium through the cell membrane [73]. The presence of cationic diffusion facilitating transporters (CDF) is also involved in resistance to HM by the flow of ions [76].

The joint use of aquatic macrophytes and microorganisms—such as bacteria originating from the rhizosphere—represents a solution for the removal of HM in contaminated water bodies. Or, in the removal of polycyclic aromatic hydrocarbons (PAH), as was the case with the study by Yan et al. [6], with the use of macrophytes *Vallisneria natans* and *Herbaspirillum* bacteria, which made use of PAH as a carbon source and promoted plant growth. Recent studies demonstrate that bacterial inoculation enhances the natural remediation ability that aquatic plant species have, making them more resistant and increasing the ability to remove these compounds [77]. Rhizopheric microorganisms, such as denitrifying bacteria, can affect "rhizobio growth" in aquatic plants, boosting wastewater purification, such as the study by Lu et al. [78], with the use of the inoculated *Pseudomonas rhizospheric* strain and *Spirodela polyrrhiza* in nitrogen removal. Therefore, the interaction between macrophytes and microorganisms can help create new environmental decontamination strategies [6].

6. Artificial Biofilter Floating Islands

Biofilter floating island systems are a variation of the wetland system built to improve water quality. They are made of vegetation on floating support, remaining under the surface of the water body [79] (Figure 2).

These AFI systems showed the upper part of the vegetation growing above the water level, while the roots perform the filtration of contaminants in hydroponics. The roots allow the development of a biofilm of microorganisms, which also present mechanisms

for the removal of contaminants [80;81]. The types of support that can be used are usually fabricated of materials such as polymers, wood, and fiberglass, and present fluctuation by foam injection or use of hollow and sealed components [40]. Different species of aquatic macrophytes have been used for the remediation of water bodies, such as water hyacinth (*Eichhornia crassipes*), lentil (*Lemna, Lemna* spp.), water lettuce (*Pistia stratiotes*), vetiver grass (*Chrysopogon zizanioides*) and reed (*Phragmites australis*) [82] and could be applied in artificial islands biofilters.

Figure 2. Representation of an artificial floating island (AFI), presenting (a) shoots, (b) floating device, (c) roots under the surface water, allowing biofilm formation. The system remain floating in water flow (d).

The use of combined technologies, such as the addition of biofilms or immobilized microorganisms, can increase the potential for removing contaminants from floating islands [83]. In the literature, the use of immobilized denitrifying bacteria, the inclusion of an aeration system, addition of rice straw and other fibers as substrates have been reported, aiming to improve the functioning of these filter systems [84].

After the process of removing contaminants, biomass must be removed from the water body before the decay phase occurs and the nutrients and HM removed reenter the system [85]. Regarding the part of the plant to be removed, some studies have already shown that, during the initial phase of plant growth, the highest concentrations of nutrients are in the aerial part, while in the senescence phase, there are higher concentrations in the roots [86]. Thus, the need for further studies is highlighted, given the capacity of contaminant retention in both parts of the vegetable [23].

It is important to know about floating islands, including their place of study, composition material, species used, and parameters analyzed, as presented in Table 3.

Table 3. Studies carried out with artificial floating islands.

Study Area	Scale	Floating Material	Plant Species	Planting Method	Evaluated Parameters	Ref.
Botanical Garden (Pakistan)	Microcosm	Container/plastic tub of 50 L capacity	*Salvinia natans; Pistia stratiotes*	Adult plants	P-accumulated in plant biomass; pH; temperature.	[87]
River (South Africa)	In situ	Free-floating macrophytes	*Pontederia (=Eichhornia) crassipes; Stuckenia pectinatus; Typha capensis; Cyperus sexangularis; Phragmites australis*	Adult plants	pH; chemical oxygen demand (COD), Zn; Fe; Cd; As; Cr; Pb; Hg; Cu.	[1]
Botanical Garden (China)	In situ	Container, ecological floating bed	*Vallisneria natans; Ludwigia adscendens; Ipomoea aquatica; Monochoria vaginalis; Saururus chinensis; Acorus calamus; Typha orientalis; Schoenoplectus juncoides*	Adult plants	Total nitrogen (TN), total phosphorus (TP), COD.	[88]

Rural area (China)	In situ	PVC tubes (40 mm) and ropes	*Oenanthe javanica; Gypsophila sp.; Rohdea Japônica; Dracaena sanderiana; Gardenia jasminoides Var. grandiflora; Gardenia jasminoides Var. prostratae Salix Babylonica.*	Seedlings	Temperature, pH, OD, SS, COD, N total; P total; chlorophyll a.	[89]
Aquaculture effluent channel (Italy)	In situ	Licence Tech-IA® (EVA)	*Phragmites australis; Carexelata; Juncus effusus; Typha Latifolia; Chrysopogon zizanioides; Sparganiumerectume Dactylisglomerata*	Adult plants	pH, temperature, conductivity, DO, BOD, COD, N total, KTN, N ammoniacal, nitrate, P total, SS.	[90]
Synthetic rainwater experiment (New Zealand)	Mesocosm	[a] license BioHaven®	*Carexvirgata; Cyperus Ustulatus; Juncusedgariae; Schoenoplectus Tabernaemontani.*	Seedlings	Cu, Zn, turbidity, temperature, DO, pH, macronutrients, and micronutrients.	[91]
Nutrient Solution Experiment (China)	Microcosm	[a] license BioHaven®	*Cannageneralis; Scirpusvalidus; Alternanthera Philoxeroides; Cyperus Alternifolius; Thalia Geniculata.*	Adult plants	BOD; COD; N total; P total; ammoniacal N and nitrate.	[92]
Urban stormwater runoff	Mesocosm	Extruded Polystyrene Circular Buoy	*Juncus Effusus Carex Riparia.*	Pozzolan as substrate with seedlings	Cd, Ni, Zn, biomass production.	[93]
Urban retention ponds (USA)	Mesocosm	Coconut fiber bristles RoLanka™ Inc.	*Pontederia cordata L., Schoenoplectus tabernaemontani*	Seedlings	P total, P particulate, orthophosphate, N total, organic N, ammoniacal N, nitrate, chlorophyll a.	[94]

Legend: Ref: reference; DO: dissolved oxygen (mg L^{-1}); BOD: biochemical oxygen demand (mg L^{-1}); COD: chemical oxygen demand (mg L^{-1}); SS: suspended solids; KTN: Kjeldahl total nitrogen; [a] Interlaced polyester fiber (95% porosity) injected with polystyrene foam to provide buoyancy. Source: Adapted from Pavlineri, Skoulikidis, and Tsihrintzis [**Erro! Fonte de referência não ncontrada.**].

The disposal of biomass after the removal of contaminants will depend on the characteristics and toxicity of the material since there is a possibility of secondary contamination. The possibilities of application/disposal of this biomass range from anaerobic fermentation, composting, combustion, phytomining, landfill, and pyrolysis [95]. Among them, pyrolysis stands out for being suitable for biomass containing HM, given the ability to promote the stabilization of metals within the carbon matrix, according to a study performed by Huang et al. [96]. Pyrolysis of biomass is responsible for reducing the mass of residues and degrading the material in pyrolytic products of added value, giving rise to the so-called biocoal, which can be used as corrective for the soil, considering the presence of basic nutrients with N, P, and K, among others [97].

7. Advantages and Disadvantages of Bioremediation

Bioremediation using only plants or its combination with microorganisms such as fungus or bacteria has an important advantage against the conventional remediation treatment, once the society is more suitable and can choose biological treatments against the conventional. The bioremediation issue for studies and applications has increased in the current years. Studies with the most different applications such as heavy metals [98,99], hydrocarbonates [100], diesel [101,102], biodiesel [101,102], persistent organic pollutants [103], pesticides [104], and others.

Phytoremediation is one of the main techniques of bioremediation applied for the removal of contaminants from the environment, once to apply bacteria, fungus and other microorganisms have some limitations for applications in the environment. The use of macrophytes as a cost-effective bioremediation method is an interesting technique to treat contaminated water [20]. According to Shen et al. [105], biological, physical, chemical, agronomic, and genetic approaches have been used to enhance phytoremediation. Nevertheless, bioremediation systems require plants with rapid growth and higher biomass accumulation [20].

It is important to understand the limitations of each technique once the microorganisms contaminate other environments, or cause other problems, e.g., the application of one bacterium such as *Pseudomonas pneumoniae* in the environment for removal of copper [106], and to know that this kind of bacteria can promote diseases in humans.

Another disadvantage is the disposal methods of contaminated biomass, such as pyrolysis, incineration, composting, and compaction, which can be effective. However, they are costly and can provide security issues with improper disposal of contaminated HM [105]. Although the biomass of these wetland plants may be used for bioenergy generation [15], it is paramount to develop research for new and economical technologies to convert the contaminated waste from bioremediation to benefit the environment.

Plants that can be seen in their growth, and measured the population, are more suitable to understand for controlling some undesirable growth or population and to reintroduce the plants for phytoremediation. Phytoremediation has the potential to remove high concentrations of contaminants from soil; despite this possibility, long-term treatment is necessary once with the time course to decrease the concentration and efficiency. Meanwhile, in the watercourses, the possibility to introduce and remove plants is more suitable for remediation and can be easily used and managed, and it can increase the results and reduce the time course of the bioremediation process. This kind of study should be well explored and used in the field.

8. Conclusions and Future Prospects

The increase in environmental contamination has culminated in a reduction in the quality of soils and aquatic environments throughout the globe. Alternatives such as macrophyte plants have been used for phytoremediation of these environments, and are an effective, efficient alternative with high potential for use. Not all plants can absorb and or adsorb toxic HM from the environment; however, by studying bioremediation methods for these metals, it is possible to highlight various resistance mechanisms and forms of bioremediation that are fundamental to the identification of the best use of the plant. Allied to plants, resistant microorganisms can exert various forms of bioremediation, helping the plant extract, modify or mitigate the toxic effect of HM. Once this step has been identified, phytoremediation can be improved by transporting or reducing the toxicity of HM.

The relationship between the type of contaminant with the phytoremediation plant affects the capacity and mechanism of bioremediation. In addition, with different contaminants, this dynamic is also affected. This theme still needs many studies to reach a common denominator, even if there would have more results, they would hardly find an exact formula because they are living organisms in often complex environmental interactions, such as type of organism, different temperatures (including on the same day), different floating concentrations of HM, and different volumes and pHs, among other environmental variants. To reduce these processes, it is recommended that, when using plants and microorganisms, they are adapted to the environment and contamination conditions.

Within the bioremediation processes of aquatic environments, the use of macrophyte plants with a high capacity for phytoremediation of metals, used with bioremediating microorganisms, such as biofilters, is an interesting perspective to remove contaminants in solution. It is still possible to promote the use of biofilters with the incorporation of

renewable materials, such as polyurethane foams, which act as adsorbents in aquatic environments. Thus, the set of environmental technologies favors remediation and bioremediation of contaminated environments.

Author Contributions: Conceptualization, C.F.D. and R.A.; methodology, C.F.D.; investigation, C.F.D., M.S.Q., F.S.C., S.P., L.B.G.A.M. and R.A.; resources, R.A.; writing—original draft preparation, C.F.D.; writing—review and editing, C.F.D., F.S.C., L.B.G.A.M. and R.A.; supervision, R.A. All authors have read and agreed to the published version of the manuscript.

Funding: This study was financed in part by the Coordenação de Aperfeiçoamento de Pessoal de Nível Superior—Brasil (CAPES)—Finance code 001, by the CNPq (National Council for Scientific and Technological Development) and FAPERGS (Research Support Foundation of the State of Rio Grande do Sul).

Institutional Review Board Statement: Not applicable.

Informed Consent Statement: Not applicable.

Data Availability Statement: Not applicable.

Conflicts of Interest: The authors declare no conflict of interest.

References

1. Lu, Y.; Song, S.; Wang, R.; Liu, Z.; Meng, J.; Sweetman, A.J.; Jenkins, A.; Ferrier, R.C.; Li, H.; Luo, W.; et al. Impacts of soil and water pollution on food safety and health risks in China. *Environ. Int.* **2015**, *77*, 5–15.
2. Ahmed, M.J.K.; Ahmaruzzaman, M. A review on potential usage of industrial waste materials for binding heavy metal ions from aqueous solutions. *J. Water Process Eng.* **2016**, *10*, 39–47.
3. Xu, J.; Jin, G.; Tang, H.; Mo, Y.; Wang, Y.-G.; Li, L. Response of water quality to land use and sewage outfalls in different seasons. *Sci. Total Environ.* **2019**, *696*, 134014.
4. Sajid, M.; Nazal, M.K.; Ihsanullah; Baig, N.; Osman, A.M. Removal of heavy metals and organic pollutants from water using dendritic polymers-based adsorbents: A critical review. *Sep. Purif. Technol.* **2018**, *191*, 400–423.
5. Couto, E.; Assemany, P.P.; Carneiro, G.C.A.; Soares, D.C.F. The potential of algae and aquatic macrophytes in the pharmaceutical and personal care products (PPCPs) environmental removal: A review. *Chemosphere* **2022**, *302*, 134808.
6. Yan, H.; Yan, Z.; Wang, L.; Hao, Z.; Huang, J. Toward understanding submersed macrophyte *Vallisneria natans*-microbe partnerships to improve remediation potential for PAH-contaminated sediment. *J. Hazard. Mater.* **2022**, *425*, 127767.
7. Hua, Z.; Li, X.; Zhang, J.; Gu, L. Removal potential of multiple perfluoroalkyl acids (PFAAs) by submerged macrophytes in aquatic environments: Tolerance of *Vallisneria natans* and PFAA removal in submerged macrophyte-microbiota systems. *J. Hazard. Mater.* **2021**, *424*, 127695.
8. Ogo, H.A.; Tang, N.; Li, X.; Gao, X.; Xing, W. Combined toxicity of microplastic and lead on submerged macrophytes. *Chemosphere* **2022**, *295*, 133956.
9. Alencar, B.T.B.; Ribeiro, V.H.V.; Cabral, C.M.; Santos, N.M.C.; Ferreira, E.A.; Francino, D.M.T.; Santos, J.B.; Silva, D.V.; Souza, M.F. Use of macrophytes to reduce the contamination of water resources by pesticides. *Ecol. Indic.* **2020**, *109*, 105785.
10. Tshithukhe, G.; Motitsoe, S.N.; Hill, M.P. Heavy Metals Assimilation by Native and Non-Native Aquatic Macrophyte Species: A Case Study of a River in the Eastern Cape Province of South Africa. *Plants* **2021**, *10*, 2676.
11. Geng, N.; Xia, Y.; Lu, D.; Bai, Y.; Zhao, Y.; Wang, H.; Ren, L.; Xu, C.; Hua, E.; Sun, G.; et al. The bacterial community structure in epiphytic biofilm on submerged macrophyte *Potamogetom crispus* L. and its contribution to heavy metal accumulation in an urban industrial area in Hangzhou. *J. Hazard. Mater.* **2022**, *430*, 128455.
12. Hadad, H.R.; Mufarrege, M.D.L.M.; Luca, G.A.D.; Denaro, A.C.; Nocetti, E.; Maine, M.A. Potential metal phytoremediation in peri-urban wetlands using rooted macrophytes. *Ecol. Eng.* **2022**, *182*, 106734.
13. Haghnazar, H.; Hudson-Edwards, K.A.; Kumar, V.; Pourakbar, M.; Mahdavianpour, M.; Aghayani, E. Potentially toxic elements contamination in surface sediment and indigenous aquatic macrophytes of the Bahmanshir River, Iran: Appraisal of phytoremediation capability. *Chemosphere* **2021**, *285*, 131446.
14. Heisi, H.D.; Awosusi, A.A.; Nkuna, R.; Matambo, T.S. Phytoextraction of anthropogenic heavy metal contamination of the Blesbokspruit wetland: Potential of wetland macrophytes. *J. Contam. Hydrol.* **2022**, 104101.https://doi.org/10.1016/j.jconhyd.2022.104101
15. Rai, P.K. Heavy metals/metalloids remediation from wastewater using free floating macrophytes of a natural wetland. *Environ. Technol. Innov.* **2019**, *15*, 100393.
16. Sattar, S.; Hussain, R.; Shah, S.M.; Bibi, S.; Ahmad, S.R.; Shahzad, A.; Zamir, A.; Rauf, Z.; Noshad, A.; Ahmad, L. Composition, impacts, and removal of liquid petroleum waste through bioremediation as an alternative clean-up technology: A review. *Heliyon* **2022**, *8*, e11101.
17. Timalsina, H.; Gyawali, T.; Ghimire, S.; Paudel, S.R. Potential application of enhanced phytoremediation for heavy metals treatment in Nepal. *Chemosphere* **2022**, *306*, 135581

18. Qing, X.; Yutong, Z.; Shenggao, L. Assessment of heavy metal pollution and human health risk in urban soils of steel industrial city (Anshan), Liaoning, Northeast China. *Ecotoxicol. Environ. Saf.* **2015**, *120*, 377–385.
19. Massoud, R.; Hadiani, M.R.; Hamzehlou, P.; Khosravi-Darani, K. Bioremediation of heavy metals in food industry: Application of *Saccharomyces cerevisiae*. *Electron. J. Biotechnol.* **2019**, *37*, 56–60.
20. Ansari, A.A.; Naeem, M.; Gill, S.S.; Alzuaibr, F.M. Phytoremediation of contaminated waters: An eco-friendly technology based on aquatic macrophytes application. *Egypt. J. Aquat. Res.* **2020**, *46*, 371–376.
21. Sudiarto, S.I.A.; Renggaman, A.; Choi, H.L. Floating aquatic plants for total nitrogen and phosphorus removal from treated swine wastewater and their biomass characteristics. *J. Environ. Manag.* **2019**, *231*, 763–769.
22. Ali, S.; Abbas, Z.; Rizwan, M.; Zaheer, I.E.; Yavaş, I.; Ünay, A.; Abdel-Daim, M.M.; Bin-Jumah, M.; Hasanuzzaman, M.; Kalderis, D. Application of floating aquatic plants in phytoremediation of heavy metals polluted water: A review. *Sustainability* **2020**, *12*, 1927.
23. Samal, K.; Kar, S.; Trivedi, S. Ecological floating bed (EFB) for decontamination of polluted water bodies: Design, mechanism and performance. *J. Environ. Manag.* **2019**, *251*, 109550.
24. Wang, W.; Wang, Y.; Sun, L.; Zheng, Y.; Zhao, J. Research and application status of ecological floating bed in eutrophic landscape water restoration. *Sci. Total Environ.* **2020**, *704*, 135434.
25. Kurniawan, S.B.; Ahmad, A.; Said, N.S.M.; Imron, M.F.; Abdullah, S.R.S.; Othman, A.R.; Purwanti, I.F.; Hasan, H.A. Macrophytes as wastewater treatment agents: Nutrient uptake and potential of produced biomass utilization toward circular economy initiatives. *Sci. Total Environ.* **2021**, *790*, 148219.
26. Hejna, M.; Gottardo, D.; Baldi, A.; Dell'Orto, V.; Cheli, F.; Zaninelli, M.; Rossi, L. Review: Nutritional ecology of heavy metals. *Animal* **2018**, *12*, 2156–2170.
27. Zhang, Y.; Long, C.; Hu, G.; Hong, S.; Su, Z.; Zhang, Q.; Zheng, P.; Wang, T.; Yu, S.; Ji, G. Two-week repair alleviates hexavalent chromium-induced hepatotoxicity, hepatic metabolic and gut microbial changes: A dynamic inhalation exposure model in male mice. *Sci. Total Environ.* **2023**, *857*, 159429.
28. Trzonkowska, L.; Leśniewska, B.; Godlewska-Żyłkiewicz, B. Development of Solid Phase Extraction Method Based on Ion Imprinted Polymer for Determination of Cr(III) Ions by ETAAS in Waters. *Water* **2022**, *14*, 529.
29. Brasil Conselho Nacional do Meio Ambiente—CONAMA. *Resolution No. 430, 13 May 2011*; It Provides for the Conditions and Patterns of Effluent Discharge, Complements and Amends Resolution No. 357 of 17 March 2005, of the National Council of the Environment—CONAMA; 2011; Published in the Diário Oficial da União—DOU No. 92; 2011; p. 89.Availabe online: http://www.ibama.gov.br/sophia/cnia/legislacao/CONAMA/RE0430-130511.PDF (acessed on 5 March 2021).
30. USEPA. United States Environmental Protection Agency. Aquatic Life Ambient Water Quality Criteria. 2006. Available online: https://www.epa.gov/wqc/national-recommended-water-quality-criteria-aquatic-life-criteria-table (accessed on5 March 2021).
31. Jin, G.; Zhang, Z.; Li, R.; Li, R.; Chen, C.; Tang, H.; Li, L.; Barry, D.A. Transport of zinc ions in the hyporheic zone: Experiments and simulations. *Adv. Water Res*. **2020**, *146*, 103775.
32. Kohzadi, S.; Shahmoradi, B.; Ghaderi, E.; Loqmani, H.; Maleki, A. Concentration, Source, and Potential Human Health Risk of Heavy Metals in the Commonly Consumed Medicinal Plants. *Biol. Trace Element Res.* **2019**, *187*, 41–50.
33. Zhang, T.; Ruan, J.; Zhang, B.; Lu, S.; Gao, C.; Huang, L.; Bai, X.; Xie, L.; Gui, M.; Qiu, R.-L. Heavy metals in human urine, foods and drinking water from an e-waste dismantling area: Identification of exposure sources and metal-induced health risk. *Ecotoxicol. Environ. Saf.* **2019**, *169*, 707–713.
34. Renieri, E.A.; Safenkova, I.V.; Alegakis, A.K.; Slutskaya, E.S.; Kokaraki, V.; Kentouri, M.; Dzantiev, B.B.; Tsatsakis, A.M. Cadmium, lead and mercury in muscle tissue of gilthead seabream and seabass: Risk evaluation for consumers. *Food Chem. Toxicol.* **2019**, *124*, 439–449.
35. WHO. *Guidelines for Drinking-Water Quality*; World Health Organization: Geneva, Switzerland, 2011.
36. Thakur, S.; Singh, L.; Wahid, Z.A.; Siddiqui, M.F.; Atnaw, S.M.; Din, M.F.M. Plant-driven removal of heavy metals from soil: Uptake, translocation, tolerance mechanism, challenges, and future perspectives. *Environ. Monit. Assess.* **2016**, *188*, 206.
37. Ali, F.; Jilani, G.; Fahim, R.; Bai, L.; Wang, C.; Tian, L.; Jiang, H. Functional and structural roles of wiry and sturdy rooted emerged macrophytes root functional traits in the abatement of nutrients and metals. *J. Environ. Manag.* **2019**, *249*, 109330.
38. Wang, J.; Wang, W.; Xiong, J.; Li, L.; Zhao, B.; Sohail, I.; He, Z. A constructed wetland system with aquatic macrophytes for cleaning contaminated runoff/storm water from urban area in Florida. *J. Environ. Manag*. **2021**, *280*, 111794.
39. Zhao, Z.; Qin, Z.; Xia, L.; Zhang, D.; Hussain, J. Dissipation characteristics of pyrene and ecological contribution of submerged macrophytes and their biofilms-leaves in constructed wetland. *Bioresour. Technol.* **2018**, *267*, 158–166.
40. Lucke, T.; Walker, C.; Beecham, S. Experimental designs of field-based constructed floating wetland studies: A review. *Sci. Total Environ.* **2019**, *660*, 199–208.
41. Bonanno, G.; Vymazal, J.; Cirelli, G.L. Translocation, accumulation and bioindication of trace elements in wetland plants. *Sci. Total Environ.* **2018**, *631–632*, 252–261.
42. Nguyen, T.Q.; Sesin, V.; Kisiala, A.; Emery, R.J.N. Phytohormonal roles in plant responses to heavy metal stress: Implications for using macrophytes in phytoremediation of aquatic ecosystems. *Environ. Toxicol. Chem.* **2021**, *40*, 7–22.
43. Nascimento, C.W.A.D.; Biondi, C.M.; Silva, F.B.V.D.; Lima, L.H.V. Using plants to remediate or manage metal-polluted soils: An overview on the current state of phytotechnologies. *Acta Sci. Agron.* **2021**, *43*, e58283.

44. Oladoye, P.O.; Olowe, O.M.; Asemoloye, M.D. Phytoremediation technology and food security impacts of heavy metal contaminated soils: A review of literature. *Chemosphere* **2022**, *288*, 132555.
45. Muthusaravanan, S.; Sivarajasekar, N.; Vivek, J.S.; Paramasivan, T.; Naushad, M.; Prakashmaran, J.; Gayathri, V.; Al-Duaij, O.K. Phytoremediation of heavy metals: Mechanisms, methods and enhancements. *Environ. Chem. Lett.* **2018**, *16*, 1339–1359.
46. Khan, A.U.; Khan, A.N.; Waris, A.; Ilyas, M.; Zamel, D. Phytoremediation of pollutants from wastewater: A concise review. *Open Life Sci.* **2022**, *17*, 488–496.
47. Etesami, H. Bacterial mediated alleviation of heavy metal stress and decreased accumulation of metals in plant tissues: Mechanisms and future prospects. *Ecotoxicol. Environ. Saf.* **2018**, *147*, 175–191.
48. Kapoor, D.; Singh, S.; Kumar, V.; Romero, R.; Prasad, R.; Singh, J. Antioxidant enzymes regulation in plants in reference to reactive oxygen species (ROS) and reactive nitrogen species (RNS). *Plant Gene* **2019**, *19*, 100182.
49. Clemente, R.; Arco-Lázaro, E.; Pardo, T.; Martín, I.; Sánchez-Guerrero, A.; Sevilla, F.; Bernal, M.P. Combination of soil organic and inorganic amendments help plants overcome trace element induced oxidative stress and allows phytostabilization. *Chemosphere* **2019**, *223*, 223–231.
50. Yilmaz, D.D.; Ercan, N.; Ercan, F.S. Heavy Metal-induced Oxidative Stress and DNA Damage as Shown by RAPD-PCR in Leaves of Elodea Canadensis. *Appl. Chem. Eng.* **2020**, *3*, 14–22
51. Yasin, N.A.; Khan, W.U.; Ahmad, S.R.; Ali, A.; Ahmed, S.; Ahmad, A. Effect of Bacillus fortis 162 on Growth, Oxidative Stress Tolerance and Phytoremediation Potential of Catharanthus roseus under Chromium Stress. *Int. J. Agric. Biol.* **2018**, *20*, 1513–1522.
52. Islam, F.; Yasmeen, T.; Ali, Q.; Ali, S.; Arif, M.S.; Hussain, S.; Rizvi, H. Influence of *Pseudomonas aeruginosa* as PGPR on oxidative stress tolerance in wheat under Zn stress. *Ecotoxicol. Environ. Saf.* **2014**, *104*, 285–293.
53. Rizwan, M.; Ali, S.; Rehman, M.Z.U.; Rinklebe, J.; Tsang, D.C.W.; Bashir, A.; Maqbool, A.; Tack, F.M.G.; Ok, Y.S. Cadmium phytoremediation potential of Brassica crop species: A review. *Sci. Total Environ.* **2018**, *631–632*, 1175–1191.
54. Bhagyawant, S.S.; Narvekar, D.T.; Gupta, N.; Bhadkaria, A.; Koul, K.K.; Srivastava, N. Variations in the antioxidant and free radical scavenging under induced heavy metal stress expressed as proline content in chickpea. *Physiol. Mol. Biol. Plants* **2019**, *25*, 683–696.
55. El-Khatib, A.A.; Youssef, N.A.; Barakat, N.A.; Samir, N.A. Responses of *Eucalyptus globulus* and *Ficus nitida* to different potential of heavy metal air pollution. *Int. J. Phytoremediation* **2020**, *22*, 986–999.
56. Kisa, D.; Elmastaş, M.; Öztürk, L.; Kayir, Ö. Responses of the phenolic compounds of *Zea* mays under heavy metal stress. *Appl. Biol. Chem.* **2016**, *59*, 813–820.
57. Manquián-Cerda, K.; Escudey, M.; Zúñiga, G.; Arancibia-Miranda, N.; Molina, M.; Cruces, E. Effect of cadmium on phenolic compounds, antioxidant enzyme activity and oxidative stress in blueberry (*Vaccinium corymbosum* L.) plantlets grown in vitro. *Ecotoxicol. Environ. Saf.* **2016**, *133*, 316–326.
58. Taie, H.A.A.; Seif El-Yazal, M.A.; Ahmed, S.M.A.; Rady, M.M. Polyamines modulate growth, antioxidant activity, and genomic DNA in heavy metal–stressed wheat plant. *Environ. Sci. Pollut. Res.* **2019**, *26*, 22338–22350.
59. Ghori, N.-H.; Ghori, T.; Hayat, M.; Imadi, S.; Gul, A.; Altay, V.; Ozturk, M. Heavy metal stress and responses in plants. *Int. J. Environ. Sci. Technol.* **2019**, *16*, 1807–1828.
60. Souza, V.L.; Silva, D.D.C.; Santana, K.B.; Mielke, M.S.; Almeida, A.-A.F.D.; Mangabeira, P.A.O.; Rocha, E.A. Efeitos do cádmio na anatomia e na fotossíntese de duas macrófitas aquáticas. *Acta Bot. Bras.* **2009**, *23*, 343–354.
61. He, L.; Su, R.; Chen, Y.; Zeng, P.; Du, L.; Cai, B.; Zhang, A.; Zhu, H. Integration of manganese accumulation, subcellular distribution, chemical forms, and physiological responses to understand manganese tolerance in Macleaya cordata. *Environ. Sci. Pollut. Res.* **2022**, *29*, 39017–39026.
62. Su, R.; Ou, Q.; Wang, H.; Luo, Y.; Dai, X.; Wang, Y.; Chen, Y.; Shi, L. Comparison of Phytoremediation Potential of Nerium indicum with Inorganic Modifier Calcium Carbonate and Organic Modifier Mushroom Residue to Lead–Zinc Tailings. *Int. J. Environ. Res. Public Health* **2022**, *19*, 10353.
63. Xin, J.; Ma, S.; Li, Y.; Zhao, C.; Tian, R. Pontederia cordata, an ornamental aquatic macrophyte with great potential in phytoremediation of heavy-metal-contaminated wetlands. *Ecotoxicol. Environ. Saf.* **2020**, *203*, 111024.
64. Costa, M.B.; Tavares, F.V.; Martinez, C.B.; Colares, I.G.; Martins, C.D.M.G. Accumulation and effects of copper on aquatic macrophytes *Potamogeton pectinatus* L.: Potential application to environmental monitoring and phytoremediation. *Ecotoxicol. Environ. Saf.* **2018**, *155*, 117–124.
65. Li, C.; Wang, M.; Luo, X.; Liang, L.; Han, X.; Lin, X. Accumulation and effects of uranium on aquatic macrophyte Nymphaea tetragona Georgi: Potential application to phytoremediation and environmental monitoring. *J. Environ. Radioact.* **2019**, *198*, 43–49.
66. Singh, H.; Kumar, D.; Soni, V. Copper and mercury induced oxidative stresses and antioxidant responses of *Spirodela polyrhiza* (L.) Schleid. *Biochem. Biophys. Rep.* **2020**, *23*, 100781.
67. Ayangbenro, A.S.; Babalola, O.O. A New Strategy for Heavy Metal Polluted Environments: A Review of Microbial Biosorbents. *Int. J. Environ. Res. Public Health* **2017**, *14*, 94.

68. Cai, X.; Zheng, X.; Zhang, D.; Iqbal, W.; Liu, C.; Yang, B.; Zhao, X.; Lu, X.; Mao, Y. Microbial characterization of heavy metal resistant bacterial strains isolated from an electroplating wastewater treatment plant. *Ecotoxicol. Environ. Saf.* **2019**, *181*, 472–480.
69. Yang, J.; Wei, W.; Pi, S.; Ma, F.; Li, A.; Wu, D.; Xing, J. Competitive adsorption of heavy metals by extracellular polymeric substances extracted from *Klebsiella* sp. J1. *Bioresour. Technol.* **2015**, *196*, 533–539.
70. Verma, S.; Kuila, A. Bioremediation of heavy metals by microbial process. *Environ. Technol. Innov.* **2019**, *14*, 100369.
71. Gupta, A.; Joia, J.; Sood, A.; Sood, R.; Sidhu, Y.; Kaur, G. Microbes as Potential Tool for Remediation of Heavy Metals: A Review. *J. Microb. Biochem. Technol.* **2016**, *8*, 364–372.
72. Kaplan, H.; Ratering, S.; Felix-Henningsen, P.; Schnell, S. Stability of in situ immobilization of trace metals with different amendments revealed by microbial 13C-labelled wheat root decomposition and efflux-mediated metal resistance of soil bacteria. *Sci. Total Environ.* **2019**, *659*, 1082–1089.
73. Yin, K.; Wang, Q.; Lv, M.; Chen, L. Microorganism remediation strategies towards heavy metals. *Chem. Eng. J.* **2019**, *360*, 1553–1563.
74. Calvo, J.; Jung, H.; Meloni, G. Copper metallothioneins. *IUBMB Life* **2017**, *69*, 236–245.
75. Liu, S.-H.; Zeng, G.-M.; Niu, Q.-Y.; Liu, Y.; Zhou, L.; Jiang, L.-H.; Tan, X.-F.; Xu, P.; Zhang, C.; Cheng, M. Bioremediation mechanisms of combined pollution of PAHs and heavy metals by bacteria and fungi: A mini review. *Bioresour. Technol.* **2017**, *224*, 25–33.
76. Kolaj-Robin, O.; Russell, D.; Hayes, K.A.; Pembroke, J.T.; Soulimane, T. Cation Diffusion Facilitator family: Structure and function. *FEBS Lett.* **2015**, *589*, 1283–1295.
77. Shahid, M.J.; Ali, S.; Shabir, G.; Siddique, M.; Rizwan, M.; Seleiman, M.F.; Afzal, M. Comparing the performance of four macrophytes in bacterial assisted floating treatment wetlands for the removal of trace metals (Fe, Mn, Ni, Pb, and Cr) from polluted river water. *Chemosphere* **2020**, *243*, 125353.
78. Lu, Y.; Kronzucker, H.J.; Shi, W. Stigmasterol root exudation arising from Pseudomonas inoculation of the duckweed rhizosphere enhances nitrogen removal from polluted waters. *Environ. Pollut.* **2021**, *287*, 117587.
79. Chang, Y.; Cui, H.; Huang, M.; He, Y. Artificial floating islands for water quality improvement. *Environ. Rev.* **2017**, *25*, 350–357.
80. Yeh, N.; Yeh, P.; Chang, Y.-H. Artificial floating islands for environmental improvement. *Renew. Sustain. Energy Rev.* **2015**, *47*, 616–622.
81. Benvenuti, T.; Hamerski, F.; Giacobbo, A.; Bernardes, A.M.; Zoppas-Ferreira, J.; Rodrigues, M.A.S. Constructed floating wetland for the treatment of domestic sewage: A real-scale study. *J. Environ. Chem. Eng.* **2018**, *6*, 5706–5711.
82. Lu, B.; Xu, Z.; Li, J.; Chai, X. Removal of water nutrients by different aquatic plant species: An alternative way to remediate polluted rural rivers. *Ecol. Eng.* **2018**, *110*, 18–26.
83. Pavlineri, N.; Skoulikidis, N.T.; Tsihrintzis, V.A. Constructed Floating Wetlands: A review of research, design, operation and management aspects, and data meta-analysis. *Chem. Eng. J.* **2017**, *308*, 1120–1132.
84. Shen, C.; Zhao, Y.Q.; Liu, R.B.; Morgan, D.; Wei, T. Enhancing wastewater remediation by drinking water treatment residual-augmented floating treatment wetlands. *Sci. Total Environ.* **2019**, *673*, 230–236.
85. Zhao, F.; Xi, S.; Yang, X.; Yang, W.; Li, J.; Gu, B.; He, Z. Purifying eutrophic river waters with integrated floating island systems. *Ecol. Eng.* **2012**, *40*, 53–60.
86. Bi, R.; Zhou, C.; Jia, Y.; Wang, S.; Li, P.; Reichwaldt, E.S.; Liu, W. Giving waterbodies the treatment they need: A critical review of the application of constructed floating wetlands. *J. Environ. Manag.* **2019**, *238*, 484–498.
87. Dean, S.; Akhtar, M.S.; Ditta, A.; Valipour, M.; Aslam, S. Microcosm Study on the Potential of Aquatic Macrophytes for Phytoremediation of Phosphorus-Induced Eutrophication. *Sustainability* **2022**, *14*, 16415.
88. Xu, L.; Chen, S.; Zhuang, P.; Xie, D.; Yu, X.; Liu, D.; Li, Z.; Qin, X.; Wang, F.; Xing, F. Purification Efficiency of Three Combinations of Native Aquatic Macrophytes in Artificial Wastewater in Autumn. *Int. J. Environ. Res. Public Health* **2021**, *18*, 6162.
89. Zhu, L.; Li, Z.; Ketola, T. Biomass accumulations and nutrient uptake of plants cultivated on artificial floating beds in China's rural area. *Ecol. Eng.* **2011**, *37*, 1460–1466.
90. De Stefani, G.; Tocchetto, D.; Salvato, M.; Borin, M. Performance of a floating treatment wetland for in-stream water amelioration in NE Italy. *Hydrobiologia* **2011**, *674*, 157–167.
91. Tanner, C.C.; Headley, T.R. Components of floating emergent macrophyte treatment wetlands influencing removal of stormwater pollutants. *Ecol. Eng.* **2011**, *37*, 474–486.
92. Zhang, C.-B.; Liu, W.-L.; Pan, X.-C.; Guan, M.; Liu, S.-Y.; Ge, Y.; Chang, J. Comparison of effects of plant and biofilm bacterial community parameters on removal performances of pollutants in floating island systems. *Ecol. Eng.* **2014**, *73*, 58–63.
93. Ladislas, S.; Gérente, C.; Chazarenc, F.; Brisson, J.; Andrès, Y. Performances of Two Macrophytes Species in Floating Treatment Wetlands for Cadmium, Nickel, and Zinc Removal from Urban Stormwater Runoff. *Water Air Soil Pollut.* **2013**, *224*, 1408.
94. Wang, C.-Y.; Sample, D.J. Assessment of the nutrient removal effectiveness of floating treatment wetlands applied to urban retention ponds. *J. Environ. Manag.* **2014**, *137*, 23–35.

95. Liu, Z.; Lu, B.; He, B.; Li, X.; Wang, L.-A. Effect of the pyrolysis duration and the addition of zeolite powder on the leaching toxicity of copper and cadmium in biochar produced from four different aquatic plants. *Ecotoxicol. Environ. Saf.* **2019**, *183*, 109517.
96. Huang, H.; Yao, W.; Li, R.; Ali, A.; Du, J.; Guo, D.; Xiao, R.; Guo, Z.; Zhang, Z.; Awasthi, M.K. Effect of pyrolysis temperature on chemical form, behavior and environmental risk of Zn, Pb, and Cd in biochar produced from phytoremediation residue. *Bioresour. Technol.* **2018**, *249*, 487–493.
97. Zhou, J.; Chen, L.H.; Peng, L.; Luo, S.; Zeng, Q.R. Phytoremediation of heavy metals under an oil crop rotation and treatment of biochar from contaminated biomass for safe use. *Chemosphere* **2020**, *247*, 125856.
98. Andreazza, R.; Okeke, B.C.; Pieniz, S.; Bortolon, L.; Lambais, M.R.; Camargo, F.A.O. Effects of Stimulation of Copper Bioleaching on Microbial Community in Vineyard Soil and Copper Mining Waste. *Biol. Trace Elem. Res.* **2012**, *146*, 124–133.
99. Santos, V.M.; Andrade, L.C.; Tiecher, T.; Andreazza, R.; Camargo, F.A.O. Phytoremediation of metals by colonizing plants developed in point bars in the channeled bed of the Dilúvio Stream, Southern Brazil. *Int. J. Phytoremediation* **2021**, *24*, 59–65.
100. Silva, A.S.; Jacques, R.J.S.; Andreazza, R.; Bento, F.M.; Roesch, L.F.W.; Camargo, F.A.O. Properties of catechol 1,2-dioxygenase in the cell free extract and immobilized extract of Mycobacterium fortuitum. *Braz. J. Microbiol.* **2013**, *44*, 291–297.
101. Meyer, D.D.; Beker, S.A.; Bücker, F.; Peralba, M.C.R.; Frazzon, A.P.G.; Osti, J.F.; Andreazza, R.; Camargo, F.A.O.; Bento, F.M. Bioremediation strategies for diesel and biodiesel in oxisol from southern Brazil. *Int. Biodeterior. Biodegrad.* **2014**, *95*, 356–363.
102. Colla, T.S.; Andreazza, R.; Bücker, F.; Souza, M.M.; Tramontini, L.; Prado, G.R.; Frazzon, A.P.G.; Camargo, F.A.O.; Bento, F.M. Bioremediation assessment of diesel–biodiesel-contaminated soil using an alternative bioaugmentation strategy. *Environ. Sci. Pollut. Res.* **2013**, *21*, 2592–2602.
103. Tufail, M.A.; Iltaf, J.; Zaheer, T.; Tariq, L.; Amir, M.B.; Fatima, R.; Asbat, A.; Kabeer, T.; Fahad, M.; Naeem, H.; et al. Recent advances in bioremediation of heavy metals and persistent organic pollutants: A review. *Sci. Total Environ.* **2022**, *850*, 157961.
104. Dash, D.M.; Osborne, W.J. A systematic review on the implementation of advanced and evolutionary biotechnological tools for efficient bioremediation of organophosphorus pesticides. *Chemosphere* **2023**, *313*, 137506.
105. Shen, X.; Dai, M.; Yang, J.; Sun, L.; Tan, X.; Peng, C.; Ali, I.; Naz, I. A critical review on the phytoremediation of heavy metals from environment: Performance and challenges. *Chemosphere* **2021**, *291*, 132979.
106. Andreazza, R.; Okeke, B.C.; Pieniz, S.; Camargo, F.A.O. Characterization of Copper-Resistant Rhizosphere Bacteria from Avena sativa and Plantago lanceolata for Copper Bioreduction and Biosorption. *Biol. Trace Elem. Res*. **2011**, *146*, 107–115.

5 Artigo 2

O artigo intitulado “**Potential Phytoremediation of Aquatic Macrophyte Species for Heavy Metals in Urban Environments in the Southern Area of Brazil”** é apresentado conforme publicado na Revista Sustainability, ISSN: 2071-1050, fator de impacto 3.889, classificação A2 na área de Materiais, tendo sido aceito em 23 de Dezembro de 2022.

sustainability

MDPI

Article

Potential Phytoremediation of Aquatic Macrophyte Species for Heavy Metals in Urban Environments in the Southern Area of Brazil

Carolina Faccio Demarco [1], Thays França Afonso [1], Simone Pieniz [2], Filipe Carlos Selau [3], Fernando Machado Machado [1] and Robson Andreazza [1,*]

[1]Center of Engineering, Graduate Program of Science and Materials Engineering, Federal University of Pelotas,Pelotas 96015-560, Rio Grande do Sul, Brazil
[2]Faculty of Nutrition, Federal University of Pelotas, Pelotas 96015-560, Rio Grande do Sul, Brazil
[3]Faculty of Agronomy, Federal University of Pelotas, Pelotas 96015-560, Rio Grande do Sul, Brazil
*Correspondence: robsonandreazza@yahoo.com.br; Tel.: +55-53-3921-1432

Abstract: This research investigated four different species of aquatic macrophytes with natural occurrence in an urban environment highly anthropized in Southern Brazil. The aim of the research was to compare the phytoremediation potential among the species *E. anagallis*, *H. grumosa*, *H. ranunculoides*, and *S. montevidensis* through Pearson´s correlation analysis and cluster analysis, using the heavy metal content identified through HNO_3 - $HClO_4$ and phytoremediation indexes. The results highlighted the bioconcentration factor (BCF) of *H. ranunculoides*, with outstanding results for Cu BCF = 667.09, Zn BCF = 149.93, Cd BCF = 26.85, Cr BCF = 31.77, Ni BCF = 35.47, and Pb BCF= 126.29. Additionally, *H. grumosa* and *S. montevidensis* were also highlighted, considering the potential phytoremoval (g ha^{-1}). Therefore, this study demonstrates the tolerance and potential for removal of heavy metals Cu, Cr, Cd, Pb, Ni, and Zn by the evaluated aquatic macrophyte species and elucidates the outstanding potential of application in phytoremediation purposes.

Citation: Demarco, C.F.; Afonso, T.F.; Pieniz, S.; Selau, F.C.; Machado, F.M.; Andreazza, R. Potential Phytoremediation of Aquatic Macrophyte Species for Heavy Metals in Urban Environments in theSouthern Area of Brazil. *Sustainability***2023**, *15*, 419. https://doi.org/10.3390/su15010419

Academic Editor: Alberto Ferraro

Received: 1 December 2022
Revised: 22 December 2022
Accepted: 23 December 2022
Published: 27 December 2022

Keywords: anthropogenic pollution; degraded areas; bioremediation; in situ removal of heavy metals;phytofiltration; aquatic macrophytes; phytoremediation application and urbanization

1. Introduction

The urbanization and industrialization processes within cities contribute to the release of contaminants into aquatic and terrestrial ecosystems. The contaminants reaching the aquatic environments are responsible for an increase in both sediments and water in these areas. In urban locations, the pollutants reach aquatic environments through rainfall runoffsthat carry different loadings depending on the area and land use. Residential areas can contribute to nitrogen and phosphorous loadings, as well as domestic sewage, along with industrial wastewater discharges with high levels of heavy metals [1]. Additionally, means of transport are a source of heavy metals, hydrocarbons, sulfur, oil, and grease [2].

Among the contaminants, the presence of heavy metals in watercourses represents a threat considering the bioaccumulation properties in the food chain and risks to environment, animals, fish, plants, and population health. General consequences of heavy metal in excess are damage to the kidneys and bones, endocrine, cardiovascular, and neurological problems, in addition to potentiating the development of cancer [3].

The entrance of heavy metals into organisms can occur due to invertebrates which absorb levels of these elements and are a food source for fish and other aquatic species. Another route is immediate absorption via water, or even via sediment deposition—which is the first location for heavy-metal accumulation in aquatic environments [4].

In Brazil, the origin of most heavy-metal content in excess is due to mining activities, along with untreated effluent discharges from agricultural, industrial, and urban areas [5].

The Santa Bárbara Stream is an important watercourse for the municipality of Pelotas/RS, south Brazil, being responsible for the water supply of most parts of this city. The presence of aquatic macrophytes is widely noticed in the area, along with a smell and foam also present, indicating a possible eutrophication condition and highlighting the polluted condition of the area [6].

Several conventional methods can be applied to remove heavy metals from these environments, such as chemical separation, dredging, and electro-oxidation [7]. However, there are some cost limitations and environmental issues that limit the wide application of these techniques. Phytoremediation is an alternative and innovative method, since the specificity of species and genotypes allows the removal of different pollutants [7,8]. However, the efficient application of phytoremediation techniques presents a straight relationship with the understanding of mechanisms in which the plants tolerate and bioaccumulate heavy metals, with attention to the limits of the toxic level. It is also important the understand how the elements are translocated in the plants [9].

Different mechanisms enable plants to accumulate heavy metals, nutrients, and other contaminants. For heavy-metal uptake, the plant performs intracellular accumulation, alteration of gene expression responsible for uptake of these elements, efflux, sequestration, and translocation [10,11]. Among phytoremediation techniques, there is: phytoextraction, the accumulation by the shoots of the plants; phytostabilization, with the immobilization of contaminants; phytodegradation, degradation through the metabolic process; rhizodegradation, degradation in the rhizosphere; phytovolatilization, elimination of contaminants through a transpiration process; and rhizofiltration, filtration in the rhizosphere area without translocation [12].

For the efficient application of phytoremediation, the first step is the screening and identification of plant species with the ability to tolerate the high levels of the selected pollutant. For this prospection of plants, the strategy of studying plants from contaminated areas is promising [13]. In addition, it is necessary to understand the main mechanism by which the plant removes the contaminant, its transport within the plant, and its tolerance, among other aspects, in order to exploit its full potential [14].

The identification of tolerant native species is essential for the proper application ofthe technique, and there are essential factors such as adaptation to local condition and competitions with invasive/exotic species [15]. Worldwide, researchers have been investigating different aquatic macrophyte species' potential for application in phytoremediation purposes, e.g., *Eichhornia*, *Lemna*, and *Azolla*, and in general, the requirements for the application are rapid growth and higher biomass production, along with tolerating higher levels of the selected contaminant [16].

Therefore, in this study, we propose the utilization of aquatic macrophyte species' characteristics of South America, i.e., *Enydra anagallis*, *Hydrocotyle ranunculoides*, *Hymenachne grumosa*, and *Sagittaria montevidensis*, for phytoremediation, as well as comparison of the potential of accumulating heavy metals of these plants. We then highlight their great potential for application in phytoremediation purposes, thus representing a sustainable alternative for decontamination of water and wastewater.

2. Materials and Methods

2.1 Study Area

The study area is located in the municipality of Pelotas/RS (31°45′43″ S and 52°21′00″ W), Brazil. The Santa Bárbara Stream is the principal watercourse from Santa Bárbara Subwatershed, with 30,000 m of total length, and presents importance for the city since it serves as a water source for a great part of the population [17]. The Stream has suffered changes in its drainage bed, along with the construction of a dam for public supply and the implementation of a flood protection system [18].

The current condition of degradation in the Santa Bárbara Stream begins with the expansion of urban areas and changes in the natural characteristics of the environment. Some aspects can be highlighted as the land use and occupation occurring in a disorderly

manner, the absence of a sanitary sewer system, resulting in the domestic and industrial release of contaminants, along with lack of environmental education [19].

2.2 Sampling Plants and Characterization

The collection of the emergent aquatic macrophytes (Figure 1) was performed in Santa Bárbara Stream, and the location (31°45′24.4″ S, 52°21′22.1″ W) was selected according to the presence of a large number of plants in the area, along with easy access to the riverbanks.The sampling occurred in the summer season, when presence of aquatic macrophytes is usually more visible, presenting the highest amount and diversity. The plants were sampled through the area and the biomass was placed in plastic bags and properly stored until in the laboratory. The plants (Table 1) were then washed and rinsed using distilled water to remove soil or sediment particles attached to plant biomass [20].

Figure 1. Studied aquatic macrophyte species: (**a**) Enydra anagallis; (**b**) Hydrocotyle ranunculoides; (**c**) Hymenachne grumosa; (**d**) Sagittaria montevidensis.

Table 1. Studied aquatic macrophyte species with family and common name, dry mass, and biomassproduction (ton ha^{-1}).

Species	Family	Common Name	Dry Mass (g)	Biomass Production (ton ha^{-1})
Enydra anagallis	Asteraceae	–	2.58	0.56
Hydrocotyle ranunculoides	Araliaceae	Floating pennywort	0.23	0.16
Hymenachne grumosa	Poaceae	Carnivão	11.69	2.92
Sagittaria montevidensis	Alismataceae	Giant arrowhead	20.04	3.20

2.3 Detection of Nutrients and Heavy-Metal Content

The roots were separated from the shoots of the plants and the different portions were dried until achieving constant mass (approximately 48 h at 60 ˚C), and subsequently ground.The ground material was used for 3:1 nitric-perchloric acid digestion (HNO_3-$HClO_4$) following the methodology described by Tedesco [20], with approximately 15 hours in HNO_3 and 5 hours in $HClO_4$. We used a Micro Tube Kjeldahl digester block (LUCADEMA, Luca-23/02, Brazil) in a gas exhaust housing (Ideoxima ORG.10, Brazil), and the element levels were detected with Inductively Coupled Plasma-Optical Emission Spectrometry (PerkinElmer®-Optima™ 8300 ICP-OES), at the Laboratory of Soil at the Federal University of Rio Grande do Sul (UFRGS). We used internal standards [21] for quality control with limits of detection (LoD) of Cu—0.6; Zn—2.0; Cd—0.2; Cr—0.4; Ni—0.4; Pb—2.0 mg kg^{-1}.

2.4 Indexes for Phytoremediation

The bioconcentration factor (BCF) and the translocation factor (TF) phytoremediation indexes were determined by applying Equations (1) and (2), respectively [22]:

$$BCF = \frac{\text{level in roots}}{\text{level in environment}} \quad (1)$$

$$TF = \frac{\text{level in shoots}}{\text{level in roots}} \quad (2)$$

where levels in roots refer to the concentration determined in the roots of the plants, in mg kg^{-1}, the level in the environment refers to the concentration of the element in water (mg L^{-1}), and the level in shoots refers to the concentration of the element in the shoots of the plants (mg kg^{-1})—aerial biomass.

In addition, we calculated the phytoremediation potential, in g ha^{-1}. For this, firstly, we estimated the biomass production (Table 2) for each species, obtained from the area occupied by one plant and its total dry weight. Secondly, the phytoremoval potential was calculated bymultiplying the biomass production by the total element levels (total mg kg^{-1}).

Table 2. Reference values for general plants (in mg kg^{-1} dry mass, according with Kabata-Pendias and Pendias [23] and Hopkins [24] and total levels found in the aquatic macrophyte species, in mg kg $^{-1}$.

Sufficient Level		Toxic Level	*H. gruMosa*	*H. ranun-culoides*	*S. Montevi-densis*	*E. anagallis*
----------mg kg^{-1}----------						
Cu	5–30 [23]	20–100 [23]	42.29	236.83	145.39	125.61
Zn	27–150 [23]	100–400 [23]	298.13	373.74	235.16	205.55
Cd	0.05–0.2 [23]	5–30 [23]	0.64	0.75	0.55	1.28
Cr	0.1–0.5 [23]	5–30 [23]	21.28	179.34	22.55	59.77
Ni	0.1–5 [23]	10–100 [23]	13.37	83.44	13.17	34.66
Pb	5–10 [23]	30–300 [23]	22.76	33.37	13.75	25.76

Table 2. *Cont.*

Sufficient Level		Toxic Level	*H. gruMosa*	*H. ranunculoides*	*S. Montevidensis*	*E. anagallis*
mmol kg^{-1}			g kg^{-1}			
P	60 [24]	-	7.23	17.05	11.63	10.64
K	250 [24]	-	15.32	35.34	28.65	29.15
Ca	125 [24]	-	13.48	25.9	20.6	20.85
Mg	80 [24]	-	4.47	8.9	8.35	6.5
S	30 [24]	-	6.81	10.17	6.31	7.1

2.5 Statistical Analysis

The experimental data were analyzed using the Statistica®software program, v. 7.0. A Pearson's analysis of correlation was run, along with cluster analysis (CA) using Ward's linkage method based on the Euclidean distance, which produced a dendrogram with well-defined clusters.

3. Results

3.1 Total Content of Heavy Metals

Some guidelines values established by Kabata-Pendias and Pendias [23] described the usual/sufficient values and toxic/exceeding levels for general plants and were used as a comparative (Table 2). *H. grumosa* exceeded the sufficient levels for Cu (42.29 mg kg^{-1}), Zn (298.13 mg kg^{-1}), Cd (0.64 mg kg^{-1}), Cr (21.28 mg kg^{-1}), Ni (13.37 mg kg^{-1}), and Pb (22.76 mg kg^{-1}), presenting then total values that were between the toxic ranges, excepting Cd and Pb. Adapted from Demarco et al. [25]; Demarco et al. [26]; Demarco et al. [6].

The *H. ranunculoides* species was detected with copper levels up to two-fold higher than the highest toxic limit of 100 mg kg^{-1}. Another outstanding ability detected for *H. ranunculoides* was the chromium total levels reaching almost six-fold higher than the highest toxic limit of 30 mg kg^{-1}.

The species *S. montevidensis* was highlighted for copper total levels (145.39 mg kg^{-1}), exceeding the toxic range for general plant species. This aquatic macrophyte presented Zn, Cr, and Ni levels standing among the toxic/exceeding levels for general plants. These results for *S. montevidensis* can be pointed out as demonstrating the plant with great capacity of tolerance for these toxic metals. *S. montevidensis* Cd and Pb levels were above sufficient. It might be mentioned that both heavy metals Cd and Pb are known for their lack in terms of biological function in plants and their toxic effects as oxidative stress [27]. Finally, *E. anagallis* presented Cu and Cr exceeding the toxic levels, with values of 125.61 mg kg^{-1} and 59.77 mg kg^{-1}. Zn and Ni stayed among the toxic range.

3.2 Correlation Analysis

The correlation in *H. grumosa* regarding total levels of macronutrients and heavy metals is shown in Table 3, which the strong positive correlation between K and Cu (r = 0.97), Kand Ni (r = 0.96), S and Zn (r = 0.90), Cu and Ni (r = 0.92), and Cr and Pb (r = 0.99).

Table 3. Correlation analysis in *H. grumosa* regarding total levels of macronutrients and heavy metals.

	P	K	Ca	Mg	S	Cu	Zn	Cd	Cr	Ni	Pb
P	1.00										
K	−0.04	1.00									
Ca	0.21	−0.12	1.00								
Mg	0.80	0.51	0.17	1.00							
S	0.43	0.85	0.13	0.77	1.00						
Cu	−0.12	0.97	−0.27	0.37	0.80	1.00					
Zn	0.44	0.83	0.21	0.88	0.90	0.70	1.00				

Table 3. *Cont.*

	P	K	Ca	Mg	S	Cu	Zn	Cd	Cr	Ni	Pb
Cd	0.12	0.70	−0.73	0.42	0.56	0.77	0.48	1.00			
Cr	0.67	0.04	−0.19	0.71	0.16	−0.08	0.42	0.34	1.00		
Ni	0.15	0.96	-0.20	0.67	0.86	0.92	0.89	0.78	0.29	1.00	
Pb	0.73	−0.08	−0.06	0.70	0.10	−0.21	0.37	0.19	0.99	0.17	1.00

In the case of *H. ranunculoides* (Table 4), the highlighted positive correlation was among Cu and Zn (r = 0.99) and Cr and Ni (r = 0.99).

Table 4. Correlation analysis in *H. ranunculoides* regarding total levels of macronutrients and heavy metals.

	P	K	Ca	Mg	S	Cu	Zn	Cd	Cr	Ni	Pb
P	1.00										
K	0.12	1.00									
Ca	−0.17	0.06	1.00								
Mg	- 0.62	-0.07	0.87	1.00							
S	0.71	0.62	−0.17	−0.47	1.00						
Cu	0.42	−0.42	0.19	−0.11	−0.19	1.00					
Zn	0.39	−0.36	0.30	0.00	−0.18	0.99	1.00				
Cd	−0.84	0.10	0.64	0.89	−0.54	−0.24	−0.14	1.00			
Cr	−0.68	0.34	0.39	0.61	−0.15	−0.32	−0.22	0.82	1.00		
Ni	−0.61	0.33	0.40	0.57	−0.14	−0.19	−0.09	0.78	0.99	1.00	
Pb	−0.08	0.38	0.81	0.66	0.15	0.16	0.28	0.58	0.61	0.66	1.00

The *S. montevidensis* correlation matrix (Table 5) showed a strong positive correlation of P and Ca (r = 0.91), P and S (r = 0.94), P and Cr (r = 0.93), K and Cu (r = 0.99), K and Zn (r = 0.96), K and Cd (r = 0.96), Ca and S (r = 0.99), Ca and Cr (r = 0.95), S and Cr (r = 0.99), Cu and Zn (r = 0.99), Cu and Cd (r = 0.99), and Zn and Cd (r = 0.99). Thus, it might be mentioned that, unlike the other species, *S. montevidensis* demonstrated that heavy-metal uptake strongly correlated with nutrient uptake.

Table 5. Correlation analysis in *S. montevidensis* regarding total levels of macronutrients and heavy metals.

	P	K	Ca	Mg	S	Cu	Zn	Cd	Cr	Ni	Pb
P	1.00										
K	−0.98	1.00									
Ca	0.91	−0.96	1.00								
Mg	−0.65	0.78	−0.88	1.00							
S	0.94	−0.98	0.99	−0.87	1.00						
Cu	−1.00	0.99	−0.92	0.68	−0.95	1.00					
Zn	−0.99	0.96	−0.85	0.59	−0.89	0.99	1.00				
Cd	−0.99	0.96	−0.87	0.57	−0.90	0.99	0.99	1.00			
Cr	0.93	−0.98	0.95	−0.86	0.99	−0.95	−0.91	−0.89	1.00		
Ni	−0.29	0.16	−0.07	−0.39	−0.03	0.26	0.28	0.40	0.06	1.00	
Pb	−0.30	0.37	−0.55	0.43	−0.43	0.32	0.17	0.32	−0.27	0.37	1.00

It can be seen that *E. anagallis* demonstrated a strong positive correlation among P and Ca (r = 0.92), P and S (r = 0.96), P and Cd (r = 0.93), Ca and S (r = 0.90), S and Cd (r = 0.96),Cu and Zn (r = 0.93), Zn and Pb (r = 0.96), and Cr and Ni (r = 0.93) (Table 6).

Table 6. Correlation analysis in *E. anagallis* regarding total levels of macronutrients and heavy metals.

P		K	Ca	Mg	S	Cu	Zn	Cd	Cr	Ni	Pb
P	1.00										
K	−0.40	1.00									
Ca	0.92	−0.60	1.00								
Mg	−0.63	−0.34	−0.41	1.00							
S	0.96	−0.23	0.90	−0.75	1.00						
Cu	0.37	−0.25	0.52	0.19	0.37	1.00					
Zn	0.49	−0.60	0.69	0.26	0.42	0.93	1.00				
Cd	0.93	−0.17	0.87	−0.64	0.96	0.58	0.57	1.00			
Cr	−0.10	0.81	−0.15	−0.46	0.15	0.13	−0.19	0.22	1.00		
Ni	−0.47	0.87	−0.48	−0.17	−0.23	−0.01	−0.34	−0.15	0.93	1.00	
Pb	0.57	−0.78	0.79	0.22	0.48	0.79	0.96	0.56	−0.36	−0.52	1.00

3.3 Phytoremediation Evaluation by Cluster Analysis

The phytoremediation indexes calculated allowed comparison between the plants for removing the toxic metals from Santa Bárbara Stream. Generally, the elements were grouped by BCF in two main groups (Figure 2a), one composed of Ca, Pb, K, and Cd, and the other presenting Ni, Cr, Zn, S, Mg, P, and Cu. *H. ranunculoides* has been classified separately from other species regarding BCF (Figure 2b). This species presented outstandingresults for the studied heavy metals: Cu BCF = 667.09, Zn BCF = 149.93, Cd BCF = 26.85, Cr BCF = 31.77, Ni BCF = 35.47, and Pb BCF = 126.29 [25].

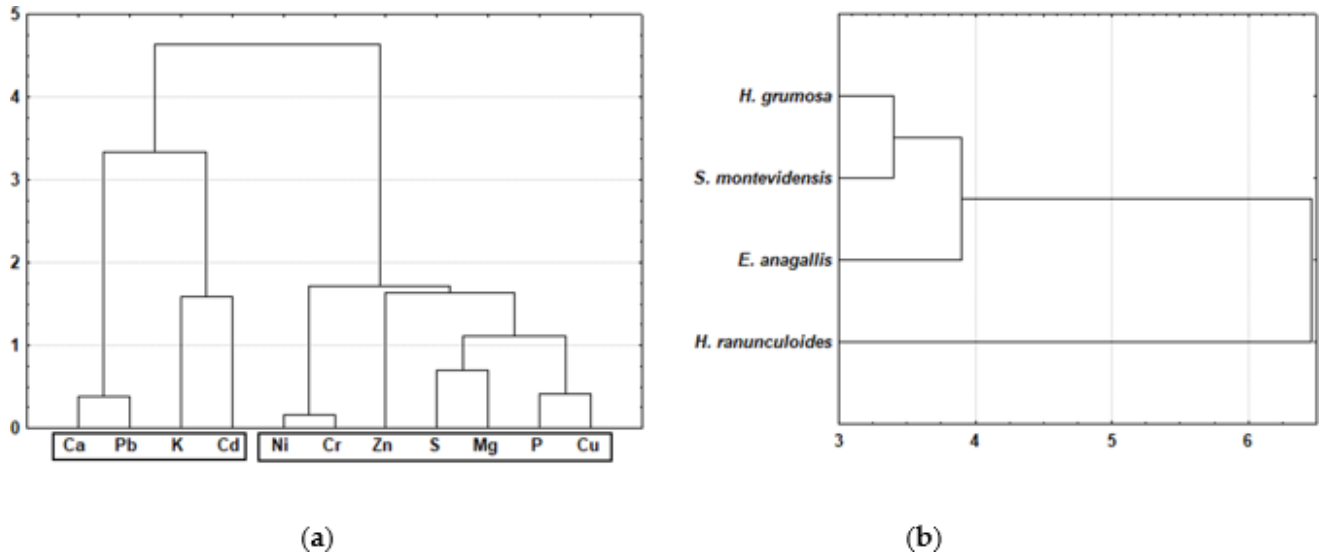

Figure 2. Dendrogram of heavy-metal and nutrient phytoremediation index BCF, demonstrating theclustering regarding (**a**) elements and (**b**) species categorization.

The cluster analysis regarding TF by element demonstrated two main groups, the first composed of Mg, Cd, Ni, S, P, K, and Zn, and the other by Ca, Cr, Pb, and Cu (Figure 3a). Plants with TF > 1.0 present the ability to translocate the element to the shoot's tissues [22]. Therefore, when BCF > 1.0 and TF > 1.0, the mechanism performed is then known as phytoextraction. *S. montevidensis* and *H. ranunculoides* were grouped in Figure 3b regarding phytoremediation index TF. This fact may be justified by the characteristic of *S. montevidensis* and *H. ranunculoides* being identified as presenting the ability of maintaining high levels of elements mainly in their roots, since TF < 1.0. Therefore, phytoremediation mechanism performed by *S. montevidensis* and *H. ranunculoides* for Zn, Cu, Cr, Cd, Ni, and Pb is rhizofiltration.

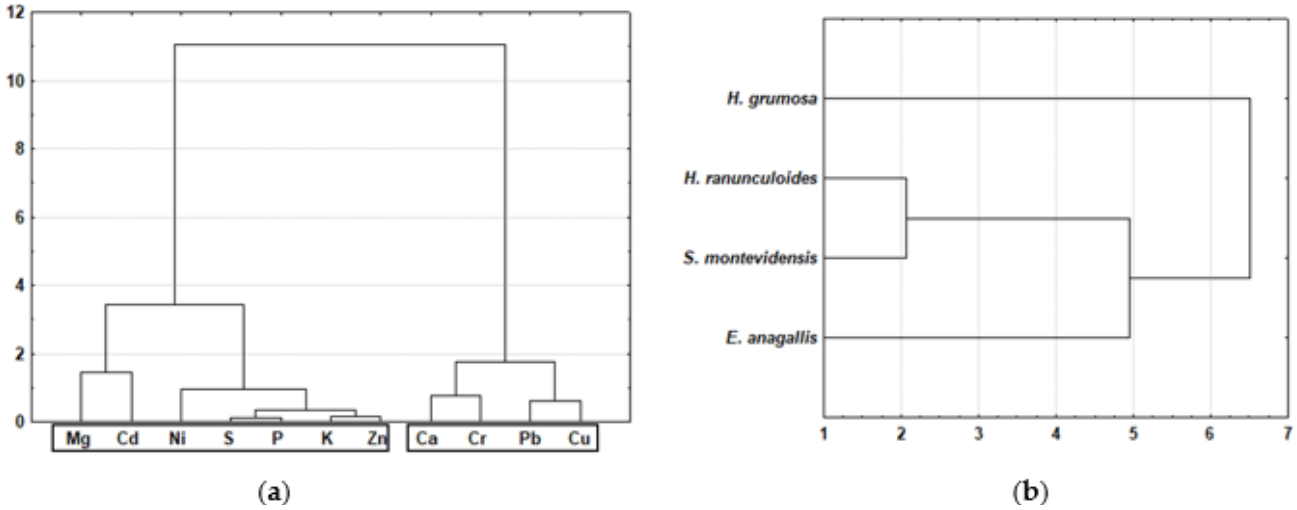

Figure 3. Dendrogram of heavy-metal and nutrient phytoremediation index TF, demonstrating the clustering regarding (**a**) elements and (**b**) species categorization.

The evaluation of phytoremoval potential was performed, aiming at the identification of the most promising plant species for application in phytoremediation technique, considering biomass production for removal estimation. The cluster analysis regarding phytoremoval potential by element demonstrated the formation of two groups, the first with the elements Cd, Pb, Zn, Cr, Ni, and S, and the second with Cu, Mg, K, Ca, and P (Figure 4a).

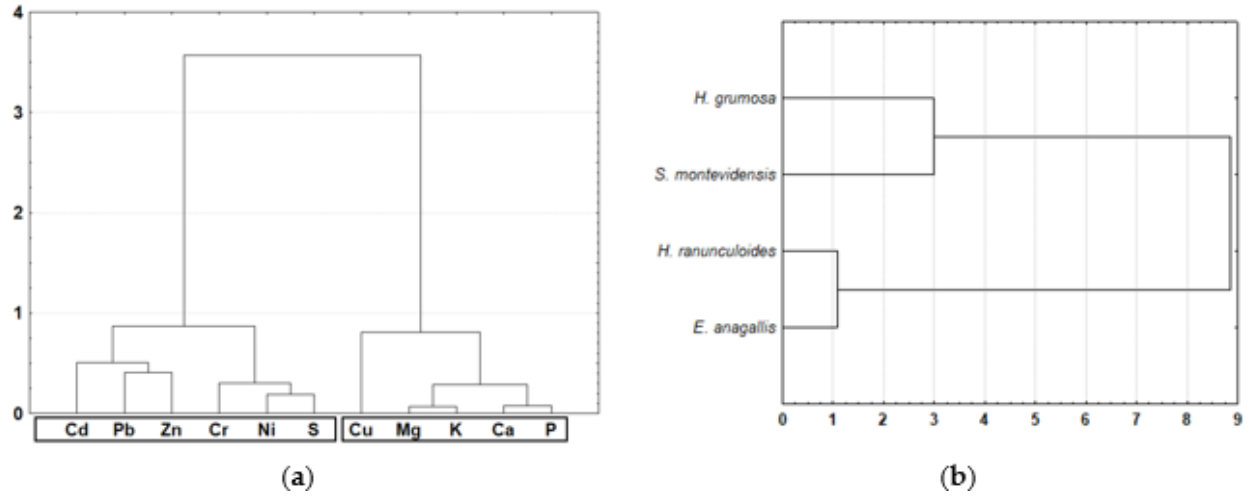

Figure 4. Dendrogram of in situ phytoremoval potential identified in the different aquatic macrophytes, demonstrating the clustering regarding (**a**) heavy metals and nutrients, and (**b**) species categorization.

Both *H. grumosa* and *S. montevidensis* were grouped (Figure 3b), considering the outstanding potential found. It should be emphasized that *H. grumosa* presented great results for all the studied heavy metals, reaching values of 871.29 g ha^{-1} for Zn. This was quite similar to the value estimated for Zn removal by *S. montevidensis*, which was 754.01 g ha^{-1}. In addition, *S. montevidensis* copper removal was detected at 466.20 g ha^{-1} and the results thus demonstrated the high tolerance of *S. montevidensis* to zinc and copper levels. Among the species, *S. montevidensis* was also detected with the highest values of Cr and Ni, being 72.31 g ha^{-1} and 42.25 g ha^{-1}, respectively.

H. grumosa was also highlighted by Pb phytoremoval potential (66.52 g ha^{-1}) and Cd (1.89 g ha^{-1}). The Cd values, besides being less than the found for other heavy

metals, represent potential for phytoremediation of cadmium, considering its toxicity and consequent damage to human and animal health [28,29].

4. Discussion

The Cr values detected for *H. ranunculoides* were impressively higher than other studies investigating the potential of different plants bioaccumulating this heavy metal from natural environments. The study of Tiwari et al. [30] investigating the biofiltration of heavy metals by *Eichhornia crassipes* in a contaminated watercourse in Bhopal, India, detected maximum chromium levels of 10.1 mg kg^{-1}.

Regarding copper content, Melo et al. [31] studied the phytoremediation potential of spontaneous species in vineyard soils contaminated with copper and detected values in plants that were similar to those found in this study in *H. ranunculoides*. It was verified that, despite the study being performed in soil, more specifically in Inceptisol, the total levels of the highlighted species were with similar magnitude, being *Lolium multiflorum* (198.6 mg kg^{-1} of Cu), *Cyperus compressus* (276 mg kg^{-1} of Cu), and *Chrysanthemum leucanthemum* (160.3 mg kg^{-1} of Cu). The authors pointed out *L. multiflorum* potential for phytostabilization among the studied plant species, considering its dry matter production and ability to maintain the highest levels in its roots.

Regarding correlation analysis, Üçüncü et al. [32], studying the removal potential ofCu, Cr, and Pb by the aquatic macrophyte *Lemna minor*, found that Cr and Pb resembled each other in the time required for achieving the maximum removal rate (48 h), along with similar variations in contaminant levels during the experiment period (144 h). Thus, the authors obtained a high degree of correlation between these two metals.

Li et al. [33], performing a meta-analysis regarding Cu, Zn, and Cd uptake by aquatic plants, found that the ability of a given species to absorb a metal was strongly correlated with its ability to remove the other studied metals. However, the authors also identified other aspects such as the water pH, the morphology of plants (submerged or emerged),and the surface area exposed to water as highly influencing the uptake ability. The authors also identified a strong correlation between Cu and Zn, suggesting that the process of concentrating could be cooperative.

Considering the results found in BCF clustering analysis, the results found were higher than the BCF found by Afonso et al. [34] in a study aiming at the bioprospection of indigenous flora grown in copper-mining tailing areas for phytoremediation of metals. The BCF of Pb ranged from 0.4 by the species *Juncus* sp. to 16.4 in *Solanum viarum* Dunal. Regarding Cu, the species highlighted by the authors were *Eryngium horridum* Malme, *Equisetum giganteum* L., and *Baccharis trimera*, presenting values of BCF for Cu of 1.1, 1.5, and 1.8, respectively. Despite being somewhat lower, this species was highlighted by the authors considering its potential for Cu toleration and accumulation in its tissues, with impressive values of 440 mg kg^{-1}, being thus indicated for phytoremediation application.

Diverging from the results of TF clustering, Gomez et al. [35] found Cu and Ni being translocated to the shoots of *S. montevidensis*. Regarding the mechanism of phytoremediation, rhizofiltration was also detected as the main mechanism performed by aquatic macrophyte plants in other studies. One example is the research conducted by Woraharn et al. [36], which pointed out *Typha angustifolia* as accumulating Cd and Zn levels mainly in roots, in all tested treatments of the experiment.

In the studied area, the Santa Bárbara stream, the application of aquatic macro- phytes could be performed in a controlled form, using the systems of floating islands for water decontamination.

Conclusions

The studied plant species showed tolerance for Cu, Cr, Cd, Pb, Ni, and Zn, demon- strating potential for application in phytoremediation. Comparison between the bioconcen- tration factors allowed the identification of *H. ranunculoides* as presenting excellent results

of accumulation. In addition, the study evaluated the phytoremoval potential of each plant, and the highlighted species were *H. grumosa* and *S. montevidensis*.

This study serves as a background for the application of aquatic macrophyte speciesfor phytoremediation purposes and for a biofilter proposal as floating-island systems for wetland treatments that combine the application of living plants with floating devices for water decontamination. In addition, it also helps other researchers to apply these aquatic macrophyte species with excellent natural potential for remediating other aquatic environments worldwide.

The correct disposal of plant biomass after remediating a contaminated area is primordial to ensuring that the metals do not re-enter the systems, affecting other sites. This study recommends the investigation of alternatives to be explored, such as heat treatment which is followed by co-product generation. Among the treatments one can mention are pyrolysis and the production of new adsorbents such as activated carbon. In addition, we recommend the bioprospection of native species in studies aiming at the remediation of other areas worldwide.

Author Contributions: Conceptualization, C.F.D. and R.A.; literature search and data analysis, C.F.D. and T.F.A.; writing—original draft preparation, C.F.D. and R.A.; writing—review and editing, S.P. and R.A.; funding acquisition: F.C.S., F.M.M. and R.A.; supervision: R.A. All authors have read and agreed to the published version of the manuscript.

Funding: This study was financed in part by the Coordenação de Aperfeiçoamento de Pessoal de Nível Superior—Brasil (CAPES)—Finance code 001, by the CNPq (National Council for Scientific and Technological Development), and FAPERGS (Research Support Foundation of the State of Rio Grande do Sul).

Institutional Review Board Statement: Not applicable.

Informed Consent Statement: Not applicable.

Data Availability Statement: Not applicable.

Conflicts of Interest: The authors declare no conflict of interest.

Ethical Statement: *E. anagallis, H. grumosa, H. ranunculoides,* and *S. montevidensis* plants were used inthis study. The plants were collected in a polluted area, where the municipal government of Pelotas perform periodical cleaning.

Abbreviations

E. anagallis	*Enydra anagallis*
H. grumosa	*Hymenachne grumosa*
H. ranunculoides	*Hydrocotyle ranunculoides*
S. montevidensis	*Sagittaria montevidensis*
HNO_3	Nitric acid
$HClO_4$	Perchloric acid
ICP-OES	Inductively Coupled Plasma-Optical Emission Spectrometry
Cu	Copper
Cr	Chromium
Cd	Cadmium
Pb	Lead
Ni	Nickel
Zn	Zinc
P	Phosphorus
K	Potassium
Ca	Calcium
Mg	Magnesium
S	Sulfur
BCF	Bioconcentration Factor
TF	Translocation Factor

References

1. Li, Q.G.; Liu, G.H.; Qi, L.; Wang, H.C.; Ye, Z.F.; Zhao, Q.L. Heavy metal-contained wastewater in China: Discharge, management and treatment. *Sci. Tot. Environ.* **2022**, *808*, 152091. [CrossRef] [PubMed]
2. Al Masum, A.; Bettman, N.; Read, S.; Hecker, M.; Brinkmann, M.; McPhedran, K. Urban stormwater runoff pollutant loadings: GIS land use classification vs. sample-based predictions. *Environ. Sci. Pollut. Res.* **2022**, *29*, 1–15. [CrossRef] [PubMed]
3. Renieri, E.A.; Safenkova, I.V.; Alegakis, A.K.; Slutskaya, E.S.; Kokaraki, V.; Kentouri, M.; Dzantiev, B.B.; Tsatsakis, A.M. Cadmium, lead and mercury in muscle tissue of gilthead seabream and seabass: Risk evaluation for consumers. *Food Chem. Toxicol.* **2019**, *124*, 439–449. [CrossRef] [PubMed]
4. Zaynab, M.; Al-Yahyai, R.; Ameen, A.; Sharif, Y.; Ali, L.; Fatima, M.; Khan, K.A.; Li, S. Health and environmental effects of heavy metals. *J. King Saud Un. Sci.* **2022**, *34*, 101653. [CrossRef]
5. Coração, A.C.D.S.; Santos, F.S.D.; Duarte, J.A.D.; Lopes-Filho, E.A.P.; De-Paula, J.C.; Rocha, L.M.; Krepsky, N.; Fiaux, S.B.; Teixeira, V.L. What do we know about the utilization of the *Sargassum* species as biosorbents of trace metals in Brazil? *J. Environ. Chem. Eng.* **2020**, *8*, 103941. [CrossRef]
6. Demarco, C.F.; Afonso, T.F.; Pieniz, S.; Quadro, M.S.; De Oliveira Camargo, F.A.; Andreazza, R. Evaluation of *Enydra anagallis* remediation at a contaminated watercourse in south Brazil. *Int. J. Phytorem.* **2020**, *22*, 1216–1223. [CrossRef]
7. Ugwu, E.I.; Othmani, A.; Nnaji, C.C. A review on zeolites as cost-effective adsorbents for removal of heavy metals from aqueous environment. *Int. J. Environ. Sci. Technol.* **2022**, *19*, 8061–8084. [CrossRef]
8. Ali, F.; Jilani, G.; Fahim, R.; Bai, L.; Wang, C.; Tian, L.; Jiang, H. Functional and structural roles of wiry and sturdy rooted emerged macrophytes root functional traits in the abatement of nutrients and metals. *J. Environ. Manag.* **2019**, *249*, 109330. [CrossRef]
9. Oladoye, P.O.; Olowe, O.M.; Asemoloye, M.D. Phytoremediation technology and food security impacts of heavy metal contaminated soils: A review of literature. *Chemosphere* **2022**, *288*, 132555. [CrossRef]
10. Garg, S.; Roy, A. Phytoremediation: An alternative approach for removal of dyes. In *Phytoremediation*; Academic Press: Cambridge, MA, USA, 2022; pp. 369–386.
11. Shah, V.; Daverey, A. Phytoremediation: A multidisciplinary approach to clean up heavy metal contaminated soil. *Environ. Technol. Innov.* **2020**, *18*, 100774.
12. Kafle, A.; Timilsina, A.; Gautam, A.; Adhikari, K.; Bhattarai, A.; Aryal, N. Phytoremediation: Mechanisms, plant selection and enhancement by natural and synthetic agents. *Environ. Adv.* **2022**, *8*, 100203. [CrossRef]
13. Yan, X.; Wang, J.; Song, H.; Peng, Y.; Zuo, S.; Gao, T.; Duan, X.; Qin, D.; Dong, J. Evaluation of the phytoremediation potential of dominant plant species growing in a chromium salt–producing factory wasteland, China. *Environ. Sci. Poll. Res.* **2020**, *27*, 7657–7671. [CrossRef] [PubMed]
14. Manorama Thampatti, K.C.; Beena, V.I.; Meera, A.V.; Ajayan, A.S. Phytoremediation of Metals by Aquatic Macrophytes. In *Phytoremediation: In-situ Applications*; Shmaefsky, B.R., Ed.; Springer International Publishing: New York, NY, USA, 2020; pp. 153–204.
15. Pires-Lira, M.F.; De Castro, E.M.; Lira, J.M.S.; De Oliveira, C.; Pereira, F.J.; Pereira, M.P. Potential of *Panicum aquanticum* Poir. (Poaceae) for the phytoremediation of aquatic environments contaminated by lead. *Ecotox. Environ. Saf.* **2020**, *193*, 110336. [CrossRef] [PubMed]
16. Ansari, A.A.; Naeem, M.; Gill, S.S.; AlZuaibr, F.M. Phytoremediation of contaminated waters: An eco-friendly technology based on aquatic macrophytes application. *Egyp. J. Aq. Res.* **2020**, *46*, 371–376. [CrossRef]
17. SANEP. *Serviço Autônomo de Saneamento de Pelotas*; Estações de Tratamento: Guaratuba, Brazil, 2019. (In Portuguese)
18. SQA. *Environmental Plan of Pelotas*; Secretaria de Qualidade Ambiental: Areal, Brazil, 2013. (In Portuguese)
19. Korb, C.C.; Suertegaray, D.M.A. Identificação de depósitos tecnogênicos em um reservatório de abastecimento de água da cidade de Pelotas (RS). *Quater. Environ. Geosci.* **2014**, *5*, 33918. [CrossRef]
20. Análises de Solo, Plantas e Outros Materiais. Available online: https://www.scribd.com/document/362494561/Analise-de-solos-plantas-e-outros-materiais-Tedesco-et-al-1995-pdf# (accessed on 1 December 2022).
21. De Andrade, L.C.; Tiecher, T.; De Oliveira, J.S.; Andreazza, R.; Inda, A.V.; De Oliveira Camargo, F.A. Sediment pollution in margins of the Lake Guaíba, Southern Brazil. *Environ. Monit. Assess.* **2018**, *190*, 1–13. [CrossRef]
22. Yoon, J.; Cao, X.; Zhou, Q.; Ma, L.Q. Accumulation of Pb, Cu, and Zn in native plants growing on a contaminated Florida site. *Sci. Total Environ.* **2006**, *368*, 456–464. [CrossRef]
23. Kabata-Pendias, A.; Pendias, H. *Trace Elements in Soils and Plants*, 3rd ed.; CRC Press: Boca Raton, FL, USA, 2001.
24. Hopkins, W.G. *Introduction to Plant Physiology*, 2nd ed.; John Wiley & Sons: New York, NY, USA, 2000; p. 512.
25. Demarco, C.F.; Afonso, T.F.; Pieniz, S.; Quadro, M.S.; Camargo, F.A.; Andreazza, R. *In situ* phytoremediation characterization of heavy metals promoted by *Hydrocotyle ranunculoides* at Santa Bárbara stream, an anthropogenic polluted site in southern of Brazil. *Environ. Sci. Pollut. Res.* **2018**, *25*, 28312–28321. [CrossRef]
26. Demarco, C.F.; Afonso, T.F.; Pieniz, S.; Quadro, M.S.; Camargo, F.A.D.O.; Andreazza, R. Phytoremediation of heavy metals and nutrients by the *Sagittaria montevidensis* into an anthropogenic contaminated site at Southern of Brazil. *Int. J. Phytor.* **2019**, *21*, 1145–1152. [CrossRef]
27. Małkowski, E.; Sitko, K.; Szopiński, M.; Gieroń, Ż.; Pogrzeba, M.; Kalaji, H.M.; Zieleźnik-Rusinowska, P. Hormesis in plants: The role of oxidative stress, auxins and photosynthesis in corn treated with Cd or Pb. *Int. J. Molec. Scie.* **2020**, *21*, 2099. [CrossRef]

28. Souza-Arroyo, V.; Fabián, J.J.; Bucio-Ortiz, L.; Miranda-Labra, R.U.; Gomez-Quiroz, L.E.; Gutiérrez-Ruiz, M.C. The mechanism ofthe cadmium-induced toxicity and cellular response in the liver. *Toxicology* **2022**, *480*, 153339. [CrossRef]
29. Zhao, D.; Wang, P.; Zhao, F.J. Dietary cadmium exposure, risks to human health and mitigation strategies. *Crit. Rev. Environ. Sci.Technol.* **2022**, *12*, 1–25. [CrossRef]
30. Tiwari, S.; Dixit, S.; Verma, N. An effective means of biofiltration of heavy metal contaminated water bodies using aquatic weed *Eichhornia crassipes*. *Environ. Monit. Assess* **2007**, *129*, 253–256. [CrossRef] [PubMed]
31. Melo, G.W.; Furini, G.; Brunetto, G.; Comin, J.J.; Simão, D.G.; Marques, A.C.R. Identification and phytoremediation potential ofspontaneous species in vineyard soils contaminated with copper. *Int. J. Phytor.* **2021**, *24*, 342–349. [CrossRef] [PubMed]
32. Üçüncü, E.; Tunca, E.; Fikirdeşici, Ş.; Altındağ, A. Decrease and increase profile of Cu, Cr and Pb during stable phase of removal by duckweed (*Lemna minor* L.). *Int. J. Phytor.* **2013**, *15*, 376–384. [CrossRef]
33. Li, J.; Yu, H.; Luan, Y. Meta-analysis of the copper, zinc, and cadmium absorption capacities of aquatic plants in heavy metal-polluted water. *Int. J. Environ. Res. Public Health* **2015**, *12*, 14958–14973. [CrossRef]
34. Afonso, T.F.; Demarco, C.F.; Pieniz, S.; Quadro, M.S.; Camargo, F.A.; Andreazza, R. Bioprospection of indigenous flora grown incopper mining tailing area for phytoremediation of metals. *J. Environ. Manag.* **2020**, *256*, 109953. [CrossRef]
35. Gomez, B.M.; Reale, M.; El Kassisse, Y.; Mujica, C.; Gómez, C.; De Cabo, L.; Salemi, V.R. Metals uptake by *Sagittaria montevidensis* in contaminated riparian Area of Matanza-Riachuelo River (Argentina). *SN Appl. Sci.* **2020**, *2*, 1–10. [CrossRef]
36. Woraharn, S.; Meeinkuirt, W.; Phusantisampan, T.; Chayapan, P. Rhizofiltration of cadmium and zinc in hydroponic systems. *Wat. Air Soil Pollut.* **2021**, *232*, 1–17.

6 Artigo 3

O artigo intitulado “**New low-cost biofilters for SARS-CoV-2 using *Hymenachne grumosa* as a precursor”** é apresentado conforme publicado na Revista Journal of Cleaner Production, ISSN: 0959-6526, fator de impacto 11.072, classificação A1 na área de Materiais, tendo sido aceito em 2 de dezembro de 2021.

Journal of Cleaner Production 331 (2022) 130000

Contents lists available at ScienceDirect

Journal of Cleaner Production

journal homepage: www.elsevier.com/locate/jclepro

New low-cost biofilters for SARS-CoV-2 using *Hymenachne grumosa* as a precursor

Carolina Faccio Demarco [a], Thays França Afonso [a], Guilherme Pereira Schoeler [b], Victor dos Santos Barboza [c], Liziane dos Santos Rocha [c], Simone Pieniz [b], Janice Luehring Giongo [c], Rodrigo de Almeida Vaucher [c], Andrei Vallerão Igansi [d], Tito Roberto Sant'Anna Cadaval Jr. [d], Robson Andreazza [a,b,*]

[a] Science and Engineering of Materials Postgraduate Program, Federal University of Pelotas, R. Gomes Carneiro 01, CEP 96010-610, Pelotas, RS, Brazil
[b] Environmental Sciences Postgraduate Program, Federal University of Pelotas. R. Benjamin Constant 989, CEP 96010-020, Pelotas, RS, Brazil
[c] Graduate Program in Biochemistry and Bioprospecting, Research Laboratory in Biochemical and Molecular Biology of Microorganisms (LaPeBBiOM), Federal University of Pelotas, Av. Eliseu Maciel, Campus Universitário, S/n, Capão do Leão, CEP 96160-000, RS, Brazil
[d] School of Chemistry and Food, Federal University of Rio Grande, Av. Itália, Km 8, S/n, Carreiros, CEP 96203-000, Rio Grande, RS, Brazil

ARTICLE INFO

Handling Editor: M.T. Moreira

Keywords:
COVID-19
SARS-CoV-2
RT-qPCR
Biofilters
Aquatic macrophytes

ABSTRACT

The ongoing global spread of COVID-19 (SARS-CoV-2 2019 disease) is causing an unprecedented repercussion on human health and the economy. Despite the primary mode of transmission being through air droplets andcontact, the transmission via wastewater is a critical concern. There is a lack of techniques able to provide complete disinfection, along with the uncertainty related to the behavior of SARS-CoV-2 in the natural envi- ronment and risks of contamination. This fact makes urgent the research towards new alternatives for virus removal from water and wastewater. Thus, this research aimed to characterize new lost-cost adsorbents for SARS-CoV-2 using *Hymenachne grumosa* as a precursor and verify its potential for removing SARS-CoV-2 from the solution. The aquatic macrophyte *H. grumosa* had *in natura* and activated carbon produced with *H. grumosa* and zinc chloride ($ZnCl_2$,1:1) impregnation and carbonization (700 °C, 1 h) were incubated for 24 h with inactivated SARS-CoV-2 viral suspension, and then the ribonucleic acid (RNA) was extracted and viral load quantified through reverse transcription-quantitative polymerase chain reaction (RT-qPCR) technique. The results demonstrated the great adsorption potential, achieving removal of 98.44% by *H. grumosa "in natura"*, and 99.61% by *H. grumosa* with carbon activation, being similar to commercial activated carbon (99.67%). Thus, this study highlights the possibility of low-cost biofilters to be used for SARS-CoV-2 removal, as an excellent alternative for wastewater treatment or watercourses decontamination.

1. Introduction

The global pandemic SARS-CoV-2 2019 disease (COVID-19) has reached 116 million cases and 2.5 million deaths reported globally since the start of the pandemic, according to WHO (2021) weekly report on 07 March 2021. Despite the primary mode of transmission of SARS-CoV-2 being through respiratory droplets and direct/indirect contact, the secondary transmission via wastewater is an outstanding concern to be overcome (Liu et al., 2020). Recently reports the persistence ability of novel coronavirus SARS-CoV-2 RNA for multiple days in wastewater without considerable degradation (Ahmed et al., 2020).

The emerging pathogens, including the SARS-CoV-2, may enter wastewater systems from different sources i.e.: hospital effluents, domestic sewage, surface water runoff, and may present serious consequences to human health (Lahrich et al., 2021). The viral load identified incoming in wastewater treatment plants (WWTP) varies from 2 copies/100 mL to 3×10^3copies mL^{-1} after dilution in the watercourse, and directly depending on the contamination level (Foladori et al., 2020).

The current methods used for virus removal include membrane filtration, reverse osmosis, nanofiltration, and adsorption, along with physical inactivation as ultraviolet light, photodynamic oxidation, and

* Corresponding author. Science and Engineering of Materials Postgraduate Program, Federal University of Pelotas, R. Gomes Carneiro 01, CEP 96010-610, Pelotas,RS, Brazil.
E-mail address: robsonandreazza@yahoo.com.br (R. Andreazza).

https://doi.org/10.1016/j.jclepro.2021.130000
Received 19 May 2021; Received in revised form 28 November 2021; Accepted 2 December 2021
Available online 7 December 2021

chemical disinfection – chlorine or ozone (Mi et al., 2020).

In addition, among the current methods applied for removal of virus, the chemical disinfection using chlorine or ozone present some restrictions in use nowadays considering the by-products generated, since reacts with composts present in surface waters as humic and fulvic acids and thus generating drinking water disinfection by-products (DBPs) as haloacetonitriles, haloacetic acids and trihalomethane (Goswami and Pugazhenthi, 2020).

The technologies with membrane filtration are efficient in virus removal, present limitations regarding operational costs, a fact that can limit the usage in low-income countries (Adelodun et al., 2020).

To achieve the complete removal of SARS-CoV-2 from wastewater, previous studies recommended the application of advanced technologies and/or hybrid treatment systems to achieve satisfactory disinfection, along with the removal of secondary metabolites produced by antiviral drugs (Kumar et al., 2021).

It might be highlighting the absence of studies regarding the com- plete removal of SARS-CoV-2 from wastewater and the presence of the virus in the environment points out the hotspots zones where there is spreading of the virus in specific populations (Venugopal et al., 2020). This surveillance of the virus in wastewater could be highly efficient for helping authorities in decision-making regarding COVID-19 crisis management (Randazzo et al., 2020).

The use of activated carbon is among the promising options aiming for virus removal, along with advanced oXidation processes, membrane use, and solar disinfection (Ghernaout et al., 2020). Activated carbon can be produced using chemical impregnation (KOH, NaOH, $ZnCl_2$, etc.) followed by carbonization (Mamaní et al., 2019). Several precursor materials are being studied to reduce the cost of the adsorption process, including lignocellulosic biomass. Among the materials investigated, the aquatic macrophytes and out considering their natural presence in the environment (González-García et al., 2020). The aquatic macrophyte Hymenachne grumosa belongs to the Poaceae family and is reported in the literature as presenting excellent results for using in constructed wetlands (CW), showing potential to remediate urban effluents (Silveira et al., 2019).

In general, viruses present the characteristic of being chargedcolloidal particles that can be adsorbed by different surfaces (Lahrichet al., 2021). The SARS-CoV-2 presents a single-stranded positive RNA genome and belongs to the family *Coronaviridae* (Yin, 2020). Its adsorption phenomena onto surfaces depend on several factors as sur- face chemistry, pH, humidity, and temperature. These aspects also drive the desorption process and the stability and persistence of SARS-CoV-2, and the literature presents a lack regarding the interaction among the virus and different surfaces (Joonaki et al., 2020).

The substantial importance of this study is related to the sanitary crisis faced currently by Brazil. The country is into a collapse in the health system in its history, as reported by Fiocruz (2021), with 25 of 27 federative units presenting occupancy rates higher than 80% in an intensive care unit (ICU) COVID-19 beds.

The epicentre of COVID-19 in America and the world is Brazil, reaching almost 4000 deaths per day. The sanitary crisis presents long- term impacts in population health, economic and social spheres.

Thus, this research aims to investigate the potential of low-cost adsorbent produced using the aquatic macrophyte *H. grumosa* as a precursor for SARS-CoV-2 removal from water. Therefore, it is highlighted a promising alternative for wastewater treatment and aquatic environments contaminated with the new SARS-CoV-2, mostly in developing countries with sanitation issues.

2 Materials and methods

2.1Adsorbent preparation

The aquatic macrophyte *H. grumosa* was collected at Santa Bárbara Stream, municipality of Pelotas/RS, Brazil (31°45′ 24.4″ S 52°21′ 22.1″ W). The biomass was then washed in tap water and distilled water for the removal of associated sediments and dried at 65 °C until constant weight.

The material named *H. grumosa in natura* was prepared using the dried biomass, followed by milling in 18-mesh granulometry. On the other hand, the *H. grumosa* activated carbon was prepared with $ZnCl_2$ impregnation (1:1), at 200 rpm for 24 h. The material was dried and then was performed carbonization at 700 °C for 1 h. After carbonization, the material was washed using an HCl (3 M) solution, followed by hot water washing, until neutrality. The methodology was adapted from Kiliç et al. (2012).

2.2. Characterization

The thermogravimetric analysis (TGA) was performed in TGA-1000 equipment (Navas Instrument), the flow of Nitrogen gas of 1 L/min and heating rate of 10 °C min.

The functional groups were obtained with Fourier-transform infrared spectroscopy (FT-IR), using Shimadzu model IRPrestige-21, scanning from 400 to 4000 cm^{-1}, 32 scans, transmittance mode, and resolution of 4 cm^{-1}.

The specific surface area of *H. grumosa* activated carbon was obtained from the Brunauer, Emmett, Teller (BET) method, and the pore size distribution was obtained from Barrett- Joyner-Halenda (BJH) method (GEMINI 2390).

The surface morphologies were evaluated using Scanning Electron Microscopy (SEM) (JEOL, JSM 6610 L V, Japan), using 15 kV and magnification of 1000×

The X-ray diffraction (XRD) patterns were obtained using a diffractometer (Brunker D–8, Germany), provided with a diffracted beam monochromator and Ni filtered CuKα radiation (λ 1.5406 Å). The voltage was 40 kV and the intensity of 40 mA. The 2ɵ angle was scanned between 10° and 60°, and the counting time was of 1.0 s at each anglestep (0.02°).

The point of zero charges (PZC) for *H. grumosa in natura*, *H. grumosa* activated carbon, and commercial activated carbon was obtained using the 24 h agitation contact (50 rpm) of adsorbent to pH solutions varying from pH 1 to 12. The initial and final pH values were measured using a pHmeter and the PZC was obtained after plotting the ΔpH (pH final – pH initial) against initial pH. This methodology was adapted from Feng et al. (2020).

The moisture content of *H. grumosa* activated carbon followed the American Society for Testing and Materials (ASTM D2867/04). The pH was determined using ASTM D3838/11, and apparent density followed ASTM D2854/09. The ash content was established according to ASTM D2866/11 and calculated as Equation (1):

$$\text{Ash content } (\%) = \frac{\text{weight}_{final}}{\text{weight}_{initial}} \times 100 \quad (1)$$

Where weight_{final} is the final weight after carbonization (g); $\text{weight}_{initial}$ refers to the initial weight of the material (g).

The yield of *H. grumosa* activated carbon was calculated as Equation (2):

$$\text{Yield } (\%) = \frac{m_f}{m_i} \times 100 \quad (2)$$

Where m_f represents the weight of the produced activated carbon (g); and m_i is the weight of raw precursor, in this case being the biomass activated with $ZnCl_2$.

The software used for data treatment was Origin Pro 2019.

2.3. Obtainment of SARS-CoV-2 inactivated

The SARS-CoV-2 virus was used to carry out the experiments with the materials which had been used as a positive control and come from a

clinical isolated in Vero-E6 cell culture (SARS-CoV-2/SP02/human2020/Br, GenBank accession number MT126808.1). This virus was provided by Prof. Dr. Edison Luiz Durigon of the Department of Microbiology, Institute of Biomedical Sciences, University of São Paulo (USP), Brazil (Dorlass et al., 2020).

2.3. Virus removal experiment

The materials *H. grumosa in natura* (10 mg) and *H. grumosa* activated carbon (10 mg) were properly dried at 37 °C for 2 h. After that time, each material was transferred to a microtube containing 1.5 mL of sterile RNAse-free ultrapure water. To each microtube containing the respective material, 150 μL of the inactivated SARS-CoV-2 viral suspension (2.5×10^6 copies/mL) was added, followed by incubation at 28 °C with shaking at 200 rpm for 24 h, pH 7.0.

2.4. RNA extraction

After incubation, each supernatant and material was transferred into a new microtube and viral RNA was extracted. The extraction of RNA of supernatant and materials were performed using the MagMax™ Core Nucleic Acid Purification kit (Thermo Fisher Scientific, Waltham, MA, USA) according to the manufacturer's instructions. After extraction, the RNAs were quantified in NanoDrop™ (Thermo Scientific, Waltham, MA, USA). A concentration of approximately 10 ng of RNA was used to perform RT-qPCR.

2.5. RT-qPCR

The primer and probe used in PCR reactions were designed according to the sequences published by the Centers for Disease Control and Prevention (CDC, 2020). Briefly, a reaction of 25 μL of the final volume was used, with the following volumes added to the 1× concentrated master mix: 5 μL of sample RNA, 12.5 μL of 2 × reaction buffer, 1 μL of Superscript™ III One-Step with Platinum™ Taq DNA Polymerase (Invitrogen, Darmstadt, Germany), 0.4 mM of each dNTP, 0.4 μL of a 50 mM $MgSO_4$ solution (Invitrogen), 1 μg of non-acetylated bovine albumin (Roche), 10 μM of each primer 2019-nCoVN1-F2019-nCoV N1 (5′ GACCCCAAAATCAGCGAAAT3′), 2019-nCoVN1-R2019-nCoV N1 (5′ TCTGGTTACTGCCAGTTGAATCTG3′) and 2019-nCoVN1-P2019-n- CoV N1 probe (5′-FAM – ACCCCGCATTACGTTTGGTGGACC– BBQ 3′) and DEPC water. The reaction occurred in StepOne™ Real-Time PCR System (Thermo Fisher Scientific, Waltham, MA, USA) in the following cycling: 55 °C for 10 min for reverse transcription, followed by 95 °C for 3 min and 40 cycles of 95 °C for 15 s, 58 °C for 30 s.

2.6. Statistical analysis

Data were expressed as mean SE± for duplicates for each experimental point. Data were analyzed by using analysis of variance (ANOVA) followed by Tukey's test.

3. Results and discussion

This research aimed to help the understanding of the interactions of viral particles of SARS-CoV-2 with the surface of the adsorbent pro- duced. The major goal is the evaluation of the feasibility of using an aquatic macrophyte plant species for developing an adsorbent for virus removal. The study of surface charge and morphology, functionalgroups, thermal degradation of the precursor material, and crystallinity was performed aiming the understand how the particles of bioadsorbent affect the adsorption of SARS-CoV-2.

Thereafter, it was evaluated the potential removal using RNA extraction and the RT-qPCR technique. Subsequently, a cost estimation was included to endorse the sustainable potential and contribution to the cleaner production sector. Finally, it was described the possibilities of real application of the new adsorbents presented by this research and the advantages of this alternative precursor use. Thus, the characterization of the biomaterial used in this work was the first step intending the elucidation of the adsorption mechanism of SARS-CoV-2 in activated carbon and raw material for water and wastewater treatment. It can be highlighted that this research supports the development of new biomaterials for virus removal worldwide.

The use of inactivated SARS-CoV-2 was performed to guarantee the biosecurity, being accordance with recommendations of previous studies. Along with careful handling of samples, the prior inactivation of SARS-CoV-2 is important to prevent accidental release into the envi- ronment, ensuring the safety of the researchers and the community (Bain et al., 2020). The inactivation process also allows the samples to reach diverse institutions and researchers, at secure conditions at different locations, and it is recommended that each laboratory mustfollow the guidelines for the correct handling of the samples.

It might be highlighted that besides being following the biosecurity guideline, the inactivated SARS-CoV-2 was used in other previousstudies performed, as Trassante et al. (2021) aimed the detection of SARS-CoV-2 in healthcare professionals with RT-LAMP (Reverse tran-scription loop-mediated isothermal amplification) and qRT-PCR techniques.

3.1 Adsorbent characterization

The thermogravimetric analysis is essential for the production of activated carbon from a new precursor that did not present previous studies in the literature (González-García, 2018). The curves obtained during the analysis demonstrate the thermal conversion structural changes in material, and the differential thermogravimetry highlights the different stages precisely (Arbeláez et al., 2019).

It can be seen in the TGA analysis of the precursor (Fig. 1), *H. grumosa* showed two main weight losses. The first was identified at 100 °C, which can be noticed along with the differential peak in this temperature. On the other hand, the second weight loss presented a slowly decreasing rate from 300 °C to 700 °C, having a differential peak at 300 °C. At the end of pyrolysis, it was shown a final content residue of 7.89%. Abovethe temperature of 700 °C, the differential thermogravimetric (DTG) and TGA lines remained constant.

Thereby, the *H. grumosa* was detected presenting its first weight loss in 100 °C mainly related to moisture elimination, and the second weight loss (300 °C) related to hemicellulose degradation (De Luna et al., 2019). The degradation of cellulose was reported occurring at 325 °C and 375 °C intervals by Di Blasi (2008) in a study modeling chemical and physical processes of wood and biomass pyrolysis, and by Burhenne et al. (2013) identifying the effect of the biomass components lignin,

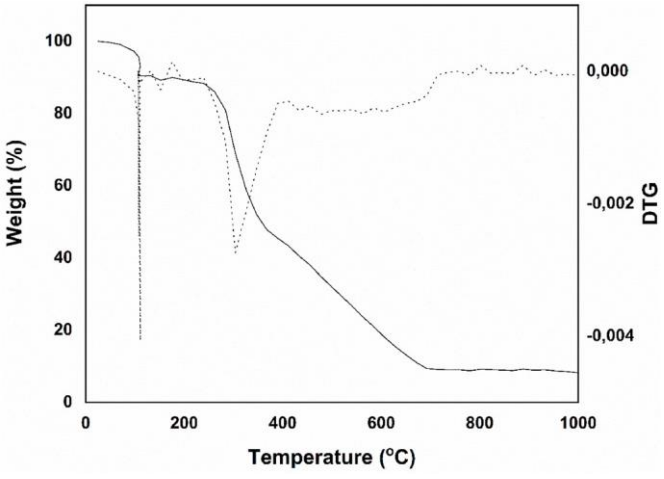

Fig. 1. TGA curve of *H. grumosa* biomass.

cellulose and hemicellulose on TGA and fixed bed pyrolysis. Regarding lignin degradation, there is a lack of studies demonstrating the weight loss of this component. Weight losses in temperatures above 400 °C might be related to secondary reactions of carbon residues. However, further studies are recommended in order the completely understand the nature of the decomposition process. The identified percentage of final residues represents the char after total decomposition (Kumar et al., 2019).

The cell wall of plant biomass presents a complex composition with several components as cellulose, hemicellulose, pectin, lignin, proteins, and other chemical compounds (Hu et al., 2018). These components affect the adsorption capacity of the biomass, considering the functional groups modifying the surface chemistry.

The functional groups for *H. grumosa in natura*, *H. grumosa* activated carbon, and commercial activated carbon was determined by FT-IR in the region of 400–4000 cm^{-1}. It was identified similar bands in *H. grumosa in natura* and *H. grumosa* activated carbon, with a major difference in 1631 cm^{-1} bands (Fig. 2a) shifting to 1579 cm^{-1} in the produced activated carbon (Fig. 2b) and 1544 cm^{-1} in commercial activated carbon (Fig. 2c).

In addition, the *H. grumosa in natura* also presented a broadband located around 3352 cm^{-1} (Fig. 2a). The main peaks detected for the adsorbents were among 1000–1220 cm^{-1} positions, 1217 cm^{-1}, 1363-1371 cm^{-1}, 1741 cm^{-1}, 2090 cm^{-1}, 2320-2343 cm^{-1} and 2918-2968 cm^{-1}.

The detected FT-IR spectra in *H. grumosa in natura* showed bands that can be attributed to O–H stretching of the hydroxyl group (broadband located around 3352 cm^{-1}) (Abdullah et al., 2020). The aliphatic C–H group was identified in *H. grumosa in natura* and *H. grumosa* activated carbon in 2918 cm^{-1} and 2968 cm^{-1}, respectively (Alves et al., 2019). The C−O free carbonyl groups were identified in *H. grumosa in natura* and *H. grumosa* activated carbon in 1741 cm^{-1} (Bind et al., 2018).

The peaks 1371 cm^{-1} and 1363 cm^{-1} in *H. grumosa in natura* and *H. grumosa* activated carbon can be assigned to O–H deformations regarding phenolic and aliphatic groups; and lastly, peaks occurring among the spectra of 1000–1220 cm^{-1} can be attributed to C–O stretching (Alves et al., 2019). The detected bands were similar to previous studies of activated carbon from different precursors (Zyoud et al., 2015; Maneerung et al., 2016).

The functional groups present in the viruses are another important factor affecting the adsorption process. The main groups found in the amino acids of SARS-CoV-2 are $–NH_2$, $–NH_3^+$, –COOH, and COO^- and the adsorption process is thus given by electrostatic interactions between the surface of virions and opposite charge from the surface (Joonaki et al., 2020).

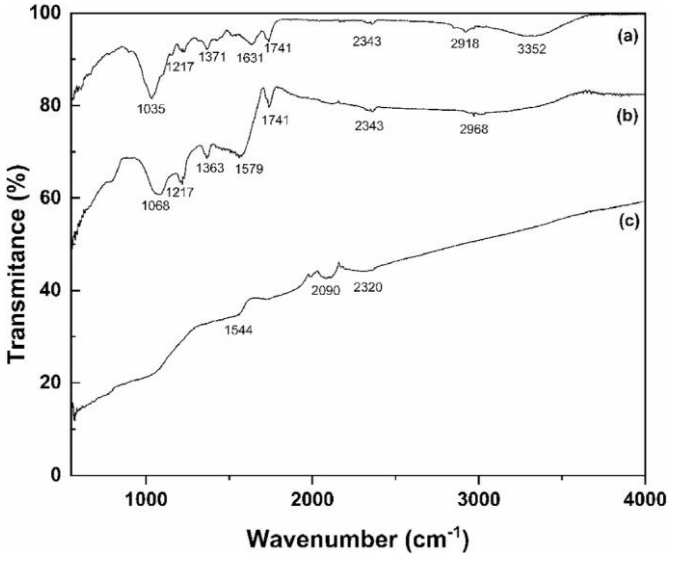

Fig. 2. FT-IR spectra of (a) *H. grumosa in natura*, (b) *H. grumosa* activated carbon, and (c) Commercial activated carbon.

The adsorption of SARS-CoV-2 is also driven by the spike (S) glycoprotein protruding from the lipidic membrane since it is responsible for giving the virus its morphology and being a component of the outer surface. The spike-glycoprotein of SARS-CoV-2 is reported as presenting a hydrophobic nature and negative charge in pH above its isoelectricpoint – pH 5.9 (Pandey, 2020). The point of zero charges (pH_{PZC}) detected for *H. grumosa* activated carbon was 6.09, and the value detected for *H. grumosa in natura* was 6.32. The commercial activated carbon presented a pH_{PZC} of 6.55. Considering the pH_{PZC} of the materialsit can be seen that the charges of the surface of the bioadsorbents are also negative in the pH condition (pH = 7.0) tested since all the materials pH_{PZC} are lower than the pH of the solution. This fact is supported by the fact that when the solution pH is lower than the pH_{PZC}, the solid material surface will be positively charged and tends to adsorb anionic species.On the other hand, when the pH of a solution is higher than the pH_{PZC},the material surface will be negatively charged and tends to adsorb cationic species due to electrostatic interactions (Nizam et al., 2021).

The specific surface area of *H. grumosa* activated carbon was 30.09 m^2 g^{-1}, and the average pore size was 3.7 nm. The produced activated carbon presented a micro/mesoporous structure. The microporous and mesoporous structures were according to the research conducted by Piriya et al. (2021), which produced activated carbon from coconut shells and chemical activation using $ZnCl_2$ aiming at the removal of malachite green dye from aqueous solutions. In addition, these structures were on par with the results found by Wang et al. (2013), a study aiming the optimization of mesoporous activated carbon produced from coconut shells and activation with H_3PO_4, which also identified mainly microporous (total volume of 37.06%) and mesoporous (total volume of 62.85%) structure formed. Kumar and Jena (2017) also identified microporous structure on activated carbon produced from fox nutshell and $ZnCl_2$ activation. The conditions used were 600 °C carbonization and 1 h impregnation.

The chemical composition of raw material influences directly on surface area and pore structure for activated carbon (Correa et al., 2017). Depending on the compost of interest for removing with adsorption, the low surface area can be efficient in removing contaminants. In lignocellulosic materials, the high content of lignin can lead to activated carbon with lower surface areas, as Nanda et al. (2014) studied lignocellulosic feedstocks and found surface areas less than 5 m^2 g^{-1} after pyrolysis (600 °C, 4 h) aiming the production of biochar for soil amending.

Carbon-based materials have already been tested for virus removal from fluids in adsorption techniques and presented promisor results. The investigation conducted by Powell et al. (2000) tested conventional granular activated carbon and an activated carbon fiber composite for removing the bacteriophage MS2. The technique used batch design to determine empirical isotherm coefficients from linear regression analysis. The authors found a removal superior for carbon fiber composite than granular activated carbon, despite the lower total surface area (840 m^2 g^{-1}) compared to the granular one (1050 m^2 g^{-1}). The authors justified that the promising results were due to different shape and size fractions of the activated carbons.

Matsushita et al. (2013) studied the removal of bacteriophages using adsorption with powdered activated carbon and super-powdered activated carbon and ended up identifying that the factors that contribute to virus removal were the hydrophobicity of the virus surface, the reduced repulsive force between the virus and activated carbon particles, and the negative surface charge of activated carbon.

The SEM of the aquatic macrophyte *H. grumosa in natura*, *H. grumosa* activated carbon, and Commercial activated carbon are shown in Fig. 3a, b, and c, respectively.

The scanning microscopy of the aquatic macrophyte *H. grumosa in natura* (Fig. 3a) showed a longitudinally striated surface, presenting the

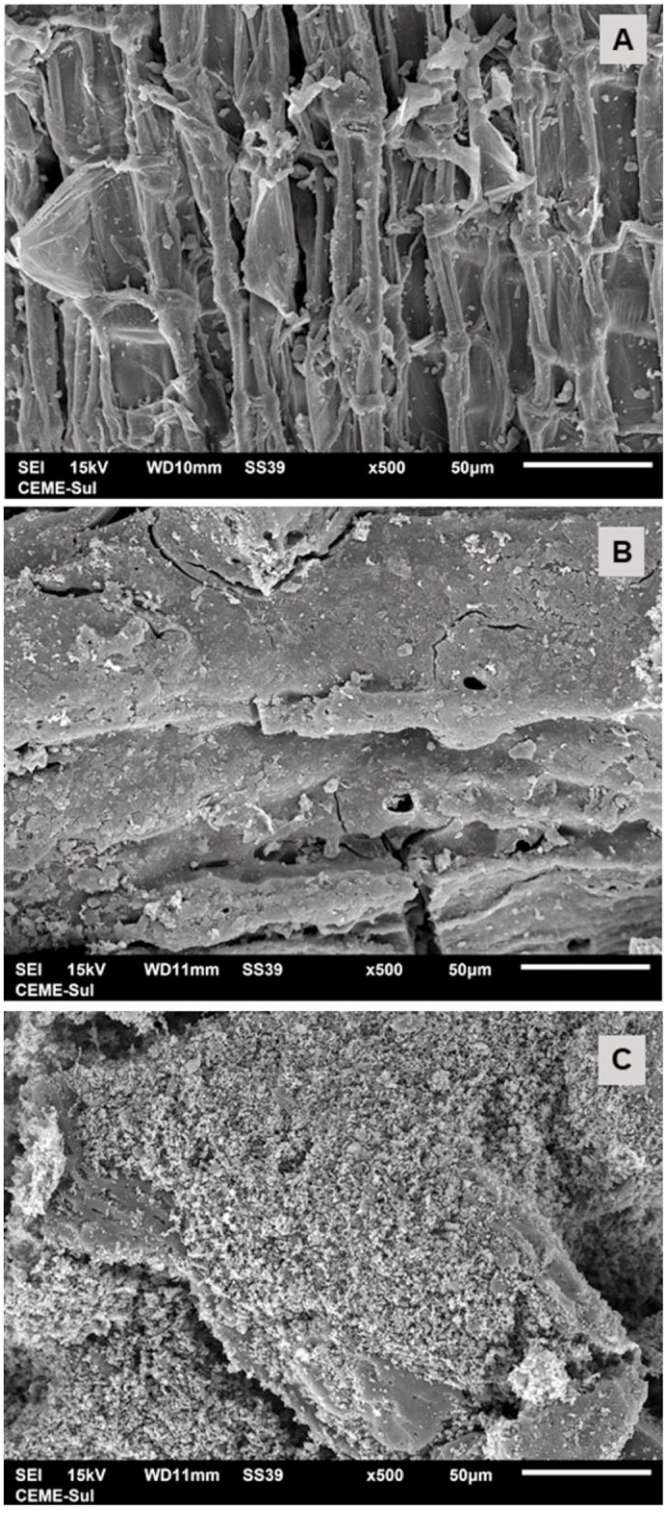

Fig. 3. SEM image of (a) *H. grumosa in natura*, (b) *H. grumosa* activated carbon, and (c) Commercial activated carbon.

topography of characteristic plant tissue. The surface of the raw material had no porous structure, being uniformly filled, thus reducing the sur- face area of the material.

However, it can be seen that after the production of activated carbon from the aquatic macrophyte *H. grumosa* (Fig. 3b), the surface of the material was significantly altered, being possible to observe the appearance of pores and a reduction in the streaks characteristic of plant tissue.

Finally, the commercial activated carbon (Fig. 3c) showed a rough and extremely porous surface, which is a desired characteristic in this type of adsorbent since the surface area is directly related to the porosity of the solid.

The X-ray diffractograms are demonstrated in Fig. 4. It can be noticed that the Commercial activated carbon (Fig. 4 a) presented a predominantly crystalline characteristic with peaks of this type of ma- terial. This crystallinity can be attributed to the high ash composition remaining after the pyrolysis of the precursor material since it is ex-pected that significant crystalline phases occur in samples rich in ash (Benedetti et al., 2018). In addition, the presence of salts of inorganic activating agents used for the production of the adsorbent is also known as responsible for increasing crystallinity. The usage of $ZnCl_2$ for the production of activated carbon with bamboo bagasse was also identified as enhancing crystallinity in a study conducted by Gunasekaran et al. (2019), whose fact did not occur when treated with iron salt.

The diffractogram of the aquatic macrophyte *H. grumosa in natura* (Fig. 4c) showed an amorphous characteristic with an elongated halo in 2θ equal to 22°, peculiar to low-fibrous plant materials. The *H. grumosa* activated carbon material (Fig. 4b) started to present crystalline char- acteristics due to the removal of volatile organic material during the production of the coal as well as the presence of the inorganic salt used during the activation phase. The temperature at which the activated carbon was transformed into a structure with better crystallinity than *H. grumosa in natura*. Lua and Yang (2004) identified the same pattern studying the activated carbon prepared from the pistachio-nut shell when evaluating the effect of activation temperature on the textural and chemical properties of the adsorbent. The authors found that the higher activation temperatures reduce the less ordered components leading to a reduction of the amorphous structure.

Adinaveen et al. (2013), in their research aiming the understand activated carbon properties produced from sugarcane bagasse also identified the formation of crystalline phases during activation at higher temperatures (700 and 800 °C) in XRD curves. The authors stated this formation, which is unusual in activated carbons, can be justified by the temperature employed.

The *H. grumosa* activated carbon presented an apparent density of 0.309 ± 0.023 g/cm^3, moisture content of 19.14 ± 0.84%, and a pH of 7.26 ± 0.30. Regarding the ash content, *H. grumosa in natura* presented
6.37 ± 1.06% and, on other hand, the *H. grumosa* activated carbon presented 25.30 ± 3.35%.

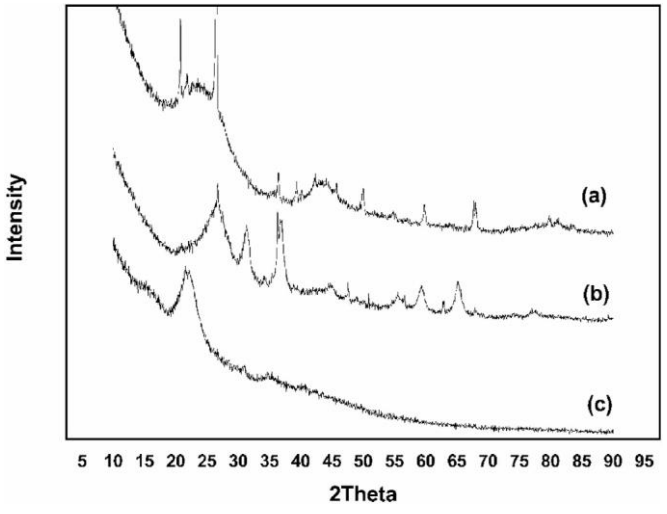

Fig. 4. XRD patterns from(a) Commercial activated carbon (b) *H. grumosa* activated carbon and (c) *H. grumosain natura*.

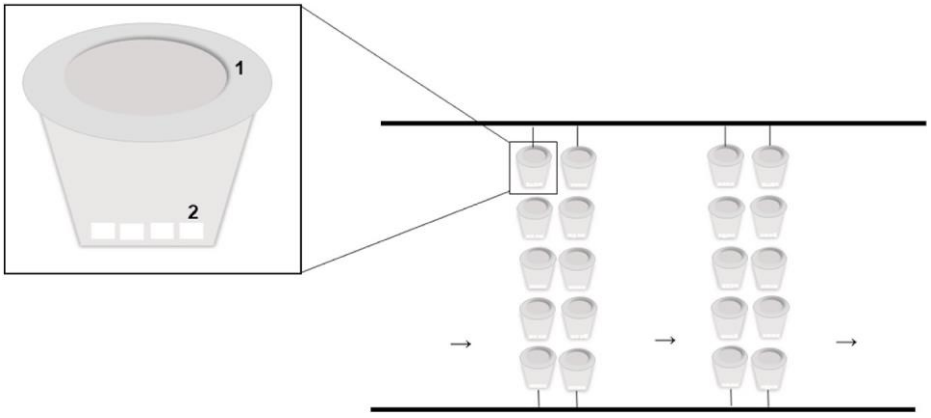

Fig. 5. Proposal of a floating device composed of polypropylene (PP) in which the bioadsorbent are placed inside. The device presents a lid (1) and an opening for thewater entrance (2).

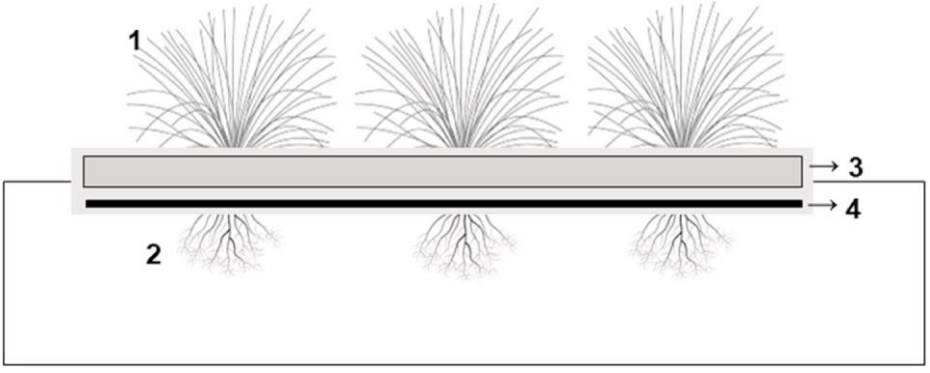

Fig. 6. Combined floating island device with living plants and using bioadsorbents composed of aerial part of the plants (1); submerged roots (2); planting media forthe species (3); adsorbent layer (4) which remains floating in the water column.

3.2 SARS-CoV-2 removal

The concentration of SARS-CoV-2 (2.5×10^6 copies/mL) used was selected to be higher than the levels found in wastewater and the environment, thus guaranteeing that the bioadsorbents developed would be able to remove the viral load efficiently in several different locations that present different background levels of viral particles. Therefore, the application of the biomaterials could attend several low income countries in different scenarios of viral propagation in actual and future pandemic situations. Table 1 presents the concentration of SARS-CoV- 2 found in wastewater in some studies.

It can be seen from Table 2 that the new adsorbents as H. grumosa in natura and H. grumosa activated carbon produced with $ZnCl_2$ impregnation did not differ from commercial activated carbon regarding supernatant and material cycle threshold (CT). The values detected for supernatant were 27.76 ± 0.38 for H. grumosa in natura, 27.3 ± 2.64 for *H. grumosa* activated carbon, and 24.73 ± 0.69 for commercial activated

Table 1
Concentration of SARS-CoV-2 identified in previous studies in wastewater.

Location	Description	Concentration (copies/mL)	Reference
France	Untreated wastewater	$>10^3$	Wurtzer et al. (2020)
Spain	Untreated wastewater	10^2–10^3	Randazzo et al. (2020)
Turkey	Untreated wastewater	1–10^3	Kocamemi et al. (2020)
USA	Primary sludge	1.7 10^3–4.6 10^5	Peccia et al. (2020)

Table 2
Cycle threshold (C_T), viral load(copies mL^{-1}), and removal obtained after 24 h incubation.

	H. grumosa in natura	*H. grumosa* activated carbon	Commercial activated carbon
Control C_T	14.85 ± 0.96		
Viral load in control (copies mL^{-1})	$2.5 \times 10^6 \pm 0.11 \times 10^6$		
Supernatant C_T	27.76 ± 0.38[a]	27.3 ± 2.64[a]	24.73 ± 0.69[a]
Viral load in supernatant (copies mL^{-1})	4.61×10^2	4.54×10^2	36.95×10^2
Material C_T	33.72 ± 1.64[a]	35.04 ± 1.40[a]	32.68 ± 6.00[a]
Viral load in material (copies mL^{-1})	7.19	1.75	12.32
Viral load removed (copies mL^{-1})	4.54×10^2	4.52×10^2	36.83×10^2
Viral load removed (copies mLg^{-1})	4.54×10^4	4.52×10^4	36.83×10^4
Removal (%)	98.44%[a]	99.61% [a]	99.67% [a]

Values are mean ± standard deviation. Means followed by the same letter are not significantly different at the 95% confidence level (Tukey's test).

carbon. In addition, the C_T was also similar for the materials, being the values 33.72 ± 1.64, 35.04 ± 1.40, and 32.68 ± 6.00, respectively. The cycle threshold value (C_T) in RT-qPCR analysis is referred to as the number of amplification cycles that are required for the gene to exceed the threshold level. The values detected for CT are inverse to viral load content, and it represents an indirect method of detection of copy number of viral RNA (Rao et al., 2020).

Regarding the viral load, it was considered a reference number of 2.5 × 10^6 copies mL^{-1} for 15 cycles. Thus, the viral load identified in the supernatant was 4.61 × 102 (copies mL^{-1}) for *H. grumosa* in natura, 4.54 × 10^2 copies mL^{-1}1 for *H. grumosa* activated carbon, and 36.95 × 10^2 copies mL^{-1} for commercial activated carbon.

On the other hand, the viral load detected in the material surface was 7.19 copies mL^{-1} for *H. grumosa* in natura, 1.75 copies mL^{-1} for *H. grumosa* activated carbon, and 12.32 copies mL^{-1} 1 for commercial activated carbon.

Then, it can be seen the viral load per gram removed by each material, being 4.54 × 10^4 copies mL^{-1} by the adsorbent *H. grumosa* in natura, 4.52 × 10^4 copies mL^{-1} for H. grumosa activated carbon, and 36.83 × 10^4 copies mL^{-1} for commercial activated carbon.

In terms of removal percentage, it can be highlighted the excellent results of removal potential of SARS-CoV-2 by the studied adsorbents. The removal potential find was 98.44% for the adsorbent *H. grumosa* in natura, 99.61% for the produced activated carbon from *H. grumosa*, and 99.67% for commercial activated carbon.

The virus surface can interact through hydrogen bonding that is present in the solid surface, which can explain the adsorption phenomena with the new adsorbents found in this study. The C_T, viral loads, and removal percentage results demonstrated the high ability of removal of SARS-CoV-2 using the new adsorbents tested – activated carbon using H. grumosa as precursor and activation with $ZnCl_2$, along with *H. grumosa* in natura, and presenting results similar with the commercial activated carbon.

The strong binding between the surface of the material and the spike S could have caused conformational changes and destabilization of the viral envelope, thus disintegrating and inactivating the SARS-CoV-2 (Pandey, 2020; Xue et al., 2020).

In addition, the hydrophobic interactions might be responsible for the adsorption of viruses to solid surfaces, being the enveloped type more strongly associated with the solids. These hydrophobic interactions depend on several aspects, as the characteristics of the virus and the medium components; and the hydrophobic amino acids present in virus proteins can explain the removal at pH levels above the isoelectric point (Mohapatra et al., 2021).

One previous study has already presented the molecular dynamics simulation of SARS-CoV-2 spike (S) glycoprotein in cellulose surface and it was detected a more stable adsorption process than other materials. This fact may be due to the high hydrogen-bonding propriety of cellulose along with the amphiphilic characteristic of this component (Malaspina and Faraudo, 2020).

The chemical activating agent $ZnCl_2$ used in the production of H. grumosa activated carbon can be highlighted as responsible for enhancing the adsorption. The selected impregnation agent is among the most used for the activation of carbonaceous material and increases the porosity, thus increasing the efficiency of the adsorption process with carbonization yield (Machado et al., 2020).

The yield of the produced activated carbon with *H. grumosa* was 25.18%. Considering the absence of studies using *H. grumosa* as a precursor of activated carbon, the yield was then compared with other lignocellulosic materials that were used in equivalent conditions. In this sense, the yield of activated carbon was similar to results found by Yorgun et al. (2009), whose aim was the preparation of activation carbons presenting high-surface-area from *Paulownia wood* using $ZnCl_2$ activation, and different impregnation ratios and temperatures, presenting a yield of approximately 26% (impregnation ratio of 1:1 and 700 ◦ C). The authors found that this result was higher than the material without activation in the same conditions.

The results of yield for the production of H. grumosa activated carbon using $ZnCl_2$ found in this study were higher than the yield found by Kiliç et al. (2012). The authors were studying the production of activated carbon from *Euphorbia rigida* using different chemical impregnation agents, detected the $ZnCl_2$ with a yield of approximately 20% in the same conditions (impregnation ratio 1:1 and 700 ◦ C).

The chemical activation using $ZnCl_2$ produces activated carbon with a high surface area and this fact is reported in the literature as a result of breaking the lateral bonds in cellulose molecules (Amran and Zaini, 2020). The $ZnCl_2$ yield improvement in activated carbon production is mentioned in several studies since it acts as a dehydrating agent pro- moting the carbonaceous material decomposition and restricts the for- mation of tar (Kaya et al., 2017). The $ZnCl_2$ is known to be largely usedas a catalyst for carbonization to induce the creation ofthree-dimensional (3D)-hierarchical porous structures (Zhang et al., 2018).

The enhancement of the adsorption process can be done through the optimization of the operational parameters including adsorbent dosage, pH, contact time, temperature, and concentration (Anfar et al., 2020). These conditions allow the identification of an optimal process that achieves the maximum removal of the target component – in this case SARS-CoV-2 removal; and each parameter is responsible for showing important information about the adsorption mechanism.

The adsorption investigations commonly start with the understanding of the adsorbent dose effect in the removal. It is expected that higher dosages of adsorbent enhance the adsorption, considering the increased binding sites in the system (Soliman and Moustafa, 2020). Regarding the optimization of contact time in adsorption, regularly, the removal of contaminants increases with increasing contact time and tends to reach stability due to saturation of adsorption sites – achieving the equilibrium and thus allowing the identification of optimum reaction time (Anfar et al., 2020).

The optimization of the pH parameter is essential for enhancing adsorption given its influence on the physicochemical behavior of the aqueous solution and in surface charge of the used adsorbent, dissociation of functional groups, and degree of ionization (Nnaji et al., 2021). Regarding the stability of SARS-CoV-2 in different environmental conditions, Chin et al. (2020) found the virus stable in a wide range of pH (from pH 3 to 10), at room temperature.

Another important parameter highly influencing the adsorption process is the temperature. The understanding of its effects in the adsorption process can be done with thermodynamic studies, pointing to the nature of the process as exothermic or endothermic. According to the nature of the interaction, the temperature presents the possibility of enhancing or reducing adsorption capacity. The parameters investigated in thermodynamic are the ΔG showing the spontaneous nature of the adsorption process, ΔH confirming the nature of adsorption, and ΔS showing the affinity of adsorbent and the nature of randomness to the solid-solution interface (Peydayesh and Rahbar-Kelishami, 2015).

Similarly, the effect of initial concentration of adsorbate affects the efficiency of the adsorption process indirectly since there is a general trend of the adsorption sites to be more easily saturated – thus leading to a reduction in removal. Despite this fact, in some cases, there is an in- crease in the removal of the target contaminant from the solution when this initial concentration is high (Al-Ghouti and Al-Absi, 2020).

One method used for enhancing adsorption is the application of Response Surface Methodology (RSM), which is a set of statistical techniques aiming at the multivariable optimization of the adsorption process, demonstrating the influence of each parameter and the interaction among them using a mathematical model (Hamidi et al., 2021). The detection of SARS-CoV-2 genetic load in wastewater was an innovation that supports the wastewater-based epidemiology (WBE) and environmental surveillance of the COVID-19 pandemic. A study conducted by Kumar et al. (2020) demonstrated the removal of theSARS-CoV-2 in a Wastewater Treatment Plant (WWTP) in India, whichreceives effluent from a hospital with COVID-19 patients. The treatmentmethod was an up flowed anaerobic sludge blanket reactor (UASB) and aeration pond and the authors noticed an increase in C_T in the samples(C_T values higher than 40), meaning minor viral load than the compared one – the effluent sample.

A previous study aiming to inactivate viruses using granular activated carbon modified with combined silver and copper oxide

nanoparticles presented a great effect in inactivation. The metals used were able to inactivate the T4 bacteriophage, one of the seven *Escherichia coli* phages (T1–T7), despite both adsorbent material and adsorbate presenting negative surface charges – occurring van der Waals repulsive electrostatic sum and retarded forces. In addition, the study identifiedthe generation of reactive oXygen species (ROS) followed by subsequent oXidation of amino acids from the proteins of the virus capsid. The copper positive charges form electrostatic bonds with negatively charged sites and the cell membrane was then allowed the silver to enter, causing attack due to binding in specific sites to DNA, RNA, en- zymes, and proteins (Shimabuku et al., 2017).

Another study investigating the agglomeration of viruses by cationic colloidal lignin particles using softwood kraft lignin identified the great potential for using this material in the water purification process in columns or membrane filtration, as long as flocculation and sedimentation agents. It is highlighted as a low-cost alternative for water disinfection along with being an alternative for the commercialization of this co-product (Rivière et al., 2020).

The cost estimation of *H. grumosa* activated carbon production is described in Table 3, considering the precursor material, chemical used in the preparation, along with drying, carbonization, and washing. The total cost for production of 1 kg is estimated at US$ 6.60, which is lower than the commercial activated carbon (approximately US$ 19.53, seen in 2021). The cost for the production of bioadsorbent *H. grumosa in natura* is based on the transportation of biomass, and it can be seen the low cost of US$ 0.01 kg^{-1}.

The cost evaluation estimation along with the removal efficiency allowed the identification of economical and sustainable alternatives for commercial activated carbon production.

Despite further studies are necessary for the implementation of biofilters using the new low-cost adsorbents from *H. grumosa* precursor, the authors idealize three main applications:

i) The system to be proposed is analogous to floating islands, thus using a fluctuant device for the adsorption of SARS-CoV-2, to be placed in the watercourse and removed before the desorption process starts to occur, thus avoiding the resuspension and re-entering of viral particles to the water column.

For such, it is idealized a device whose bioadsorbent remains fixed and whose water passes through and it remains fixed in both sides of the margin when applied in the watercourse (Fig. 5).

ii) The other option is the application of a combined artificial floating island, which uses living plants in a buoyant system, in which the roots of the plants remain in water rizhofiltrating and the shoots arein the upper part of the device (Fig. 6). This combined device pre- sents the benefits of living plants promotes the effects of improving water quality through plant absorption of nutrients and other con- taminants. In addition, there is a natural formation of biofilm in the roots of the plants presenting bacterial and other activities of or- ganisms. The adsorbent layer is then composed of the bioadsorbents produced: *H. grumosa* activated carbon or *H. grumosa in natura.*

The *H. grumosa* usage in constructed wetlands (CW) was reported in several studies. For example, it can be mentioned the research conducted by Horn et al. (2014); Lutterbeck et al. (2017); Dell'Osbel et al. (2020); da Silva et al. (2021). It is highlighted that *H. grumosa* is knownfor its potential in removing contaminants, easy acclimatization and dense root system, and pruning allowed in three or four months (Machado et al., 2015).

In addition, it is highly recommended the evaluation of kinetic along with the equilibrium study in different experimental conditions to understand which kinetics and isotherm models could predict the adsorption process of SARS-CoV-2 onto the bioadsorbent. It might betested the possibility of reuse of adsorbent with specific eluent, along with a recommendation for disposal in the appropriate waste site.

iii) The third application proposal is the use of bioadsorbents in WWTP, in the tertiary treatment stage, as a low-cost substitution of commercial activated carbon. This application stands out as a relevant contributor for conventional treatment, since the first treatment phase, whose physical processes aim to reduce the solids already are responsible for the first viral removal; however, being unable to completely remove the viral load. In addition, the secondary treatment besides presents good removal rates using membrane bioreactor, i.e, it was reported with high energy demanding by previous studies - around 0.45 and 0.65 $kWh{\cdot}m^3$ in higher efficiency (Teymoorian et al., 2021).

It is highlighted also the relevance of treatment options presenting low toXic products aiming at the reduction of secondary pollution along with being an alternative for managing a future crisis. The current need for redesigned treatment options considering a multi-barrier method forviral pathogens is in agreement with the pandemic control measures (Mohan et al., 2021).

4. Conclusions

In this study, it can be pointed out the high ability of the new bioadsorbents in the removal of SARS-CoV-2 from the solution through the adsorption process. The aquatic macrophyte *H. grumosa in natura* and the activated carbon produced with *H. grumosa* biomass and $ZnCl_2$ activating agent demonstrated excellent potential for the virus removal and viral load reduction per gram of the material.

The identification of new adsorbents able to reduce the viral load is extremely important since the behavior and infectiousness of the SARS-CoV-2 in the environment are still unclear. It might be highlighted that despite the immunization program using the SARS-CoV-2 vaccine hav- ing already started in Brazil and the World, it is still unknown how longit will take to reach the critical immunization threshold in the country. Also, using a biomaterial eco-friendly, and cheap is a sustainable alternative for cleaning and also for biomonitoring the occurrence of the virus widespread in the environment.

This research stands out as an innovative alternative for wastewater treatment along with decontamination of watercourses to preventfurther contamination of COVID-19 through waterborne. In addition, it

Table 3
Cost estimation for the production of bioadsorbent *H. grumosa* activated carbon and *H. grumosa in natura* (US$/kg).

	Breakup cost	Temperature/duration/ amount	Unit cost (US $)	Power rating (kWh)	*H. grumosa* activated carbon (US$)	*H. grumosa in natura* (US$)
Biomass collection and transportation			0.01		0.01	0.01
Activation	$ZnCl_2$	1 L	5.21		5.21	–
	Agitation	200 rpm, 24 h	0.06	0.1	(24 × 0.06 x 0.1) 0.144	–
Drying		25 °C, 48 h			0.0	0.0
Carbonization	Heating	700 °C, 1 h	0.06	1.5	(0.06 × 1.5 x 1) 0.09	–
Washing	HCl (3 M)	200 mL	1.15		1.15	–
Total					**6.60**	**0.01**

is highlighted the reduced costs for the production of these adsorbents, since this plant species presents natural growth in polluted watercourses.

This research aimed to provide a complete characterization of the produced activated carbon in accordance with current researches aiming at the production of low-cost activated carbons with low environmental impacts. The characteristic of environment-friendly productionis based mainly on the utilization of a plant species of aquatic macrophyte naturally occurring in contaminated watercourses as the precursor of the material. These plants are phytoremediating these contaminated sites, and sometimes, the presence of this plant in excess causes problems of reducing the light entrance in aquatic environments, along with reducing the available oxygen leading to the death of several organisms. Therefore, in many cases in urban areas, there is a needing of removing this plant to avoid the eutrophication process. This biomass might be then correctly disposed of in specific waste areas as landfills or incineration.

The process of using this phytoremediated biomass as bioadsorbent and for activated carbon production represents a sustainable alternative for re-evaluating this biomass, leading to a high-value product. It might be highlighted that despite presenting a cost estimation for its production, further studies are necessary for the detailed quantification of environmental impacts. However, this research represents a great innovative first step toward environmental and health global issues and aims to assist the protective measures for coping with the SARS-CoV-2 pandemic and future similar conditions mainly in low-incoming countries dealing with basic sanitation issues.

Funding

This study was financed in part by the Coordenação de Aperfeiçoamento de Pessoal de Nível Superior – Brasil (CAPES) – Finance code 001, by the CNPq (National Council for Scientific and Technological Development) and FAPERGS (Research Support Foundation of the State of Rio Grande do Sul) [20/2551-0000263-2].

CRediT authorship contribution statement

Carolina Faccio Demarco: Conceptualization, Data curation, Formal analysis, Investigation, Roles, Writing – original draft, Writing – review & editing. **Thays França Afonso:** Data curation, Formal analysis. **Guilherme Pereira Schoeler:** Data curation, Formal analysis. **Victor dos Santos Barboza:** Data curation. **Liziane dos Santos Rocha:** Data curation. **Simone Pieniz:** Visualization. **Janice Luehring Giongo:** Visualization. **Rodrigo de Almeida Vaucher:** Conceptualization, Data curation, Formal analysis. **Andrei Vallerão Igansi:** Methodology. **Tito Roberto Sant'Anna Cadaval:** Methodology. **Robson Andreazza:** Conceptualization, Funding acquisition, Investigation, Project administration, Resources, Supervision, Writing – original draft, Writing – review & editing.

Declaration of competing interest

The authors declare that they have no known competing financial interests or personal relationships that could have appeared to influence the work reported in this paper.

References

Abdullah, A., Ahmed, A., Akhter, P., Razzaq, A., Zafar, M., Hussain, M., Park, Y.K., 2020. Bioenergy potential and thermochemical characterization of lignocellulosic biomass residues available in Pakistan. Kor. J. Chem. Eng. 1–8. https://doi.org/10.1007/s11814-020-0624-0.

Adelodun, B., Ajibade, F.O., Ighalo, J.O., Odey, G., Ibrahim, R.G., Kareem, K.Y., Bakare, H.O., Tiamiyu, A.O., Ajibade, T.F., Abdulkadir, T.S., Adeniran, K.A., Choi, K. S., 2020. Assessment of socioeconomic inequality based on virus-contaminated water usage in developing countries: a review. Environ. Res. 110309 https://doi.org/10.1016/j.envres.2020.110309.

Adinaveen, T., Kennedy, L.J., Vijaya, J.J., Sekaran, G., 2013. Studies on structural, morphological, electrical and electrochemical properties of activated carbon prepared from sugarcane bagasse. J. Ind. Eng. Chem. 19 (5), 1470–1476. https://doi.org/10.1016/j.jiec.2013.01.010.

Ahmed, W., Bertsch, P.M., Bibby, K., Haramoto, E., Hewitt, J., Huygens, F., Bivins, A., 2020. Decay of SARS-CoV-2 and surrogate murine hepatitis virus RNA in untreated wastewater to inform application in wastewater-based epidemiology. Environ. Res. 191, 110092. https://doi.org/10.1016/j.envres.2020.110092.

Al-Ghouti, M.A., Al-Absi, R.S., 2020. Mechanistic understanding of the adsorption and thermodynamic aspects of cationic methylene blue dye onto cellulosic olive stones biomass from wastewater. Sci. Rep. 10 (1), 1–18. https://doi.org/10.1038/s41598-020-72996-3.

Alves, J.L.F., da Silva, J.C.G., da Silva Filho, V.F., Alves, R.F., de Araujo Galdino, W.V., De Sena, R.F., 2019. Kinetics and thermodynamics parameters evaluation of pyrolysis of invasive aquatic macrophytes to determine their bioenergy potentials. Biomass Bioenergy 121, 28–40. https://doi.org/10.1016/j.biombioe.2018.12.015.

Amran, F., Zaini, M.A.A., 2020. Effects of chemical activating agents on physical properties of activated carbons–a commentary. Water Pract. Technol. 15 (4), 863–876. https://doi.org/10.2166/wpt.2020.094.

Anfar, Z., Ait Ahsaine, H., Zbair, M., Amedlous, A., Ait El Fakir, A., Jada, A., El Alem, N., 2020. Recent trends on numerical investigations of response surface methodology for pollutants adsorption onto activated carbon materials: a review. Crit. Rev. Environ. Sci. Technol. 50 (10), 1043–1084. https://doi.org/10.1080/10643389.2019.1642835.

Arbeláez, A.A., Giraldo, N.D., Pérez, J.F., Atehortúa, L., 2019. Pyrolysis kinetics using TGA and simulation of gasification of the microalga *Botryococcus braunii*. BioEnergyRes. 12 (4), 1077–1089. https://doi.org/10.1007/s12155-019-10037-2.

Bain, W., Lee, J.S., Watson, A.M., Stitt-Fischer, M.S., 2020. Practical guidelines for collection, manipulation and inactivation of SARS-CoV-2 and COVID-19 clinical specimens. Curr. Protoc. Cytom. 93 (1), e77.

Benedetti, V., Patuzzi, F., Baratieri, M., 2018. Characterization of char from biomass gasification and its similarities with activated carbon in adsorption applications. Appl. Energy 227, 92–99. https://doi.org/10.1016/j.apenergy.2017.08.076.

Bind, A., Goswami, L., Prakash, V., 2018. Comparative analysis of floating and submerged macrophytes for heavy metal (copper, chromium, arsenic and lead) removal: sorbent preparation, characterization, regeneration and cost estimation. Geol. Ecol. Landsc. 2 (2), 61–72. https://doi.org/10.1080/24749508.2018.1452460.

Burhenne, L., Messmer, J., Aicher, T., Laborie, M.P., 2013. The effect of the biomass components lignin, cellulose and hemicellulose on TGA and fixed bed pyrolysis. J. Anal. Appl. Pyrol. 101, 177–184. https://doi.org/10.1016/j.jaap.2013.01.012.

CDC, 2020. Centers for Disease Control and Prevention Home Page. Available from. https://www.cdc.gov/coronavirus/2019-ncov/downloads/rt-pcr-panel-fordetection-instructions.pdf. (Accessed 14 February 2020).

Chin, A.W., Chu, J.T., Perera, M.R., Hui, K.P., Yen, H.L., Chan, M.C., Poon, L.L., 2020. Stability of SARS-CoV-2 in different environmental conditions. Lancet Microbe 1 (1), e10. https://doi.org/10.1016/S2666-5247(20)30003-3.

Correa, C.R., Otto, T., Kruse, A., 2017. Influence of the biomass components on the pore formation of activated carbon. Biomass Bioenergy 97, 53–64. https://doi.org/10.1016/j.biombioe.2016.12.017.

da Silva, F.P., Lutterbeck, C.A., Colares, G.S., Oliveira, G.A., Rodrigues, L.R., Dell'Osbel, N., Rodriguez, A.L., Lopez, D.A.R., Gehlen, G., Machado, ÊL., 2021. Treatment of university campus wastewaters by anaerobic reactor and multi-stage constructed wetlands. J. Water Process Eng. 42, 102119. https://doi.org/10.1016/j.jwpe.2021.102119.

De Luna, M.Y., Marcelo Rodrigues, P., Antônia Mabrysa Torres, G., Antônio Eufrázio, D. C.J., Jackson Queiroz, M., Selma Elaine, M., Maria Alexsandra de Sousa, R., 2019. A thermogravimetric analysis of biomass wastes from the northeast region of Brazil as fuels for energy recovery. Energy Sources, Part A Recovery, Util. Environ. Eff. 41 (13), 1557–1572. https://doi.org/10.1080/15567036.2018.1549132.

Dell'Osbel, N., Colares, G.S., Oliveira, G.A., Rodrigues, L.R., da Silva, F.P., Rodriguez, A. L., López, D.A.R., Lutterbeck, C.A., Silveira, E.O., Kist, L.T., Machado, ÊL., 2020. Hybrid constructed wetlands for the treatment of urban wastewaters: increased nutrient removal and landscape potential. Ecol. Eng. 158, 106072. https://doi.org/10.1016/j.ecoleng.2020.106072.

Di Blasi, C., 2008. Modeling chemical and physical processes of wood and biomass pyrolysis. Prog. Energy Combust. Sci. 34 (1), 47–90. https://doi.org/10.1016/j.pecs.2006.12.001.

Dorlass, E.G., Monteiro, C.O., Viana, A.O., Soares, C.P., Machado, R.R.G., Thomazelli, L. M., Araujo, D.B., Leal, F.B., Candido, E.D., Telezynski, B.L., Valério, C.A., Chalup, V. N., Mello, R., Almeida, F.J., Aguiar, A.S., Barrientos, A.C.M., Sucupira, C., De Paulis, M., Sáfadi, M.A.P., Silva, D.G.B.P., Sodré, J.J.M., Soledade, M.P., Matos, S.F., Ferreira, S.R., Pinez, C.M.N., Buonafine, C.P., Pieroni, L.N.F., Malta, F.M., Santana, R.A.F., Souza, E.C., Fock, R.A., Pinho, J.R.R., Ferreira, L.C.S., Botosso, V.F., Durigon, E.L., Oliveira, D.B.L., 2020 Sep. Lower cost alternatives for molecular diagnosis of COVID-19: conventional RT-PCR and SYBR Green-based RT-qPCR. Braz. J. Microbiol. 51 (3), 1117–1123. https://doi.org/10.1007/s42770-020-00347-5. Epub 2020 Aug 7. PMID: 32767275; PMCID: PMC7411266.

Feng, C., Zhang, S., Wang, Y., Wang, G., Pan, X., Zhong, Q., Yao, P., 2020. Synchronous removal of ammonium and phosphate from swine wastewater by two agricultural waste based adsorbents: performance and mechanisms. Bioresour. Technol. 123231. https://doi.org/10.1016/j.biortech.2020.123231.

Foladori, P., Cutrupi, F., Segata, N., Manara, S., Pinto, F., Malpei, F., La Rosa, G., 2020. SARS-CoV-2 from faeces to wastewater treatment: what do we know? A review. Sci. Total Environ. 743, 140444. https://doi.org/10.1016/j.scitotenv.2020.140444.

Ghernaout, D., Elboughdiri, N., Al Arni, S., 2020. New insights towards disinfecting viruses–short notes. J. Water Reuse Desalination 10 (3), 173–186. https://doi.org/10.2166/wrd.2020.050.

González-García, P., 2018. Activated carbon from lignocellulosics precursors: a review of the synthesis methods, characterization techniques and applications. Renew. Sustain. Energy Rev. 82, 1393–1414. https://doi.org/10.1016/j.rser.2017.04.117.

González-García, P., Gamboa-González, S., Andrade Martínez, I., Hernández-Quiroz, T., 2020. Preparation of activated carbon from water hyacinth stems by chemical activation with K_2CO_3 and its performance as adsorbent of sodium naproxen. Environ. Prog. Sustain. Energy 39 (3), e13366. https://doi.org/10.1002/ep.13366.

Goswami, K.P., Pugazhenthi, G., 2020. Credibility of polymeric and ceramic membrane filtration in the removal of bacteria and virus from water: a review. J. Environ. Manag. 268, 110583. https://doi.org/10.1016/j.jenvman.2020.110583.

Gunasekaran, S.S., Bose, R.S., Raman, K., 2019. Electrochemical capacitive performance of zncl2 activated carbon derived from bamboo bagasse in aqueous and organic electrolyte. Orient. J. Chem. 35 (1), 302. https://doi.org/10.13005/ojc/350136.

Hamidi, D., Fard, M.B., Yetilmezsoy, K., Alavi, J., Zarei, H., 2021. Application of Orchis mascula tuber starch as a natural coagulant for oily-saline wastewater treatment: modeling and optimization by multivariate adaptive regression splines method and response surface methodology. J. Environ. Chem. Eng. 9 (1), 104745. https://doi.org/10.1016/j.jece.2020.104745.

Horn, T.B., Zerwes, F.V., Kist, L.T., Machado, ÊL., 2014. Constructed wetland and photocatalytic ozonation for university sewage treatment. Ecol. Eng. 63, 134–141. https://doi.org/10.1016/j.ecoleng.2013.12.012.

Hu, H., Zhang, R., Tao, Z., Li, X., Li, Y., Huang, J., Peng, L., 2018. Cellulose synthase mutants distinctively affect cell growth and cell wall integrity for plant biomass production in *Arabidopsis*. Plant Cell Physiol. 59 (6), 1144–1157. https://doi.org/10.1093/pcp/pcy050.

Joonaki, E., Hassanpouryouzband, A., Heldt, C.L., Areo, O., 2020. Surface chemistry can unlock drivers of surface stability of SARS-CoV-2 in variety of environmental conditions. Inside Chem. 6 (9), 2135–2146. https://doi.org/10.1016/j.chempr.2020.08.001.

Kaya, M., Şahin, Ö., Saka, C., 2017. Preparation and TG/DTG, FT-IR, SEM, BET surface area, iodine number and methylene blue number analysis of activated carbon from pistachio shells by chemical activation. Int. J. Chem. React. Eng. 16 (2) https://doi.org/10.1515/ijcre-2017-0060.

Kiliç, M., Apaydın-Varol, E., Pütün, A.E., 2012. Preparation and surface characterization of activated carbons from *Euphorbia rigida* by chemical activation with $ZnCl_2$, K_2CO_3, NaOH and H_3PO_4. Appl. Surf. Sci. 261, 247–254. https://doi.org/10.1016/j.apsusc.2012.07.155.

Kocamemi, B.A., Kurt, H., Sait, A., Sarac, F., Saatci, A.M., Pakdemirli, B., 2020. SARS-CoV-2 detection in Istanbul wastewater treatment plant Sludges. MedRxiv. https://doi.org/10.1101/2020.05.12.20099358, 2020.05.12.20099358.

Kumar, A., Jena, H.M., 2017. Adsorption of Cr (VI) from aqueous phase by high surface area activated carbon prepared by chemical activation with $ZnCl_2$. Process Saf. Environ. Protect. 109, 63–71. https://doi.org/10.1016/j.psep.2017.03.032.

Kumar, M., Upadhyay, S.N., Mishra, P.K., 2019. A comparative study of thermochemical characteristics of lignocellulosic biomasses. Biores. Technol. Rep. 8, 100186. https://doi.org/10.1016/j.biteb.2019.100186.

Kumar, M., Patel, A.K., Shah, A.V., Raval, J., Rajpara, N., Joshi, M., Joshi, C.G., 2020. First proof of the capability of wastewater surveillance for COVID-19 in India through detection of genetic material of SARS-CoV-2. Sci. Total Environ. 746, 141326. https://doi.org/10.1016/j.scitotenv.2020.141326.

Kumar, M., Mazumder, P., Mohapatra, S., Thakur, A.K., Dhangar, K., Taki, K., Mukherjee, S., Patel, A.K., Bhattacharya, P., Mohapatra, P., Rinklebe, J., Kitajima, M., Hai, F.I., Khursheed, A., Furumai, H., Sonne, C., Kuroda, K., 2021. A chronicle of SARS-CoV-2: seasonality, environmental fate, transport, inactivation, and antiviral drug resistance. J. Hazard Mater. 405, 124043. https://doi.org/10.1016/j.jhazmat.2020.124043.

Lahrich, S., Laghrib, F., Farahi, A., Bakasse, M., Saqrane, S., El Mhammedi, M.A., 2021. Review on the contamination of wastewater by COVID-19 virus: impact and treatment. Sci. Total Environ. 751, 142325. https://doi.org/10.1016/j.scitotenv.2020.142325.

Liu, D., Thompson, J.R., Carducci, A., Bi, X., 2020. Potential secondary transmission of SARS-CoV-2 via wastewater. Sci. Total Environ. 749, 142358. https://doi.org/10.1016/j.scitotenv.2020.142358.

Lua, A.C., Yang, T., 2004. Effect of activation temperature on the textural and chemical properties of potassium hydroxide activated carbon prepared from pistachio-nut shell. J. Colloid Interface Sci. 274 (2), 594–601. https://doi.org/10.1016/j.jcis.2003.10.001.

Lutterbeck, C.A., Kist, L.T., Lopez, D.R., Zerwes, F.V., Machado, ÈL., 2017. Life cycle assessment of integrated wastewater treatment systems with constructed wetlands in rural areas. J. Clean. Prod. 148, 527–536. https://doi.org/10.1016/j.jclepro.2017.02.024.

Machado, ÈL., Lourenço, A.M., Kist, L.T., Schneider, R.C.S., Kern, D., Lobo, E.A.A., Lutterbeck, C.A., Silveira, D.D., Horn, T.B., Zerwes, F.V., 2015. Constructed wetlands integrated with advanced oxidation processes in wastewater treatment for reuse. In: Fatta-Kassinos, D., Dionysiou, D., Kümmerer, K. (Eds.), Advanced Treatment Technologies for Urban Wastewater Reuse. The Handbook of Environmental Chemistry, vol. 45. Springer, Cham. https://doi.org/10.1007/698_2015_372.

Machado, L.M., Lütke, S.F., Perondi, D., Godinho, M., Oliveira, M.L., Collazzo, G.C., Dotto, G.L., 2020. Treatment of effluents containing 2-chlorophenol by adsorption onto chemically and physically activated biochars. J. Environ. Chem. Eng. 8 (6), 104473. https://doi.org/10.1016/j.jece.2020.104473.

Malaspina, D.C., Faraudo, J., 2020. Computer Simulations of the interaction between SARS-CoV-2 spike glycoprotein and different surfaces. Biointerphases 15 (5), 051008. https://doi.org/10.1116/6.0000502.

Mamaní, A., Ramírez, N., Deiana, C., Giménez, M., Sardella, F., 2019. Highly microporous sorbents from lignocellulosic biomass: different activation routes and their application to dyes adsorption. J. Environ. Chem. Eng. 7 (5), 103148. https://doi.org/10.1016/j.jece.2019.103148.

Maneerung, T., Liew, J., Dai, Y., Kawi, S., Chong, C., Wang, C.H., 2016. Activated carbon derived from carbon residue from biomass gasification and its application for dye adsorption: kinetics, isotherms and thermodynamic studies. Bioresour. Technol. 200, 350–359. https://doi.org/10.1016/j.biortech.2015.10.047.

Matsushita, T., Suzuki, H., Shirasaki, N., Matsui, Y., Ohno, K., 2013. Adsorptive virus removal with super-powdered activated carbon. Separ. Purif. Technol. 107, 79–84. https://doi.org/10.1016/j.seppur.2013.01.017.

Mi, X., Albukhari, S.M., Heldt, C.L., Heiden, P.A., 2020. Virus and chlorine adsorption onto guanidine modified cellulose nanofibers using covalent and hydrogen bonding. Carbohydr. Res. 498, 108153. https://doi.org/10.1016/j.carres.2020.108153.

Mohan, S.V., Hemalatha, M., Kopperi, H., Ranjith, I., Kumar, A.K., 2021. SARS-CoV-2 in environmental perspective: occurrence, persistence, surveillance, inactivation and challenges. Chem. Eng. J. 405, 126893. https://doi.org/10.1016/j.cej.2020.126893.

Mohapatra, S., Menon, N.G., Mohapatra, G., Pisharody, L., Pattnaik, A., Menon, N.G., Mukherji, S., 2021. The Novel SARS-CoV-2 Pandemic: Possible Environmental Transmission, Detection, Persistence and Fate during Wastewater and Water Treatment. Science of the Total Environment, p. 142746. https://doi.org/10.1016/j.scitotenv.2020.142746.

Nanda, S., Azargohar, R., Kozinski, J.A., Dalai, A.K., 2014. Characteristic studies on the pyrolysis products from hydrolyzed Canadian lignocellulosic feedstocks. BioEnergy Res. 7 (1), 174–191. https://doi.org/10.1007/s12155-013-9359-7.

Nizam, N.U.M., Hanafiah, M.M., Mahmoudi, E., Halim, A.A., Mohammad, A.W., 2021. The removal of anionic and cationic dyes from an aqueous solution using biomass-based activated carbon. Sci. Rep. 11 (1), 1–17. https://doi.org/10.1038/s41598-021-88084-z.

Nnaji, C.C., Agim, A.E., Mama, C.N., Emenike, P.C., Ogarekpe, N.M., 2021. Equilibrium and thermodynamic investigation of biosorption of nickel from water by activated carbon made from palm kernel chaff. Sci. Rep. 11 (1), 1–20. https://doi.org/10.1038/s41598-021-86932-6.

Pandey, L.M., 2020. Surface engineering of personal protective equipments (PPEs) to prevent the contagious infections of SARS-CoV-2. Surf. Eng. 36 (9), 901–907. https://doi.org/10.1080/02670844.2020.1801034.

Peccia, J., Zulli, A., Brackney, D.E., Grubaugh, N.D., Kaplan, E.H., Casanovas-Massana, A., Ko, A.I., Malik, A.A., Wang, D., Wang, M., Warren, J.L., Weinberger, D. M., Omer, S.B., 2020. SARSCoV-2 RNA concentrations in primary municipal sewage sludge as a leading indicator of COVID-19 outbreak dynamics. medRxiv. https://doi.org/10.1101/2020.05.19.20105999, 2020.05.19.20105999.

Peydayesh, M., Rahbar-Kelishami, A., 2015. Adsorption of methylene blue onto Platanus orientalis leaf powder: kinetic, equilibrium and thermodynamic studies. J. Ind. Eng. Chem. 21, 1014–1019. https://doi.org/10.1016/j.jiec.2014.05.010.

Piriya, R.S., Jayabalakrishnan, R.M., Maheswari, M., Boomiraj, K., Oumabady, S., 2021. Coconut shell derived $ZnCl_2$ activated carbon for malachite green dye removal. Water Sci. Technol. 83 (5), 1167–1182. https://doi.org/10.2166/wst.2021.050.

Powell, T., Brion, G.M., Jagtoyen, M., Derbyshire, F., 2000. Investigating the effect of carbon shape on virus adsorption. Environ. Sci. Technol. 34 (13), 2779–2783. https://doi.org/10.1021/es991097w.

Randazzo, W., Truchado, P., Cuevas-Ferrando, E., Simón, P., Allende, A., Sánchez, G., 2020. SARS-CoV-2 RNA in wastewater anticipated COVID-19 occurrence in a low prevalence area. Water Res. 181, 115942. https://doi.org/10.1016/j.watres.2020.115942.

Rao, S.N., Manissero, D., Steele, V.R., Pareja, J., 2020. A narrative systematic review of the clinical utility of cycle threshold values in the context of COVID-19. Infect. Dis. Ther. 1–14. https://doi.org/10.1007/s40121-020-00324-3.

Rivière, G.N., Korpi, A., Sipponen, M.H., Zou, T., Kostiainen, M.A., Österberg, M., 2020. Agglomeration of viruses by cationic lignin particles for facilitated water purification. ACS Sustain. Chem. Eng. 8 (10), 4167–4177. https://doi.org/10.1021/acssuschemeng.9b06915.

Shimabuku, Q.L., Arakawa, F.S., Fernandes Silva, M., Ferri Coldebella, P., Ueda-Nakamura, T., Fagundes-Klen, M.R., Bergamasco, R., 2017. Water treatment with exceptional virus inactivation using activated carbon modified with silver (Ag) and copper oxide (CuO) nanoparticles. Environ. Technol. 38 (16), 2058–2069. https://doi.org/10.1080/09593330.2016.1245361.

Silveira, E.O., Wink, M., Zappe, A.L., Kist, L.T., Machado, ÊL., 2019. Sistema integrado com microalgas e wetland construído de fluxo vertical no tratamento de efluentes urbanos. Eng. Sanitária Ambient. 24 (2), 305–313. https://doi.org/10.1590/S1413-41522019161655.

Soliman, N.K., Moustafa, A.F., 2020. Industrial solid waste for heavy metals adsorption features and challenges; a review. J. Mater. Res. Technol. 9 (5), 10235–10253. https://doi.org/10.1016/j.jmrt.2020.07.045.

Teymoorian, T., Teymourian, T., Kowsari, E., Ramakrishna, S., 2021. Direct and indirect effects of SARS-CoV-2 on wastewater treatment. J. Water Process Eng. 42, 102193. https://doi.org/10.1016/j.jwpe.2021.102193.

Trassante, C.M., dos Santos Barboza, V., dos Santos Rocha, L., Correa, P.M., Luchese, C., Wilhelm, E.A., de Pereira, C.M.P., Baldissera, M.D., Rech, V.C., Giongo, J.L., de Almeida Vaucher, R., 2021. Detection of SARS-CoV-2 virus using an alternative molecular method and evaluation of biochemical, hematological, inflammatory, andoxidative stress in healthcare professionals. Microb. Pathog. 158, 104975. https:// doi.org/10.1016/j.micpath.2021.104975.

Venugopal, A., Ganesan, H., Raja, S.S.S., Govindasamy, V., Arunachalam, M., Narayanasamy, A., Vellingiri, B., 2020. Novel wastewater surveillance strategy for early detection of SARS-CoV-2 disease 2019 hotspots. Curr. Opin. Environ. Sci. Health 17, 8–13. https://doi.org/10.1016/j.coesh.2020.05.003.10.1016/j.coesh.2020.05.003.

Wang, X., Li, D., Li, W., Peng, J., Xia, H., Zhang, L., Guo, S., Chen, G., 2013. Optimizationof mesoporous activated carbon from coconut shells by chemical activation withphosphoric acid. BioResources 8 (4), 6184–6195

World Health Organization (WHO), 2021. Novel SARS-CoV-2 disease (COVID-19) Situation Report. https://www.who.int/publications/m/item/weekly-epidemiological-update—12-january-2021.

Wurtzer, S.S., Marechal, V., Mouchel, J.M., Moulin, L., 2020. Time course quantitative detection of SARS-CoV-2 in Parisian wastewaters correlates with COVID-19 confirmed cases. medRxiv. https://doi.org/10.1101/2020.04.12.20062679, 2020.04.12.20062679.

Xue, X., Ball, J.K., Alexander, C., Alexander, M.R., 2020. All surfaces are not equal incontact transmission of SARS-CoV-2. Matter 3, 1433–1441. https://doi.org/ 10.1016/j.matt.2020.10.006.

Yin, C., 2020. Genotyping coronavirus SARS-CoV-2: methods and implications. Genomics112, 3588–3596. https://doi.org/10.1016/j.ygeno.2020.04.016.

Yorgun, S., Vural, N., Demiral, H., 2009. Preparation of high-surface area activated carbons from Paulownia wood by ZnCl2 activation. Microporous Mesoporous Mater.122 (1–3), 189–194. https://doi.org/10.1016/j.micromeso.2009.02.032.

Zhang, L., Wang, M., Lai, Y., Li, X., 2018. Oil/molten salt interfacial synthesis of hybridthin carbon nanostructures and their composites. J. Mater. Chem. 6 (12), 4988–4996. https://doi.org/10.1039/x0xx00000x.

Zyoud, A., Nassar, H.N., El-Hamouz, A., Hilal, H.S., 2015. Solid olive waste in environmental cleanup: enhanced nitrite ion removal by $ZnCl_2$-activated carbon. J. Environ. Manag. 152, 27–35. https://doi.org/10.1016/j.jenvman.2015.01.001.

7 Artigo 4

O artigo intitulado “**Resistance mechanisms of *Hydrocotyle ranunculoides* to Cr(VI): a biolfilter plant**” é apresentado conforme submetido na Revista Journal of Cleaner Production, ISSN: 0959-6526, fator de impacto 11.072, classificação A1 na área de Materiais.

Resistance mechanisms of *Hydrocotyle ranunculoides* to Cr(VI): a biolfilter plant

Carolina Faccio Demarco[a], Daisa Hakbart Bonemann[b], Anderson Schwingel Ribeiro[b], Tito Roberto Sant'Anna Cadaval Jr[c], Marcos Alexandre Gelesky[c], Marcelo Godinho[d], Simone Pieniz[e], Robson Andreazza[a*]

[a]*Science and Engineering of Materials Postgraduate Program, Federal University of Pelotas, R. Gomes Carneiro 01, CEP 96010-610, Pelotas, RS, Brazil*

[b]*Chemistry Postgraduate Program, Federal University of Pelotas,Campus Capão do Leão, S/n, Jardim América, CEP96010-900, Capão do Leão, RS, Brazil.*

[c] *School of Chemistry and Food, Federal University of Rio Grande, Av. Itália, Km 8, S/n, Carreiros, CEP 96203-000, Rio Grande, RS, Brazil*

[d]*Process Engineering and Technologies Postgraduate Program, University of Caxias do Sul, Rua Francisco Getúlio Vargas 130, Petropólis, CEP 95070-560, Caxias do Sul, RS, Brazil.*

[e]*Environmental Sciences Postgraduate Program, Federal University of Pelotas. R. Benjamin Constant 989, CEP 96010-020, Pelotas, RS, Brazil*

*Corresponding author: e-mail: robsonandreazza@yahoo.com.br; Phone +55 53 3921 1432; Fax +55 53 3921 1432.

Abstract

Hydrocotyle ranunculoides is an aquatic macrophyte with natural ability of removing heavy metals from environment. The understand of the mechanisms that makes this plant species tolerant and able to remove Cr(VI) are essential for proposing biofilters devices for watercourses decontamination. Therefore, this research aimed to identify the main effects in *H. ranunculoides* that could explain its tolerance to this heavy metal. For such, a treatment with $K_2Cr_2O_7$ with 7 days exposure was performed, along with evaluation regarding growth parameters, photosynthetic pigment, lipid peroxidation via TBARS assay, total phenolic compounds, antioxidant enzymes, FT-IR, chromium and nutrients contents, phytoremediation indexes, surface and cytological observations along with TGA analysis. The main results found suggested that *H. ranunculoides* demonstrated adaptive response to chromium. Considering all the tolerance and excellent removal potential by this plant, it is then proposed a floating biofilter device in order to apply this plant species for chromium decontamination purposes.

Keywords: bioaccumulation, floating island,chromium phytoremediation, sustainable biofilter.

1. Introduction

The increase of chromium release in environment have raised concern worldwide in light of its toxicity and bioaccumulation proprieties (Ukhurebor et al. 2021). The activities that promotes its discharge are industrial sectors as dye production, steel manufacturing and metal smelting (Qu et al. 2021).

This metal can occurs in several oxidation states, being the most commons the Cr (0), Cr (III) and Cr (VI).The chromium in trivalent form is an essentialmicronutrient, being responsible for assisting growth boost and increasing productivity in plants. On the other hand, the hexavalent presentno biological function, along with the characteristic of being highly soluble in water and seriously moretoxic than the other forms of chromium, due to its high oxidizing potential and impacts in nutrient uptake and photosynthesis (Saravanan et al. 2021).

Among the deleterious effects of chromium in plants, it can be cited the inhibition of germination, degradation of photosynthetic pigment, chloroplasts damage,modifications in antioxidant enzymes and cell membrane, along with stress oxidative induction (Sharma et al. 2020).

The oxidative injury by redox metals - such as chromium,can be caused via Haber-Weiss and Fenton reactions, which lead to production of reactive oxygen species (ROS)(Sinha et al. 2018). Plants normally produce these ROS, as superoxide radicals (O_2^-), hydroxyl radicals (OH), hydrogen peroxide (H_2O_2) and oxygen (O_2) in small amounts. However, in stress conditions the production increase significantly, which can cause proteins defragmentation, damage in cell membrane, photosynthetic pigments and DNA, leading to cell death (Adhikari et al. 2020).

The compounds that are responsible for coping with these ROS are antioxidant enzymes, as superoxide dismutase (SOD, E.C. 1.15.1.1), that comprises the first line of defense from oxidative stress (Kumar et al. 2020). Other important enzymes widely studied in plants are the peroxidase (POD, E.C. 1.11.1.7) and catalase (CAT, E.C. 1.11.1.6), mainly eliminating the H_2O_2 (da Conceicão Gomes et al. 2017).

The species *H. ranunculoides* L.,known as floating pennywortis an aquatic floating macrophyte from the Araliaceae family and it occurs in a wide diversity of environments, being native from Americas and invasive in Europe(Walsh and Maestro, 2017). It is a perennial plant with rhizomatous and creeping characteristics, and as other aquatic weeds, *H. ranunculoides* tolerates high amounts of nutrients, therefore being easily found in eutrophic watercourses (Simbanegavi et al. 2018). It was already reported by several studies the ability of this aquatic

plant in removing nutrients and other contaminants, including heavy metalsthough several mechanisms as rhizofiltration and phytoextraction (Demarco et al. 2018; Custodio et al. 2020).

Recent low-cost biofiltersusing aquatic macrophytes were proposed using adsorbents produced with *Hymenachne grumosa*species – in natura and activated carbon forms. The produced adsorbents achievedremoval potential higher than 98% for SARS-CoV-2 and the proposal aimed the application of floating devices using the produced adsorbents and living plants for watercourses decontamination and wastewater treatment(Demarco et al. 2022).

Thus, the aim of this research is to understand the effects of Chromium (VI) in *H. ranunculoides* in order to clarify the mechanisms that makes this species tolerant to this heavy metal. This study intends to assist the proposal and construction of floating devices – biofilters, for decontamination of watercourses.

2. Materials and Methods

2.1 Plant material

The plant material was obtained in the municipality of Pelotas/RS, Brazil. Plants were collected, washed for removing the associated sediments and kept on Clark (1975) nutrient solution for environmentalization. The light period selected was 16h/8h, with a temperature of 25 ºC. Plants were exposed to Cr (VI) different concentrations for 7 days. The Cr (VI) stock solution (1000 mg/L) was prepared with potassium dichromate ($K_2Cr_2O_7$) and was used for preparing the following concentrations: 1 mg L^{-1}, 2 mg L^{-1}, 4 mg L^{-1}, 6 mg $L^{-1}$and 10 mg L^{-1}. The pH was adjusted to 6.5 with NaOH (0.1M). It might be highlighted that the solutions with chromium were prepared with nutrient solution, and the control (0 mgL^{-1}) was composed of only Clark (1975) solution.

Expressed in molarity, the test concentrations were the following:19.23µM(C1); 38.40 µM (C2); 76.92 µM (C3); 115.38 µM (C4) and192.30 µM (C5).

2.2 Plant growth and photosynthetic pigments

The leaf area was measured using graph paper, and the root length was obtained using a digital calliper (150mm, Lorbes). The plant biomass was oven dried (65 ºC) until constant weight, and dry matter production was calculated as follows (Eq. 1):

$$\%\, DM = (100 \times m_{final})/m_{initial} \quad (1)$$

The chlorophyll and carotenoids content were determined using acetone extraction. For this, 500 mg of leaf was grounded in 5mL of acetone (80%), without the presence of light, in order to avoid photo-degradation. For the chlorophyll determination, the absorbance was measured at 661 nm (chlorophyll*a*) and 644 nm (chlorophyll*b*). For carotenoids determination, the absorbance was 470 nm. The concentrations were evaluated as μg g^{-1} (Lichtenthaler 1987).

2.3 Quantification of lipid peroxidation

The thiobarbituric acid-reactive substances (TBARS) was determined according to Ohkawa; Ohishi;Yagi, (1979).The sample – 500 mg of leaf, was then incubatedin acetic acid (20%) pH 3.5, and thiobarbituric acid (0.67%), pH 4.0. The incubation was performed at 95ºC for 60 min, andquickly transferred in iceand then centrifuged at 3500 rpm for 10 min. The reaction products were determined at 532 nm. The concentration was calculated using a standard curve and the results were expressed in nmol of MDA g^{-1} sample.

2.4 Total Phenolic Compounds

The total phenolic compounds were determined with the Folin–Ciocalteu method, using gallic acid as standard (adapted from Swain and Hillis, 1959). The sample was homogenized in methanol, centrifuged in 5000 rpm for 15 minutes. In the supernatant (250 μL), it was added 4 mL of distilled water and 250 μL of Folin–Ciocalteu reagent. The tubes were agitated, and then 0.5 mL of Na_2CO_3(7%) was homogenized and after 2h, the absorbance was measured at 725 nm and the results are expressed in μg of gallic acid per g of sample (μg g^{-1}).

2.5 Assay of antioxidant enzymes

For the assay of antioxidant enzymes, it was prepared an extract containing 500 mg of the leaf tissue of *H. ranunculoides*grounded in 50 nM Tris-HCl buffer (pH=7.5) with 3mM $MgCl_2$and 1mM EDTA. The extract was then centrifuged at 4000 rpm for 20 min.

The superoxide dismutase (SOD) was estimated by measuring the inhibition of the photochemical reduction of nitroblue tetrazolium (NBT) by the enzyme in the reaction mixture containing50 μL extract and 3 mL of a reaction solution (containing 63 μM nitroblue tetrazolium, 1.3 μM riboflavin, 13 mM methionine, 0.1 mM EDTA, 50 mM Tris–HCl pH 8.0). The extract with the reaction solution was kept under light for 20 min, and then the absorbance was measured at 560 nm in spectrophotometer (GIANNOPOLITIS; RIES, 1977).One unit of SOD is defined as the enzyme quantity capable of inhibiting 50% NBT reduction under the assay conditions and the results were expressed as U SOD activity g^{-1}fresh weight.

The catalase (CAT) was determined using 0.3 mL of extract in a solution of 2.5 mL of 50 mM phosphate buffer pH 7.0, and 0.2 mL of hydrogen peroxide (1%). The decrease in absorbance of H_2O_2 was measured at 240 nm, considering a molar extinction rate of 43.6 M cm^{-1} (AEBI, 1984).

Peroxidase (POD) was evaluated using 20 μL of extract in a solution containing 1 mL of H_2O_2(1%), 2.5 mL of 50 mM phosphate buffer (pH 6.1) and 1 mL of guaiacol (1%). The absorbance was determined at 420 nm (UPADHYAYA et al., 1985).

2.6 FT-IR

The functional groupswere identified by using the Fourier Transform Infrared Spectroscopy (FT-IR Shimadzu, IRPrestige-21), in the transmission mode ranging from 400 to 4000 cm^{-1}, with a resolution of 4 cm^{-2} and 32 scans.The software used for plotting the graphics was OriginPro 2019 (Originlab Corporation, Northampton, MA, USA).

2.7 TGA

The thermogravimetric analysis was performed in the TGA-1000 equipment (Navas Instrument), flow of nitrogen gas of 1 L min^{-1} and heating rate of 10 ºC min^{-1}. The software used for plotting the graphics was SigmaPlot 10.0.

2.8 Surface area and pore size characterization

The specific surface area and pore size were estimated by N_2 adsorption using Quantachrome Instruments (Nova 1200e) at 77 K. The methods were the Brunauer, Emmett and Teller (BET) and Barrett- Joyner-Halenda (BJH). The sample followed the degassing temperature of 80 ºC.

2.9 Element content in plant tissues

The chromium content in plant tissues – roots and shoots were determined with HNO_3-$HClO_4$ digestion followed by detection in microwave-induced plasma optical emission spectrometer (MIP OES, Agilent 4200, Australia), equipped with a nebulizer (OneNeb series 2) and a cyclonic nebulizer chamber. The nitrogen was extracted from the atmospheric air using a nitrogen generator (model 4107, Agilent Technologies, Australia), with flow rates of 20 L min^{-1} and 1.5 L min^{-1} for the plasma gas and 1.5 L min^{-1} for the auxiliary gas (nebulization). To plasmaignition, a small flow of Argon gas (Ar) was used, supplied by an internal storage cylinder installed in the device (Agilent Technologies, USA).

2.10 Phytoremediation index

169 The phytoremediation indexes calculated were the Bioconcentration Factor (BCF) and
170 Translocation Factor (TF). The BCF was calculated using the following the equation (Yoon et
171 al. 2006; Chanu and Gupta 2016; Pandey 2016; Sidhu et al. 2018):
172
173 $$BCF = \frac{[Concentration]_{roots}}{[Concentration]_{water}} \quad (2)$$
174
175 Where$[Concentration]_{roots}$ refers to chromium levels in the roots of the plant (mg kg^{-1})
176 and $[Concentration]_{water}$ refers to the chromium content in solution (mg L^{-1}). The Translocation
177 Factor (TF) from the roots to the shoots of the plants was calculated according to Yoon et al.
178 (2006) and Cui et al. (2007), as described in Equation 3, where $[Concentration]_{shoots}$ is the
179 concentration of element in the plant shoots (mg kg^{-1} of aerial biomass).
180 $$TF = \frac{[Concentration]_{shoots}}{[Concentration]_{roots}} \quad (3)$$
181
182 *2.11 Surface morphology*

183 The evaluation of surface morphology was performed using Scanning Electron
184 Microscopy (SEM) with 15 kV(JEOL, JSM 6610 L V, Japan).
185 *2.12 Cyto-histological observations*

186 The cyto-histological analysis by semi-thin sections of shoots of *H. ranunculoides*. The
187 plant tissues were stained with toluidine blue (O'Brien et al. 1964). The tissues were then
188 investigated under light microscope (Olympus CX41).
189 *2.13 Statistical analysis*

190 The experimental design was completely randomized and the software Statistica® version 7.0
191 was used. It was performed the Analysis of Variance (ANOVA), Tukey test ($p<0.05$).
192
193 **3. Results and discussions**
194
195 *3.1 Plant growth and photosynthetic pigments*
196
197 The growth parameters were evaluated to investigate the $K_2Cr_2O_7$effect in this aquatic
198 macrophyte plant species after the contact time. The leaf area (cm^2 $plant^{-1}$), of *H. ranunculoides*
199 (Table 1) presented values ranging from 4.04 ± 0.67cm^2 $plant^{-1}$ to 9.17 ± 1.99 cm^2 $plant^{-1}$. The
200 lowest values were detected in the treatments of 6 and 10 mg L^{-1} hexavalent chromium.

Regarding root length (cm plant $^{-1}$), the values presented a slight decrease as the levels of Cr(VI) increased, with control being detected with 7.43 ± 0.54 cm plant^{-1} and the lowest value was 2.44 ± 0.41cm plant $^{-1}$.

The percentage of dry matter production obtained for *H. ranunculoides* species after 7 days exposure also presented a decreased in values, going from 7.58 % in control treatment to 4.24 % in 10 mg L^{-1}.

Gautam et al. (2021) also detected decreased in these parameters when evaluating the stress protective effect of methanol extract of *Rhododendron arboreum* Leaves in *Vigna radiate* plants exposed to Cr. The authors reported the hexavalent chromium considerably reducing the dry and fresh weight, along with root and shoot length reduction and justified the heavy metal influencing cell division or chromosomes abnormalities leading to issues in mitosis.

The pigment analysis involved the chlorophyll*a*, chlorophyll *b*, chlorophyll*a* + *b* and carotenoids evaluation in *H. ranunculoides* (Fig. 1).The chlorophyll *a* was reported increasing with the incrementing levels of Cr (VI), being the lowest value detected in control (0 mg L^{-1}of Cr (VI), presenting 0.158 µg g^{-1}of chlorophyll *a*), and the highest was at 4mg L^{-1}of Cr (VI), with values of 0.397 µg g^{-1} of chlorophyll *a.*

Contrastingly, regarding chlorophyll *b*, the lowest value was verified at 2 mg L^{-1}ofCr (VI), being 0.038 µg g^{-1}and the highest at4 mg L^{-1}ofCr (VI), being 0.1532µg g^{-1}. The chlorophyll *a* + *b*content verified did not differ among the treatments; and the carotenoids were detected presenting lower values in the control treatment (0 mg L^{-1} of Cr (VI)) with value of0.051 µg g^{-1}and the highest value (0.121 µg g^{-1}) also in the treatment of 4 mg L^{-1} of Cr (VI).

The results obtained in chlorophyll *a*, chlorophyll *b*, chlorophyll *a* + *b* and carotenoids suggested that the tested concentrations of Cr (VI) did not interfere negatively in the photosynthetic pigment production during the experiment duration.

Despite it is widely reported in literature that stress levels may reduce the pigment content in plants, some studies already reported the opposite. Recent advances in area support these studies, which considered that pigment in plants as chlorophyll and carotenoid content can act as scavengers of reactive chemical species, performing defense mechanisms in response to stress (Agathokleous et al. 2020).

The results found in this research are thus in accordance with some studies, as the research conducted by Christou et al. (2021) which evaluate the hexavalent chromium in two different crop species, lettuce (*Lactuca sativa* L.) and wheat (*Triticum aestivum* L.). The authors identified that lettuce leaves presented increased photosynthetic pigments' levels in the higher content of $K_2Cr_2O_7$ (5 and 10 mg L^{-1}).

Zou et al.(2009) investigating the antioxidant response system and chlorophyll in maize seedlings detected that the pigment content increased in seedlings treated with 1 μM Cr(VI) during the first 14 days. In addition, the authors detected that the inhibition of pigments production was strengthened with the duration of stress, being higher with superior exposure time.

The results are also in line with the research of Kundu et al. (2018), whose levels of chlorophyll and carotenoid in leaves of the species *Plantago ovata* also presented an increase with hexavalent chromium exposure up to a certain level, demonstrating an adaptive response to stress with pigment formation and restoration.

3.2 Estimation of lipid peroxidation (TBARS)

The lipid peroxidation in *H. ranunculoides*was estimated using the thiobarbituric acid reactive substances (TBARS) method, being quantified in terms of malondialdehyde (MDA) content (Fig. 2). The treatment with the highest Cr (VI) levels: 6 mgL^{-1} and 10 mgL^{-1} presented a significant increase in MDA content in leaves of *H. ranunculoides.* These values were 1067.81 ± 30.22nmol MDA g^{-1} FW and 823.49 ± 14.84 nmol MDA g^{-1} FW, respectively, while in the control treatment the value was 496.46 ± 29.68 nmol MDA g^{-1} FW, thus indicating enhanced lipid peroxidation in these treatments.

Previous results in the literature demonstrated the incrementing lipid peroxidation with the increasing Cr (VI) levels. Liu et al. (2014), while studying the Cr (III) pre-treatment to alleviate hexavalent chromium oxidative stress in wheat plants, also detected increased TBARS content. This fact was minimized by the pre-treatment whose delay the TBARS accumulation in the studied plants by the Cr (VI), serving as a stress defense.

Another research detecting the increased MDA content in TBARS assay was in a study conducted by Sinha et al. (2014).The investigation aims to screen the biochemical and antioxidant alterations caused by hexavalent chromium in a succulent perennial herb named *Tradescantia pallida*. As mentioned, when referring to TBARS, the authors found that in the three experimental periods, 30, 60, and 90 days, the levels of malondialdehyde were higher than in control samples in both roots and shoots of the plants. The antioxidant activities were detected also with increased levels – such as ascorbate peroxidase, catalase, and peroxidase, thus suggesting that these activities were an essential part for the plant to overcoming Cr-induced oxidative stress.

An additional report demonstrating that the lipid peroxidation levels were higher in Cr (VI) treatment than in control samples was the study performed by Sharmin et al. (2012). The authors were identifying the proteomic and physiological alterations in the roots of the plant species *Miscanthus sinensis* and verified higher levels of lipid peroxidation and H_2O_2 in chromium treated plants. These results indicated that an extensive oxidative damage could have occurred to the root cells. The authors identified around 170 nmol MDA g^{-1}in control samples, against more than 250 nmol MDA g^{-1}inthe higher chromium content (1000 µM). These results were further confirmed by a histochemical assay using Schiff's reagent, which allowed the localization of TBA reactive products *in situ* with high sensitivity, corroborating thus with other studies that reported increased peroxidation induced by heavy metals as arsenic(Ahmad et al. 2021), lead (Huang et al. 2017) and aluminum (Riaz et al. 2018).

Diverging from these results, Kundu et al. (2018), studying the induced stress response in the plant *Plantago ovata* Forsk by Cr (VI), the MDA content was found to be lower in the plants with Cr (VI) treatment than the control. This fact suggests that the membrane damage caused by free radical generation was not noticeable possibly due to an increase in antioxidant levels, also reported by the authors. The MDA values detected by the authors were around 0.7 µmol /L/g FW in control, while inthe Cr (VI) exposure these values range from 0.15 to 0.4µmol /L/g FW with Cr levels of 0.1 mM to 1.8 mM.

The malondialdehyde (MDA)is formed as a product of lipid peroxidation and is considered an indicator of oxidative damage, which may destroy membrane functionality and integrity (Rizvi and Khan 2018). The increase found in MDA content in this study in the highest's Cr (VI) treatment (6 and 10 mg L^{-1}) may indicate that only in these levels the *H. ranunculoides* presented the deleterious effects of oxidative stress.

The chromium-induced generation of reactive oxygen species (ROS) was reported as being closely related to an increase in lipid peroxidation, as several studies indicated (Shahid et al 2017). In addition, heavy metals in general stimulate the formation of ROS by direct transferring of electrons or inhibiting metabolic reactions (Scoccianti et al. 2016). Despite being normally produced by plants, the unbalance among ROS produced by environmental constraints can overwhelm the systems and cause oxidative stress (Berni et al. 2019).

3.3 Total phenolic content

The total phenolic content (TPC) determination in the shoots of the aquatic macrophyte *H. ranunculoides* are shown in Fig. 3.

It can be seen a slight decrease in TPC levels, with exception of the treatment of 4 mg L^{-1} of hexavalent chromium, which showed an increase in TPC, with values of 207.96 ± 12.80µg g^{-1} FW. This resultcan be explained by the fact that this amount of Cr (VI) seems to be the limit before the damages in cell membrane starts to occur in this plant species, previously detected by the TBARS assay.

The defencing characteristic of phenolic compounds can explain the modulation of its different levels depending directly of the stressing factors and the environment circumstance (Kisa et al. 2016). In general, the decrease in phenolic content under chromium stress may be justified by the malfunctioning of the key enzymes responsible for the biosynthesis of these compounds (Levizou et al. 2019).

Islam et al. (2016) showed also a decrease in total phenolic content investigating the use of plant growth promoting bacteria (PGPB) and salicylic acid (SA) aiming to reduce the chromium stress in maize plants. Control was detected presenting around 75 mg g^{-1} FW against 50 mg g^{-1} FW detected in other treatments. The authors identified relative higher amounts of phenolic content under PGPB and SA application, pointing out the improvement of metabolic activity of these plants and activating of antioxidant defense system, according with other assays employed, demonstrating thus the alleviation of oxidative stress at the same time that the TPC was higher.

Another study showing decrease in total phenol content was conducted by Tripathi et al. (2012), investigating the impact of silicon (Si) in rice seedlings exposed to Cr (VI) in hydroponic experiments. The results demonstrated that control was detected presenting approximately 6 mg $g^{-1}$of TPC, and while the Cr treated presented around 3 mg $g^{-1}$of TPC. The authors identified that the Si addition was able to improve the TPC (around 7 mg g^{-1}), thus suggesting a protective role avoiding oxidative stress as indicated also by lower MDA levels.

The phenolic compounds are among the secondary metabolites produced by plants, and presents at least one aromatic ring, with hydroxyl groups. These phenolic compounds are classified in different groups, accordingly with the number of carbon atoms with the basic structure of phenolic –and the main classification are the flavonoids and non-flavonoid groups (i.e. benzoic acids) (Tsimogiannis and Oreopoulou, 2019).In plants, these compounds presents great importance in growth and reproduction, in addition to antioxidant and antimicrobial activities. The antioxidant activity helps to protect the plant against the oxidative stress, since

throughout stress conditions of heavy metal exposure, the phenolic compounds act as metal chelators or even can scavenge the reactive species of oxygen (Vuolo et al. 2019).

Regarding the total phenolic previously identified in aquatic macrophytes, Smolders et al. (2000) has reported some differences in values according with the morphology and classification of these plants, with the fluctuant type presenting 85 µg g^{-1}TPC. The species with floating or emergent leaves were detected with higher TPC than submerged species, and this was related with the own chemical protection of the plant, since the submerged ones are less vulnerable to herbivores and UV radiation.

There is a lack in the literature regarding the total phenolic levels found in *H. ranunculoides.* Maulidiani et al. (2014) aiming to understand the antioxidant activity and chemical characterization of medical herbs, quantified the total phenolic content in *Hydrocotyle bonariensis* and *Hydrocotyle sibthorpioides*and found 28.55 and 56.2 mg GAE. 100 g^{-1} DW, being therefore higher than the values found for *H. ranunculoides.*

3.4 Assay of antioxidant enzymes

Among the antioxidant enzymes, the superoxide dismutase (SOD) in *H. ranunculoides* activity were detected with values of 172.11 U g^{-1} FW in control and the highest value was identified for 4 mg L^{-1} treatment, with SOD activity 195.27U g^{-1} FW (Fig. 4).

SOD activity results were similar with found by Prado et al (2012), investigating summer and winter activities of antioxidative enzymes (G-POD, SOD and CAT) in floating and submerged leaves of *Salvinia minima*, an aquatic macrophyte whose mechanism of Cr (VI) detoxification was detected being related with seasonal alterations. The authors found no significant difference in SOD activity when analysing the floating leaves of *S. minima* species in summer. The tested concentrations tested by the authors were 0,2, 5, 10, and 20 mg L^{-1}Cr(VI) and SOD remained practically unchanged. On the other hand, the submerged leaves in summer presented an increase in this enzymatic response, suggesting that the aquatic macrophytes presents other mechanisms as soluble phenolics (SP) and protein- and non-protein-thiol-containing compounds (THCC) being correlated and involved in antioxidative mechanism of these leaves.

The SOD results were also in accordance with Dazy et al. (2008),studying antioxidant enzyme activities affected by trivalent and hexavalent chromium in *Fontinalis antipyretica* Hedw species. The authors found antioxidant enzyme activity of SOD responding to $K_2Cr_2O_7$ only with Cr concentrations higher than 50 mM. The studied species *Fontinalis antipyretica*

Hedw demonstrated SOD and APX activities being more sensitive to the other analysed salts: $Cr(NO_3)_3$and $CrCl_3$.

The slight increase in SOD activity in Cr (VI) treatment in concentration of 4 mg L^{-1} represent an enhancement of 13.45%. The increased in 4 mgL^{-1} treatment may be related with the accumulation of ROS species activating antioxidative defence and probably justified by the induction of the expression of genes encoding SOD. This result can be demonstrating the oxidative damage occurring in concentrations higher than 4 mg L^{-1} as previously described in TBARS assay. Thus, it can be seen that in this concentrations (6 mgL^{-1} and 10 mgL^{-1}) it was exceeded the scavenging ability of this enzyme (Li et al. 2021). Superoxide dismutase is the first enzyme in ROS detoxification process of converting O_2^- in H_2O_2andcan be located in cytosol, chloroplast, and mitochondria in plant cell (Emamverdian et al. 2018).

The CAT enzyme is responsible for catalysing the dismutation of H_2O_2 into O_2 and H_2O and presents great importance in detoxification of ROS in plant, despite its mechanism being not well understood (da Conceicão Gomes et al. 2017; Prasad et al. 2021). The effect of Cr in catalase (CAT)activity in aquatic macrophytes varies greatly depending on the species being investigated.Therefore,the identification of its levels in *H. ranunculoides* are from great importance.

The CAT activity was detected presenting a slight increase in low Cr treatments (1 mgL^{-1} and 2 mgL^{-1}). However, the CAT remains very similar among all the tested treatments. Adki et al. (2013) studying a potential hyperaccumulator of Cr (VI), *Nopalea cochenillifera,* using a micropropagation protocol identified that concentrations lower than 10 μM of $K_2Cr_2O_7$(lower than the tested levels of this study) induced catalase. On the other hand, levels higher than 100 μM inhibited the activities of CAT, thus presenting activity equal or lower than control. The authors justified the induction of activity with activation of genes encoding CAT, and the inhibition due to protein oxidation.

Haokip et al. (2021) studying the biochemical and antioxidant responses of the aquatic marcrophyte *Ipomoea aquatic* exposed to different concentrations of chromium also did not observe statistical differences in CAT activity in upper stem of the plant. More specifically, for *Ipomoea aquatic*, the Cr (VI) increase catalase in leaf and lower stem in concentrations of 1 – 2 mg L^{-1}. As conclusions, the authors'states that the early oxidative stress was in part mitigated and tolerated and by the activation of antioxidant defense system, in which catalase and proline play significant role. Therefore, the *I. aquatic*easy adaptation to chromium could make possible the use for phytoremediation purposes.

Similar results regarding CAT activity in Cr stress was found by Bah et al. (2011).The authors were identifying the effects on growth, uptake and antioxidative capacity in *Typha angustifolia* after 30 days exposure of 1mM level in soil of Cd, Cr and Pb also found no difference in CAT in *Typha angustifolia* challenged with high doses of Cr. The catalase activity in shoots of Pb presented an increase, while the Cd and Cr treated plant did not differ from control.

The investigation of peroxidase (POD, E.C. 1.11.1.7) in the *H. ranunculoides* species with different Cr (VI) demonstrated an increase in 1 mg L^{-1} treatment. Precisely, the activity of POD in 1mg L^{-1},4 mg L^{-1} and 6 mg $L^{-1}$was 2.05, 1.35, and 1.61 fold higher than control. On the other hand, the highest Cr (VI) concentration – 10 mg L^{-1} was 1.80 fold lower than control, suggesting that this chromium content was responsible for supressing POD activity. The results found were in accordance with previous finding that heavy metals can induce or supress antioxidant enzymes activity (Nagajyoti et al. 2010).

Yan et al. (2020) found the same pattern as this study for the plant species *M. azedarach* while evaluating the phytoremediation potential of plants growing in a large chromium salt–producing factory wasteland in China. The authors found that the peroxidase demonstrated positive responses to a certain level of Cd (II) and Cr (VI) exposure - 5 mg L^{-1} and 10 mg L^{-1}, and higher concentrations (20 mg L^{-1})was responsible for reducing it. The research also revealed that non-enzymatic antioxidants as glutathione (GSH), proline and soluble protein involved in ROS detoxification were correlated with higher levels of metals accumulation potential.

Fan et al (2020) investigating the genes promoting ROS metabolism in subcellular organelles of *Oryza sativa* after Cr (III) and Cr (VI) exposure found POD activity also around 1 – 2 fold higher than control in roots treated with both form of this heavy metal in levels of 2 mg L^{-1}, 8 mg $L^{-1}$and 16 mg L^{-1}.

3.5 Fourier-transform infrared spectroscopy (FT-IR)

The functional groups investigated in *H. ranunculoides* roots and shoots, in different concentration of Cr (VI) in 7 days of exposure are exhibited in Fig. 5. The FT-IR spectra showed peaks between the region of 3500 and 3200 cm^{-1} in both roots and shoots, which refers to the stretching of O-H and N-H groups (Rafi et al. 2017). The peak around 2900 cm^{-1}in both parts of *H. ranunculoides* specifies C–H stretching. 1650 and 1730 cm^{-1} were assigned to C=O from aldehydes and ketones.

The peaks around 1309 and 1423cm^{-1}were related to stretching of C–H. On the other hand, the band around 1000 and 1115 cm^{-1} is related to C–O group, which is the characteristic peak for polysaccharides (Srividya and Mohanty 2009). The increased band in this peak could indicate a binding capacity of this metal in polysaccharide network of *H. ranunculoides.* The mechanisms of entrapment in intra and inter-fibrilliar capillaries/sites of carbohydrateare a result of the concentration gradient and diffusion in cell walls and membranes (Vankar et al. 2008).

An interesting fact to note is that for *H.ranunculoides* shoots there was an increase in band intensity at 3309 cm^{-1}inthe treatment of highest Cr (VI) levels – 10 mg L^{-1}in shoots of the plants, which corresponds to O-H, thus meaning that the hydroxyl groups interacts in Cr(VI) binding. Usman et al. (2019) studying the tolerance and bioaccumulation potential of heavy metals to *Tetraena qataranse*, an shrub plant species, in Qatar, identified through FT-IR analysis the mechanism in which heavy metals were being removed by this plant. The authors states that ion exchange via carboxyl groups in plant´s surface was the predominant process. In addition, it was found bind interactions with the following functional groups: hydroxyl, amide and phosphate.

Another relevant found was the visible alterations in intensity in FT-IR spectra in the roots of *H. ranunculoides*, when comparing the control and the Cr(VI) treatments. This fact demonstrates that the roots were modified greatly regarding functional groups in the exposure time.

3.6 Element content and phytoremediation indexes

The chromium, macronutrients and micronutrients content in plant tissues of *H. ranunculoides* are described in Table 2. The chromium uptake was increased mostly in roots of *H. ranunculoides* in the highest treatment of hexavalent chromium (levels of 6 and 10 mg L^{-1}), presenting values of 1715.49 ± 177.03 mg kg^{-1} and 2327.43 ± 519.79 mg kg^{-1}, respectively. The shoots also presented an increased in Cr uptake, ranging from 223.68 ± 26.32 mg kg^{-1}in control (0 mg L^{-1}) to 2228.63 ± 324.34mg kg^{-1}(10 mg L^{-1}). These results show then that *H. ranunculoides* was found to be an excellent chromium accumulator.

Similar results were found in research aiming the understanding of bioremediation of hexavalent chromium by *Callitriche cophocarpa*, an aquatic macrophyte species. The authors tested the exposure in hydroponic culture up to 3 weeks, and found a significant increase in Cr accumulation levels, reaching almost 4000 mg kg^{-1} after 10 days incubation in 700 µM –

concentration that is more than 3 times higher than the tested in this study. It was highly recommended the *Callitriche cophocarpa*species for hexavalent chromium remediation and for studying the phytoremediation mechanisms of this heavy metal (Augustynowicz et al. 2010).

The Ca content was detected higher in 10 mg L^{-1} treatment in both shoots and roots of *H. ranunculoides,* with concentration of 37257.86 ± 788.79 mg $kg^{-1}$and 17925.83 ± 1645.89 mg kg^{-1}, respectively. Similar results werefound by Gardea-Torresdey et al. (2005) which found calcium content in roots of *Salsola kali* plant species increasing after Cr(VI) exposure – levels of 20 mg L^{-1}. However, theshoots levels of Ca were found to decrease.

The Fe levels were not significant different in shoots of the plant; however, in the roots, the levels of 1mg L^{-1}, 2 mg $L^{-1}$and 4mg $L^{-1}$of hexavalent chromium demonstrated influence in increasing Fe content in this aquatic macrophyte. This result of Fe increasing levels is in accordance with earlier study performed by Kovácik et al.(2014), in which the exposure of chamomile plants to hexavalent chromium also presented an surprising increase in Fe, Ca, Zn, and Cu uptake in its roots.

The uptake of Mn and Mg did not differ statistically in both shoots and roots of *H. ranunculoides.*On the other hand, it can be noticed that Na and K content in roots showed a decresed in the highest treatment of hexavalent Cr (10 mg L^{-1}) comparing with the control, presenting values of 3607.80 ± 127.26 mg kg^{-1} and 37622.67 ± 571.77 mg kg^{-1}, respectively. This fact could be justified by the similarity of chromium structure with other ions, thus interfering in the absorption of other elements, reducing the uptake of some essential nutrients. Other study detected K decreasing levels after chromium exposure was conducted by Gardea-Torresdey et al. (2005). The authors were investigating the Tumbleweed (*Salsola kali*), and after the highest hexavalent Cr treatments (10 and 20 mg L^{-1}), the potassium uptake also presented a significant decrease in the roots.

The B uptake was found to increase in 6 mg L^{-1} in the shoots of the *H. ranunculoides,* at the same time that decrease at 1 and 2 mg L^{-1} in the roots of the plants. Depending on the plant species, the uptake of essential nutrient can vary drastically. Previous study already reported the influence of both Cr III and Cr VI in nutrient uptake in other plants. For example, Liu et al. (2008),investigated the behaviour of *Amaranthus viridis* after hexavalent chromium exposure and it was detected that heavy metal induced decrease in the levels of Zn, Cu, Fe and Mn.

The Translocation Factor (TF) calculated for *H. ranunculoides*is described in Table 3. The other phytoremediation index calculated was theBioconcentration Factor (BCF) of chromium, and the results obtained were 532 ± 42 (for 1 mg L^{-1}treatment), 662 ± 109 (for 2 mg

L^{-1} treatment), 288 ± 32 (for 4 mg L^{-1}treatment), 255 ± 61 (for 6 mg L^{-1}treatment) and 273 ± 12 (for 10 mg L^{-1} treatment).

Regarding Translocation Factor (TF), it can be seen from Table 3 that Na, Ca and Mgpresented translocation factor higher than 1.0 in all hexavalent chromium treatment. The macronutrient K also presented TF>1.0, excepting in the highest treatment tested (6 and 10 mg L^{-1}). Then, It can be noticed that for K, the higher levels of Cr seems to affect the tranloscation ability.

Regarding the Translocation Factor (TF) of Cr, it can be seen that the values >1.0 were identified also in the highest treatment of hexavalent chromium (levels of 6 and 10 mg L^{-1}). It is widely known in literature that plants presenting a good translocation ability (TF > 1) along with high BCF values (BCF > 1) are recommended for use in phytoextraction technique – a phytoremediation application in which the plant accumulate the contaminant in question in its shoots (Yoon et al. 2006). Thus, it was verified that *H. ranunculoides* could be applied in phytoextraction technique when the levels of hexavelent chromium are higher than 6 mg L^{-1} in environment.

On the oher hand, when the plant presents low translocation potential (TF < 1) and high BCF values (BCF > 1.0), the mechanisms performed is the rhizofiltration – meaning that the plant retain the most Cr content in its roots. This aspect thus highlight the recommendation for application of *H. ranunculoides*in rhizofiltration technique, when the levels of Cr (VI) are lower than 6 mg L^{-1}. This fact was in accordance with the results already found in previous study identifying the natural potential of *H. ranunculoides*in situ phytoremediation of heavy metals at Santa Bárbara stream, in southern Brazil (Demarco et al. 2018). The plant in the study exhibited high potential to uptake higher levels of chromium in the roots, thus naturally rhizofiltrating chromium in the contaminated environment.

The elements Fe and Mn, in all treatments, presented TF <1.0, and demonstrated that the hexavalent chromium did not change the translocation of these elements, despite the iron levels exhibited an increase in roots, as previously described.

3.7 Scanning Electron Microscopy (SEM)

The surface morphology of *H. ranunculoides*evaluated by Scanning Electron Microscopy (SEM) (Fig. 6) revealed that the aquatic macrophyte species presented alterations mainly regarding the appearance of microorganisms as a response to heavy metal tolerance, as several algae (Fig. S1 g and h), and cocci bacteria (Fig. S1 a, c and d).

Zhang et al. (2016) investigating the submerged aquatic macrophytes and its surface biofilms also verified some algae presence and mainly cocci bacterial in SEM images of plant surface. The authors aimed to understand the bacterial community structure and denitrifiers exposed to nitrate.

It is thus highly recommended the identification of bacterial species Cr-resistant, which may be able to tolerate, reduce or bioaccumulate chromium. This identification could be done based on rRNA 16S gene sequence analysis and might point out interesting species for bioremediation purposes, revealing the richness and diversity of microbial communities under Cr(VI) stress.

3.8 Cyto-histological analysis

The observations of *H. ranunculoides*shoots stained with toluidine blue are adaxialepidermal cells (Fig. 7).

The epidermal cells in the highest Cr(VI) treatment (Fig. 7f) were jigsaw puzzle in shape with deeply lobed anticlinal cell walls. The reason of this alteration in cell walls to puzzle shape remains unclear in literature until now. However, it is known that the formation is a result of the cell growth in confined space and the theory is that might exist a signalling mechanism linking neighbouring cells and the mechanisms in which this cells are formed seems to be related with microfilaments and microtubules (Bidhendi et al. 2019).

Meanwhile, Punwong et al. (2017) studying the effects of other contaminants - oil spills in leaf anatomical characteristics of *Terminalia catappa* L. found different results. The authors detected the cell walls with puzzle-form in plants located in control site (non-contaminated), instead the straight form found in shoots of the plant in contaminated site with oil spills. In the research, it was reported that the leaf anatomy could be used as an alternative method for monitoring environmental pollutants, using the plant as bio-indicators.

The analysis of epidermal cells also allowed the identification of alteration and closure of stomata (Fig. 7f), plant organ responsible to regulate the influx of carbon dioxide and efflux of transpiration water. The stomatal movement can be a response of several factors in plants, as environmental conditions, biotic stress or intracellular signalling. However, heavy metals can directly induce the stomata closure as an early effect of the toxicity in plants and there are several studies reporting the anomalous/non-functioning stomata appearance as a response to heavy metals (Rucinska-Sobkowiak 2016).

Faisal and Hasnain (2005) detected Cr(VI) reducing bacteria influencing in sunflower mechanisms of coping with this heavy metal stress. The authors identified that the bacterial

inoculation alleviates the damage in guard cell of stomata caused by hexavalent chromium. It was also verified the disintegration of leaf cells and tissues in plants without the inoculation of the selected bacteria.

Another study showing the stomatal damage after Cr(VI) exposure was performed by Gautam et al.(2021). The authors were studying the protective effect of methanol extract of *Rhododendron arboreum* Leaves (MEL) on Chromium-Treated *Vigna radiata* plants and detected the more open a nicely shaped stomata, with proper functioning when compared to the control sample as signal of stress amelioration. Other findings were related with reduction of H_2O_2 accumulation and reduction of MDA content.

Considering the excellent results of this research, a proposal of floating biofilters using *H. ranunculoides* aquatic macrophyte species could be easily proposed. According with new low cost biofilters proposal using *Hymenachne grumosa* as precursor (Demarco et al. 2022), it is thus recommended an adaptation for applying *H. ranunculoides*in the floating system. It is then developed an new model proposal for this species, as can be seen in Fig. 8.

The functioning is based in the ability of the plant removing the target contaminant until reaching its capacity support, and to be removed from the environment before the plant dying, thus avoiding the contaminant to re-enter in the water column.

3.9 TGA analysis and BET/BJH

The thermogravimetric analysis (Fig. 9) was performed aiming the proposal of using the biomass from biolfilters as precursor for new adsorbents for heavy metals, after its natural cycle of removing contaminants in floating devices. In addition, the alternative aim to indicate another option for treating wastewater using this new adsorbent produced, at the same time that redirect this heavy metal loaded biomass. The correct management of contaminated phytoremediation biomass is essential to avoid the secondary pollution.

Along with thermogravimetric analysis, other characteristics of the raw material highly influencing the bioadsorbents to be produced are the specific surface area and pore size. The results found for *H. ranunculoides* regarding these analyses were 8.24 $m^2 g^{-1}$for specific surface area, and pore diameter of 4.36 nm.

As is noticeable, the thermal degradation of *H. ranunculoides* showed two main weight losses (Fig. 9). The first was detected in 100^{o}C, related with moisture elimination. The second was found from 240^{o}C to 850^{o}C, presenting an endothermic peak in 308^{o}C. For *H. ranunculoides*, over 400 ^{o}C, the weight loss may be due the carbon residues reactions, and the final percentage found of 7.44% was related to the char after decomposition.

The temperature around 300ºC was found to be related with hemicellulose degradation (De Luna et al., 2019). The degradation of cellulose is commonly reported occurring in the range of 325 and 375ºC. Similar patters was found by Muradov et al. (2014) studying the thermic behaviour of aquatic macrophytes *Azolla filiculoides* and duckweed *Landoltia punctata* aiming the application of this species in renewable fuels and petrochemicals production. The authors also found the second phase of thermic decomposition around 200 and 400 ºC, referring to the start of breaking chemical bonds, with less thermally stable compounds degrading first.

It is recommended supplemental studies aiming the characterisation of the generated pyrolysis products, for the environmental risk assessment. Huang et al. (2018) studying the effects of pyrolysis temperature in biochar from phytoremediation found that higher temperatures (over 550 ºC) were able to decrease the soluble fraction of the studied heavy metals, reducing thus its bioavailability and risks of bioaccumulation in organisms. The selected metals for the investigation were Pb (II), Cd (II) and Zn (II). The authors characterized the phytoremediation residue - *Brassica juncea* harvest residue as presenting a specific surface area (S_{BET}) of 1.15 m^2 g^{-1}. The produced biochars from phytoremediation residue increased considerably the S_{BET}, reaching 241.33 m^2g^{-1}in the treatment with 750ºC pyrolysis.

The pyrolysis was already reported as efficient sustainable alternative for disposal of biomass from phytoremediation. He et al. (2019), studying the pyrolysis of heavy metal contaminated *Avicennia marina* biomass from phytoremediation, identified that in overall, the technique was effective in converting metal loaded biomass in high added value products. The authors tested temperature ranging from 300 to 800 ºC and identified that the factors: temperature and presence of heavy metals - affected the properties of the generated products. In addition, the heavy metals in plant biomass were found to contribute to higher biochar and pyrolytic gas yield in bio-oil production.

4. Conclusions

H. ranunculoides has been studied as a high potential phytoremediator plant for heavy metals and with important biofilter characteristics. Also, this study could represent the first communication of *H. ranunculoides* resistance mechanisms for Cr(VI) exposure. The chromium levels in plant shoots and roots, along with phytoremediation indexes exhibited great potencial for removing this extremely toxic metal. It is then highlighted the outstanding innovative character presented in this research, unreveling the mechanisms in which this aquatic

macrophyte tolerates and bioacumulates chromium and it is proposed a practical application of biofilters.

Among the main results found, some aspects need to be reinforced. Firstly, the pigment analysis demonstrated that *H. ranunculoides* seems to be able to restore its photosyntetic pigment production as a form of adaptation to this stress condition. Another important found was that the damage measured as lipid peroxidation reveals that only above 6 mg L^{-1} that Cr(VI) could affect this plant species. Regarding enzymatic activitites, it was found CAT inhibition occuring maybe due protein oxidation.

The study of functional groups through FT-IR analysis demonstrated alteration in *H. ranunculoides*, highlighting that the shoots of this plant, in the highest Cr(VI) treatment of 10 mg L^{-1}, the O-H groups seems to interacts in the metal binding and could have a role in chromium resistance mechanisms in the studied plant.

Another important find was the formation of puzzle shape epidermal cells, found clearly in the 10 mg L^{-1} Cr(VI) treatment. With further studies, this found can be used also as a bioindicator of chromium stress condition. The analysis also allowed to verify stomatal damage as a consequence of metal exposure.

A biofilter device was proposed in this study, aiming the removal of chromium from watercourses and represents an innovative solution for Cr polluted aquatic environments. Considering another use for plant biomass after biofiltration, the TGA analysis was performed and demonstrated the thermal behaviour of the aquatic macrophyte. The authors point out that the production of new adsorbents using the pyrolysis are quite possible and allow the sustainable re-use of the biomass, being able to remove other heavy metals in its dry form.

Further studies are recommended focusing on other antioxidant enzymes activities, as ascorbate peroxidase (APX), and glutathione peroxidase (GPX) activities in order to better understand the tolerance mechanisms, considering that other studies demonstrated that they present a role in Cr detoxification in plants. Despite that, this first understand reported in our study can certainly help to clarify other plant – metal resistance mechanisms, and to propose new biofilters systems for water decontamination.

Acknowledgments

This study was financed in part by the Coordenação de Aperfeiçoamento de Pessoal de Nível Superior – Brasil (CAPES) – Finance code 001, by the CNPq (National Council for Scientific

668 and Technological Development) and FAPERGS (Research Support Foundation of the State of
669 Rio Grande do Sul).
670

671 **Table 1 –**Effect of Cr(VI) in aquatic macrophyte *H. ranunculoides* leaf area, root length, fresh
672 weight and dry matter production after 7 days of exposure.

Cr(VI) treatment	**Leaf area ($cm^2 plant^{-1}$)**	**Root length (cm $plant^{-1}$)**	**Dry matter (%)**
0 mg L^{-1}	6.47 ± 0.70[a]	7.43 ± 0.54[a]	7.58 %
1 mg L^{-1}	7.64 ± 1.36[a]	4.83 ± 1.38[a]	5.51 %
2 mg L^{-1}	8.05 ± 1.10[a]	3.81 ± 1.09[a]	5.28 %
4 mg L^{-1}	9.17 ± 1.99[a]	2.44 ± 0.41[a]	6.07 %
6 mg L^{-1}	4.04 ± 0.67[a]	4.87 ± 0.24[a]	4.08 %
10 mg L^{-1}	4.19 ± 1.34[a]	4.15 ± 1.90[a]	4.24 %

673

674 Values are mean ± standard error; Means followed by the same letter in column are not significantly different at
675 the 95% confidence level (Tukey's test).

Table 2– Effects in elements uptake in roots and shoots of *H. ranunculoides* after different hexavalent chromium exposure.

		0 mg L^{-1}	1 mg L^{-1}	2 mg L^{-1}	4 mg L^{-1}	6 mg L^{-1}	10 mg L^{-1}
Cr	Shoots	223.68 ± 26.32b	392.89 ± 61.34ab	549.01 ±129.68ab	661.28 ± 38.35ab	1943.31 ± 777.51 ab	2228.63 ± 324.34a
	Roots	249.84 ± 44.05 c	531.99 ± 41.99 bc	1323.54 ± 218.52 abc	1153.99 ± 127.07 abc	1715.49 ± 177.03 ab	2327.43 ± 519.79 a
Ca	Shoots	20805.92 ± 1069.08 b	16918.49 ± 912.39 b	21283.78 ± 2533.78 b	19471.15 ±721.15 b	22195.31 ± 2765.26 b	37257.86 ± 788.79 a
	Roots	12645.75 ±755.51 b	12996.22 ± 273.01 b	12321.51 ± 139.31 b	12344.90 ± 116.64 b	16513.98 ± 425.27 ab	17925.83 ± 1645.89 a
B	Shoots	223.68 ± 26.32 b	192.57 ± 9.64 b	176.13 ± 3.58 b	165.11 ± 3.15 b	303.47 ± 7.41 a	213.40 ± 5.67 b
	Roots	202.50 ± 26.16 ab	117.69 ± 2.31 c	150.56 ± 2.26 bc	176.63 ± 1.94 abc	180.87 ± 0.58 ab	218. 71 ± 5.39 a
Fe	Shoots	2486.84 ±513.16 a	2125.08 ±410.14 a	2523.31 ±7.35 a	2567.96 ± 76.27 a	3049.97 ± 447.44 a	3499.52 ± 406.73 a
	Roots	6662.64 ±197.12 d	10978.95 ± 978.95 abc	14355.43 ± 13.73 a	12575.13 ± 463.33 ab	9111.02 ± 1050.27 bcd	8561.56 ± 253.18 cd
Mn	Shoots	344.89±117.61 a	694.15±87.54a	747.00±12.20 a	827.41±254.32 a	1154.11±207.73a	1105.31±67.37 a
	Roots	2255.57±518.73 a	2838.43±98.43 a	2904.42±591.34 a	2764.88±235.12 a	2883.80±597.51 a	3583.41±649.38 a
Mg	Shoots	5281.93±406.93 ab	4527.21±68.37 b	4200.95±400.28 b	3851.94±114.40 b	3620.64±265.37 b	6862.11±612.11 a
	Roots	3539.64±12.99 a	3369.77±169.77 a	2375.55±272.75 a	2487.71±42.05a	3266.51±121.34a	2692.82±899.99a
Na	Shoots	6219.43 ±530.57 a	5349.32 ±595.80 a	5223.97 ±47.59 a	4770.96 ±36.74 a	4596.75 ± 929.56 a	3781.82 ± 44.71 a
	Roots	6028.99±83.87 a	4176.92±23.08 bc	4223.01±226.14 bc	4577.51±35.58 b	4399.12±76.69 b	3607.80 ± 127.26 c
K	Shoots	66780.96±5780.96 a	73166.25±4.48 a	71837.43±4429.46 a	61696.19±5205.80 a	27691.35±8743.98 b	20529.33 ±5709.74 b
	Roots	60660.70±523.51 a	52501.15±4801.15 ab	46119.41±1960.53 bc	44914.72±892.98 bc	52011.42±609.55 ab	37622.67 ± 571.77 c

* Values are Mean ± standard error. Different lowercase letters in lines indicate a statistical difference in *H. ranunculoides* according to Tukey's test ($p < 0.05$).

679 **Table 3–**Translocation Factor (TF) detected in the *H. ranunculoides*after hexavalent chromium
680 exposure.

	0 mg L^{-1}	**1 mg L^{-1}**	**2 mg L^{-1}**	**4 mg L^{-1}**	**6 mg L^{-1}**	**10 mg L^{-1}**
Cr	0.94 ± 0.27 a	0.73 ± 0.06 a	0.44 ± 0.17 a	0.58 ± 0.03 a	1.10 ± 0.34 a	1.07 ± 0.38 a
B	1.11± 0.01b	1.64 ± 0.11 a	1.17 ± 0.01b	0.93 ± 0.01b	1.68 ± 0.04 a	0.98 ± 0.002b
Fe	0.37 ± 0.07 ab	0.19 ± 0.02 b	0.18 ± 0.001 b	0.20 ± 0.001 ab	0.33 ± 0.01 ab	0.41 ± 0.06 a
Mn	0.15 ±0.02 a	0.24 ± 0.02 a	0.27 ± 0.05 a	0.31 ± 0.12 a	0.43 ± 0.16 a	0.32 ± 0.04 a
Na	1.03 ± 0.10 a	1.28 ± 0.14 a	1.24 ± 0.08 a	1.04 ± 0.0001 a	1.04 ± 0.19 a	1.05 ± 0.05 a
			Macronutrients			
Ca	1.66 ±0.18 a	1.30 ±0.10 a	1.73 ± 0.19 a	1.58 ±0.04 a	1.34 ±0.13 a	2.10 ± 0.24 a
Mg	1.49 ±0.11 a	1.35 ±0.05 a	1.77 ± 0.45 a	1.55 ± 0.02 a	1.11 ± 0.12 a	2.95 ± 1.21 a
K	1.10 ± 0.09 a	1.41 ± 0.13 a	1.56 ± 0.16 a	1.38 ± 0.14 a	0.53 ± 0.17 a	0.54 ± 0.14 a

681 * Values are Mean ± standard error. Different lowercase letters in lines indicate a statistical
682 difference in *H. ranunculoides* according to Tukey's test ($p < 0.05$).
683
684

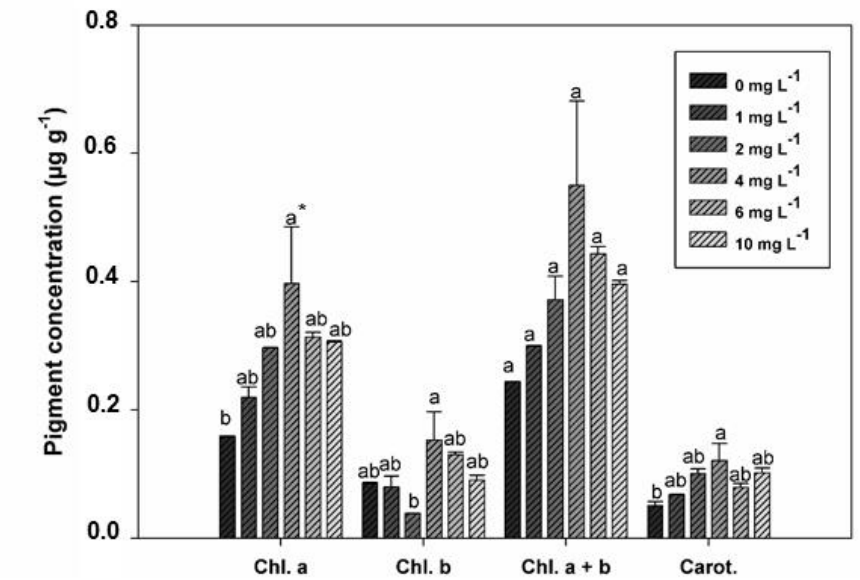

Fig. 1- Photosynthetic pigments levels in *H. ranunculoides* in different Cr (VI) treatments. *Means followed by the same letter are not significantly different at the 95% confidence level (Tukey's test).

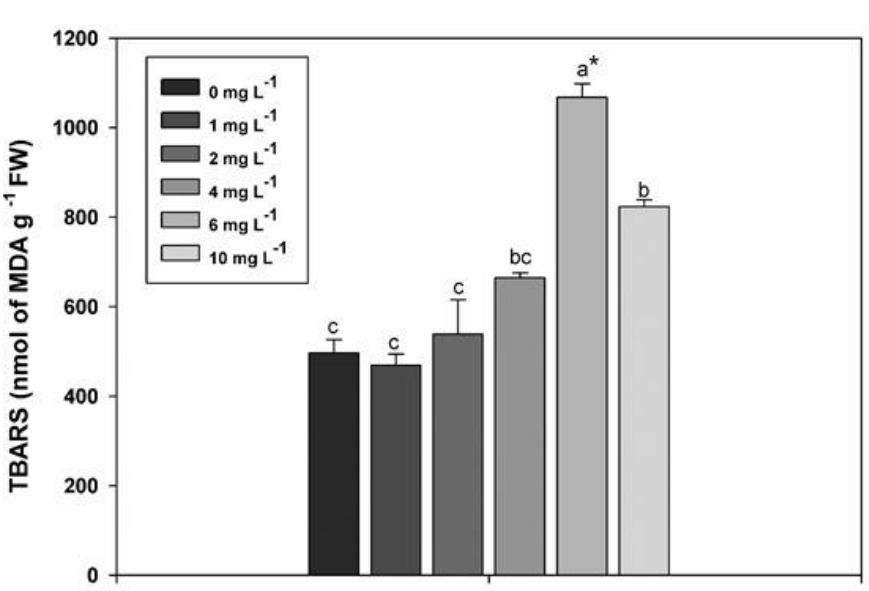

692 **Fig. 2 -**TBARS levels (nm MDA g^{-1} FW) in *H. ranunculoides* in different Cr (VI) treatments.
693 *Means followed by the same letter are not significantly different at the 95% confidence level
694 (Tukey's test).
695
696

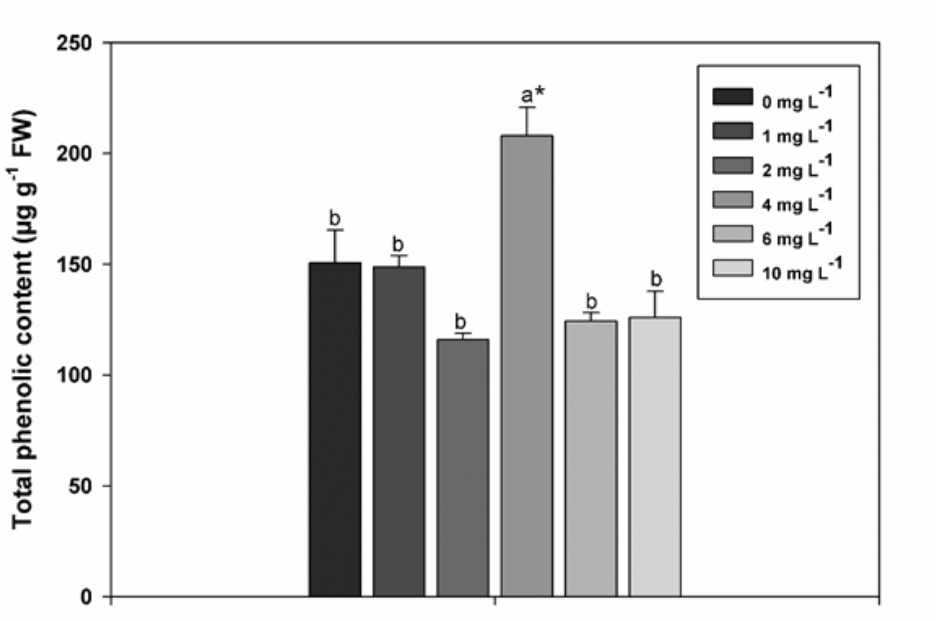

Fig. 3 -Total phenolic content (µg g^{-1} FW) in *H. ranunculoides* in different Cr (VI) treatments. *Means followed by the same letter are not significantly different at the 95% confidence level (Tukey's test).

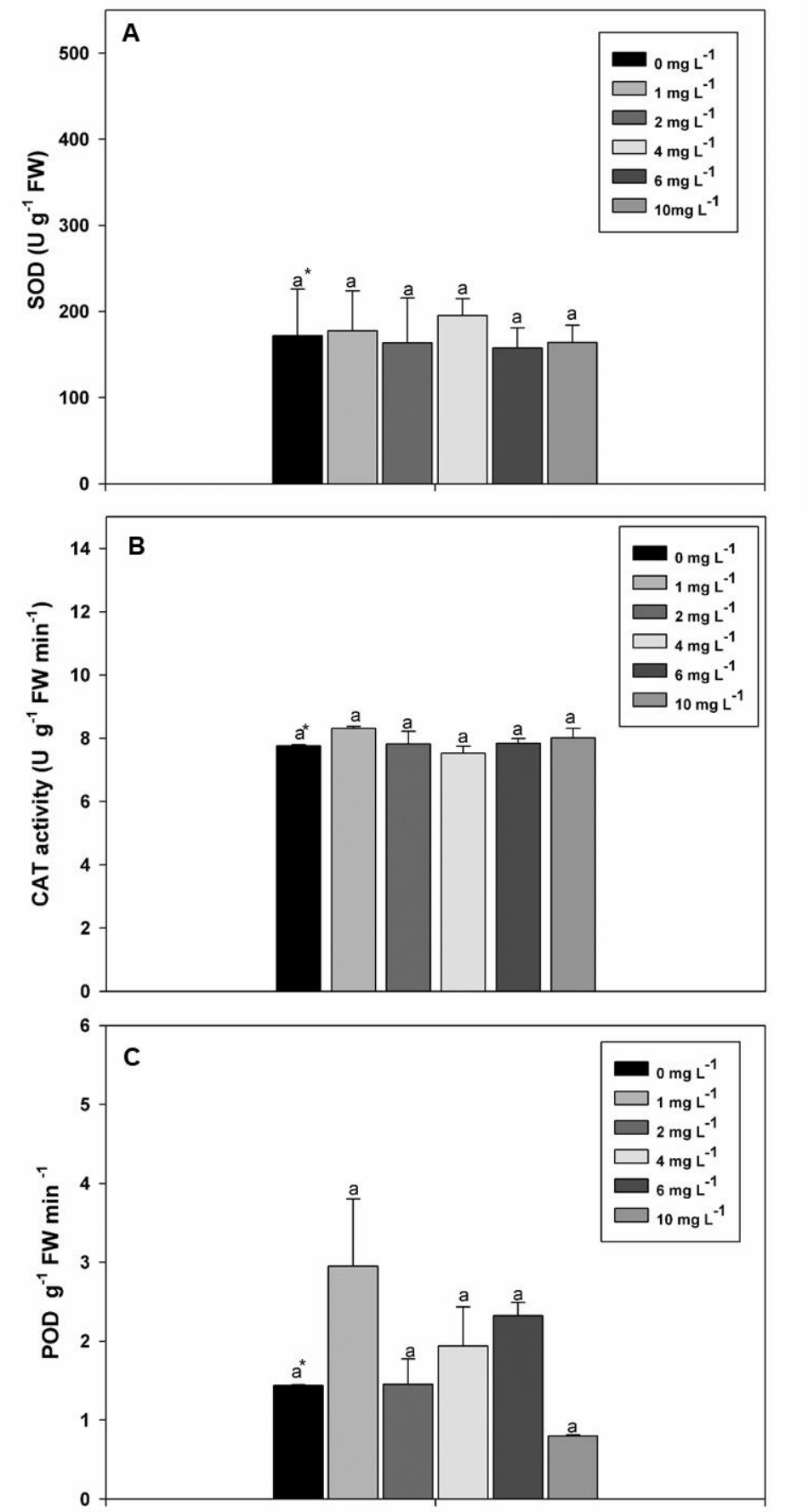
A
SOD (U g-1 FW)
0
100
200
300
400
500
a*
a
a
a
a
a
0 mg L-1
1 mg L-1
2 mg L-1
4 mg L-1
6 mg L-1
10mg L-1
B
CAT activity (U g-1 FW min-1)
0
2
4
6
8
10
12
14
a*
a
a
a
a
a
0 mg L-1
1 mg L-1
2 mg L-1
4 mg L-1
6 mg L-1
10 mg L-1
C
POD g-1 FW min-1
0
1
2
3
4
5
6
a*
a
a
a
a
a
0 mg L-1
1 mg L-1
2 mg L-1
4 mg L-1
6 mg L-1
10 mg L-1

702
703

704 **Fig. 4 –**Enzymatic antioxidant activities in *H. ranunculoides* in different Cr (VI) treatments; a)
705 Superoxide dismutase (SOD) (U g^{-1} FW); b) Catalase (CAT) activity (U g^{-1} FW min^{-1};
706 c)Peroxidase (POD)g^{-1} FW min^{-1}. *Means followed by the same letter are not significantly
707 different at the 95% confidence level (Tukey's test).
708

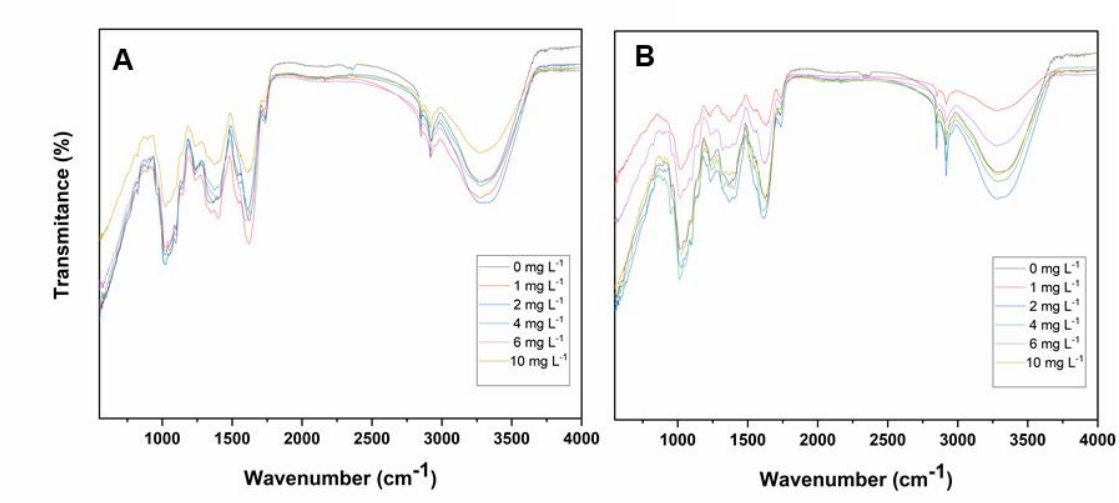

709
710 **Fig. 5 –** Functional groups observed in *H. ranunculoides* (a) shoots and (b) roots in different
711 concentration of Cr (VI) in 7 days of exposure.
712
713

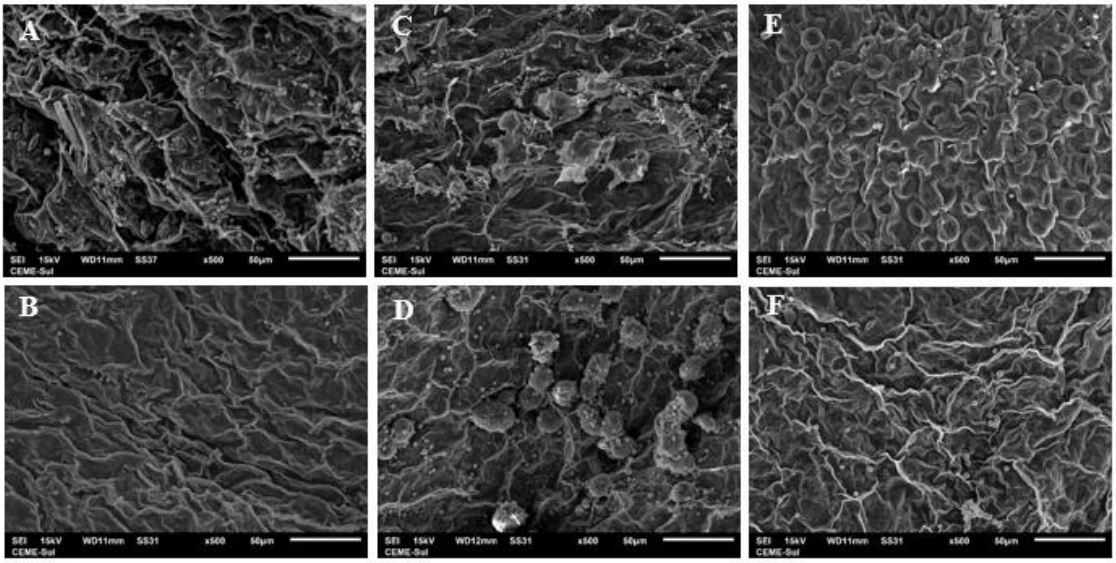

Fig. 6 - SEM image of *H. ranunculoides* shoots surface at different Cr(VI) treatments (a) control - 0 mg L^{-1}, (b) 1mg L^{-1} (c) 2mg L^{-1} (d) 4mg L^{-1} (e) 6 mg $L^{-1}$and (f) 10mg L^{-1} after 7 days exposure.

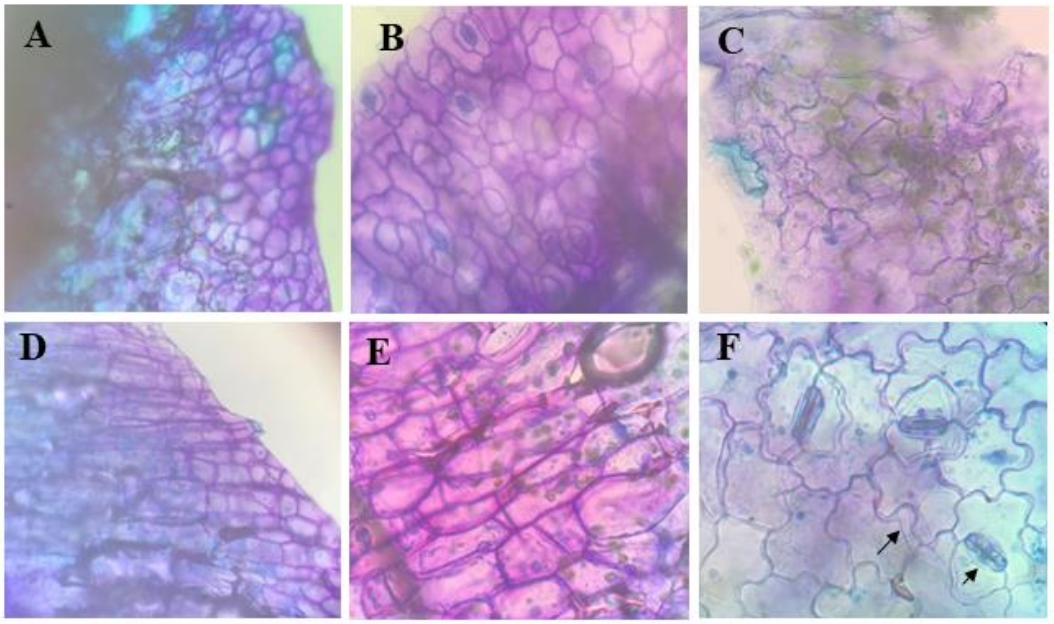

Fig. 7–*H. ranunculoides* shoots sections stained with toluidine blue showing the variation in epidermal cells after 7 days exposure to Cr(VI) treatments (a) 0 mg L^{-1} (b)1 mg L^{-1} (c) 2mg L^{-1} (d) 4mg L^{-1}(e) 6 mg $L^{-1}$and (f)10mg L^{-1}.

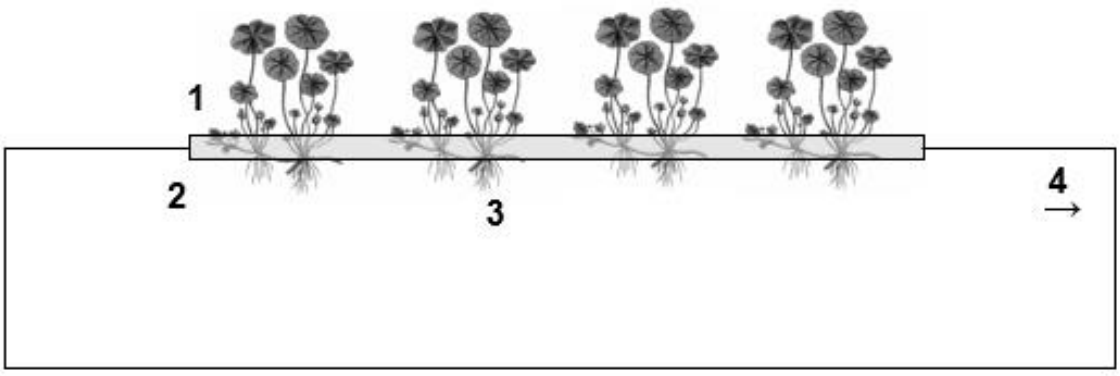

Fig. 8 –Floating biofilter proposal for *H. ranunculoides*being(1) shoots of the plant (2) plant substract (3) roots submerged (4)water eflux.

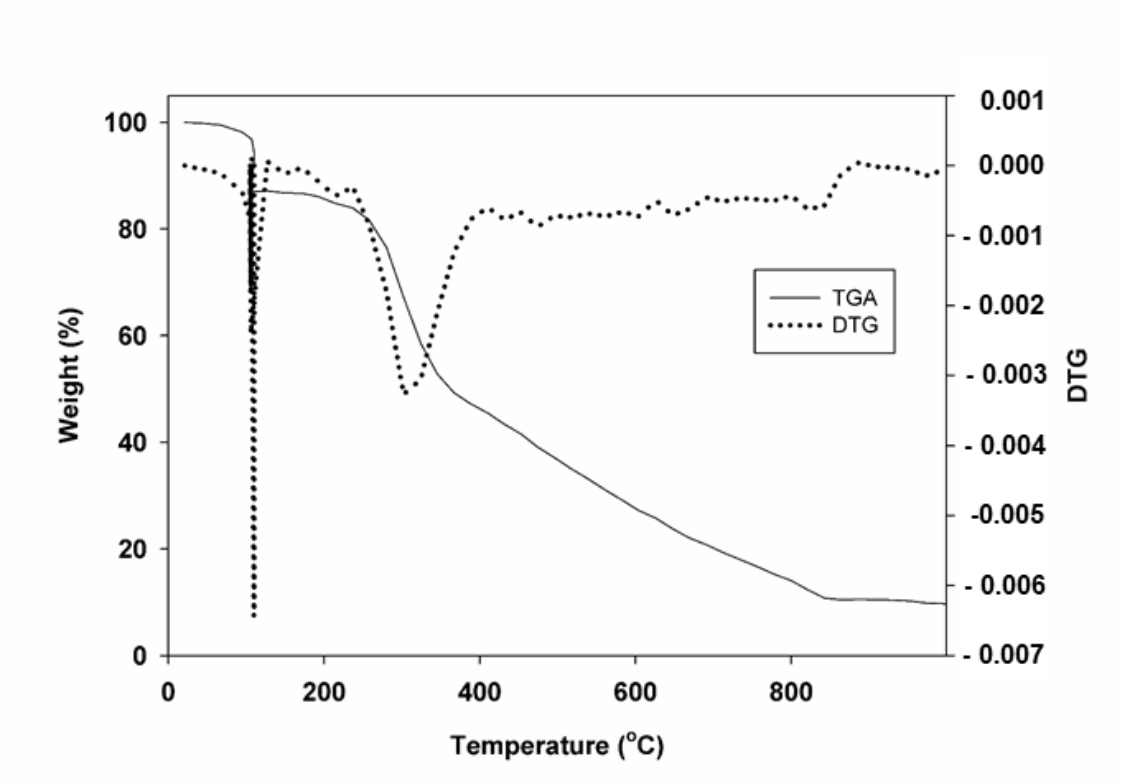

730

731 **Fig. 9 –** Thermogravimetric analysis of the biomass of the aquatic macrophyte *H.*

732 *ranunculoides.*

733

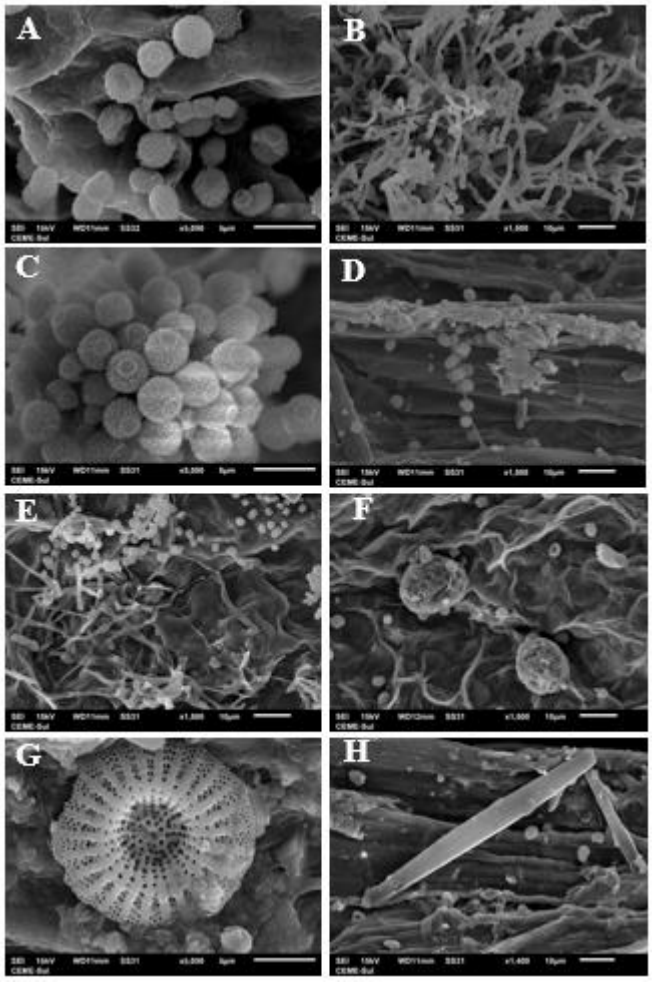

Fig. S1 - Microorganisms found in *H. Ranunculoides* in different treatments(a) 0 mg L^{-1}(b) 1 mg L^{-1} (c) 1 mg L^{-}(d) 1 mg L^{-1} (e) 2 mg L^{-1} (f) 4 mg L^{-1} (g) 6 mg L^{-1} (h) 6 mg L^{-1}.· All images represent shoots of the aquatic macrophyte, with exception of d, g and h that are images from roots.

References

Adki, V. S., Jadhav, J. P., Bapat, V. A. 2013. *Nopalea cochenillifera*, a potential chromium (VI) hyperaccumulator plant. Environmental Science and Pollution Research, 20(2), 1173-1180.

Aebi, H. 1984. Catalase *in vitro*. Methods in enzymology, 105, 121-126.

Ahmad, A., Khan, W. U., Shah, A. A., Yasin, N. A., Naz, S., Ali, A., .Batool, A. I. 2021. Synergistic effects of nitric oxide and silicon on promoting plant growth, oxidative stress tolerance and reduction of arsenic uptake in Brassica juncea. Chemosphere, 262, 128384.

Adhikari, A., Adhikari, S., Ghosh, S., Azahar, I., Shaw, A. K., Roy, D., Roy, S., Saha, S., Hossain, Z. 2020. Imbalance of redox homeostasis and antioxidant defense status in maize under chromium (VI) stress. Environmental and Experimental Botany, 169, 103873.

Augustynowicz, J., Grosicki, M., Hanus-Fajerska, E., Lekka, M., Waloszek, A., Kołoczek, H. 2010. Chromium (VI) bioremediation by aquatic macrophyte Callitriche cophocarpa Sendtn. Chemosphere, 79(11), 1077-1083.

Agathokleous, E., Feng, Z., Peñuelas, J. 2020. Chlorophyll hormesis: are chlorophylls major components of stress biology in higher plants?. Science of The Total Environment, 726, 138637.

Bah, A. M., Dai, H., Zhao, J., Sun, H., Cao, F., Zhang, G., Wu, F. 2011. Effects of cadmium, chromium and lead on growth, metal uptake and antioxidative capacity in *Typha angustifolia*. Biological trace element research, 142(1), 77-92.

Bidhendi, A. J., Altartouri, B., Gosselin, F. P., Geitmann, A. 2019. Mechanical stress initiates and sustains the morphogenesis of wavy leaf epidermal cells. Cell reports, 28(5), 1237-1250.

Berni, R., Luyckx, M., Xu, X., Legay, S., Sergeant, K., Hausman, J. F., Lutts, S., Cai, G., Guerriero, G. 2019. Reactive oxygen species and heavy metal stress in plants: Impact on the cell wall and secondary metabolism. Environmental and Experimental Botany, 161, 98-106.

Brand-Williams, W., Cuvelier, M. E., Berset, C. L. W. T. 1995. Use of a free radical method to evaluate antioxidant activity. LWT-Food science and Technology, 28(1), 25-30.

Chanu LB, Gupta A. 2016. Phytoremediation of lead using *Ipomoea aquatica* Forsk. in hydroponic solution. Chemosphere. 156:407–411. doi:10.1016/j.chemosphere.2016.05.001.

Christou, A., Georgiadou, E. C., Zissimos, A. M., Christoforou, I. C., Christofi, C., Neocleous, D., Dalias, P., Fotopoulos, V. 2021. Uptake of hexavalent chromium by *Lactuca sativa* and *Triticum aestivum* plants and mediated effects on their performance, linked with associated public health risks. Chemosphere, 267, 128912.

Clark, R. B. 1975. Characterization of phosphatase of intact maize roots. Journal of Agricultural and Food Chemistry, 23(3), 458-460.

Custodio, M., Orellana-Mendoza, E., Peñaloza, R., la Cruz-Solano, D., Bulege-Gutiérrez, W., Quispe-Mendoza, R. 2020. Heavy Metal Accumulation in Sediment and Removal Efficiency in the Stabilization Ponds with the Hydrocotyle ranunculoides Filter. Journal of Ecological Engineering, 21(5).

Cui S, Zhou Q, Chao L. 2007. Potential hyperaccumulation of Pb, Zn, Cu and Cd in endurant plants distributed in an old smeltery, northeast China. Environ Geol. 51(6):1043–1048. doi:10.1007/s00254-006-0373-3.

da Conceicao Gomes, M. A., Hauser-Davis, R. A., Suzuki, M. S., Vitoria, A. P. 2017. Plant chromium uptake and transport, physiological effects and recent advances in molecular investigations. Ecotoxicology and environmental safety, 140, 55-64.

Dazy, M., Béraud, E., Cotelle, S., Meux, E., Masfaraud, J. F., Férard, J. F. 2008. Antioxidant enzyme activities as affected by trivalent and hexavalent chromium species in *Fontinalis antipyretica* Hedw. Chemosphere, 73(3), 281-290.

De Luna, M.Y., Marcelo Rodrigues, P., Antonia Mabrysa Torres, G., Antonio Eufrazio, D.C.J., Jackson Queiroz, M., Selma Elaine, M., Maria Alexsandra de Sousa, R., 2019. A thermogravimetric analysis of biomass wastes from the northeast region of Brazil as fuels for energy recovery. Energy Sources, Part A Recovery, Util. Environ. Eff. 41(13), 1557–1572.

Demarco, C. F., Afonso, T. F., Pieniz, S., Quadro, M. S., Camargo, F. A., Andreazza, R. 2018. In situ phytoremediation characterization of heavy metals promoted by Hydrocotyle ranunculoides at Santa Bárbara stream, an anthropogenic polluted site in southern of Brazil. Environmental Science and Pollution Research, 25(28), 28312-28321.

Demarco, C. F., Afonso, T. F., Schoeler, G. P., dos Santos Barboza, V., dos Santos Rocha, L., Pieniz, S., Giongo, J. L., Vaucher, R. A., Igansi. A. V., Cadaval Jr, T.R.S., Andreazza, R. 2022. New low-cost biofilters for SARS-CoV-2 using *Hymenachne grumosa* as a precursor. Journal of Cleaner Production, 331, 130000.

Emamverdian, A., Ding, Y., Xie, Y., Sangari, S. 2018. Silicon mechanisms to ameliorate heavy metal stress in plants. BioMed Research International, 1-10.

Faisal, M., Hasnain, S. 2005. Bacterial Cr (VI) reduction concurrently improves sunflower (*Helianthus annuus* L.) growth. Biotechnology letters, 27(13), 943-947.

Fan, W. J., Feng, Y. X., Li, Y. H., Lin, Y. J., Yu, X. Z. 2020. Unraveling genes promoting ROS metabolism in subcellular organelles of *Oryza sativa* in response to trivalent and hexavalent chromium. Science of The Total Environment, 744, 140951.

Gardea-Torresdey, J. L., De la Rosa, G., Peralta-Videa, J. R., Montes, M., Cruz-Jimenez, G., Cano-Aguilera, I. 2005. Differential uptake and transport of trivalent and hexavalent chromium by tumbleweed (*Salsola kali*). Archives of Environmental Contamination and Toxicology, 48(2), 225-232.

Gautam, V., Kohli, S. K., Kapoor, D., Bakshi, P., Sharma, P., Arora, S.,Ahmad, P. 2021. Stress protective effect of rhododendron arboreum leaves (MEL) on chromium-treated Vigna radiata Plants. Journal of Plant Growth Regulation, 40(1), 423-435.

Giannopolitis, C. N., Ries, S. K. 1977. Superoxide dismutases: I. Occurrence in higher plants. Plant physiology, 59(2), 309-314.

Haokip, N., Gupta, A. 2021. Biochemical and antioxidant responses of *Ipomoea aquatica* exposed to graded concentrations of chromium. Biologia, 1-8.

He, J., Strezov, V., Kumar, R., Weldekidan, H., Jahan, S., Dastjerdi, B. H., Zhou, X., Kan, T. 2019. Pyrolysis of heavy metal contaminated *Avicennia marina* biomass from phytoremediation: Characterisation of biomass and pyrolysis products. Journal of Cleaner Production, 234, 1235-1245.

Huang, C., Lai, C., Xu, P., Zeng, G., Huang, D., Zhang, J., Wang, R. 2017. Lead-induced oxidative stress and antioxidant response provide insight into the tolerance of *Phanerochaete chrysosporium* to lead exposure. Chemosphere, 187, 70-77.

Huang, H., Yao, W., Li, R., Ali, A., Du, J., Guo, D., Xiao, R., Guo, Z., Zhanga, Z., Awasthi, M. K. 2018. Effect of pyrolysis temperature on chemical form, behavior and environmental risk of Zn, Pb and Cd in biochar produced from phytoremediation residue. Bioresource technology, 249, 487-493.

Islam, F., Yasmeen, T., Arif, M. S., Riaz, M., Shahzad, S. M., Imran, Q., Ali, I. 2016. Combined ability of chromium (Cr) tolerant plant growth promoting bacteria (PGPB) and salicylic acid (SA) in attenuation of chromium stress in maize plants. Plant Physiology and Biochemistry, 108, 456-467.

JOHANSEN, D. A. Plant microtechnique New York: Mcgraw-Hill Book, 1940. 523 p.

Kısa, D., Elmastaş, M., Öztürk, L., Kayır, Ö. 2016. Responses of the phenolic compounds of *Zea mays* under heavy metal stress. Applied Biological Chemistry, 59(6), 813-820.

Kováčik, J., Babula, P., Hedbavny, J., Klejdus, B. 2014. Hexavalent chromium damages chamomile plants by alteration of antioxidants and its uptake is prevented by calcium. Journal of hazardous materials, 273, 110-117.

Kumar, A., Dubey, A. K., Kumar, V., Ansari, M. A., Narayan, S., Kumar, S., Meenakshi Kumar, S., Pandey, V., Shirke, P.A.,Pande, V., Sanyal, I. 2020. Over-expression of chickpea glutaredoxin (CaGrx) provides tolerance to heavy metals by reducing metal accumulation and improved physiological and antioxidant defence system. Ecotoxicology and environmental safety, 192, 110252.

Kundu, D., Dey, S., Raychaudhuri, S. S. 2018. Chromium (VI)–induced stress response in the plant *Plantago ovata* Forsk in vitro. Genes and Environment, 40(1), 1-13.

Levizou, E., Zanni, A. A., Antoniadis, V. 2019. Varying concentrations of soil chromium (VI) for the exploration of tolerance thresholds and phytoremediation potential of the oregano (*Origanum vulgare*). Environmental Science and Pollution Research, 26(1), 14-23.

Li, N., Qin, L., Jin, M., Zhang, L., Geng, W., Xiao, X. 2021. Extracellular adsorption, intracellular accumulation and tolerance mechanisms of *Cyclotella* sp. to Cr (VI) stress. Chemosphere, 270, 128662.

Lichtenthaler, H. K. Chlorophylls and carotenoids: pigments of photosynthetic biomembranes. Methods in Enzymology, 148:350-382, 1987.

Liu, D., Zou, J., Wang, M., Jiang, W. 2008. Hexavalent chromium uptake and its effects on mineral uptake, antioxidant defence system and photosynthesis in *Amaranthus viridis* L. Bioresource Technology, 99(7), 2628-2636.

Liu, C., Du, W., Cai, H., Jia, Z., Dong, H. 2014. Trivalent chromium pretreatment alleviates the toxicity of oxidative damage in wheat plants exposed to hexavalent chromium. Acta Physiologiae Plantarum, 36(3), 787-794.

Maulidiani, Abas, F., Khatib, A., Shaari, K., Lajis, N. H. 2014. Chemical characterization and antioxidant activity of three medicinal Apiaceae species. Industrial Crops and Products, 55, 238-247.

Muradov, N., Taha, M., Miranda, A. F., Kadali, K., Gujar, A., Rochfort, S., Stevenson, T.,Ball, A. S., Mouradov, A. 2014. Dual application of duckweed and azolla plants for wastewater treatment and renewable fuels and petrochemicals production. Biotechnology for biofuels, 7(1), 1-17.

Nagajyoti, P. C., Lee, K. D., Sreekanth, T. V. M. 2010. Heavy metals, occurrence and toxicity for plants: a review. Environmental chemistry letters, 8(3), 199-216.

O'Brien, T., Feder, N., & McCully, M. E. 1964. Polychromatic staining of plant cell walls by toluidine blue O. Protoplasma, 59(2), 368-373.

Ohkawa, H., Ohishi, N., Yagi, K. 1979. Assay for peroxides in animal tissues by thiobarbituric acid reaction. Analitical Biochemistry 95: 351-358.

Pandey VC. 2016. Phytoremediation efficiency of *Eichhornia crassipes*in fly ash pond. International J Phytoremediation. 18(5):450–452. doi:10.1080/15226514.2015.1109605.

Prado, C., Pagano, E., Prado, F., Rosa, M. 2012. Detoxification of Cr (VI) in *Salvinia minima*is related to seasonal-induced changes of thiols, phenolics and antioxidative enzymes. Journal of hazardous materials, 239, 355-361.

Prasad, S., Yadav, K. K., Kumar, S., Gupta, N., Cabral-Pinto, M. M., Rezania, S., Radwan, N., Alam, J. 2021. Chromium contamination and effect on environmental health and its remediation: A sustainable approaches. Journal of Environmental Management, 285, 112174.

Punwong, P., Juprasong, Y., Traiperm, P. 2017. Effects of an oil spill on the leaf anatomical characteristics of a beach plant (*Terminalia catappa* L.). Environmental Science and Pollution Research, 24(27), 21821-21828.

Qu, J., Wang, Y., Tian, X., Jiang, Z., Deng, F., Tao, Y., Zhang, Y. 2021. KOH-activated porous biochar with high specific surface area for adsorptive removal of chromium (VI) and

naphthalene from water: Affecting factors, mechanisms and reusability exploration. Journal of Hazardous Materials, 401, 123292.

Rafi, S., Shoaib, A., Awan, Z. A., Rizvi, N. B., Shafiq, M. 2017. Chromium tolerance, oxidative stress response, morphological characteristics, and FTIR studies of phytopathogenic fungus *Sclerotium rolfsii*. Folia microbiologica, 62(3), 207-219.

Riaz, M., Yan, L., Wu, X., Hussain, S., Aziz, O., Imran, M., Jiang, C. 2018. Boron reduces aluminum-induced growth inhibition, oxidative damage and alterations in the cell wall components in the roots of trifoliate orange. Ecotoxicology and environmental safety, 153, 107-115.

Rizvi, A., Khan, M. S. 2018. Heavy metal induced oxidative damage and root morphology alterations of maize (*Zea may*s L.) plants and stress mitigation by metal tolerant nitrogen fixing *Azotobacter chroococcum*. Ecotoxicology and environmental safety, 157, 9-20.

Rucińska-Sobkowiak, R. 2016. Water relations in plants subjected to heavy metal stresses. Acta Physiologiae Plantarum, 38(11), 1-13.

Saravanan, A., Kumar, P. S., Govarthanan, M., George, C. S., Vaishnavi, S., Moulishwaran, B., Yaashikaa, P. R. 2021. Adsorption characteristics of magnetic nanoparticles coated mixed fungal biomass for toxic Cr (VI) ions in aquatic environment. Chemosphere, 267, 129226.

Scoccianti, V., Bucchini, A. E., Iacobucci, M., Ruiz, K. B., Biondi, S. 2016. Oxidative stress and antioxidant responses to increasing concentrations of trivalent chromium in the Andean crop species *Chenopodium quinoa* Willd. Ecotoxicology and environmental safety, 133, 25-35.

Shahid, M., Shamshad, S., Rafiq, M., Khalid, S., Bibi, I., Niazi, N. K., Dumat, C., Rashid, M. I. 2017. Chromium speciation, bioavailability, uptake, toxicity and detoxification in soil-plant system: a review. Chemosphere, 178, 513-533.

Sharma, A., Kapoor, D., Wang, J., Shahzad, B., Kumar, V., Bali, A. S., Yan, D. 2020. Chromium bioaccumulation and its impacts on plants: an overview. Plants, 9(1), 100.

Sharmin, S. A., Alam, I., Kim, K. H., Kim, Y. G., Kim, P. J., Bahk, J. D., Lee, B. H. 2012. Chromium-induced physiological and proteomic alterations in roots of *Miscanthus sinensis*. Plant science, 187, 113-126.

Sidhu GPS, Bali AS, Singh HP, Batish DR, Kohli RK. 2018. Phytoremediation of lead by a wild, non-edible Pb accumulator *Coronopus didymus (L.)* Brassicaceae. Int J Phytoremediation. 20(5):483–489. doi:10.1080/15226514.2017.1374331.

Sinha, V., Pakshirajan, K., Chaturvedi, R. 2014. Chromium (VI) accumulation and tolerance by *Tradescantia pallida*: biochemical and antioxidant study. Applied biochemistry and biotechnology, 173(8), 2297-2306.

Sinha, V., Pakshirajan, K., Chaturvedi, R. 2018. Chromium tolerance, bioaccumulation and localization in plants: an overview. Journal of environmental management, 206, 715-730.

Simbanegavi, T. T., Ndagurwa, H. G., Mundava, J., Mundy, P. J. 2018. Response of the waterbird community to floating pennywort (*Hydrocotyle ranunculoides*) cover at Ngamo dam, Antelope Park, Zimbabwe. African Journal of Ecology, 56(1), 20-27.

Smolders, A. J. P., Vergeer, L. H. T., Van der Velde, G., Roelofs, J. G. M. 2000. Phenolic contents of submerged, emergent and floating leaves of aquatic and semi-aquatic macrophyte species: why do they differ?. Oikos, 91(2), 307-310.

Srividya, K., Mohanty, K. 2009. Biosorption of hexavalent chromium from aqueous solutions by *Catla catla* scales: equilibrium and kinetics studies. Chemical Engineering Journal, 155(3), 666-673.

Swain, T., Hillis, W. E. 1959. The phenolic constituents of *Prunus domestica.* I.—The quantitative analysis of phenolic constituents. Journal of the Science of Food and Agriculture, 10(1), 63-68.

Tripathi, D. K., Singh, V. P., Kumar, D., Chauhan, D. K. 2012. Impact of exogenous silicon addition on chromium uptake, growth, mineral elements, oxidative stress, antioxidant capacity, and leaf and root structures in rice seedlings exposed to hexavalent chromium. Acta physiologiae plantarum, 34(1), 279-289.

Tsimogiannis, D., Oreopoulou, V. 2019. Classification of phenolic compounds in plants. In Polyphenols in plants (pp. 263-284). Academic Press.

Ukhurebor, K. E., Aigbe, U. O., Onyancha, R. B., Nwankwo, W., Osibote, O. A., Paumo, H. K., Siloko, I. U. 2021. Effect of hexavalent chromium on the environment and removal techniques: A review. Journal of environmental management, 280, 111809.

Upadhyaya, A., Sankhla, D., Davis, T. D., Sankhla, N., & Smith, B. N. (1985). Effect of paclobutrazol on the activities of some enzymes of activated oxygen metabolism and lipid peroxidation in senescing soybean leaves. Journal of plant physiology, 121(5), 453-461.

Usman, K., Al-Ghouti, M. A., Abu-Dieyeh, M. H. 2019. The assessment of cadmium, chromium, copper, and nickel tolerance and bioaccumulation by shrub plant *Tetraena qataranse*. Scientific reports, 9(1), 1-11.

Vankar, P. S., Bajpai, D. 2008. Phyto-remediation of chrome-VI of tannery effluent by *Trichoderma* species. Desalination, 222 (1–3), 255–262.

Vuolo, M. M., Lima, V. S., Junior, M. R. M. 2019. Phenolic compounds: Structure, classification, and antioxidant power. In Bioactive compounds (pp. 33-50). Woodhead Publishing.

Yan, X., Wang, J., Song, H., Peng, Y., Zuo, S., Gao, T., Duan, X., Qin., D., Dong, J. 2020. Evaluation of the phytoremediation potential of dominant plant species growing in a chromium salt–producing factory wasteland, China. Environmental Science and Pollution Research, 27(7), 7657-7671.

Yoon J, Cao X, Zhou Q, Ma LQ. 2006. Accumulation of Pb, Cu, and Zn in native plants growing on a contaminated Florida site. Science ofTotal Environment. 368(2–3):456–464. doi:10.1016/j.scitotenv.2006.01.016.

Walsh, G. C., Maestro, M. 2017. Assessing the specificity of a herbivore on a plant of uncertain phylogenetic placing: *Listronotus elongatus* a herbivore of *Hydrocotyle ranunculoides*. BioControl, 62(2), 269-279.

Zhang, S., Pang, S., Wang, P., Wang, C., Guo, C., Addo, F. G., Li, Y. 2016. Responses of bacterial community structure and denitrifying bacteria in biofilm to submerged macrophytes and nitrate. Scientific Reports, 6(1), 1-10.

Zou, J., Yu, K., Zhang, Z., Jiang, W., Liu, D. 2009. Antioxidant response system and chlorophyll fluorescence in chromium (VI)-treated *Zea mays* L. seedlings. Acta Biologica Cracoviensia Series Botanica, 51(1), 23-33.

8 Considerações finais

A urgente necessidade de remediação de ambientes aquáticos contaminados com metais pesados e SARS-CoV-2, devido principalmente à ameaça à saúde da população foi o grande norteador do desenvolvimento dessa pesquisa. Os resultados dessa pesquisa comprovam que a biorremediação pode ser uma alternativa eficiente para remover contaminantes desses ambientes degradados. A utilização de plantas e microrganismos como agentes de descontaminação demonstrou ser uma perspectiva futura para a recuperação desses locais.

As descobertas dessa pesquisa são evidentes: as macrófitas aquáticas representam alternativas altamente eficientes para a remoção de contaminantes do meio, incluindo metais pesados. As espécies *E. anagallis*, *H. grumosa*, *H. ranunculoides* e *S. montevidensis*, em particular, apresentaram um potencial promissor para a aplicação em técnicas de fitorremediação em áreas altamente antropizadas do município de Pelotas/RS

Por meio de uma comparação entre o potencial natural das espécies de macrófitas aquáticas, uma delas foi selecionada para um estudo aprofundado dos mecanismos de resistência ao Cr(VI), e outra para o estudo da remoção do SARS-CoV-2. Os resultados desses estudos apontam para uma perspectiva futura promissora para a aplicação de macrófitas aquáticas na remediação de ambientes aquáticos contaminados. Com base nesses achados, é possível afirmar que a fitorremediação com macrófitas aquáticas pode ser uma abordagem altamente eficaz para mitigar os riscos ambientais e de saúde pública causados por contaminantes.

Os resultados obtidos na avaliação dos mecanismos de resistência ao Cr(VI) por meio da espécie de macrófita *H. ranunculoides* foram altamente promissores. Essa espécie mostrou-se altamente tolerante a esse metal tóxico, indicando sua grande capacidade de adaptação em ambientes contaminados. Além disso, a pesquisa revelou prováveis mecanismos que permitem a tolerância da planta ao Cr(VI), mesmo com seu alto potencial de dano devido ao poder oxidativo. Essas descobertas podem ter implicações significativas na remediação de ambientes contaminados com metais pesados, fornecendo informações valiosas sobre as espécies que podem ser utilizadas com eficácia na fitorremediação.

Os resultados da pesquisa realizada com a espécie *H. grumosa* para a remoção de SARS-CoV-2 são extremamente promissores. Os bioadsorventes produzidos com a planta in natura e em forma de carvão ativado apresentaram uma eficiência de remoção do vírus de 98,44% e 99,61%, respectivamente. Esses resultados são especialmente significativos, uma vez que há poucos estudos disponíveis sobre a adsorção do SARS-CoV-2 em diferentes materiais, bem como há preocupação com a transmissão do vírus por meio de águas residuárias. Além disso, considerando a ausência de uma vacina para aplicação na população na época da realização da pesquisa, a descoberta dessas alternativas para a remoção do vírus em águas e efluentes demonstrou-se de grande relevância para a proteção da saúde pública. Esses achados podem ter um impacto significativo no controle de futuras pandemias, bem como na melhoria da qualidade da água em ambientes naturais e urbanos.

Compreender os mecanismos de absorção e adsorção em biofiltros é essencial para a aplicação eficiente dessas novas propostas de biorremediação em ambientes aquáticos contaminados com SARS-CoV-2 e metais pesados. Para validar a eficiência desses dispositivos, destaca-se a necessidade de conduzir testes *in situ*, a fim de avaliar a sua capacidade real de remoção de contaminantes. Além disso, é possível aprimorar ainda mais os biofiltros por meio da identificação de microrganismos tolerantes aos compostos de interesse, que podem ser inoculados nas plantas, aumentando assim a sua capacidade de remoção. Com essas abordagens, pode-se contribuir para a melhoria da qualidade da água em ambientes naturais e urbanos, bem como para a saúde pública, ao mitigar a contaminação por SARS-CoV-2 e metais pesados.

A pesquisa realizada abriu caminho para o desenvolvimento de novas tecnologias ambientais que favoreçam a remediação de ambientes aquáticos contaminados a partir da utilização de biofiltros ilhas flutuantes. No entanto, ainda há uma vasta possibilidade de explorar novos materiais que possam ser utilizados como suporte e adsorvente ao mesmo tempo, como as espumas de poliuretano. A utilização desses materiais pode aumentar a eficiência e a praticidade das técnicas de biorremediação, além de contribuir para a preservação dos ecossistemas e para a proteção da saúde pública. Portanto, a continuidade desses estudos é essencial para o avanço da ciência e para a aplicação de soluções inovadoras e sustentáveis na remediação de ambientes aquáticos contaminados.

Referências

ABDOLALI, A.; NGO, H. H.; GUO, W.; ZHOU, J. L.; DU, B.; WEI, Q.; WANG, X. C.; NGUYEN, P. D. Characterization of a multi-metal binding biosorbent: Chemical modification and desorption studies. **Bioresource Technology**, v.193, p.477-487, 2015.

ABDULLAH, A. AHMED, A.; AKHTER, P.; RAZZAQ, A.; ZAFAR, M.; HUSSAIN, M.; SHAHZAD, N.; MAJEED, K.; KHURRUM, S.; ABU BAKAR, M. S.; PARK, Y. Bioenergy potential and thermochemical characterization of lignocellulosic biomass residues available in Pakistan. **Korean Journal of Chemical Engineering**, v. 37, n. 11, p. 1899-1906, 2020.

ADELODUN, B.; AJIBADE, F.O.; IGHALO, J.O.; ODEY, G.; IBRAHIM, R.G.; KAREEM, K.Y.; BAKARE, H.O.; TIAMIYU, A.O.; AJIBADE, T.F.; ABDULKADIR, T.S.; ADENIRAN, K.A.; CHOI, K. S. Assessment of socioeconomic inequality based on virus-contaminated water usage in developing countries: a review. **Environmental Research**, v. 192, p. 110309, 2021.

ADINAVEEN, T.; KENNEDY, L.J.; VIJAYA, J.J.; SEKARAN, G. Studies on structural, morphological, electrical and electrochemical properties of activated carbon prepared from sugarcane bagasse. **Journal of industrial and Engineering Chemistry**, v. 19, n. 5, p. 1470-1476, 2013.

ADKI, V. S.; JADHAV, J. P.; BAPAT, V. A. *Nopalea cochenillifera*, a potential chromium (VI) hyperaccumulator plant. **Environmental Science and Pollution Research**, v. 20, n. 2, p. 1173-1180, 2013.

ADHIKARI, A; ADHIKARI, S.; GHOSH, S.; AZAHAR, I.; SHAW, A. K.; ROY, D.; ROY, S.; SAHA, S., HOSSAIN, Z. Imbalance of redox homeostasis and antioxidant defense status in maize under chromium (VI) stress. **Environmental and Experimental Botany**, v. 169, p. 103873, 2020.

AEBI, Hugo. [13] Catalase in vitro. In: Methods in enzymology. Academic press, 1984. p. 121-126.

AFONSO, T. F.; DEMARCO, C. F.; PIENIZ, S.; QUADRO, M. S.; CAMARGO, F. A.; ANDREAZZA, R. Bioprospection of indigenous flora grown in copper mining tailing area for phytoremediation of metals. **Journal of Environmental Management**, v. 256, p. 109953, 2020.

AGATHOKLEOUS, E.; FENG, Z.; PEÑUELAS, J. Chlorophyll hormesis: are chlorophylls major components of stress biology in higher plants? **Science of The Total Environment**, v. 726, p. 138637, 2020.

AHMAD, A.; KHAN, W. U.; SHAH, A. A.; YASIN, N. A.; NAZ, S.; ALI, A.; BATOOL, A. I. Synergistic effects of nitric oxide and silicon on promoting plant growth, oxidative stress tolerance and reduction of arsenic uptake in *Brassica juncea*. **Chemosphere**, v. 262, p. 128384, 2021.

AHMED, M. J. K.; AHMARUZZAMAN, M. A review on potential usage of industrial waste materials for binding heavy metal ions from aqueous solutions. **Journal of Water Process Engineering**, v.10, p.39-47, 2016.

AHMED, W.; BERTSCH, P.M.; BIBBY, K.; HARAMOTO, E.; HEWITT, J.; HUYGENS, F.; BIVINS, A. Decay of SARS-CoV-2 and surrogate murine hepatitis virus RNA in untreated wastewater to inform application in wastewater-based epidemiology. **Environmental Research**, v. 191, p. 110092, 2020.

AL MASUM, A.; BETTMAN, N.; READ, S.; HECKER, M.; BRINKMANN, M.; MCPHEDRAN, K. Urban stormwater runoff pollutant loadings: GIS land use classification vs. sample-based predictions. **Environmental Science and Pollution Research**, p. 1-15, 2022.

ALENCAR, B.T.B.; RIBEIRO, V.H.V.; CABRAL, C.M.; SANTOS, N.M.C.; FERREIRA, E.A.; FRANCINO, D.M.T.; SANTOS, J.B.; SILVA, D.V.; SOUZA, M.F. Use of macrophytes to reduce the contamination of water resources by pesticides. **Ecological Indicators**, v. 109, p. 105785, 2020.

ALI, F.; JILANI, G.; FAHIM, R.; BAI, L.; WANG, C.; TIAN, L.; JIANG, H. Functional and structural roles of wiry and sturdy rooted emerged macrophytes root functional traits in the abatement of nutrients and metals. **Journal of Environmental Management**, 2019, 249, 109330.

ALI, S.; ABBAS, Z.; RIZWAN, M.; ZAHEER, I.E.; YAVA, I.; ÜNAY, A.; ABDEL-DAIM, M.M.; BIN-JUMAH, M.; HASANUZZAMAN, M.; KALDERIS, D. Application of floating aquatic plants in phytoremediation of heavy metals polluted water: a review. **Sustainability**, v. 12, n. 5, p. 1927, 2020.

ALMEIDA, J. C.; CARDOSO, C. E. D.; TAVARES, D. S.; FREITAS, R.; TRINDADE, T.; VALE, C.; PEREIRA, E. Chromium removal from contaminated waters using nanomaterials – A review TrAC. **Trends in Analytical Chemistry**, v.118, p.277-291, 2019.

AL-GHOUTI, M.A., AL-ABSI, R.S. Mechanistic understanding of the adsorption and thermodynamic aspects of cationic methylene blue dye onto cellulosic olive stones biomass from wastewater. **Sci. Rep**. v.10, n.1, p. 1–18, 2020.

ALVES, J.L.F.; DA SILVA, J.C.G.; DA SILVA FILHO, V.F.; ALVES, R.F.; DE ARAUJO GALDINO, W.V.; DE SENA, R.F. Kinetics and thermodynamics parameters evaluation of pyrolysis of invasive aquatic macrophytes to determine their bioenergy potentials. **Biomass Bioenergy**, v. 121, p. 28–40, 2019.

AMRAN, F., Zaini, M.A.A. Effects of chemical activating agents on physical properties of activated carbons–a commentary. **Water Pract. Technol**, v. 15, n.4, p. 863–876, 2020.

ANASTOPOULOS, I.; ANAGNOSTOPOULOS, V. A.; BHATNAGAR, A.; MITROPOULOS, A. C.; KYZAS, G. Z. A review for chromium removal by carbon nanotubes. **Chemistry and Ecology**, v.33, n.6, p.572-588, 2017.

ANDREAZZA, R.; OKEKE, B. C; PIENIZ, S.; BORTOLON, L.; LAMBAIS, M. R.; CAMARGO, F. A. Effects of stimulation of copper bioleaching on microbial community in vineyard soil and copper mining waste. **Biological trace element research**, v. 146, n. 1, p. 124-133, 2012.

ANDREAZZA, R.; OKEKE, B. C.; PIENIZ, S.; CAMARGO, F. A. Characterization of copper-resistant rhizosphere bacteria from *Avena sativa* and *Plantago lanceolata* for copper bioreduction and biosorption. **Biological Trace Element Research**, v. 146, n. 1, p. 107-115, 2012.

ANFAR, Z.; AIT AHSAINE, H.; ZBAIR, M.; AMEDLOUS, A.; AIT EL FAKIR, A.; JADA, A.; EL ALEM, N. Recent trends on numerical investigations of response surface methodology for pollutants adsorption onto activated carbon materials: A review. **Critical Reviews in Environmental Science and Technology**, v. 50, n. 10, p. 1043-1084, 2020.

ANSARI, A.A.; NAEEM, M.; GILL, S.S.; ALZUAIBR, F.M. Phytoremediation of contaminated waters: An eco-friendly technology based on aquatic macrophytes application. **The Egyptian Journal of Aquatic Research**, v. 46, n. 4, p. 371-376, 2020.

ARBELÁEZ, A.A.; GIRALDO, N.D.; PEREZ, J.F.; ATEHORTÚA, L. Pyrolysis kinetics using TGA and simulation of gasification of the microalga *Botryococcus braunii*. **BioEnergy Research**, v. 12, n. 4, p. 1077-1089, 2019.

AUGUSTYNOWICZ, J.; GROSICKI, M.; HANUS-FAJERSKA, E.; LEKKA, M.; WALOSZEK, A.; KOŁOCZEK, H. Chromium (VI) bioremediation by aquatic macrophyte *Callitriche cophocarpa* Sendtn. **Chemosphere**, v. 79, n. 11, p. 1077-1083, 2010.

AYANGBENRO, A.S.; BABALOLA, O.O. A new strategy for heavy metal polluted environments: a review of microbial biosorbents. **International journal of environmental research and public health**, v. 14, n. 1, p. 94, 2017.

BAH, A. M.; DAI, H.; ZHAO, J.; SUN, H.; CAO, F.; ZHANG, G.; WU, F. Effects of cadmium, chromium and lead on growth, metal uptake and antioxidative capacity in *Typha angustifolia*. **Biological trace element research**, v. 142, n. 1, p. 77-92, 2011.

BAIN, W.; LEE, J.S.; WATSON, A.M.; STITT-FISCHER, M.S.; Practical guidelines for collection, manipulation and inactivation of SARS-CoV-2 and COVID-19 clinical specimens. **Current protocols in cytometry**, v. 93, n. 1, p. e77, 2020.

BARAKAT, M. A. New trends in removing heavy metals from industrial wastewater. **Arabian Journal of Chemistry**, v.4, n.4, p.361-377, 2011.

BARDHAN, R.; BYRD, T.; BOYD, J. Workforce Management during the Time of COVID-19—Lessons Learned and Future Measures. **COVID**, v. 3, n. 1, p. 1-27, 2023.

BENEDETTI, V., PATUZZI, F., BARATIERI, M. Characterization of char from biomass gasification and its similarities with activated carbon in adsorption applications. **Applied Energy**, v. 227, p. 92-99, 2018.

BENVENUTI, T.; HAMERSKI, F.; GIACOBBO, A.; BERNARDES, A.M.; ZOPPAS-FERREIRA, J.; RODRIGUES, M.A.S. Constructed floating wetland for the treatment of domestic sewage: a real-scale study. **Journal of Environmental Chemical Engineering**, v. 6, n. 5, p. 5706-5711, 2018.

BHAGYAWANT, S.S.; NARVEKAR, D.T.; GUPTA, N.; BHADKARIA, A.; KOUL, K.K.; SRIVASTAVA, N. Variations in the antioxidant and free radical scavenging under induced heavy metal stress expressed as proline content in chickpea. **Physiology and Molecular Biology of Plants**, v. 25, n. 3, p. 683-696, 2019.

BI, R.; ZHOU, C.; JIA, Y.; WANG, S.; LI, P.; REICHWALDT, E.S.; LIU, W. Giving waterbodies the treatment they need: a critical review of the application of constructed floating wetlands. **Journal of Environmental Management**, v. 238, p. 484-498, 2019.

BIND, A.; GOSWAMI, L.; PRAKASH, V. Comparative analysis of floating and submerged macrophytes for heavy metal (copper, chromium, arsenic and lead) removal: sorbent preparation, characterization, regeneration and cost estimation. **Geology, Ecology, and Landscapes**, v.2, n.2, p.61-72, 2018.

BIDHENDI, A. J.; ALTARTOURI, B.; GOSSELIN, F. P.; GEITMANN, A. Mechanical stress initiates and sustains the morphogenesis of wavy leaf epidermal cells. **Cell reports**, v. 28, n. 5, p. 1237-1250. e6, 2019.

BERNI, R.; LUYCKX, M.; XU, X.; LEGAY, S.; SERGEANT, K.; HAUSMAN, J. F.; LUTTS, S.; CAI, G.; GUERRIERO, G. Reactive oxygen species and heavy metal stress in plants: Impact on the cell wall and secondary metabolism. **Environmental and Experimental Botany**, v. 161, p. 98-106, 2019.

BRASIL. **Resolução nº 430, de 13 de maio de 2011**. Dispõe sobre as condições e padrões de lançamento de efluentes, complementa e altera a Resolução no 357, de 17 de março de 2005, do Conselho Nacional do Meio Ambiente-CONAMA.Diário Oficial da República Federativa do Brasil. Brasília.

BRAND-WILLIAMS, W.; CUVELIER, M. E.; BERSET, C. L. W. T. Use of a free radical method to evaluate antioxidant activity. **LWT-Food science and Technology**, v. 28, n. 1, p. 25-30, 1995.

BURAKOV, A. E.; GALUNIN, E. V.; BURAKOVA, I. V.; KUCHEROVA, A. E.; AGARWAL, S.; TKACHEV, A. G.; GUPTA, V. K. Adsorption of heavy metals on conventional and nanostructured materials for wastewater treatment purposes: A review. **Ecotoxicology and environmental safety**, v.148, p.702-712, 2018.

BURHENNE, L.; MESSMER, J.; AICHER, T.; LABORIE, M.P. The effect of the biomass components lignin, cellulose and hemicellulose on TGA and fixed bed pyrolysis. **Journal of Analytical and Applied Pyrolysis**, v. 101, p. 177-184, 2013.

BONANNO, G.; VYMAZAL, J.; CIRELLI, G. L. Translocation, accumulation and bioindication of trace elements in wetland plants. **Science of the Total Environment**, v. 631, p. 252-261, 2018.

CAI, X.; ZHENG, X.; ZHANG, D.; IQBAL, W.; LIU, C.; YANG, B.; ZHAO, X.; LU, X.; MAO, Y. Microbial characterization of heavy metal resistant bacterial strains isolated from an electroplating wastewater treatment plant. Ecotoxicology and environmental safety, v. 181, p. 472-480, 2019.

CALVO, J.; JUNG, H.; MELONI, G. Copper metallothioneins. **Iubmb Life**, v. 69, n. 4, p. 236-245, 2017.

COUTO, E.; ASSEMANY, P.P.; CARNEIRO, G.C.A.; SOARES, D.C.F. The potential of algae and aquatic macrophytes in the pharmaceutical and personal care products (PPCPs) environmental removal: a review. **Chemosphere**, p. 134808, 2022.

CDC, 2020. Centers for Disease Control and Prevention Home Page. Disponível em: https://www.cdc.gov/coronavirus/2019-ncov/downloads/rt-pcr-panel-fordetection-instructions.pdf. Acesso em 14 Fevereiro de 2020.

CHANG, Y.; CUI, H.; HUANG, M.; HE, Y. Artificial floating islands for water quality improvement. **Environmental Reviews**, v. 25, n. 3, p. 350-357, 2017.

CHANU, L. B.; GUPTA, A. Phytoremediation of lead using *Ipomoea aquatica* Forsk in hydroponic solution. **Chemosphere**, v. 156, p. 407-411, 2016.

CHEN, Z.; MA, W.; HAN, M. Biosorption of nickel and copper onto treated alga (*Undaria pinnatifida*): Application of isotherm and kinetic models. **Journal of Hazardous Materials**, v.155, n.1, p.327-333, 2008.

CHIN, A.W.; CHU, J.T.; PERERA, M.R.; HUI, K.P.; YEN, H.L.; CHAN, M.C.; POON, L.L. Stability of SARS-CoV-2 in different environmental conditions. **The Lancet Microbe**, v. 1, n. 1, p. e10, 2020.

CHRISTOU, A.; GEORGIADOU, E. C.; ZISSIMOS, A. M.; CHRISTOFOROU, I. C.; CHRISTOFI, C.; NEOCLEOUS, D.; DALIAS, P.; FOTOPOULOS, V. Uptake of hexavalent chromium by *Lactuca sativa* and *Triticum aestivum* plants and mediated effects on their performance, linked with associated public health risks. **Chemosphere**, v. 267, p. 128912, 2021.

CLARK, R. B. Characterization of phosphatase of intact maize roots. **Journal of Agricultural and Food Chemistry**, v. 23, n. 3, p. 458-460, 1975.

CLEMENTE, R.; ARCO-LÁZARO, E.; PARDO, T.; MARTÍN, I.; SÁNCHEZ-GUERRERO, A.; SEVILLA, F.; BERNAL, M.P. Combination of soil organic and

inorganic amendments helps plants overcome trace element induced oxidative stress and allows phytostabilisation. **Chemosphere**, v. 223, p. 223-231, 2019.

COLLA, T.S.; ANDREAZZA, R.; BÜCKER, F.; SOUZA, M.M.; TRAMONTINI, L.; PRADO, G.R.; FRAZZON, A.P.G.; CAMARGO, F.A.O.; BENTO, F.M. Bioremediation assessment of diesel–biodiesel-contaminated soil using an alternative bioaugmentation strategy. **Environmental science and pollution research**, v. 21, n. 4, p. 2592-2602, 2013.

CORAÇÃO, A. C. D. S.; SANTOS, F. S. D.; DUARTE, J. A. D.; LOPES-FILHO, E. A. P.; DE-PAULA, J. C.; ROCHA, L. M.; TEIXEIRA, V. L. What do we know about the utilization of the *Sargassum species* as biosorbents of trace metals in Brazil? **Journal of Environmental Chemical Engineering**, v. 8, n. 4, p. 103941, 2020.

CORREA, C.R.; OTTO, T.; KRUSE, A. Influence of the biomass components on the pore formation of activated carbon. **Biomass Bioenergy,** v. 97, p. 53–64, 2017.

COSTA, M.B.; TAVARES, F.V.; MARTINEZ, C.B.; COLARES, I.G.; MARTINS, C.D.M.G. Accumulation and effects of copper on aquatic macrophytes *Potamogeton pectinatus* L.: Potential application to environmental monitoring and phytoremediation. **Ecotoxicology and Environmental Safety**, v. 155, p. 117-124, 2018.

CUSTODIO, M.; ORELLANA-MENDOZA, E.; PEÑALOZA, R.; LA CRUZ-SOLANO, D.; BULEGE-GUTIÉRREZ, W.; QUISPE-MENDOZA, R. Heavy metal accumulation in sediment and removal efficiency in the stabilization ponds with the *Hydrocotyle ranunculoides* Filter. **Journal of Ecological Engineering**, v. 21, n. 5, 2020.

CUI, S.; ZHOU, Q.; CHAO L. Potential hyperaccumulation of Pb, Zn, Cu and Cd in endurant plants distributed in an old smeltery, northeast China. **Environ Geol.,** v. 51, n. 6, p. 1043–1048, 2007.

DA CONCEICAO GOMES, M.A.; HAUSER-DAVIS, R. A.; SUZUKI, M. S.; VITORIA, A. P. Plant chromium uptake and transport, physiological effects and recent advances in molecular investigations. **Ecotoxicology and Environmental Safety**, v. 140, p. 55-64, 2017.

DA SILVA, F.P.; LUTTERBECK, C.A., COLARES, G.S.; OLIVEIRA, G.A.; RODRIGUES, L.R.; DELL'OSBEL, N.; RODRIGUEZ, A.L.; LOPEZ, D.A.R.; GEHLEN, G.; MACHADO, E.L. Treatment of university campus wastewaters by anaerobic reactor and multi-stage constructed wetlands. **Journal of Water Process Engineering**, v. 42, p. 102119, 2021.

DASH, D.M.; OSBORNE, W.J. A systematic review on the implementation of advanced and evolutionary biotechnological tools for efficient bioremediation of organophosphorus pesticides. **Chemosphere**, p. 137506, 2022.

DAZY, M.; BÉRAUD, E.; COTELLE, S.; MEUX, E.; MASFARAUD, J. F.; FÉRARD, J. F. Antioxidant enzyme activities as affected by trivalent and hexavalent chromium species in *Fontinalis antipyretica* Hedw. **Chemosphere**, v. 73, n. 3, p. 281-290, 2008.

DEAN, S.; AKHTAR, M. S.; DITTA, A.; VALIPOUR, M.; ASLAM, S. Microcosm Study on the Potential of Aquatic Macrophytes for Phytoremediation of Phosphorus-Induced Eutrophication. **Sustainability**, v. 14, n. 24, p. 16415, 2022.

DE ANDRADE, L.C.; TIECHER, T.; DE OLIVEIRA, J.S.; ANDREAZZA, R.; INDA, A.V.; DE OLIVEIRA CAMARGO, F.A. Sediment pollution in margins of the Lake Guaíba, Southern Brazil. **Environmental Monitoring and Assessment**, v. 190, n. 1, p. 1-13, 2018.

DEMARCO, C. F.; AFONSO, T. F.; PIENIZ, S.; QUADRO, M. S.; CAMARGO, F. A.; ANDREAZZA, R. In situ phytoremediation characterization of heavy metals promoted by *Hydrocotyle ranunculoides* at Santa Bárbara stream, an anthropogenic polluted site in southern of Brazil. **Environmental Science and Pollution Research**, v. 25, n. 28, p. 28312-28321, 2018.

DEMARCO, C. F.; AFONSO, T. F.; PIENIZ, S.; QUADRO, M. S.; CAMARGO, F. A. D. O.; ANDREAZZA, R. Phytoremediation of heavy metals and nutrients by the *Sagittaria montevidensis* into an anthropogenic contaminated site at Southern of Brazil. **International Journal of Phytoremediation**, v. 21, n. 11, p. 1145-1152, 2019.

DEMARCO, C. F., AFONSO, T. F., PIENIZ, S., QUADRO, M. S., DE OLIVEIRA CAMARGO, F. A., ANDREAZZA, R. Evaluation of *Enydra anagallis* remediation at a contaminated watercourse in south Brazil. **International Journal of Phytoremediation**, v. 22, n. 12, p. 1216-1223, 2020.

DE LUNA, M.Y.; RODRIGUES, P. M.; TORRES, G.A.M; EUFRAZIO, C.J.A; QUEIROZ, M.J; ELAINE, M.S.; SOUSA, R.M.A. A thermogravimetric analysis of biomass wastes from the northeast region of Brazil as fuels for energy recovery. **Energy Sources Part A: Recovery Util. Environ**. Eff, v. 41, p. 1557-1572, 2019.

DE STEFANI, G.; TOCCHETTO, D.; SALVATO, M.; BORIN, M. Performance of a floating treatment wetland for in-stream water amelioration in NE Italy. **Hydrobiologia**, v. 674, n. 1, p. 157-167, 2011.

DELL'OSBEL, N.; COLARES, G.S.; OLIVEIRA, G.A.; RODRIGUES, L.R.; DA SILVA, F.P.; RODRIGUEZ, A. L.; L´OPEZ, D.A.R.; LUTTERBECK, C.A.; SILVEIRA, E.O.; KIST, L.T., MACHADO, E.L. Hybrid constructed wetlands for the treatment of urban wastewaters: increased nutrient removal and landscape potential. **Ecological Engineering,** v. 158, p. 106072, 2020.

DEMARCO, C. F.; AFONSO, T. F.; PIENIZ, S.; QUADRO, M. S.; CAMARGO, F. A.; ANDREAZZA, R. In situ phytoremediation characterization of heavy metals promoted by *Hydrocotyle ranunculoides* at Santa Bárbara stream, an anthropogenic polluted site in southern of Brazil. **Environmental Science and Pollution Research**, v. 25, n. 28, p. 28312-28321, 2018.

DEMARCO, C. F; AFONSO, T. F.; SCHOELER, G. P.; DOS SANTOS BARBOZA, V.; DOS SANTOS ROCHA, L.; PIENIZ, S.; GIONGO, J. L.; VAUCHER, R. A.; IGANSI. A. V.; CADAVAL JR, T.R.S.; ANDREAZZA, R. New low-cost biofilters for SARS-CoV-2

using Hymenachne grumosa as a precursor. **Journal of Cleaner Production**, v. 331, p. 130000, 2022.

DI BLASI, C. Modeling chemical and physical processes of wood and biomass pyrolysis. **Prog. Energy Combust. Sci.** v. 34, n.1, p. 47–90, 2008

DORLASS, E.G., MONTEIRO, C.O., VIANA, A.O., SOARES, C.P., MACHADO, R.R.G., THOMAZELLI, L.M., ARAUJO, D.B., LEAL, F.B., CANDIDO, E.D., TELEZYNSKI, B.L., VAL´ERIO, C.A., CHALUP, V.N., MELLO, R., ALMEIDA, F.J., AGUIAR, A.S., BARRIENTOS, A.C.M., SUCUPIRA, C., DE PAULIS, M., S´AFADI, M.A.P., SILVA, D.G.B.P., SODR´E, J.J.M., SOLEDADE, M.P., MATOS, S.F., FERREIRA, S.R., PINEZ, C.M.N., BUONAFINE, C.P., PIERONI, L.N.F., MALTA, F.M., SANTANA, R.A.F., SOUZA, E.C., FOCK, R.A., PINHO, J.R.R., FERREIRA, L.C.S., BOTOSSO, V.F., DURIGON, E.L., OLIVEIRA, D.B.L Lower cost alternatives for molecular diagnosis of COVID-19: conventional RT-PCR and SYBR Green-based RT-qPCR. **Braz. J. Microbiol**, v. 51, n.3, p.1117–1123, 2020.

EL-KHATIB, A.A.; YOUSSEF, N.A.; BARAKAT, N.A.; SAMIR, N.A. Responses of *Eucalyptus globulus* and *Ficus nitida* to different potential of heavy metal air pollution. **International Journal of Phytoremediation**, v. 22, n. 10, p. 986-999, 2020.

ETESAMI, H. Bacterial mediated alleviation of heavy metal stress and decreased accumulation of metals in plant tissues: mechanisms and future prospects. **Ecotoxicology and environmental safety**, v. 147, p. 175-191, 2018.

EMAMVERDIAN, A.; DING, Y.; XIE, Y.; SANGARI, S. Silicon mechanisms to ameliorate heavy metal stress in plants. **BioMed Research International**, v. 2018, 2018.

FAISAL, M.; HASNAIN, S. Bacterial Cr (VI) reduction concurrently improves sunflower (*Helianthus annuus* L.) growth. **Biotechnology letters**, v. 27, n. 13, p. 943-947, 2005.

FAN, W. J.; FENG, Y. X.; LI, Y. H.; LIN, Y. J.; YU, X. Z. Unraveling genes promoting ROS metabolism in subcellular organelles of *Oryza sativa* in response to trivalent and hexavalent chromium. Science of the Total Environment, v. 744, p. 140951, 2020.

FENG, C.; ZHANG, S.; WANG, Y.; WANG, G.; PAN, X.; ZHONG, Q.; YAO, P. Synchronous removal of ammonium and phosphate from swine wastewater by two agricultural waste based adsorbents: Performance and mechanisms. **Bioresource technology**, v. 307, p. 123231, 2020.

FOLADORI, P.; CUTRUPI, F.; SEGATA, N.; MANARA, S.; PINTO, F.; MALPEI, F.; LA ROSA, G.; SARS-CoV-2 from faeces to wastewater treatment: What do we know? A review. **Science of the Total Environment**, v. 743, p. 140444, 2020.

GARDEA-TORRESDEY, J. L.; DE LA ROSA, G.; PERALTA-VIDEA, J. R.; MONTES, M.; CRUZ-JIMENEZ, G.; CANO-AGUILERA, I. Differential uptake and transport of trivalent and hexavalent chromium by tumbleweed (*Salsola kali*). Archives of **Environmental Contamination and Toxicology**, v. 48, n. 2, p. 225-232, 2005.

GARG, S.; GAUNS, M. Marine environmental chemistry and ecotoxicology of heavy metals. **In:** Metals in Water. Elsevier, 2023. p. 195-211.

GARG, S.; ROY, A. Phytoremediation: An alternative approach for removal of dyes. **In:** Phytoremediation. Academic Press, 2022. p. 369-386.

GAUTAM, V.; KOHLI, S. K.; KAPOOR, D.; BAKSHI, P.; SHARMA, P.; ARORA, S.; AHMAD, P. Stress protective effect of *Rhododendron arboreum* leaves (MEL) on chromium-treated *Vigna radiata* plants. **Journal of Plant Growth Regulation**, v. 40, n. 1, p. 423-435, 2021.

GENG, N.; XIA, Y.; LU, D.; BAI, Y.; ZHAO, Y.; WANG, H.; REN, L.; XU, C.; HUA, E.; SUN, G. The bacterial community structure in epiphytic biofilm on submerged macrophyte *Potamogetom crispus* L. and its contribution to heavy metal accumulation in an urban industrial area in Hangzhou. **Journal of Hazardous Materials**, v. 430, p. 128455, 2022.

GHERNAOUT, D.; ELBOUGHDIRI, N.; AL ARNI, S. New insights towards disinfecting viruses–short notes. **J. Water Reuse Desalination,** v.10, n.3, p. 173–186, 2020.

GHORI, N.-H.; GHORI, T.; HAYAT, M.; IMADI, S.; GUL, A.; ALTAY, V.; OZTURK, M. Heavy metal stress and responses in plants. **International Journal of Environmental Science and Technology,** v. 16, n. 3, p. 1807-1828, 2019.

GIANNOPOLITIS, C. N., RIES, S. K. Superoxide dismutases: I. Occurrence in higher plants. **Plant physiology**, v. 59, n. 2, p. 309-314, 1977.

GOMEZ, B. M.; REALE, M.; EL KASSISSE, Y.; MUJICA, C.; GÓMEZ, C.; DE CABO, L.; RODRÍGUEZ SALEMI, V. Metals uptake by *Sagittaria montevidensis* in contaminated riparian Area of Matanza-Riachuelo river (Argentina). **SN Applied Sciences**, v. 2, n. 12, p. 1-10, 2020.

GONZÁLEZ-GARCÍA, P.; GAMBOA-GONZÁLEZ, S.; ANDRADE MARTÍNEZ, I.; HERNÁNDEZ-QUIROZ, T. Preparation of activated carbon from water hyacinth stems by chemical activation with K_2CO_3 and its performance as adsorbent of sodium naproxen. **Environmental Progress & Sustainable Energy**, p.e13366, 2019.

GONZALEZ, R.; CURTIS, K.; BIVINS, A.; BIBBY, K.; WEIR, M. H.; YETKA, K.; GONZALEZ, D. COVID-19 surveillance in Southeastern Virginia using wastewater-based epidemiology. **Water research**, v. 186, p. 116296, 2020.

GONZALEZ-GARCÍA, P. Activated carbon from lignocellulosics precursors: a review of the synthesis methods, characterization techniques and applications. Renew. Sustain. **Energy Rev.** 82, 1393–1414, 2018.

GONZALEZ-GARCÍA, P., GAMBOA-GONZALEZ, S., ANDRADE MARTÍNEZ, I., HERNANDEZ-QUIROZ, T. Preparation of activated carbon from water hyacinth stems by chemical activation with K_2CO_3 and its performance as adsorbent of sodium naproxen. **Environmental Progress & Sustainable Energy**, v. 39, n. 3, p. e13366, 2020.

GORNY, J.; BILLON, G.; NOIRIEL, C.; DUMOULIN, D.; LESVEN, L.; MADÉ, B. Chromium behavior in aquatic environments: a review. **Environmental Reviews**, v.24, n.4, p.503-516, 2016.

GRUBE, A. M.; COLEMAN, C. K.; LAMONTAGNE, C. D.; MILLER, M. E.; KOTHEGAL, N. P.; HOLCOMB, D. A.; STEWART, J. R. Detection of SARS-CoV-2 RNA in wastewater and comparison to COVID-19 cases in two sewersheds, North Carolina, USA. **Science of The Total Environment**, v. 858, p. 159996, 2023.

GOSWAMI, K.P.; PUGAZHENTHI, G. Credibility of polymeric and ceramic membrane filtration in the removal of bacteria and virus from water: a review. **J. Environ. Manag.**, v. 2**6**8, p. 110583, 2020.

GUNASEKARAN, S.S.; BOSE, R.S.; RAMAN, K. Electrochemical capacitive performance of $ZnCl_2$ activated carbon derived from bamboo bagasse in aqueous and organic electrolyte. **Oriental Journal of Chemistry**, v. 35, n. 1, p. 302, 2019.

GUPTA, A.; JOIA, J.; SOOD, A.; SOOD, R.; SIDHU, C.; KAUR, G. Microbes as potential tool for remediation of heavy metals: a review. **Journal of Microbial & Biochemical Technology**, v. 8, n. 4, p. 364-372, 2016.

HADAD, H.R.; MUFARREGE, M.D.L.M.; LUCA, G.A.D; DENARO, A.C.; NOCETTI, E.; MAINE, M.A. Potential metal phytoremediation in peri-urban wetlands using rooted macrophytes. **Ecological Engineering**, v. 182, p. 106734, 2022.

HAGHNAZAR, H.; HUDSON-EDWARDS, K.A.; KUMAR, V.; POURAKBAR, M.; MAHDAVIANPOUR, M.; AGHAYANI, E. Potentially toxic elements contamination in surface sediment and indigenous aquatic macrophytes of the Bahmanshir River, Iran: Appraisal of phytoremediation capability. **Chemosphere**, v. 285, p. 131446, 2021.

HAMIDI, D.; FARD, M.B.; YETILMEZSOY, K.; ALAVI, J.; ZAREI, H. Application of *Orchis mascula* tuber starch as a natural coagulant for oily-saline wastewater treatment: modeling and optimization by multivariate adaptive regression splines method and response surface methodology. **J. Environ. Chem. Eng.,** v. 9, n.1, p. 104745, 2021.

HAOKIP, N.; GUPTA, A. Biochemical and antioxidant responses of *Ipomoea aquatica* exposed to graded concentrations of chromium. **Biologia**, v. 76, n. 9, p. 2477-2484, 2021.

HE, J.; STREZOV, V.; KUMAR, R.; WELDEKIDAN, H.; JAHAN, S.; DASTJERDI, B. H.; ZHOU, X.; KAN, T. Pyrolysis of heavy metal contaminated *Avicennia marina* biomass from phytoremediation: Characterisation of biomass and pyrolysis products. **Journal of Cleaner Production**, v. 234, p. 1235-1245, 2019.

HE, L.; SU, R.; CHEN, Y.; ZENG, P.; DU, L.; CAI, B.; ZHANG, A.; ZHU, H. Integration of manganese accumulation, subcellular distribution, chemical forms, and physiological responses to understand manganese tolerance in *Macleaya cordata*. **Environmental Science and Pollution Research**, p. 1-10, 2022.

HEIDARINEJAD, Z.; DEHGHANI, M. H.; HEIDARI, M.; JAVEDAN, G.; ALI, I.; SILLANPÄÄ, M. Methods for preparation and activation of activated carbon: a review. **Environmental Chemistry Letters**, p.1-23, 2020.

HEISI, H.D.; AWOSUSI, A.A.; NKUNA, R.; MATAMBO, T.S. Phytoextraction of anthropogenic heavy metal contamination of the Blesbokspruit wetland: Potential of wetland macrophytes. **Journal of Contaminant Hydrology**, p. 104101, 2022.

HEJNA, M.; GOTTARDO, D.; BALDI, A.; DELL'ORTO, V.; CHELI, F.; ZANINELLI, M.; ROSSI, L. Nutritional ecology of heavy metals. **Animal**, v. 12, n. 10, p. 2156-2170, 2018.

HOPKINS, W.G. Introduction to Plant Physiology, 2nd ed.; John Wiley & Sons: New York, NY, USA, 2000; p. 512.

HORN, T.B.; ZERWES, F.V.; KIST, L.T.; MACHADO, E.L. Constructed wetland and photocatalytic ozonation for university sewage treatment. **Ecological Engineering**, v. 63, p. 134-141, 2014.

HU, H.; ZHANG, R.; TAO, Z.; LI, X.; LI, Y.; HUANG, J.; PENG, L. Cellulose synthase mutants distinctively affect cell growth and cell wall integrity for plant biomass production in Arabidopsis. **Plant Cell Physiol**., v. 59, n. 6, p. 1144–1157, 2018.

HUA, Z. L.; LI, X. Q.; ZHANG, J. Y.; GU, L. Removal potential of multiple perfluoroalkyl acids (PFAAs) by submerged macrophytes in aquatic environments: Tolerance of Vallisneria natans and PFAA removal in submerged macrophyte-microbiota systems. **Journal of Hazardous Materials**, v. 424, p. 127695, 2022.

HUANG, C.; LAI, C.; XU, P.; ZENG, G.; HUANG, D.; ZHANG, J.; WANG, R. Lead-induced oxidative stress and antioxidant response provide insight into the tolerance of *Phanerochaete chrysosporium* to lead exposure. **Chemosphere**, v. 187, p. 70-77, 2017.

HUANG, H.; YAO, W.; LI, R.; ALI, A.; DU, J.; GUO, D.; XIAO, R.; GUO, Z.; ZHANGA, Z. Effect of pyrolysis temperature on chemical form, behavior and environmental risk of Zn, Pb and Cd in biochar produced from phytoremediation residue. **Bioresource technology**, v. 249, p. 487-493, 2018.

ISLAM, F.; YASMEEN, T.; ALI, Q.; ALI, S.; ARIF, M.S.; HUSSAIN, S.; RIZVI, H. Influence of *Pseudomonas aeruginosa* as PGPR on oxidative stress tolerance in wheat under Zn stress. **Ecotoxicology and Environmental Safety**, v.104, p.285-293, 2014.

ISLAM, F.; YASMEEN, T.; ARIF, M. S.; RIAZ, M.; SHAHZAD, S. M.; IMRAN, Q.; ALI, I. Combined ability of chromium (Cr) tolerant plant growth promoting bacteria (PGPB) and salicylic acid (SA) in attenuation of chromium stress in maize plants. **Plant Physiology and Biochemistry**, v. 108, p. 456-467, 2016.

INOBEME, A., MATHEW, J. T., ADETUNJI, C. O., AJAI, A. I., INOBEME, J., MALIKI, M., EZIUKWU, C. A. Recent advances in nanotechnology for remediation of heavy metals. **Environmental Monitoring and Assessment**, v. 195, n. 1, p. 1-24, 2023.

JIN, G.; ZHANG, Z.; LI, R.; CHEN, C.; TANG, H.; LI, L.; BARRY, D. A. Transport of zinc ions in the hyporheic zone: Experiments and simulations. **Advances in Water Resources**, v. 146, p. 103775, 2020.

JOHANSEN, Donald Alexander. Plant microtechnique. McGraw-Hill Book Company, Inc: London; 530p, 1940.

JOONAKI, E.; HASSANPOURYOUZBAND, A.; HELDT, C.L.; AREO, O. Surface chemistry can unlock drivers of surface stability of SARS-CoV-2 in variety of environmental conditions. **Inside Chem.** v.6, n.9, p. 2135–2146, 2020.

JOSEPH, L.; JUN, B.-M.; FLORA, J. R. V.; PARK, C. M.; YOON, Y. Removal of heavy metals from water sources in the developing world using low-cost materials: A review. **Chemosphere**, v.229, p.142-159, 2019.

KABATA-PENDIAS, A.; PENDIAS, H. **Trace elements in soils and plants**, 3rd edn. 2001, CRC Press, Boca Raton.

KAFLE, A.; TIMILSINA, A.; GAUTAM, A.; ADHIKARI, K.; BHATTARAI, A.; ARYAL, N. Phytoremediation: mechanisms, plant selection and enhancement by natural and synthetic agents. **Environmental Advances**, p. 100203, 2022.

KAPLAN, H.; RATERING, S.; FELIX-HENNINGSEN, P.; SCHNELL, S. Stability of in situ immobilization of trace metals with different amendments revealed by microbial 13C-labelled wheat root decomposition and efflux-mediated metal resistance of soil bacteria. **Science of The Total Environment**, v. 659, p. 1082-1089, 2019.

KAPOOR, D.; SINGH, S.; KUMAR, V.; ROMERO, R.; PRASAD, R.; SINGH, J. Antioxidant enzymes regulation in plants in reference to reactive oxygen species (ROS) and reactive nitrogen species (RNS). **Plant Gene**, v. 19, p. 100182, 2019.

KAUR, S.; RANI, S.; MAHAJAN, R. K. Adsorption Kinetics for the removal of Hazardous Dye Congo Red by Biowaste Materials as Adsorbents. **Journal of Chemistry** p.12, 2012.

KAYA, M.; SAHIN, O.; SAKA, C. Preparation and TG/DTG, FT-IR, SEM, BET surface area, iodine number and methylene blue number analysis of activated carbon from pistachio shells by chemical activation. **Int. J. Chem. React. Eng.** v. 16, n.2, 2017.

KHAN, A.U.; KHAN, A.N.; WARIS, A.; ILYAS, M.; ZAMEL, D. Phytoremediation of pollutants from wastewater: A concise review. **Open Life Sciences**, v. 17, n. 1, p. 488-496, 2022.

ZHAO, D.; WANG, P.; ZHAO, F.J. Dietary cadmium exposure, risks to human health and mitigation strategies. **Critical Reviews in Environmental Science and Technology**, p. 1-25, 2022.

KILIÇ, M., APAYDIN-VAROL, E., PÜTÜN, A.E. Preparation and surface characterization of activated carbons from *Euphorbia rigida* by chemical activation with $ZnCl_2$, K_2CO_3, NaOH and H_3PO_4. **Appl. Surf. Sci.** 261, 247–254, 2012.

KISA, D.; ELMASTAŞ, M.; ÖZTÜRK, L.; KAYIR, Ö. Responses of the phenolic compounds of *Zea mays* under heavy metal stress. **Applied Biological Chemistry**, v. 59, n. 6, p. 813-820, 2016.

KOBIELSKA, P. A.; HOWARTH, A. J.; FARHA, O. K.; NAYAK, S. Metal–organic frameworks for heavy metal removal from water. **Coordination Chemistry Reviews**, v.358, p.92-107, 2018.

KOCAMEMI, B.A.; KURT, H.; SAIT, A.; SARAC, F.; SAATCI, A.M.; PAKDEMIRLI, B. SARS-CoV-2 detection in Istanbul wastewater treatment plant sludges. **MedRxiv**, v. 7, p. 10.1101, 2020

KOLAJ-ROBIN, O.; RUSSELL, D.; HAYES, K.A.; PEMBROKE, J.T.; SOULIMANE, T. Cation diffusion facilitator family: structure and function. **FEBS letters**, v. 589, n. 12, p. 1283-1295, 2015.

KORB, C. C.; SUERTEGARAY, D. M. A. Identificação de depósitos tecnogênicos em um reservatório de abastecimento de água da cidade de Pelotas (RS). **Quaternary and Environmental Geosciences**, v. 5, n. 1, 2014.

KOVÁČIK, J.; BABULA, P.; HEDBAVNY, J.; KLEJDUS, B. Hexavalent chromium damages chamomile plants by alteration of antioxidants and its uptake is prevented by calcium. **Journal of hazardous materials**, v. 273, p. 110-117, 2014.

KOHZADI, S.; SHAHMORADI, B.; GHADERI, E.; LOQMANI, H.; MALEKI, A. Concentration, source, and potential human health risk of heavy metals in the commonly consumed medicinal plants. **Biological trace element research**, v. 187, n. 1, p. 41-50, 2019.

KURNIAWAN, S.B.; AHMAD, A.; SAID, N.S.M.; IMRON, M.F.; ABDULLAH, S.R.S.; OTHMAN, A.R.; PURWANTI, I.F.; HASAN, H.A. Macrophytes as wastewater treatment agents: Nutrient uptake and potential of produced biomass utilization toward circular economy initiatives. **Science of The Total Environment**, v. 790, p. 148219, 2021.

KUMAR, A.; DUBEY, A. K.; KUMAR, V.; ANSARI, M. A.; NARAYAN, S.; KUMAR, S.; MEENAKSHI KUMAR, S.; PANDEY, V.; SHIRKE, P.A.; PANDE, V.; SANYAL, I. Over-expression of chickpea glutaredoxin (CaGrx) provides tolerance to heavy metals by reducing metal accumulation and improved physiological and antioxidant defence system. **Ecotoxicology and Environmental Safety**, v. 192, p. 110252, 2020.

KUMAR, A.; JENA, H.M. 2017. Adsorption of Cr (VI) from aqueous phase by high surface area activated carbon prepared by chemical activation with $ZnCl_2$. **Process Saf. Environ. Protect.** v.109, p. 63–71.

KUMAR, M.; UPADHYAY, S.N.; MISHRA, P.K. A comparative study of thermochemical characteristics of lignocellulosic biomasses. **Bioresource Technology Reports**, v. 8, p. 100186, 2019.

KUMAR, M., PATEL, A.K., SHAH, A.V., RAVAL, J., RAJPARA, N., JOSHI, M., JOSHI, C.G. First proof of the capability of wastewater surveillance for COVID-19 in India through detection of genetic material of SARS-CoV-2. **Sci. Total Environ.** 746, 141326, 2020.

KUMAR, M., MAZUMDER, P., MOHAPATRA, S., THAKUR, A.K., DHANGAR, K., TAKI, K., MUKHERJEE, S., PATEL, A.K., BHATTACHARYA, P., MOHAPATRA, P., RINKLEBE, J., KITAJIMA, M., HAI, F.I., KHURSHEED, A., FURUMAI, H., SONNE, C., KURODA, K. A chronicle of SARS-CoV-2: seasonality, environmental fate, transport, inactivation, and antiviral drug resistance. **J. Hazard Mater**, v. 405, p. 124043, 2021.

KUNDU, D.; DEY, S.; RAYCHAUDHURI, S. S. Chromium (VI)–induced stress response in the plant *Plantago ovata* Forsk in vitro. **Genes and Environment**, v. 40, n. 1, p. 1-13, 2018.

LADISLAS, S.; GÉRENTE, C.; CHAZARENC, F.; BRISSON, J.; ANDRÈS, Y. Performances of two macrophytes species in floating treatment wetlands for cadmium, nickel, and zinc removal from urban stormwater runoff. **Water, Air, & Soil Pollution**, v. 224, n. 2, p. 1-10, 2013.

LAHRICH, S., LAGHRIB, F. FARAHI, A., BAKASSE, M., SAQRANE, S., EL MHAMMEDI, M.A. Review on the contamination of wastewater by COVID-19 virus: Impact and treatment. **Science of the Total Environment**, v. 751, p. 142325, 2021.

LEVIZOU, E.; ZANNI, A. A.; ANTONIADIS, V. Varying concentrations of soil chromium (VI) for the exploration of tolerance thresholds and phytoremediation potential of the oregano (*Origanum vulgare*). **Environmental Science and Pollution Research**, v. 26, n. 1, p. 14-23, 2019.

LI, J.; YU, H.; LUAN, Y. Meta-analysis of the copper, zinc, and cadmium absorption capacities of aquatic plants in heavy metal-polluted water. **International Journal of Environmental Research and Public Health**, v. 12, n. 12, p. 14958-14973, 2015.

LI, Q.G.; LIU, G.H.; QI, L.; WANG, H.C.; YE, Z.F.; ZHAO, Q.L. Heavy metal-contained wastewater in China: Discharge, management and treatment. **Science of The Total Environment**, v. 808, p. 152091, 2022.

LI, C.; WANG, M.; LUO, X.; LIANG, L.; HAN, X.; LIN, X. Accumulation and effects of uranium on aquatic macrophyte *Nymphaea tetragona* Georgi: Potential application to phytoremediation and environmental monitoring. **Journal of environmental radioactivity**, 2019, 198, 43-49.

LI, N.; QIN, L.; JIN, M.; ZHANG, L.; GENG, W.; XIAO, X. Extracellular adsorption, intracellular accumulation and tolerance mechanisms of *Cyclotella* sp. to Cr (VI) stress. **Chemosphere**, v. 270, p. 128662, 2021.

LICHTENTHALER, Hartmut K. Chlorophylls and carotenoids: pigments of photosynthetic biomembranes. In: Methods in enzymology. Academic Press, 1987. p. 350-382.

LIEW, R. K.; CHONG, M. Y.; OSAZUWA, O. U.; NAM, W. L.; PHANG, X. Y.; SU, M. H.; CHENG, C. K.; CHONG, C. T.; LAM, S. S. Production of activated carbon as catalyst support by microwave pyrolysis of palm kernel shell: a comparative study of chemical versus physical activation. **Research on Chemical Intermediates**, v.44, n.6, p.3849-3865, 2018.

LIU, Z.; LU, B.; HE, B.; LI, X.; WANG, L.-A. Effect of the pyrolysis duration and the addition of zeolite powder on the leaching toxicity of copper and cadmium in biochar produced from four different aquatic plants. **Ecotoxicology and environmental safety**, v. 183, p. 109517, 2019.

LIU, D.; ZOU, J.; WANG, M.; JIANG, W. Hexavalent chromium uptake and its effects on mineral uptake, antioxidant defence system and photosynthesis in *Amaranthus viridis* L., **Bioresource Technology**, v. 99, n. 7, p. 2628-2636, 2008.

LIU, C.; DU, W.; CAI, H.; JIA, Z.; DONG, H. Trivalent chromium pretreatment alleviates the toxicity of oxidative damage in wheat plants exposed to hexavalent chromium. **Acta Physiologiae Plantarum**, v. 36, n. 3, p. 787-794, 2014.

LIU, S.-H.; ZENG, G.-M.; NIU, Q.-Y.; LIU, Y.; ZHOU, L.; JIANG, L.-H.; TAN, X.-F.; XU, P.; ZHANG, C.; CHENG, M. Bioremediation mechanisms of combined pollution of PAHs and heavy metals by bacteria and fungi: A mini review. **Bioresource technology**, v.224, p.25-33, 2017.

LIU, D., THOMPSON, J.R., CARDUCCI, A., BI, X., Potential secondary transmission of SARS-CoV-2 via wastewater. **Science of the Total Environment**, v.749, p. 142358, 2020.

LU, Y.; SONG, S.; WANG, R.; LIU, Z.; MENG, J.; SWEETMAN, A. J.; JENKINS, A.; FERRIER, R. C.; LI, H.; LUO, W.; WANG, T. Impacts of soil and water pollution on food safety and health risks in China. **Environment International**, v.77, p.5-15, 2015.

LU, B.; XU, Z.; LI, J.; CHAI, X. Removal of water nutrients by different aquatic plant species: An alternative way to remediate polluted rural rivers. **Ecological Engineering**, v. 110, p. 18-26, 2018.

LU, Y.; KRONZUCKER, H.J.; SHI, W. Stigmasterol root exudation arising from *Pseudomonas* inoculation of the duckweed rhizosphere enhances nitrogen removal from polluted waters. **Environmental Pollution**, v. 287, p. 117587, 2021.

LUA, A.C., YANG, T. Effect of activation temperature on the textural and chemical properties of potassium hydroxide activated carbon prepared from pistachio-nut shell. **J. Colloid Interface Sci.,** v. 274, n. 2, p. 594–601, 2004.

LUCKE, T.; WALKER, C.; BEECHAM, S. Experimental designs of field-based constructed floating wetland studies: A review. **Science of the Total Environment**, v. 660, p. 199-208, 2019.

LUTTERBECK, C.A.; KIST, L.T.; LOPEZ, D.R.; ZERWES, F.V.; MACHADO, E.L. Life cycle assessment of integrated wastewater treatment systems with constructed wetlands in rural areas. **J. Clean. Prod.** v. 148, p. 527–536, 2017.

MACHADO, E.L; LOURENÇO, A.M.; KIST, L.T.; SCHNEIDER, R.C.S.; KERN, D.; LOBO, E.A.A.; LUTTERBECK, C.A.; SILVEIRA, D.D.; HORN, T.B.; ZERWES, F.V. Constructed wetlands integrated with advanced oxidation processes in wastewater treatment for reuse. In: Fatta-Kassinos, D., Dionysiou, D., Kümmerer, K. (Eds.), Advanced Treatment Technologies for Urban Wastewater Reuse. The Handbook of Environmental Chemistry, vol. 45. Springer, Cham., 2015

MACHADO, L.M.; LÜTKE, S.F.; PERONDI, D.; GODINHO, M.; OLIVEIRA, M.L.; COLLAZZO, G.C.; DOTTO, G.L. Treatment of effluents containing 2-chlorophenol by adsorption onto chemically and physically activated biochars. **J. Environ. Chem. Eng.** v. 8, n.6, p. 104473, 2020.

MAIA, Luisa Cardoso; SOARES, Liliane Catone; GURGEL, Leandro Vinícius Alves. A review on the use of lignocellulosic materials for arsenic adsorption. **Journal of Environmental Management**, v. 288, p. 112397, 2021.

MALASPINA, D.C., FARAUDO, J., 2020. Computer Simulations of the interaction between SARS-CoV-2 spike glycoprotein and different surfaces. **Biointerphases**, v. 15, n. 5, p. 051008, 2020.

MAŁKOWSKI, E.; SITKO, K.; SZOPIŃSKI, M.; GIEROŃ, Ż.; POGRZEBA, M.; KALAJI, H. M.; ZIELEŹNIK-RUSINOWSKA, P. Hormesis in plants: The role of oxidative stress, auxins and photosynthesis in corn treated with Cd or Pb. **International journal of molecular sciences**, v. 21, n. 6, p. 2099, 2020.

MAMANÍ, A.; RAMÍREZ, N.; DEIANA, C.; GIMENEZ, M.; SARDELLA, F. Highly microporous sorbents from lignocellulosic biomass: different activation routes and their application to dyes adsorption. **Journal of Environmental Chemical Engineering**, v. 7, n. 5, p. 103148, 2019.

MANEERUNG, T.; LIEW, J.; DAI, Y.; KAWI, S.; CHONG, C.; WANG, C.H. Activated carbon derived from carbon residue from biomass gasification and its application for dye adsorption: kinetics, isotherms and thermodynamic studies. **Bioresource technology**, v. 200, p. 350-359, 2016.

MANORAMA THAMPATTI, K. C., BEENA, V. I., MEERA, A. V., & AJAYAN, A. S. Phytoremediation of metals by aquatic macrophytes. **In:** Phytoremediation. Springer, Cham, 2020. p. 153-204.

MANQUIÁN-CERDA, K.; ESCUDEY, M.; ZÚÑIGA, G.; ARANCIBIA-MIRANDA, N.; MOLINA, M.; CRUCES, E. Effect of cadmium on phenolic compounds, antioxidant enzyme activity and oxidative stress in blueberry (*Vaccinium corymbosum* L.)

plantlets grown in vitro. **Ecotoxicology and environmental safety**, v. 133, p. 316-326, 2016.

MASSOUD, R.; HADIANI, M.R.; HAMZEHLOU, P.; KHOSRAVI-DARANI, K. Bioremediation of heavy metals in food industry: Application of *Saccharomyces cerevisiae*. **Electronic Journal of Biotechnology**, v. 37, p. 56-60, 2019.

MATSUSHITA, T.; SUZUKI, H.; SHIRASAKI, N.; MATSUI, Y.; OHNO, K. Adsorptive virus removal with super-powdered activated carbon. Separation and Purification Technology, v. 107, p. 79-84, 2013.

MAULIDIANI, ABAS, F.; KHATIB, A.; SHAARI, K.; LAJIS, N. H. Chemical characterization and antioxidant activity of three medicinal Apiaceae species. **Industrial Crops and Products**, v. 55, p. 238-247, 2014.

MELO, G. W.; FURINI, G.; BRUNETTO, G.; COMIN, J. J.; SIMÃO, D. G.; MARQUES, A. C. R.; ZALAMENA, J. Identification and phytoremediation potential of spontaneous species in vineyard soils contaminated with copper. **International Journal of Phytoremediation**, v. 24, n. 4, p. 342-349, 2021.

MEYER, D. D.; BEKER, S. A.; BÜCKER, F.; PERALBA, M. D. C. R.; FRAZZON, A. P. G.; OSTI, J. F.; BENTO, F. M. Bioremediation strategies for diesel and biodiesel in oxisol from southern Brazil. **International Biodeterioration & Biodegradation**, v. 95, p. 356-363, 2014.

MI, X., ALBUKHARI, S.M., HELDT, C.L., HEIDEN, P.A. Virus and chlorine adsorption onto guanidine modified cellulose nanofibers using covalent and hydrogen bonding. **Carbohydrate research**, v. 498, p. 108153, 2020.

MISHRA, S.; BHARAGAVA, R. N. Toxic and genotoxic effects of hexavalent chromium in environment and its bioremediation strategies. **Journal of Environmental Science and Health**, Part C, v.34, n.1, p.1-32, 2016.

MOHAN, S.V., HEMALATHA, M., KOPPERI, H., RANJITH, I., KUMAR, A.K. SARS-CoV-2 in environmental perspective: occurrence, persistence, surveillance, inactivation and challenges. **Chemical Engineering Journal**, v. 405, p. 126893, 2021.

MOHAPATRA, S.; MENON, N.G.; MOHAPATRA, G.; PISHARODY, L.; PATTNAIK, A.; MENON, N.G.; MUKHERJI, S. The Novel SARS-CoV-2 Pandemic: Possible Environmental Transmission, Detection, Persistence and Fate during Wastewater and Water Treatment. **Science of the Total Environment**, p. 142746, 2021.

MURADOV, N.; TAHA, M.; MIRANDA, A. F.; KADALI, K.; GUJAR, A.; ROCHFORT, S.; STEVENSON, T. BALL, A. S.; MOURADOV, A. Dual application of duckweed and azolla plants for wastewater treatment and renewable fuels and petrochemicals production. **Biotechnology for biofuels**, v. 7, n. 1, p. 1-17, 2014.

MUTHUSARAVANAN, S.; SIVARAJASEKAR, N.; VIVEK, J.S.; PARAMASIVAN, T.; NAUSHAD, M.; PRAKASHMARAN, J.; GAYATHRI, V.; AL-DUAIJ, O. K.

Phytoremediation of heavy metals: mechanisms, methods and enhancements. **Environmental chemistry letters**, v. 16, n. 4, p. 1339-1359, 2018.

NGUYEN, T.Q.; SESIN, V.; KISIALA, A.; EMERY, R.J.N. Phytohormonal roles in plant responses to heavy metal stress: Implications for using macrophytes in phytoremediation of aquatic ecosystems. **Environmental Toxicology and Chemistry**, 2021, 40, 1, 7-22.

NASCIMENTO, C.W.A.D.; BIONDI, C.M.; SILVA, F.B.V.D.; LIMA, L.H.V. Using plants to remediate or manage metal-polluted soils: an overview on the current state of phytotechnologies. **Acta Scientiarum. Agronomy**, v. 43, 2021.

NAGAJYOTI, P. C.; LEE, K. D.; SREEKANTH, T. V. M. Heavy metals, occurrence and toxicity for plants: a review. **Environmental chemistry letters**, v. 8, n. 3, p. 199-216, 2010.

NANDA, S.; AZARGOHAR, R.; KOZINSKI, J.A.; DALAI, A.K. Characteristic studies on the pyrolysis products from hydrolyzed Canadian lignocellulosic feedstocks. **BioEnergy Research**, v.7, n.1, p. 174–191, 2014.

NAYAK, A.; BHUSHAN, B.; GUPTA, V.; SHARMA, P. Chemically activated carbon from lignocellulosic wastes for heavy metal wastewater remediation: Effect of activation conditions. **Journal of Colloid and Interface Science**, v.493, p.228-240, 2017.

NIZAM, N.U.M.; HANAFIAH, M.M.; MAHMOUDI, E.; HALIM, A.A.; MOHAMMAD, A.W. The removal of anionic and cationic dyes from an aqueous solution using biomass-based activated carbon. **Sci. Rep**. 11, 8623. 2021.

NNAJI, C.C.; AGIM, A.E.; MAMA, C.N.; EMENIKE, P.C.; OGAREKPE, N.M. Equilibrium and thermodynamic investigation of biosorption of nickel from water by activated carbon made from palm kernel chaff. **Sci. Rep**., v. 11, n.1, p. 1–20, 2021.

O'BRIEN, T.; FEDER, N.; MCCULLY, M. E. Polychromatic staining of plant cell walls by toluidine blue O. **Protoplasma**, v. 59, n. 2, p. 368-373, 1964.

OGO, H. A.; TANG, N.; LI, X.; GAO, X.; XING, W. Combined toxicity of microplastic and lead on submerged macrophytes. **Chemosphere**, v. 295, p. 133956, 2022.

OHKAWA, H.; OHISHI, N.; YAGI, K. Assay for lipid peroxides in animal tissues by thiobarbituric acid reaction. **Analytical biochemistry**, v. 95, n. 2, p. 351-358, 1979.

OJEDOKUN, A. T.; BELLO, O. S. Sequestering heavy metals from wastewater using cow dung. **Water Resources and Industry**, v.13, p.7-13, 2016.

OLADOYE, P.O.; OLOWE, O.M.; ASEMOLOYE, M.D. Phytoremediation technology and food security impacts of heavy metal contaminated soils: A review of literature. **Chemosphere**, v. 288, p. 132555, 2022.

PAN, L.; WANG, J.; WANG, X.; JI, J. S.; YE, D.; SHEN, J., LI, L.; LIU, H.; ZHANG, L.; SHI, X.; WANG, L. Prevention and control of coronavirus disease 2019 (COVID-19) in public places. **Environmental Pollution,** v. 292, p. 118273, 2022.

PANDEY, V.C. Phytoremediation efficiency of *Eichhornia crassipes* in fly ash pond. **International Journal of Phytoremediation**, v. 18, n. 5, p. 450-452, 2016.

PANDEY, L.M. Surface engineering of personal protective equipments (PPEs) to prevent the contagious infections of SARS-CoV-2. **Surface Engineering**, v. 36, n. 9, p. 901-907, 2020.

PAVLINERI, N.; SKOULIKIDIS, N.T.; TSIHRINTZIS, V.A. Constructed floating wetlands: a review of research, design, operation and management aspects, and data meta-analysis. **Chemical Engineering Journal**, v. 308, p. 1120-1132, 2017.

PECCIA, J.; ZULLI, A.; BRACKNEY, D.E.; GRUBAUGH, N.D.; KAPLAN, E.H.; CASANOVAS-MASSANA, A.; KO, A.I.; MALIK, A.A.; WANG, D.; WANG, M.; WARREN, J.L.; WEINBERGER, D.M.; OMER, S.B. SARS-CoV-2 RNA concentrations in primary municipal sewage sludge as a leading indicator of COVID-19 outbreak dynamics. **MedRxiv**, 2020.

PEYDAYESH, M., RAHBAR-KELISHAMI, A. Adsorption of methylene blue onto *Platanus orientalis* leaf powder: kinetic, equilibrium and thermodynamic studies. **Journal of Industrial and Engineering Chemistry**, v. 21, p. 1014-1019, 2015.

PIRES-LIRA, M. F.; DE CASTRO, E. M.; LIRA, J. M. S.; DE OLIVEIRA, C.; PEREIRA, F. J.; PEREIRA, M. P. Potential of *Panicum aquanticum* Poir.(Poaceae) for the phytoremediation of aquatic environments contaminated by lead. **Ecotoxicology and Environmental Safety**, v. 193, p. 110336, 2020.

PIRIYA, R.S., JAYABALAKRISHNAN, R.M., MAHESWARI, M., BOOMIRAJ, K., OUMABADY, S. Coconut shell derived $ZnCl_2$ activated carbon for malachite green dye removal. **Water Sci. Technol.** v. 83, n.5, p. 1167–1182, 2021.

POWELL, T., BRION, G.M., JAGTOYEN, M., DERBYSHIRE, F. Investigating the effect of carbon shape on virus adsorption. **Environ. Sci. Technol.** v. 34, n.13, p. 2779–2783, 2000.

PRADO, C.; PAGANO, E.; PRADO, F.; ROSA, M. Detoxification of Cr (VI) in *Salvinia minima* is related to seasonal-induced changes of thiols, phenolics and antioxidative enzymes. **Journal of hazardous materials**, v. 239, p. 355-361, 2012.

PRASAD, S.; YADAV, K. K.; KUMAR, S.; GUPTA, N.; CABRAL-PINTO, M. M.; REZANIA, S.; RADWAN, N.; ALAM, J. Chromium contamination and effect on environmental health and its remediation: A sustainable approaches. **Journal of Environmental Management**, v. 285, p. 112174, 2021.

PUNWONG, P.; JUPRASONG, Y.; TRAIPERM, P. Effects of an oil spill on the leaf anatomical characteristics of a beach plant (*Terminalia catappa* L.). **Environmental Science and Pollution Research**, v. 24, n. 27, p. 21821-21828, 2017.

QING, X.; YUTONG, Z.; SHENGGAO, L. Assessment of heavy metal pollution and human health risk in urban soils of steel industrial city (Anshan), Liaoning, Northeast China. **Ecotoxicology and Environmental Safety**, v.120, p.377-385, 2015

QU, J.; WANG, Y.; TIAN, X.; JIANG, Z.; DENG, F.; TAO, Y.; ZHANG, Y. KOH-activated porous biochar with high specific surface area for adsorptive removal of chromium (VI) and naphthalene from water: affecting factors, mechanisms and reusability exploration. **Journal of Hazardous Materials**, v. 401, p. 123292, 2021.

RIZWAN, M.; ALI, S.; ZIA UR REHMAN, M.; RINKLEBE, J.; TSANG, D.C.W.; BASHIR, A.; MAQBOOL, A.; TACK, F.M.G.; OK, Y.S. Cadmium phytoremediation potential of Brassica crop species: a review. **Science of the Total Environment**, v. 631, p. 1175-1191, 2018.

RAI, P.K. Heavy metals/metalloids remediation from wastewater using free floating macrophytes of a natural wetland. **Environmental Technology & Innovation**, v. 15, p. 100393, 2019.

RAFI, S., SHOAIB, A., AWAN, Z. A., RIZVI, N. B., SHAFIQ, M. Chromium tolerance, oxidative stress response, morphological characteristics, and FTIR studies of phytopathogenic fungus *Sclerotium rolfsii*. **Folia microbiologica**, v. 62, n. 3, p. 207-219, 2017.

RANDAZZO, W.; TRUCHADO, P.; CUEVAS-FERRANDO, E.; SIMON, P.; ALLENDE, A.; SANCHEZ, G. SARS-CoV-2 RNA in wastewater anticipated COVID-19 occurrence in a low prevalence area. **Water Res.** v. 181, p. 115942, 2020

RAO, S.N.; MANISSERO, D.; STEELE, V.R.; PAREJA, J. A narrative systematic review of the clinical utility of cycle threshold values in the context of COVID-19. **Infect. Dis. Ther**. 1–14, 2020.

RENIERI, E.A.; SAFENKOVA, I.V.; ALEGAKIS, A.K.; SLUTSKAYA, E.S.; KOKARAKI, V.; KENTOURI, M.; DZANTIEV, B.B.; TSATSAKIS, A.M. Cadmium, lead and mercury in muscle tissue of gilthead seabream and seabass: Risk evaluation for consumers. **Food and Chemical Toxicology**, 2019, 124, 439-449.

RIAZ, M.; YAN, L.; WU, X.; HUSSAIN, S.; AZIZ, O.; IMRAN, M.; JIANG, C. Boron reduces aluminum-induced growth inhibition, oxidative damage and alterations in the cell wall components in the roots of trifoliate orange**. Ecotoxicology and environmental safety**, v. 153, p. 107-115, 2018.

RIVIERE, G.N.; KORPI, A.; SIPPONEN, M.H.; ZOU, T.; KOSTIAINEN, M.A.; OSTERBERG, M. Agglomeration of viruses by cationic lignin particles for facilitated water purification. **ACS Sustain. Chem. Eng.** v. 8, n.10, p. 4167–4177, 2020.

RIZVI, A.; KHAN, M. S. Heavy metal induced oxidative damage and root morphology alterations of maize (Zea mays L.) plants and stress mitigation by metal tolerant nitrogen fixing *Azotobacter chroococcum*. **Ecotoxicology and Environmental safety**, v. 157, p. 9-20, 2018.

RUCIŃSKA-SOBKOWIAK, R. Water relations in plants subjected to heavy metal stresses. **Acta Physiologiae Plantarum**, v. 38, n. 11, p. 1-13, 2016.

SAJID, M.; NAZAL, M. K.; IHSANULLAH; BAIG, N.; OSMAN, A. M. Removal of heavy metals and organic pollutants from water using dendritic polymers based adsorbents: A critical review. **Separation and Purification Technology**, v.191, p.400-423, 2018.

SARAVANAN, A.; KUMAR, P. S.; GOVARTHANAN, M.; GEORGE, C. S.; VAISHNAVI, S., MOULISHWARAN, B.; YAASHIKAA, P. R. Adsorption characteristics of magnetic nanoparticles coated mixed fungal biomass for toxic Cr (VI) ions in aquatic environment. **Chemosphere**, v. 267, p. 129226, 2021.

SATTAR, S.; HUSSAIN, R.; SHAH, S.M.; BIBI, S.; AHMAD, S.R.; SHAHZAD, A.; ZAMIR, A.; RAUF, Z.; NOSHAD, A.; AHMAD, L. Composition, impacts, and removal of liquid petroleum waste through bioremediation as an alternative clean-up technology: A review. **Heliyon**, p. e11101, 2022.

SATTERFIELD, B. A.; BHATT, D. L.; GERSH, B. J. Cardiac involvement in the long-term implications of COVID-19. **Nature Reviews Cardiology**, v. 19, n. 5, p. 332-341, 2022.

SCOCCIANTI, V.; BUCCHINI, A. E.; IACOBUCCI, M.; RUIZ, K. B.; BIONDI, S. Oxidative stress and antioxidant responses to increasing concentrations of trivalent chromium in the Andean crop species *Chenopodium quinoa* Willd. **Ecotoxicology and Environmental Safety**, v. 133, p. 25-35, 2016.

SAMAL, K.; KAR, S.; TRIVEDI, S. Ecological floating bed (EFB) for decontamination of polluted water bodies: Design, mechanism and performance. **Journal of Environmental Management**, v.251, p.109550, 2019.

SANEP. Serviço Autônomo de Saneamento de Pelotas. 2019. **Estações de tratamento.**

SANTOS, V.M.; ANDRADE, L.C.; TIECHER, T.; ANDREAZZA, R.; CAMARGO, F.A.O. Phytoremediation of metals by colonizing plants developed in point bars in the channeled bed of the Dilúvio Stream, Southern Brazil. **International Journal of Phytoremediation**, v. 24, n. 1, p. 59-65, 2022.

SHAH, V.; DAVEREY, A. Phytoremediation: A multidisciplinary approach to clean up heavy metal contaminated soil. **Environmental Technology & Innovation**, v.18 p. 100774, 2020.

SHEN, C.; ZHAO, Y.Q.; LIU, R.B.; MORGAN, D.; WEI, T. Enhancing wastewater remediation by drinking water treatment residual-augmented floating treatment wetlands. **Science of The Total Environment**, 2019, 673, 230-236.

SHEN, X.; DAI, M.; YANG, J.; SUN, L.; TAN, X.; PENG, C.; ALI, I.; NAZ, I. A critical review on the phytoremediation of heavy metals from environment: Performance and challenges. **Chemosphere**, p. 132979, 2021.

SHAHID, M., SHAMSHAD, S., RAFIQ, M., KHALID, S., BIBI, I., NIAZI, N. K., DUMAT, C., RASHID, M. I. Chromium speciation, bioavailability, uptake, toxicity and detoxification in soil-plant system: A review. **Chemosphere**, v. 178, p. 513-533, 2017.

SHAHID, M.J.; ALI, S.; SHABIR, G.; SIDDIQUE, M.; RIZWAN, M.; SELEIMAN, M.F.; AFZAL, M. Comparing the performance of four macrophytes in bacterial assisted floating treatment wetlands for the removal of trace metals (Fe, Mn, Ni, Pb, and Cr) from polluted river water. **Chemosphere**, v. 243, p. 125353, 2020.

SHARMA, A.; KAPOOR, D.; WANG, J.; SHAHZAD, B.; KUMAR, V.; BALI, A. S.; YAN, D. Chromium bioaccumulation and its impacts on plants: an overview. **Plants**, v. 9, n. 1, p. 100, 2020.

SHARMIN, S. A.; ALAM, I.; KIM, K. H.; KIM, Y. G.; KIM, P. J.; BAHK, J. D.; LEE, B. H. Chromium-induced physiological and proteomic alterations in roots of *Miscanthus* sinensis. **Plant science**, v. 187, p. 113-126, 2012.

SHIMABUKU, Q.L.; ARAKAWA, F.S.; FERNANDES SILVA, M.; FERRI COLDEBELLA, P.; UEDA-NAKAMURA, T.; FAGUNDES-KLEN, M.R.; BERGAMASCO, R. Water treatment with exceptional virus inactivation using activated carbon modified with silver (Ag) and copper oxide (CuO) nanoparticles. **Environ. Technol.** v. 38, n.16, p. 2058–2069, 2017.

SIDHU G.P.S.; BALI A.S.; SINGH H.P.; BATISH D.R.; KOHLI R.K. Phytoremediation of lead by a wild, non-edible Pb accumulator *Coronopus didymus* (L.) Brassicaceae. **International Journal of phytoremediation**, v. 20, n. 5, p. 483-489, 2018.

SILVA, A. S. D.; JACQUES, R. J. S.; ANDREAZZA, R.; BENTO, F. M.; ROESCH, L. F. W.; CAMARGO, F. A. D. O. Properties of catechol 1, 2-dioxygenase in the cell free extract and immobilized extract of *Mycobacterium fortuitum*. **Brazilian Journal of Microbiology**, v. 44, p. 291-297, 2013.

SINGH, H.; KUMAR, D.; SONI, V. Copper and mercury induced oxidative stresses and antioxidant responses of *Spirodela polyrhiza* (L.) Schleid. Biochemistry and Biophysics Reports, v. 23, p. 100781, 2020.

SINHA, V., PAKSHIRAJAN, K., CHATURVEDI, R. Chromium (VI) accumulation and tolerance by *Tradescantia pallida*: biochemical and antioxidant study. **Applied biochemistry and biotechnology**, v. 173, n. 8, p. 2297-2306, 2014.

SINHA, V.; PAKSHIRAJAN, K.; CHATURVEDI, R. Chromium tolerance, bioaccumulation and localization in plants: an overview. **Journal of environmental management**, v. 206, p. 715-730, 2018.

SIMBANEGAVI, T. T.; NDAGURWA, H. G.; MUNDAVA, J.; MUNDY, P. J. Response of the waterbird community to floating pennywort (*Hydrocotyle ranunculoides*) cover at Ngamo dam, Antelope Park, Zimbabwe. **African Journal of Ecology**, v. 56, n. 1, p. 20-27, 2018.

SILVEIRA, E.O.; WINK, M.; ZAPPE, A.L.; KIST, L.T.; MACHADO, E.L. Sistema integrado com microalgas e wetland construído de fluxo vertical no tratamento de efluentes urbanos. **Eng. Sanitaria Ambient., v.** 24, n.2, p. 305–313, 2019.

SMOLDERS, A. J. P.; VERGEER, L. H. T.; VAN DER VELDE, G.; ROELOFS, J. G. M. Phenolic contents of submerged, emergent and floating leaves of aquatic and semi-aquatic macrophyte species: why do they differ? **Oikos**, v. 91, n. 2, p. 307-310, 2000.

SOLIMAN, N.K.; MOUSTAFA, A.F. Industrial solid waste for heavy metals adsorption features and challenges; a review. **J. Mater. Res. Technol.**, v. 9, n. 5, p. 10235–10253, 2020.

SOLO-GABRIELE,H. M.; KUMAR, S.; ABELSON, S.; PENSO, J.; CONTRERAS, J.; BABLER, K. M.; KUMAR, N. Predicting COVID-19 cases using SARS-CoV-2 RNA in air, surface swab and wastewater samples. **Science of The Total Environment**, v. 857, p. 159188, 2023.

SOUZA, V.L.; SILVA, D.D.C.; SANTANA, K.B.; MIELKE, M.S.; ALMEIDA, A.-A.F.D.; MANGABEIRA, P. A. O.; ROCHA, E. A. Efeitos do cádmio na anatomia e na fotossíntese de duas macrófitas aquáticas. **Acta Botanica Brasilica**, v. 23, p. 343-354, 2009.

SOUZA-ARROYO, V.; FABIÁN, J.J.; BUCIO-ORTIZ, L.; MIRANDA-LABRA, R.U.; GOMEZ-QUIROZ, L.E.; GUTIÉRREZ-RUIZ, M.C. The mechanism of the cadmium-induced toxicity and cellular response in the liver. **Toxicology**, p. 153339, 2022.

SRIVIDYA, K., MOHANTY, K. Biosorption of hexavalent chromium from aqueous solutions by *Catla catla* scales: equilibrium and kinetics studies. **Chemical Engineering Journal**, v. 155, n. 3, p. 666-673, 2009.

SQA. 2013. Environmental plan of Pelotas. Secretaria de Qualidade Ambiental.

SU, R.; OU; Q., WANG, H.; LUO, Y.; DAI, X.; WANG, Y.; SHI, L. Comparison of Phytoremediation Potential of *Nerium indicum* with Inorganic Modifier Calcium Carbonate and Organic Modifier Mushroom Residue to Lead–Zinc Tailings. **International Journal of Environmental Research and Public Health**, v. 19, n. 16, p. 10353, 2022.

SUDIARTO, S. I.A.; RENGGAMAN, A.; CHOI, H. L. Floating aquatic plants for total nitrogen and phosphorus removal from treated swine wastewater and their biomass characteristics. **Journal of environmental management**, v. 231, p. 763-769, 2019.

SWAIN, T.; HILLIS, W. E. The phenolic constituents of *Prunus domestica*. I.—The quantitative analysis of phenolic constituents. **Journal of the Science of Food and Agriculture**, v. 10, n. 1, p. 63-68, 1959.

TANNER, C.C.; HEADLEY, T.R. Components of floating emergent macrophyte treatment wetlands influencing removal of stormwater pollutants. **Ecological Engineering**, v. 37, n. 3, p. 474-486, 2011.

TAIE, H.A.A.; SEIF EL-YAZAL, M.A.; AHMED, S.M.A.; RADY, M.M. Polyamines modulate growth, antioxidant activity, and genomic DNA in heavy metal–stressed wheat plant. **Environmental Science and Pollution Research**, v. 26, n. 22, p. 22338-22350, 2019.

TEDESCO M.J.; GIANELLO, C.; BISSANI, C.A.; BOHNEN, H.; VOLKWEISS, S.J. **Análises de solo, plantas e outros materiais.** Porto Alegre: Universidade Federal do Rio Grande do Sul, 1995, Faculdade de Agronomia.

TEYMOORIAN, T.; TEYMOURIAN, T.; KOWSARI, E.; RAMAKRISHNA, S. Direct and indirect effects of SARS-CoV-2 on wastewater treatment. **J. Water Process Eng**. 42, 102193, 2021.

TIMALSINA, H.; GYAWALI, T.; GHIMIRE, S.; PAUDEL, S.R. Potential application of enhanced phytoremediation for heavy metals treatment in Nepal. **Chemosphere**, v. 306, p. 135581, 2022.

TIWARI, S.; DIXIT, S.; VERMA, N. An effective means of biofiltration of heavy metal contaminated water bodies using aquatic weed *Eichhornia crassipes*. **Environmental monitoring and assessment**, v. 129, n. 1, p. 253-256, 2007.

THAKUR, S.; SINGH, L.; WAHID, Z.A.; SIDDIQUI, M.F.; ATNAW, S.M.; DIN, M.F.M. Plant-driven removal of heavy metals from soil: uptake, translocation, tolerance mechanism, challenges, and future perspectives. **Environmental Monitoring and Assessment**, 2016, 188, 4, 1-11.

TRASSANTE, C.M., DOS SANTOS BARBOZA, V., DOS SANTOS ROCHA, L., CORREA, P.M., LUCHESE, C., WILHELM, E.A., DE PEREIRA, C.M.P., BALDISSERA, M.D., RECH, V.C., GIONGO, J.L., DE ALMEIDA VAUCHER, R. Detection of SARS-CoV-2 virus using an alternative molecular method and evaluation of biochemical, hematological, inflammatory, and oxidative stress in healthcare professionals. **Microb. Pathog.** v. 158, p. 104975, 2021.

TRIPATHI, D. K.; SINGH, V. P.; KUMAR, D.; CHAUHAN, D. K. Impact of exogenous silicon addition on chromium uptake, growth, mineral elements, oxidative stress, antioxidant capacity, and leaf and root structures in rice seedlings exposed to hexavalent chromium. **Acta physiologiae plantarum**, v. 34, n. 1, p. 279-289, 2012.

TRZONKOWSKA, L.; LEŚNIEWSKA, B.; GODLEWSKA-ŻYŁKIEWICZ, B. Development of Solid Phase Extraction Method Based on Ion Imprinted Polymer for Determination of Cr (III) Ions by ETAAS in Waters. **Water**, v. 14, n. 4, p. 529, 2022.

TSHITHUKHE, G.; MOTITSOE, S. N.; HILL, M. P. Heavy Metals Assimilation by Native and Non-Native Aquatic Macrophyte Species: A Case Study of a River in the Eastern Cape Province of South Africa. **Plants**, v. 10, n. 12, p. 2676, 2021.

TSIMOGIANNIS, D.; OREOPOULOU, V. 2019. Classification of phenolic compounds in plants. In: Polyphenols in plants. Academic Press, 2019. p. 263-284.

TUFAIL, M. A.; ILTAF, J.; ZAHEER, T.; TARIQ, L.; AMIR, M. B.; FATIMA, R.; AYYUB, M. Recent advances in bioremediation of heavy metals and persistent organic pollutants: A review. **Science of The Total Environment**, p. 157961, 2022.

ÜÇÜNCÜ, E.; TUNCA, E.; FIKIRDEŞICI, Ş.; ALTINDAĞ, A. Decrease and increase profile of Cu, Cr and Pb during stable phase of removal by duckweed (*Lemna minor* L.). **International Journal of Phytoremediation**, v. 15, n. 4, p. 376-384, 2013.

UGWU, E. I.; OTHMANI, A.; NNAJI, C. C. A review on zeolites as cost-effective adsorbents for removal of heavy metals from aqueous environment. **International Journal of Environmental Science and Technology**, v. 19, n. 8, p. 8061-8084, 2022.

UKHUREBOR, K. E.; AIGBE, U. O.; ONYANCHA, R. B.; NWANKWO, W.; OSIBOTE, O. A.; PAUMO, H. K.; SILOKO, I. U. Effect of hexavalent chromium on the environment and removal techniques: a review. **Journal of Environmental Management**, v. 280, p. 111809, 2021.

UPADHYAYA, A.,; SANKHLA, D.; DAVIS, T. D.; SANKHLA, N.; SMITH, B. N. Effect of paclobutrazol on the activities of some enzymes of activated oxygen metabolism and lipid peroxidation in senescing soybean leaves. **Journal of plant physiology**, v. 121, n. 5, p. 453-461, 1985.

USEPA. 2006. United States Environmental Protection Agency. Aquatic life ambient water quality criteria. Disponível em: https://www.epa.gov/wqc/national-recommended-water-quality-criteria-aquatic-life-criteriatable. [accessed 2021 Mar 1].

USMAN, K.; AL-GHOUTI, M. A.; ABU-DIEYEH, M. H. The assessment of cadmium, chromium, copper, and nickel tolerance and bioaccumulation by shrub plant *Tetraena qataranse*. **Scientific reports**, v. 9, n. 1, p. 1-11, 2019.

VAN KESSEL, S. A.; OLDE HARTMAN, T. C.; LUCASSEN, P. L.; VAN JAARSVELD, C. H. Post-acute and long-COVID-19 symptoms in patients with mild diseases: a systematic review. **Family practice**, v. 39, n. 1, p. 159-167, 2022.

VANKAR, P. S.; BAJPAI, D. Phyto-remediation of chrome-VI of tannery effluent by Trichoderma species. **Desalination**, v. 222, n. 1-3, p. 255-262, 2008.

VELEMPINI, T; PILLAY, K. Sulphur functionalized materials for Hg(II) adsorption: A review. **Journal of Environmental Chemical Engineering**, p.103350, 2019.

VERMA, S.; KUILA, A. Bioremediation of heavy metals by microbial process. **Environmental Technology & Innovation**, v. 14, p. 100369, 2019.

VENUGOPAL, A.; GANESAN, H.; RAJA, S.S.S.; GOVINDASAMY, V.; ARUNACHALAM, M.; NARAYANASAMY, A.; VELLINGIRI, B. Novel wastewater surveillance strategy for early detection of SARS-CoV-2 disease 2019 hotspots. **Curr. Opin. Environ. Sci. Health,** v. 17, p. 8–13, 2020.

VUOLO, M. M.; LIMA, V. S.; JUNIOR, M. R. M. Phenolic compounds: Structure, classification, and antioxidant power. In: Bioactive compounds. **Woodhead Publishing**, 2019. p. 33-50.

WALSH, G. C.; MAESTRO, M. Assessing the specificity of a herbivore on a plant of uncertain phylogenetic placing: Listronotus elongatus a herbivore of Hydrocotyle ranunculoides. **BioControl**, v. 62, n. 2, p. 269-279, 2017.

WANG, W.; WANG, Y.; SUN, L.; ZHENG, Y.; ZHAO, J. Research and application status of ecological floating bed in eutrophic landscape water restoration. **Science of The Total Environment**, v. 704, p. 135434, 2020.

WANG, X.; LI, D.; LI, W.; PENG, J.; XIA, H.; ZHANG, L.; GUO, S.; CHEN, G. Optimization of mesoporous activated carbon from coconut shells by chemical activation with phosphoric acid. **BioResources** 8 (4), 6184–6195, 2013.

WANG, J.; WANG, W.; XIONG, J.; LI, L.; ZHAO, B.; SOHAIL, I.; HE, Z. A constructed wetland system with aquatic macrophytes for cleaning contaminated runoff/storm water from urban area in Florida. **Journal of Environmental Management**, v. 280, p. 111794, 2021.

WANG, C.-Y.; SAMPLE, D. J. Assessment of the nutrient removal effectiveness of floating treatment wetlands applied to urban retention ponds. **Journal of Environmental Management**, v. 137, p. 23-35, 2014.

WHO (World Health Organization), 2011. **Guidelines for Drinking-water Quality.** Geneva, Switzerland: Series World Health Organization.

WHO (World Health Organization), 2020. **Coronavirus disease 2019 (COVID-19) situation report—51**. World Health Organization. Disponível em: https://www.who.int/docs/default-source/coronaviruse/situationreports/20200311-sitrep-51-covid-19.pdf?sfvrsn¼1ba62e57_10. Accesso em 29 de Setembro de 2022.

WHO (World Health Organization), 2021. **Novel SARS-CoV-2 disease (COVID-19) Situation Report**. Disponível em: https://www.who.int/publications/m/item/weekly-epidemiological-update—12-january-2021. Acesso em 12 de Janeiro de 2021.

WHO (World Health Organization), 2023a. **WHO Coronavirus (COVID-19) Dashboard**. Disponível em: https://covid19.who.int/. Acesso em 3 de Janeiro de 2023.

WHO (World Health Organization), 2023b. **Tracking SARS-CoV-2 variants.** Disponível em: https://www.who.int/activities/tracking-SARS-CoV-2-variants. Acesso em 8 de Janeiro de 2023.

WOJTUSIAK, J.; BAGAIS, W.; VANG, J.; ROESS, A.; ALEMI, F. Order of Occurrence of COVID-19 Symptoms. **Quality Management in Healthcare**, v. 32, n. Supplement 1, p. S29-S34, 2023.

WORAHARN, S.; MEEINKUIRT, W.; PHUSANTISAMPAN, T.; CHAYAPAN, P. Rhizofiltration of Cadmium and Zinc in Hydroponic Systems. **Water, Air and Soil Pollution**, v. 232, n. 5, 2021.

WURTZER, S.S.; MARECHAL, V.; MOUCHEL, J.M.; MOULIN, L. Time course quantitative detection of SARS-CoV-2 in Parisian wastewaters correlates with COVID-19 confirmed cases. **MedRxiv**, 2020.

XIN, J.; MA, S.; LI, Y.; ZHAO, C.; TIAN, R. *Pontederia cordata*, an ornamental aquatic macrophyte with great potential in phytoremediation of heavy-metal-contaminated wetlands. **Ecotoxicology and Environmental Safety**, v. 203, p. 111024, 2020.

XU, J.; JIN, G.; TANG, H.; MO, Y.; WANG, Y. G.; LI, L. Response of water quality to land use and sewage outfalls in different seasons. **Science of The Total Environment**, v. 696, p. 134014, 2019.

XU, L.; CHEN, S.; ZHUANG, P.; XIE, D.; YU, X.; LIU, D.; XING, F. Purification Efficiency of Three Combinations of Native Aquatic Macrophytes in Artificial Wastewater in Autumn. **International Journal of Environmental Research and Public Health**, v. 18, n. 11, p. 6162, 2021.

XUE, X.; BALL, J.K.; ALEXANDER, C.; ALEXANDER, M.R. All surfaces are not equal in contact transmission of SARS-CoV-2. **Matter** 3, p. 1433–1441, 2020.

YAHYA, M. A.; AL-QODAH, Z.; NGAH, C. W. Z. Agricultural bio-waste materials as potential sustainable precursors used for activated carbon production: A review. **Renewable and Sustainable Energy Reviews**, v.46, p.218-235, 2015.

YAN, X.; WANG, J.; SONG, H.; PENG, Y.; ZUO, S.; GAO, T.; DUAN, X.; QIN., D.; DONG, J. Evaluation of the phytoremediation potential of dominant plant species growing in a chromium salt–producing factory wasteland, China. **Environmental Science and Pollution Research**, v. 27, n. 7, p. 7657-7671, 2020.

YAN, H.; YAN, Z.; WANG, L.; HAO, Z.; HUANG, J. Toward understanding submersed macrophyte *Vallisneria natans*-microbe partnerships to improve remediation potential for PAH-contaminated sediment. **Journal of Hazardous Materials**, v. 425, p. 127767, 2022

YANG, J.; WEI, W.; PI, S.; MA, F.; LI, A.; WU, D.; XING, J. Competitive adsorption of heavy metals by extracellular polymeric substances extracted from *Klebsiella* sp. J1. **Bioresource technology**, v. 196, p. 533-539, 2015.

YASIN, N.A.; KHAN, W.U.; AHMAD, S.R.; ALI, A.; AHMED, S.; AHMAD, A. Effect of Bacillus fortis 162 on growth, oxidative stress tolerance and phytoremediation potential of *Catharanthus roseus* under chromium stress. **International Journal of Agriculture and Biology**, v. 20, n. 7, p. 1513-1522, 2018.

YEH, N.; YEH, P.; CHANG, Y.-H. Artificial floating islands for environmental improvement. **Renewable and Sustainable Energy Reviews**, v. 47, p. 616-622, 2015.

YILMAZ, D.D.; ERCAN, N.; ERCAN, F.S. Heavy metal-induced oxidative stress and DNA damage as shown by RAPD-PCR in leaves of *Elodea canadensis*. **Applied Chemical Engineering**, v. 3, n. 1, p. 14-22, 2020.

YIN, K.; WANG, Q.; LV, M.; CHEN, L. Microorganism remediation strategies towards heavy metals. **Chemical Engineering Journal**, v. 360, p. 1553-1563, 2019.

YIN, C. Genotyping coronavirus SARS-CoV-2: methods and implications. **Genomics**, v. 112, p. 3588–3596, 2020.

YORGUN, S.; VURAL, N.; DEMIRAL, H. Preparation of high-surface area activated carbons from Paulownia wood by $ZnCl_2$ activation. **Microporous Mesoporous Mater**. v. 122, n. 1–3, p. 189–194, 2009.

YOON, J.; CAO, X.; ZHOU, Q.; MA, L.Q. Accumulation of Pb, Cu, and Zn in native plants growing on a contaminated Florida site. **Science of the total environment**, v. 368, n. 2-3, p. 456-464, 2006.

ZAMHURI, S. A.; SOON, C. F.; NORDIN, A. N.; AB RAHIM, R.; SULTANA, N.; KHAN, M. A.; TEE, K. S. A review on the contamination of SARS-CoV-2 in water bodies: Transmission route, virus recovery and recent biosensor detection techniques. **Sensing and Bio-Sensing Research**, p. 100482, 2022.

ZAYNAB, M.; AL-YAHYAI, R.; AMEEN, A.; SHARIF, Y.; ALI, L.; FATIMA, M.; KHAN, K.A.; LI, S. Health and environmental effects of heavy metals. **Journal of King Saud University-Science**, v. 34, n. 1, p. 101653, 2022.

ZHANG, C.-B.; LIU, W.-L.; PAN, X.-C.; GUAN, M.; LIU, S.-Y.; GE, Y.; CHANG, J. Comparison of effects of plant and biofilm bacterial community parameters on removal performances of pollutants in floating island systems. **Ecological Engineering**, v. 73, p. 58-63, 2014.

ZHANG, S.; PANG, S.; WANG, P.; WANG, C.; GUO, C.; ADDO, F. G.; LI, Y. Responses of bacterial community structure and denitrifying bacteria in biofilm to submerged macrophytes and nitrate. **Scientific Reports**, v. 6, n. 1, p. 1-10, 2016.

ZHANG, L.; WANG, M.; LAI, Y.; LI, X. Oil/molten salt interfacial synthesis of hybrid thin carbon nanostructures and their composites. **J. Mater. Chem.**, v.6, n. 12, 4988–4996, 2018.

ZHANG, T.; RUAN, J.; ZHANG, B.; LU, S.; GAO, C.; HUANG, L.; BAI, X.; XIE, L.; GUI, M.; QIU, R.-L. Heavy metals in human urine, foods and drinking water from an e-waste dismantling area: Identification of exposure sources and metal-induced health risk. **Ecotoxicology and environmental safety**, v. 169, p. 707-713, 2019.

ZHANG, Y.; LONG, C.; HU, G.; HONG, S.; SU, Z.; ZHANG, Q.; ZHENG, P.; WANG, T.; YU, S.; JI, G. Two-week repair alleviates hexavalent chromium-induced hepatotoxicity, hepatic metabolic and gut microbial changes: A dynamic inhalation exposure model in male mice. **Science of The Total Environment**, v. 857, p. 159429, 2023.

ZHAO, F.; XI, S.; YANG, X.; YANG, W.; LI, J.; GU, B.; HE, Z. Purifying eutrophic river waters with integrated floating island systems. **Ecological Engineering**, v. 40, p. 53-60, 2012.

ZHAO, Z.; QIN, Z.; XIA, L.; ZHANG, D.; HUSSAIN, J. Dissipation characteristics of pyrene and ecological contribution of submerged macrophytes and their biofilms-leaves in constructed wetland. **Bioresource technology**, v. 267, p. 158-166, 2018.

ZHOU, J.; CHEN, L.H.; PENG, L.; LUO, S.; ZENG, Q.R. Phytoremediation of heavy metals under an oil crop rotation and treatment of biochar from contaminated biomass for safe use. **Chemosphere**, v. 247, p. 125856, 2020.

ZHU, L.; LI, Z.; KETOLA, T. Biomass accumulations and nutrient uptake of plants cultivated on artificial floating beds in China's rural area. **Ecological Engineering**, v. 37, n. 10, p. 1460-1466, 2011.

ZYOUD, A.; NASSAR, H.N.; EL-HAMOUZ, A.; HILAL, H.S. Solid olive waste in environmental cleanup: enhanced nitrite ion removal by $ZnCl_2$-activated carbon. **J. Environ. Manag.,** v. 152, p. 27–35, 2015.

ZOU, J.; YU, K.; ZHANG, Z.; JIANG, W.; LIU, D. Antioxidant response system and chlorophyll fluorescence in chromium (VI)-treated *Zea mays* L. seedlings. **Acta Biologica Cracoviensia Series Botanica**, v. 51, n. 1, p. 23-33, 2009.